# UNIVERSITY OF LONDON THESIS

Degree PhD Year 2006 Name of Author JENKINS
Dagan

# The Genetics of Human Renal Tract Malformations

by

Dagan Jenkins

A thesis submitted to the University of London in fulfillment
of the requirement for the degree of
Doctor of Philosophy

May, 2006

Nephro-Urology Unit and Clinical and Molecular Genetics Unit,
UCL Institute of Child Health, 30 Guilford Street,
London, WC1N 1EH.





ProQuest LLC
789 East Eisenhower Parkway
P.O. Box 1346
Ann Arbor, MI 48106-1346

To Claire and 'Bloggs'

# ABSTRACT

The identification of mechanisms by which congenital renal tract malformations arise is an important area of research given that these defects account for approximately half of all children who progress to end-stage renal failure. Understanding the genetic contribution to this pathogenesis is of particular value, facilitating the counselling of families with a history of disease, serving to highlight the critical window(s) during which the course of development is altered, and aiding in the identification of molecular pathways that might be amenable to therapy in the future. This thesis is focused on furthering our understanding of how non-syndromic renal tract malformations are genetically determined.

It was hypothesised that human renal tract malformations may be caused by mutations of genes in the *Uroplakin* (*UP*) family and *Sonic hedgehog* (*SHH*), and that these genes are expressed at specific sites in tissues during normal human renal tract development.

It was shown that *UPIIIa*, a gene expressed in early human development, is mutated in a subset of patients with severe bilateral renal adysplasia. However, no definitive evidence was found that *UPII* mutations cause renal tract malformations, although variants in this gene might be a rare predisposing factor. Furthermore, no support was found for *SHH* mutations in human persistent cloaca, although *UPIIIa* mutations are occasionally associated with this condition. The expression patterns of SHH signalling proteins in normal human renal tract development is consistent with a variety of signalling modes, namely epithelial-to-epithelium canonical signalling in the cloaca, epithelial-to-

mesenchyme canonical signalling in the urogenital sinus and epithelial-to-epithelium non-canonical signalling in kidney medullary collecting ducts.

The discovery of mutations in children with renal tract malformations will provide families with long-sought explanations regarding the pathogenesis of disease and may also have implications for genetic counselling. The proposed studies will also shed light on the cell biology of normal human renal tract development.

# ACKNOWLEDGEMENTS

I would like to thank a number of individuals who collectively made this work possible. In particular, I would like to thank my supervisors, Adrian Woolf, Maria Bitner-Glindzicz and Sally Feather, as well as Sue Malcolm, who provided support and encouragement throughout my MRC-funded PhD Studentship, and whose intellectual insight and scientific rigour resounds throughout this work; I am very grateful for the unique educational experience that they have collectively provided me with.

I would also like to thank those individuals who collected DNA and assessed patients, most of whom were treated at Great Ormond Street Hospital: Ambrose Gullett, Jennifer Allison and Louise Thomasson collected DNA samples from patients who had been assessed by Adrian Woolf, Duncan Wilcox, Richard Trompeter, Lesley Rees, Sally Feather, David Thomas, Rachel Belk and Rose de Bruyn.

A number of people in the Nephro-Urology and Clinical & Molecular Genetics Units, headed by Adrian Woolf and Maria Bitner-Glindzicz respectively, at the Institute of Child Health, gave me ongoing support and advice: thanks to Simon Welham, Paul Rutland, Paul Winyard, David Gonzalez-Martinez, Jolanta Pitera, Liam McCarthy, David Long, Miliyun Chiu, Claire Gannon and Kate Hillman. I am also indebted to the Human Developmental Biology Resource for the provision of tissues.

I would also like to thank my collaborators in this work, Henry (Tung-Tien) Sun and Andrew (Chih-Chi) Hu at New York University Medical Center, and Jenny Southgate and Lisa Clements at the University of York, for hosting me in their laboratories, for the provision of materials and for their expert advice, but most of all for freely sharing their results and resources in true scientific spirit.

# CONTENTS

# LIST OF TABLES

## LIST OF FIGURES

## ABBREVIATIONS

| | |
|---|---|
| ARM | Anorectal Malformation |
| AUM | Asymmetric Unit Membrane |
| bp | Base Pair |
| CAPD | Continuous Ambulatory Peritoneal Dialysis |
| CK | Cytokeratin |
| CNBr | Cyanogen Bromide |
| °C | Degrees Celsius |
| DAB | Di-Amino Benzidine |
| DNA | Deoxyribose Nucleic Acid |
| cDNA | Complementary DNA |
| dNTP | Deoxynucleotide Triphosphate |
| ESRF | End-Stage Renal Failure |
| GFP | Green Fluorescent Protein |
| kDa | Kilodaltons |
| MCDK | Multicystic Dysplastic Kidney |
| MDCK | Madine Darby Canine Kidney cells |
| MPF | Mitosis Promoting Factor |
| NES | Nuclear Export Signal |
| PAGE | Polyacrylamide Gel Electrophoresis |
| PBS | Phosphate Buffered Saline |
| PCNA | Proliferating Cell Nuclear Antigen |
| PCR | Polymerase Chain Reaction |
| PTCH | Patched |
| PUV | Posterior Urethral Valves |
| RACE | Rapid Amplification of Complementary Ends |
| RNA | Ribonucleic Acid |
| mRNA | Messenger RNA |
| SDS | Sodium Didecyl Sulphate |
| SHH | Sonic Hedgehog |
| αSMA | α-Smooth Muscle Actin |
| SMO | Smoothened |
| SNP | Single Nucleotide Polymorphism |
| UGS | Urogenital Sinus |
| UP | Uroplakin |
| UTR | Untranslated Region |
| VACTERL | Vertebral Anorectal Cardiac Tracheoesophageal Renal Limb |
| VUR | Vesicoureteric Reflux |

# Preface. HYPOTHESES, AIMS AND OVERVIEW

## OVERALL HYPOTHESIS

I hypothesise that human renal tract malformations may be caused by mutations of genes in the *Uroplakin* (*UP*) family and *Sonic hedgehog* (*SHH*), and that these genes are expressed at specific sites and tissues during normal human renal tract development.

## OVERALL AIM

The aim of this thesis is to seek mutations of the *UPs* and *SHH* in patients with a range of renal tract malformations and to establish the expression patterns of these genes in human embryos.

## OVERVIEW

I have arranged the *Results* chapter into four sections as follows:

*Study I. Mutational analyses of* UPIIIa *and* UPIb *in patients with renal adysplasia.*

Hypothesis - Mutations in *UPIIIa* and *UPIb* cause human renal tract malformations;

Aim - To seek *UPIIIa* and *UPIb* mutations in patients with bilateral renal adysplasia.

*Study II. Mutational analyses of* UPII *in patients with renal adysplasia.*

Hypothesis - Mutations in *UPII* cause human renal tract malformations;

Aim - To seek *UPII* mutations in patients with bilateral renal adysplasia.

*Study III. Mutational analyses of* UPIIIa *and* SHH *in persistent cloaca and associated malformations.*

Hypothesis - Mutations in *UPIIIa* and *SHH* cause persistent cloaca;

Aim - To seek *UPIIIa* and *SHH* mutations in patients with persistent cloaca.

*Study IV. Expression analyses of Sonic hedgehog pathway proteins in human renal tract tissues.*

Hypothesis - Sonic hedgehog signalling proteins are expressed at key stages during human renal tract development;

Aim - To immunolocalise the core SHH signalling proteins during human renal tract development.

**LONG-TERM SIGNIFICANCE**

The discovery of mutations in children with renal tract malformations will provide families with long-sought explanations regarding the pathogenesis of disease and may also have implications for genetic counselling. The proposed studies will also shed light on the cell biology of normal human renal tract development.

# Chapter 1. INTRODUCTION

Approximately half of all children who progress to end-stage renal failure are born with congenital renal tract malformations. In most, these malformations are not accompanied by other-organ defects; their disease is non-syndromic. In order to understand the aetiology of human renal tract malformations a knowledge of normal human development and the molecular pathways associated with this category of disease is absolutely necessary.

Here, in the *Introduction* to this thesis, I will review normal development of the renal tract and consider some of the important molecules involved in these processes. Two groups of molecules will be concentrated on, the Uroplakins (UP) and the Sonic hedgehog (SHH) signalling proteins. The purpose is to provide a framework to understand the mechanisms by which renal tract malformations arise and to establish candidate genes for mutational analyses.

# Part I. RENAL TRACT DEVELOPMENT

## 1-1 ANATOMY OF NORMAL HUMAN KIDNEY DEVELOPMENT

The anatomy of kidney development described here is largely based on a number of previous reports (Potter 1972; Woolf et al. 2003; Osathanondh & Potter 1963a; Osathanondh & Potter 1963b; Osathanondh & Potter 1963c; Osathanondh & Potter 1966a; Osathanondh & Potter 1966b; Larsen 2001; Moore & Persaud 2003; Woolf & Jenkins 2006) and developmental stages are those of the human, except where indicated differently. The main components of the mature kidney are shown in Figure 1.

There are three embryonic kidneys, the pronephros, mesonephros and metanephros. The pronephros gives rise to the mesonephros from which the metanephros, the adult kidney, is derived; each of these structures forms sequentially such that as each forms, its predecessor regresses, although there is some overlap in the existence of the pronephros and mesonephros, and later the mesonephros and metanephros. Indeed, although the pronephros and mesonephros are clearly distinct from the metanephros, it has been suggested (Torrey 1954) that this whole system might be better viewed as a single entity, the holonephros.

### 1-1-1 The pronephros and mesonephros

In the 3$^{rd}$ week after conception, the nephrogenic cord arises between the 7$^{th}$ and 13$^{th}$ somites, forming from intermediate mesoderm. This associates with a few rudimentary tubules that form the pronephros, the first embryonic kidney, although this is non-

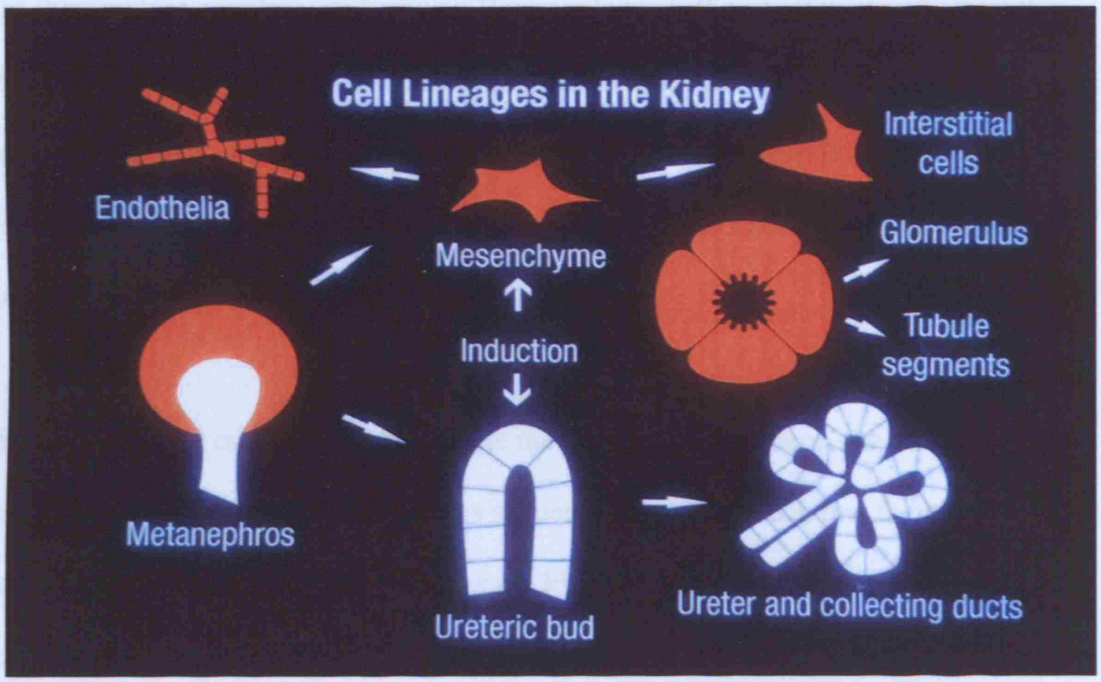


**Figure 1. Key structures in the differentiated kidney.**
The metanephros forms from two distinct embryonic structures, the ureteric bud and the metanephric mesenchyme that it invades. These two structures induce one another to survive and to form the various components of the mature kidney. The mesenchyme forms both glomerular and proximal nephron epithelia and interstitial cells of the renal stroma (and probably also some endothelia). The ureteric bud is induced to branch to form the collecting system, with the stem remaining as the ureter and renal pelvis. Figure reproduced from the personal collection of Prof. Adrian Woolf (UCL Institute of Child Health) with permission.

functional in humans and only acts as an excretory organ in amphibians. The caudal region of the nephrogenic cord becomes the mesonephric duct on day 24 of gestation, and is associated with glomeruli and blood vessels that are the first functioning excretory units in the human; though very basic, these excretory units (nephrons) are essentially the same as their mature counterparts having a Bowman's capsule and afferent and efferent tubules, and only lacking a loop of Henle as compared to the adult metanephric kidney. The mesonephric duct continues to migrate toward the cloaca, the primordium of the bladder and rectum, and the two become fused at about 4 weeks gestation, at the level of somite 25.

As this formation and caudal migration of the mesonephros takes place, the cranial regions of the pronephros and mesonephros sequentially regress, such that there is a 'caudal relocation' of these transient embryonic kidneys. The pronephros completely involutes by 25 days gestation, while the mesonephric glomeruli have completely regressed by the end of the first trimester. In adult males, the mesonephric duct does persist; following its implantation into the cloaca early in development, it subsequently migrates to connect with the urethra, where it forms the epididymis, seminal vesicle and ejaculatory duct.

### 1-1-2 The metanephros

The metanephros gives rise to the mature kidney. Between 4 and 5 weeks gestation, as the cranial portion of the mesonephros regresses, the ureteric bud emerges from the mesonephric duct opposite somite 28. The ureteric bud is a hollow epithelial structure

that grows dorsally and cranially, extending toward the metanephric mesenchyme, a group of cells situated between the peritoneal cavity and the umbilical artery that are specified to become the stroma of the kidney and to form nephrons (Figure 2). The ureteric bud lineage will eventually give rise to the collecting ducts, calyces, renal pelvis and ureter; the ureteric bud and metanephric mesenchyme communicate with one another resulting in branching morphogenesis, and the tips of the ureteric ampullae induce the metanephric mesenchyme to condense and undergo a mesenchymal-to-epithelial transition to form new nephrons.

### 1-1-3 Formation of the renal pelvis and calyces

The renal pelvis and major calyces form from the first three to six generations of ureteric bud branches and the subsequent branches give rise to the minor calyces; in the period when the renal pelvis is formed, branching occurs most rapidly at the poles of the kidney. At this initial stage of kidney development, branching is so rapid that the interstitial portions of the branches are sufficiently short that several branches appear to arise from a single stem. As the nephrons start to function, the newly produced urine causes distension of the entire collecting system, and this is thought to cause the first generations of branches to collapse into a single unit, forming the pelvicalyceal system by twelve weeks. Once the minor calyces are formed, some 20 or so ampullae are related to each minor calyx, from which the papillary collecting ducts originate. These ampullae then branch further, although progressively more slowly, and induce the formation of nephrons. By the fourteenth week of gestation the pelvicalyceal system has taken on a more mature

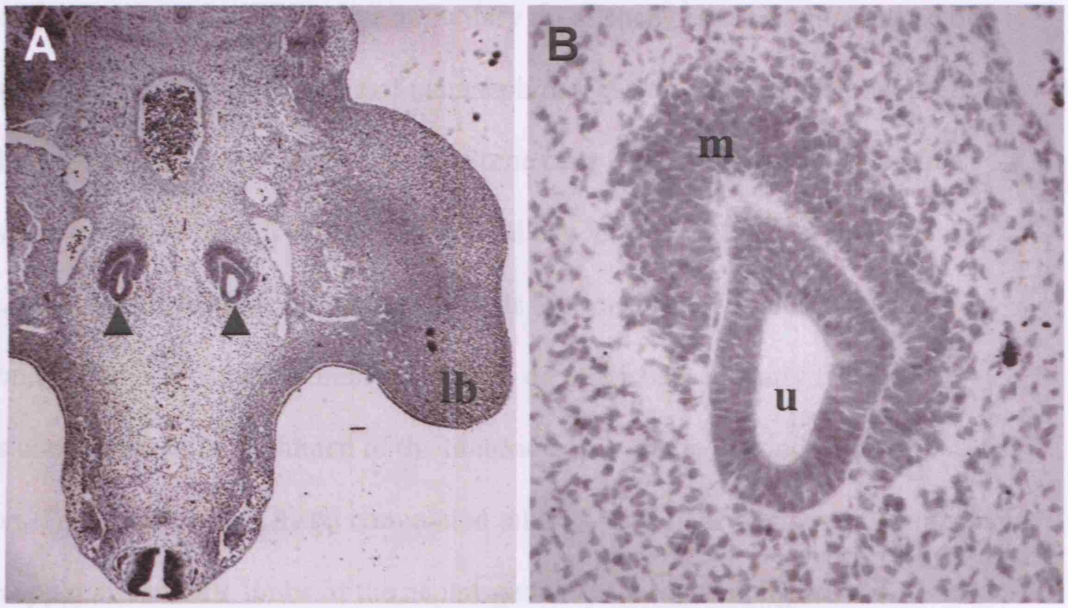


**Figure 2. Human metanephros at the 'ureteric bud' stage.**
(**A**) Transverse section of a human embryo, approximately five weeks gestation, showing paired metanephric kidneys (arrowheads), one on each side of the midline. A lower limb bud (lb) is seen on the right. Stained with hematoxylin. Original magnification X12.5. (**B**) High power of A shows one of the ureteric buds (u) capped by metanephric mesenchyme (m) which is demarcating from surrounding, loosely-packed, intermediate mesoderm. (Modified from Woolf & Jenkins 2006).

structure that is essentially the same as the adult kidney (see Figure 2.3 and 2.4 in Woolf & Jenkins 2006).

### 1-1-4 Formation of the collecting duct system and nephrons

From the eighth week of gestation, the ampullary tip of each branch of the ureteric bud is associated with an oval condensation of metanephric mesenchymal cells that will each eventually give rise to a nephron (Figure 3). Some cells in each condensation form a hollow vesicle, while others form a separate solid cap for the next subdivision of the ampulla. Each hollow vesicle elongates and folds to form first a comma- then an S-shaped body (Figure 4), the proximal upper limb of which subsequently fuses and becomes contiguous with the lumen of the ureteric bud ampulla that induced its formation. The proximal and distal convoluted tubules, as well as the loop of Henle, form from the upper and middle limbs of the nephrogenic vesicle as it elongates and differentiates while the so-called glomerular tuft, which is composed of capillaries, forms next to the lower limb of the vesicle. The outer-layer cells flatten and become Bowman's capsule, and the columnar inner layer cells form the glomerular epithelium. The nephrons, attached to the growing ureteric bud tips, expand radially and the interstitial portions of the collecting ducts eventually become the future medullary collecting ducts.

Between fourteen and twenty weeks gestation nephron arcades are formed; branching of the ampullae stops and each will induce only a further three to six nephrons. As a new nephron is induced, the connecting tubule of the older nephron shifts the position of its point of attachment away from the ampulla to the connecting tubule of the next-formed

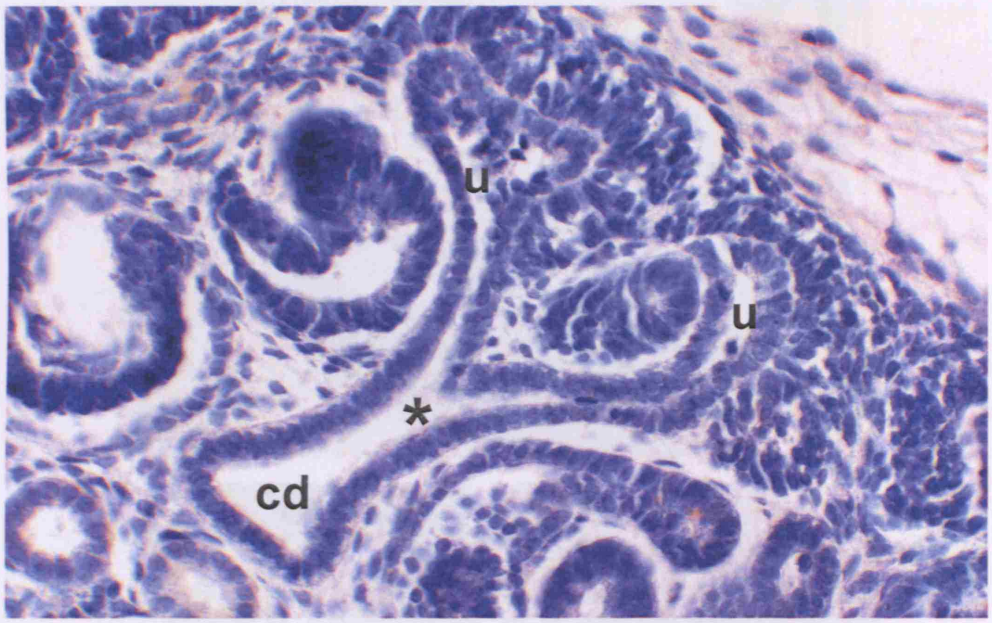


**Figure 3.** **Metanephros from a 7-week human foetus.**
A branch point (*) of the ureteric bud/collecting duct (cd) lineage leading to two ureteric bud ampullae (u). Stained with hematoxylin. Original magnification X100. (Modified from Woolf & Jenkins 2006).

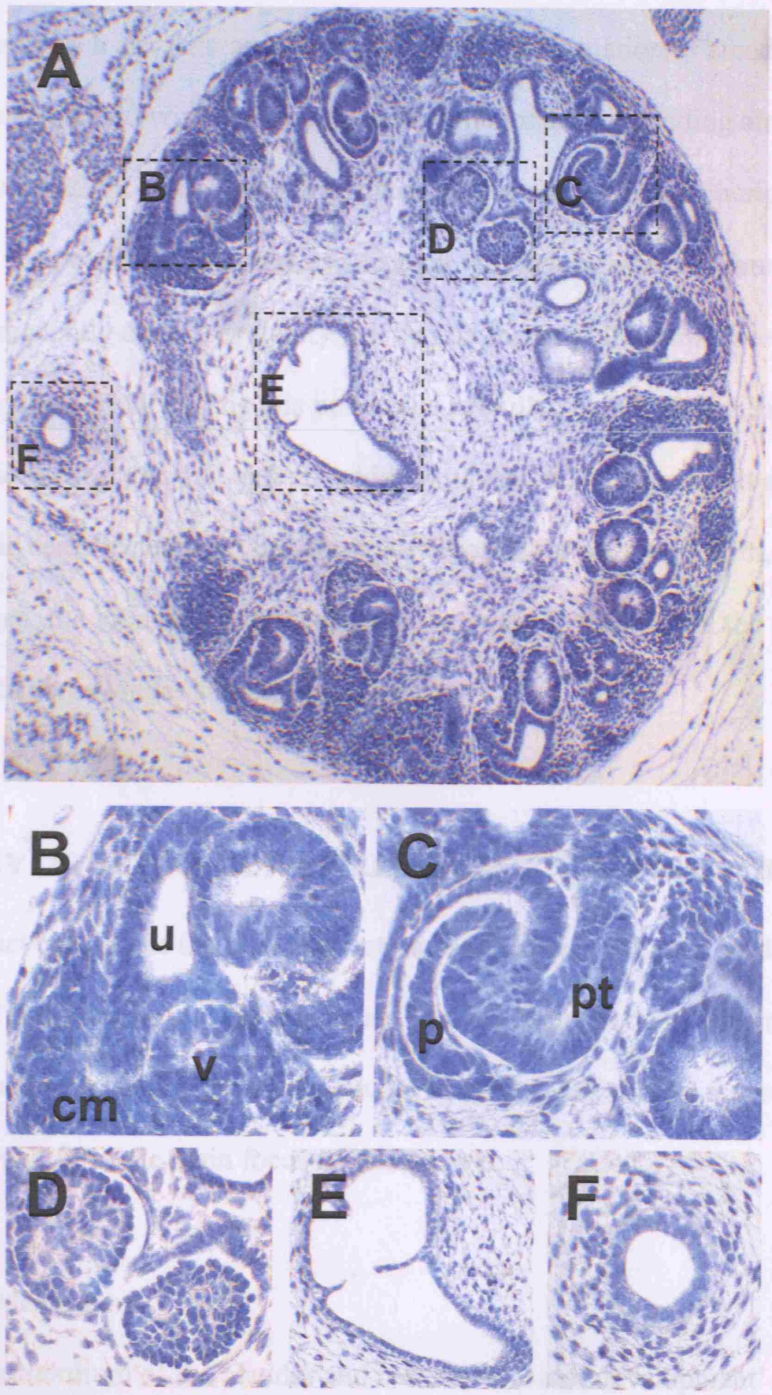


**Figure 4. Metanephros from a 7-week human foetus.**
(**A**) Low power view of whole metanephros. Boxed areas are shown in higher powers in subsequent frames. Stained with hematoxylin. Original magnification x12.5. (**B**) Nephrogenic zone showing the ampulla of a ureteric bud (u) branch, condensed metanephric mesenchyme (cm) and a primitive nephron vesicle (v) which has just undergone the mesenchymal to epithelial transition. (**C**) An 'S-shaped body': the primitive nephron is segmenting into the glomerulus, with cuboidal podocytes (p) with the adjacent proximal tubule (pt). (**D**) The first layer of glomeruli are noted in the deep cortex. (**E**) The renal pelvis lined by a monolayer of urothelium. (**F**) The ureter consists of a monolayer of urothelium surrounded by mesenchyme differentiating into smooth muscle. (Modified from Woolf & Jenkins 2006).

nephron so they are joined together in an arcade of between four and seven nephrons. The innermost nephron in each arcade was made first, before the formation of arcades, and the loops of Henle associated with these nephrons are the longest, extending almost to the papillary tip. Between 22-36 weeks gestation, the ampullae advance to the peripheral cortex beyond the region of nephron arcades and each will induce a further four to seven nephrons that subsequently attach separately just behind the ampullary tips (see Figure 2.7 in Woolf & Jenkins 2006). During this period the ampullae do not divide, and they advance toward the cortical surface with the addition of each new nephron. At about 36 weeks the ampullae cease to function and disappear. From 36 weeks until birth, no new nephrons are formed, the loops of Henle continue to increase in length, and the proximal and distal tubules become longer and more tortuous.

## 1-2 ANATOMY OF HUMAN LOWER RENAL TRACT DEVELOPMENT

The lower renal tract consists of the bladder, ureters and urethra. While the bladder and urethra are derived from the cloaca, the ureters are derived from the distal ureteric bud, formation and branching of which have been reviewed above. The earliest stages of lower tract development will form the main focus of this section.

### 1-2-1 Cloacal Development

The cloaca is the primordium of the bladder and rectum. 'Cloacal development' is a generic term used to describe the septation of the cloaca into ventral and dorsal compartments (the future bladder and rectum, respectively), the formation of the perineum and urethra, and the establishment of the genital tubercle. The anatomy of

cloacal development has been studied in a variety of mammals including sheep, pigs, dogs, rabbits, guinea pigs, squirrels, mice, rats and humans, although recent studies have focused on the latter three and will thus form the focus of this review. A variety of terminology has been used to describe different tissue domains in cloacal development, and so the description below represents an amalgam of these terms. Furthermore, different studies have described the stages of human development in terms of Carnegie stages, crown rump lengths and gestational age; here, I have described cloacal development in terms of gestational age according to observations in cited references. The anatomy of cloacal development is summarised in Figure 5.

### 1-2-2 Anatomy of cloacal development

After gastrulation, the human embryo emerges as a trilaminar structure, composed of ectoderm (adjacent to the amniotic cavity), endoderm (contiguous with the yolk sac) and (splanchnic) mesoderm. By 20-22 days gestation, the cloacal cavity is defined by the endoderm in the tail-end of the embryo, in a region beyond the allantois, a ventral offshoot that runs into the body stalk that will drain urine produced by the embryonic kidneys (Gilbert 2000). The posterior-most region of this endoderm-bound cavity is the tailgut. At about 26-28 days gestation, a fold between the hindgut and allantois is formed – the mesenchyme filling this space is the urorectal septum (Nievelstein et al. 1998). The tip of the urorectal septum marks the cranial border of the cloaca, while the endoderm of the caudal border contacts the surface ectoderm at this stage forming the cloacal membrane (Nievelstein et al. 1998). This juxtaposition of ectoderm and endoderm at the

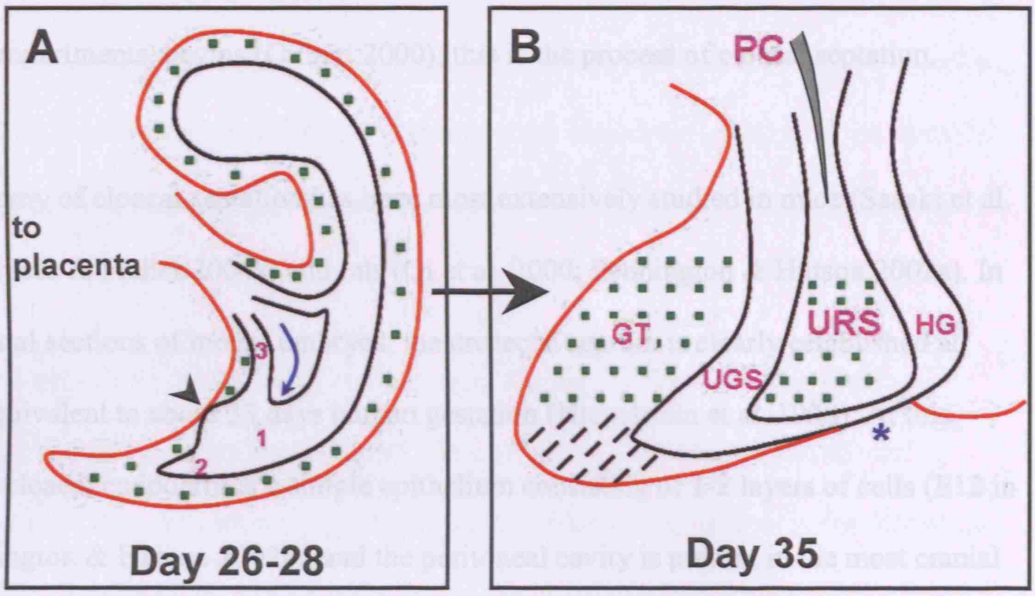


**Figure 5. Septation of the human cloaca.**

(**A**) Cartoon of the human embryo following gastrulation. The embryo is trilaminar consisting of ectoderm (red), mesoderm (green dots) and endoderm (black). Where the endoderm meets ectoderm to exclude the mesoderm (arrowhead) defines the cloacal membrane where the genital swellings form. The cloaca (1) is progressively separated by invasion of the urorectal septum (blue arrow) between the allantois (3) that migrates toward the tailgut (2). (**B**) By day 35 the urogenital sinus (UGS) and hindgut (HG) are joined only by a thin cloacal canal. The urethral plate (black dashes) will form the urethra. At this stage the cloacal plate has reverted to a cloacal membrane (*) that will rupture by apoptosis 13 days later. The endoderm lining the urorectal septum (URS) will subsequently protrude to form the perineum. GT, genital tubercle; PC, peritoneal cavity.

level of the cloacal membrane excludes mesenchymal cells in the midline, and forms the cloacal groove; the presence of mesenchyme either side of the cloacal membrane forms the labioscrotal swellings (Hynes & Fraher 2004a; Hynes & Fraher 2004b). By 28 days the invasion of the urorectal septum into the cloacal cavity, separating it into ventral and dorsal compartments, begins (Gilbert 2000); this is the process of cloacal septation.

The anatomy of cloacal septation has been most extensively studied in mice (Sasaki et al. 2004a; Hynes & Fraher 2004a) and rats (Qi et al. 2000; Pennington & Hutson 2002a). In mid-sagittal sections of mouse embryos, the urorectal septum is clearly established at E11.5, equivalent to about 33 days human gestation (Nievelstein et al. 1998). At this stage the cloacal endoderm is a simple epithelium consisting of 1-2 layers of cells (E12 in rat, Pennington & Hutson 2002a), and the peritoneal cavity is present in the most cranial area of the urorectal septal mesenchyme (Nievelstein et al. 1998). The urorectal septum progressively separates the cloacal cavity, and at E12-12.5 the common channel connecting the urogenital sinus (ventral; UGS) and hindgut (dorsal) cavities has been reduced to a thin canal. Also by E12.5, the tailgut has fully regressed, and the cloacal membrane has thickened to form the cloacal plate (Pennington & Hutson 2002a; 35 days in human, Nievelstein et al. 1998; E14 in rat, Qi et al. 2000). For many years, since the descriptions of Rathke (1832), Tourneaux (1888) and Retterer (1890), a major point of debate has been whether or not the urorectal septum fuses with the cloacal plate. In humans, while the cloacal canal still remains (i.e. while the urorectal septum and cloacal plate are still not fused), the dorsal part of the cloacal plate reverts to a membrane of only 1-2 cells thick at 46 days, and by 48 days this membrane has ruptured to expose the UGS

and hindgut to the amniotic cavity (Sasaki et al. 2004a; Nievelstein et al. 1998; Qi et al. 2000). Regression of the dorsal cloacal plate might involve apoptotic cell death, since several studies have reported pyknotic (Nievelstein et al. 1998) and apoptotic (Sasaki et al. 2004a; Pennington & Hutson 2002a) nuclei in this region at the stage when the urorectal septum becomes apposed to the cloacal plate. In between the UGS and hindgut, the tip of the urorectal septum (lined by what was the endoderm of the cloacal cavity) also protrudes into the amnion (Nievelstein et al. 1998) and forms the future perineum.

As the process of cloacal septation is taking place, inception of the future phallus is occurring in parallel. Before cloacal septation has begun, formation of the cloacal membrane (and thus the cloacal groove and labioscrotal swellings) marks the formation of the genital tubercle and at this stage the cloacal cavity fills almost the entire genital tubercle. Two days later in human development (one day in rodents), the mesenchyme immediately cranial to the cloacal membrane (sometimes called infraumbilical mesenchyme, or rostral mesenchyme of the genital tubercle) begins to expand ventrocaudally and, together with the ongoing unfolding of the whole embryo through early development (Gilbert 2000), causes the cloacal cavity to be displaced caudally and dorsally and the cloacal membrane to rotate in a likewise fashion (Sasaki et al. 2004a; Pennington & Hutson 2002a); it has been postulated that this process may contribute to changes in the spatial relationship between the urorectal septum and cloacal membrane/cloacal plate over time. This leads to further apposition of the side walls of the cloacal cavity by 33-37 days, forming the cloacal plate that extends along the entire genital tubercle. Regression of the dorsal cloacal plate to complete cloacal septation

marks the next stage in cloacal development – formation of the urethra. At this stage the cloacal plate is called the urethral plate (Hynes & Fraher 2004b, Pennington & Hutson 2002b). The genital tubercle and urethral plate extend distally, and at 49 days the genital tubercle is composed entirely of mesenchyme except for the urethral plate, a thick wedge of epithelium at the ventral surface that is contiguous with the ectoderm at the cloacal groove that surrounds the entire tubercle (Nievelstein et al. 1998; Pennington & Hutson 2002b). Studies of transverse sections of the genital tubercle in mice have shown that the distal urethral plate has no lumen, since the two walls are tightly apposed, while the proximal urethral plate is patent; indeed, between E11-E12 (28-49 days, human gestation; Nievelstein et al. 1998), the distal urethral plate becomes canalized in a proximal-distal sequence (Hynes & Fraher 2004b, Pennington & Hutson 2002b). Over the same period, the mesenchyme surrounding the urethral plate expands; in particular, the wedges of mesenchyme either side of the cloacal (now the urethral) groove, that originated as the labioscrotal swellings, indent the proximal, but less so the distal, urethral plate (Hynes & Fraher 2004b). As a result the proximal urethral plate (that is patent) at the urethral groove is composed of only 1-4 squamous cell diameters. Indeed, the accumulation of mesenchymal cells 'between' the urethral plate and the ventral surface ectoderm of the genital tubercle has been suggested to be important for normal development of the urethra (Qi et al. 2000; Pennington & Hutson 2002b). Shortly before birth (rat E19), the male urethral plate is finally canalized to the tip of the tubercle. Apoptosis has been observed in the urethral plate during this process, although ectodermal ingrowths at the tip of the tubercle have not, suggesting that the urethra is of entirely endodermal origin (Pennington & Hutson 2002b). In contrast, the female urethral plate undergoes "massive

apoptosis" (Pennington & Hutson 2002b) before birth causing the genital tubercle to collapse down onto the perineum, explaining the differences in genitalia between the two sexes.

At day 44, after rupture of the cloacal membrane/cloacal plate, the anorectal canal is closed off due to contact, perhaps even fusion, of the epithelial walls (Nievelstein et al. 1998). In support of a possible fusion event, a little later, at 50 days gestation, apoptotic cells can be observed in the anal epithelium, and at day 54 a plug has been observed (Nievelstein et al. 1998). By 60 days gestation, the anus has re-canalised to become patent once again. Obliteration followed by re-canalisation has been reported in other human lumens, including that of the ureter (Alcaraz et al. 1991), and the fact that it occurs in the anus might be relevant for an aetiological understanding of anorectal malformations, such as anal stenosis. These descriptions highlight the intricate relationship between the development of the lower digestive and urinary tracts during the first 6-7 weeks gestation, and suggest that anorectal malformations form part of the same spectrum of disorders as the more severe cloacal malformations; indeed, support for this possibility comes from studies of cloacal malformations in transgenic mice (see below).

The above anatomic studies describe how the epithelial architecture of the lower urinary tract is moulded. Another important consideration is how the musculature of the perineum is determined. One recent study has delineated this in great depth using a combination of chick fate mapping and mouse genetic analyses. By implanting quail cells, and injecting replication-deficient *lacZ*-retrovirus, into chick somites, Valasek et al.

(2005) were able to show that somites 30-34 were the source of myogenic cells of the cloacal sphincter complex, and that a precise precursor domain existed with no contribution from the adjacent somites; the same studies also showed that leg muscle was derived from an overlapping source of somites, 26-33. *In situ* hybridisation studies for the marker pax-3 identified the migrating somite-derived muscle precursors and showed that they migrated individually rather than as a sheet (known as myotomal extension), since they lacked myoD expression; moreover, these precursors migrated into the limb, but, surprisingly, no stream of cells could be detected that migrated toward the cloaca. Quail cell implantation studies, retroviral injection and *in situ* hybridisation showed that at a later stage of development, between the time when the ventral and dorsal muscle masses of the chick hindlimb are undergoing cleavage into distinct muscle groups (Schroeter & Tosney 1991) until the stage at which the cloacal anlage reaches the genital tubercle, migration of cells from the proximo-ventral muscle group of the hindlimb constitutes the cloacal musculature, and that these cells express myoD indicating that they move by myotomal extension.

Finally, these authors were also able to show that the same mechanism was also involved in forming the muscles of the perineum in mice. Expression of myoD identified a similar wave of cells migrating ventrally from the hindlimb to the cloaca in mice between E11 and E15.5 (approximately equivalent to 58 days human development). Furthermore, mice null-mutant for *met*, a gene absolutely required for all myogenic precursor migration, have an absence of all perineal muscles. Unilateral surgical ablation of a hindlimb bud in chicks at a stage before myogenic precursors had reached the limb resulted in ipsilateral

loss of cloacal muscles, and a complete absence of cloacal muscles was also observed in an equivalent non-surgical model, the *legless* mutant chick that lacks limbs owing to defects of the apical ectodermal ridge. Interestingly, in both the surgically modified chicks, as well as the genetic mouse and chick models that lacked cloacal/perineal musculature, no overt cloacal or bladder malformations were observed, showing that the processes that establish the cloacal musculature are independent of the processes that sculpt the lower urinary tract.

### 1-2-3 The urinary bladder and ureter

As the initial steps of metanephric development occur, the lower renal tract is beginning to form. By 28 days of gestation, the mesonephric duct drains into the UGS which is forming as the cloaca is divided into the sinus and rectum by the caudal extension of the urorectal septum. The epithelia of the sinus and mesonephric duct fuse, and the ureteric bud arises as described above. By 33 days of gestation, the mesonephric duct below the ureteric bud fuses with the UGS and will contribute to the trigone. As part of these morphogenetic steps, the ureteric bud origin 'enters' the bladder directly by day 37 to become the ureteric orifice. Between 28 and 35 days of gestation, the ureter appears to be patent but, from 37 to 47 days gestation, a membrane temporarily blocks the vesicoureteric junction (Alcaraz et al. 1991) and the ureter becomes occluded. This is followed by 'recanalisation' of the elongating ureter which is complete by 8 weeks (Ruano-Gil et al. 1975). By the end of the first trimester, the epithelium of the ureter differentiates into the pseudo-stratified urothelium, and the ureter has a submucosal course upon entering the bladder. Myogenesis begins in the upper part of the ureter at 12

weeks (Matsuno et al. 1984). The first layer of vascularized glomeruli is present by 8-9 weeks and would be expected to filter blood to produce urine which would enter the lower renal tract. The urogenital membrane ruptures on day 48 of gestation, thus providing a connection between the nascent bladder and the outside of the body. At ten weeks gestation, the urinary bladder appears as a cylinder of epithelium surrounded by mesenchymal tissue; the latter will form the smooth muscle layers of the detrusor from 13-20 weeks gestation. The allantois, a second outflow tract on the anterior of the developing bladder, appears at 21 days of gestation; it regresses by the end of the first trimester at 12 weeks of gestation, and its remnant is marked by the median umbilical ligament.

## 1-3 HUMAN RENAL TRACT MALFORMATIONS

A selection of genes expressed in the developing renal tract that, when mutated, cause human kidney malformations are listed in Table 1.

### 1-3-1 Foetal impairment of urine flow

Renal malformations often coexist with blocked ureters or urethras; such disorders occur in one fifth of children with end-stage renal failure (Lewis & Shaw 2002). Data from sheep show that foetal bladder outflow obstruction mimicking posterior urethral valves (PUV) perturbs kidney and bladder morphogenesis (Glick et al. 1984; Edouga et al. 2001; Nyirady et al. 2002; Thiruchelvam et al. 2003). When obstruction is initiated early, renal histology often resembles Potter type IV dysplasia, with a nephrogenic zone replaced by

***Table 1. Selected genes expressed in the developing renal tract which, when mutated cause human and mouse kidney malformations.***

| |
|---|
| *Branchio-oto-renal syndrome*<br>Human disease: Dominant *EYA1* mutation with renal agenesis, dysplasia and calyceal anomalies. Also features branchial fistulae and deafness[1].<br>Mouse mutant model: [2,3] |
| *Fraser syndrome*<br>Human disease: Recessive *FRAS1* and *FREM2* mutations[4,5]. Renal agenesis and cystic dysplasia. Also features fused digits and cryptophthalmos.<br>Mouse mutant model: [6,7] |
| *Renal-coloboma syndrome*<br>Human disease: Dominant *PAX2* mutation with VUR and renal hypoplasia. Also features optic nerve colobomas[6].<br>Mouse mutant models: [7,8] |
| *Renal cysts and diabetes syndrome*<br>Human disease: Dominant *HNF1β* mutation with solitary functioning kidney, cystic dysplasia glomerular cysts; also features diabetes mellitus and uterus malformations[9,10].<br>Mouse mutant model: [11] |
| *Townes-Brocks syndrome*<br>Human disease: Dominant *SALL1* mutation with spectrum of renal tract malformations including renal agenesis and hypoplasia, horseshoe kidney and posterior urethral valves. Also features imperforate anus and digit malformations[12].<br>Mouse mutant model: [13] |

[1] Abdelhak et al. (1997)
[2] Xu et al. (1999)
[3] Xi et al. (2003)
[4] McGregor et al. (2003)
[5] Jadeja et al. (2005)
[6] Sanyanusin et al. (1995)
[7] Torres et al. (1995)
[8] Keller et al. (1994)
[9] Kolatsi-Joannou et al. (2001)
[10] Bingham et al. (2002)
[11] Gresh et al. (2004)
[12] Salerno et al. (2000)
[13] Nishinakamra et al. (2001)

cysts; fibrosis and hypoplasia (too few nephrons) typically follow obstruction initiated later in gestation. Somewhat similar phenotypes result from complete ureteric obstruction before nephrogenesis is complete in sheep (Attar et al. 1998; Yang et al. 2001), marsupials (Steinhardt et al. 1995) and rats (Chevalier et al. 2000). The foetal sheep experiments generate several other effects known to occur in human congenital obstructive nephropathy including failure to dilute fetal urine, and reabsorb sodium from it (failed loop of Henle and collecting duct functions, respectively), apoptotic ablation of renal precursors, generation of cysts expressing PAX-2 transcription factor, pathological epithelial-to-mesenchymal/smooth muscle transformation and increased transforming growth factor β1 (TGFβ1) (Winyard et al. 1996a; Attar et al. 1998; Yang et al. 2001; Winyard et al. 1996b). TGFβ1 induces transdifferentiation of dysplastic human epithelia *in vitro* (Yang et al. 2000) and inhibits branching morphogenesis in several organs (Hardman et al. 1994). At present, the primary causes of anatomical obstruction of the human fetal renal tract remain obscure, although preliminary evidence has been presented by Weber et al. (2005) that PUV may have a genetic basis. Prune Belly syndrome (PBS) presents as a triad of undescended testes and 'pruning' of the abdomen, secondary to a large bladder with hypoplastic musculature. Although no anatomic obstruction is attributed to the disease, one school of thought is that 'kinking' of the urethra might obstruct urine flow.

### 1-3-2 Renal adysplasia

Technical advances in dialysis and transplantation mean that a new cohort of young children with end-stage renal failure (ESRF) is surviving (Rees 2002). Around 1000 UK

children have ESRF and, in approximately half of these individuals, the cause is a congenital abnormality of both kidneys (Lewis 2003), usually renal dysplasia, in which kidneys begin to form but contain undifferentiated and metaplastic tissues, sometimes with cysts (Woolf et al. 2004). Some such organs spontaneously involute to give an aplastic phenotype (Belk et al. 2002; Hiraoka et al. 2002), and therefore a spectrum of anomalies is recognised, called renal 'adysplasia' (McPherson et al. 1987; Squiers et al. 1987). Severe bilateral renal adysplasia occurs in about 1/10,000 births (Woolf et al. 2004). Some boys with renal adysplasia have PUV and this lesion causes the renal malformation by impairment of foetal urine flow (Nyirady et al. 2002). In the other renal adysplasia patients, there is no overt urinary tract obstruction, although these individuals may also have non-obstructive lesions such as vesicoureteric reflux (VUR), the retrograde passage of urine from the bladder, and some females have persistent cloaca (Warne et al. 2002a), where bladder, gut and genital tract open into a common distal passage. In some cases of renal adysplasia, there coexist anomalies of the female genital tract, and this has been called 'urogenital adysplasia' (OMIM 191830). Other renal dysplasia variants are 'multicystic renal dysplasia' (OMIM 143400; Groenen et al. 1998) and 'diffuse cystic renal dysplasia' (OMIM 601331; Sase et al. 1996). Multicystic dysplastic kidneys (MCDK) are classically thought to be caused by atresia of the ureter, and these organs usually involute to give an aplastic phenotype in the adult (Woolf et al. 2004). In her classic studies of normal and abnormal kidney development, Edith Potter emphasized that, although there is some variation in terms of extent of disease within a kidney and presence or absence of cysts, there are common histological features in all

dysplastic kidneys e.g. dysplastic tubules surrounded by poorly differentiated/metaplastic stroma (Woolf et al. 2004; Potter 1972).

On occasion, renal adysplasia exists as one part of a multiorgan syndrome (Woolf et al. 2004) caused by mutations of genes expressed during kidney development, including branchio-oto-renal (*EYA1* and *SIX1* mutations; Abdelhak et al. 1997; Ruf et al. 2004), Fraser (*FRAS1*; McGregor et al. 2003), hypoparathyroidism-deafness-renal (*GATA3*; van Esch et al. 2000), and renal-cysts-diabetes (*HNF1β*; Bingham et al. 2002) syndromes. However, in clinical practice, most children with renal adysplasia and renal failure do not have an overt syndrome affecting organs beyond the genitourinary tract. Radiographic screening of first-degree relatives shows that, in most individuals, bilateral renal adysplasia is 'sporadic' (Roodhooft et al. 1984). Perhaps multiple genes interact to generate the anomaly: indeed, Nishimura et al. (1999) found an association with a common polymorphism of the *angiotensin II receptor type 2* (*AT2*) gene with diverse urinary tract malformations; however, this could not be replicated (Hiraoka et al. 2001). In rare families with more than one affected individual, renal adysplasia might have a dominant inheritance with reduced penetrance and variable expressivity (McPherson et al. 1987; Squiers et al. 1987; Battin et al. 1993). Another possibility to explain the sporadic occurrence of bilateral renal adysplasia is that such individuals have *de novo* dominant mutations of genes expressed in renal tract differentiation; because such individuals would often have severe renal failure, they would not generally have lived to reproduce in the era before the advent of modern dialysis and transplantation.

### 1-3-3 Cloacal malformation

A 'cloaca' is a single conduit which links the urinary, genital, and alimentary tracts with the exterior of an organism. In the adult duck-billed platypus and echidna, both monotremes, a cloaca is the norm (Grutzner & Graves 2004), whereas in all other adult mammals, each of these tracts exits the body through a separate opening. The UGS and the rectum form by partition of the cloaca, as reviewed above. In the female genital tract, the lower part of the vagina forms from the dorsal wall of the UGS, while the upper vagina, cervix, uterus and fallopian tubes form from the paramesonephric ducts (Simpson 1999; Shapiro et al. 2000). About 1:50,000 human births have a 'persistent cloaca' (Forrester & Merz 2004), a failure of cloacal septation that, owing to the vaginal/uterine involvement, is defined as being a female sex-limited malformation. Persistent cloaca is a potentially devastating disease, generally requiring multiple rounds of corrective surgery and, even with the best current treatments, significant urological and gynaecological sequelae can occur, including incontinence and infertility (Warne et al. 2002a, 2003, 2004). Upper renal tract malformations are common associations. For example, of 64 patients with persistent cloaca, Warne et al. (2002b) reported VUR in 36, renal dysplasia in 17, ectopic kidney in nine, solitary kidney in eight, duplex kidney in six and pelviureteric junction obstruction in three: about half had chronic renal failure, and eleven had ESRF when assessed at an average age of 11 years. Malformations of other organ systems can accompany persistent cloaca, with anomalies of the bony sacrum being common (Warne et al. 2002b), and a subset of patients (Rink et al. 2005) having the VACTERL association (vertebral anomalies, anal atresia, cardiovascular malformations, tracheoesophageal fistula, renal and limb anomalies) (Kim et al. 2001).

## 1-4 MOLECULAR CONTROL OF KIDNEY DEVELOPMENT

### 1-4-1 The site of formation of the ureteric bud

The precise position at which the ureteric bud arises on the mesonephric duct is under strict control from many molecules expressed in the mesonephric duct and surrounding metanephric mesenchyme. Indeed, a number of genetically engineered mice have been generated in which ureteric bud formation occurs at ectopic sites on the mesonephric duct, and these mouse models serve to identify the role that some of these molecules have to play in this process and the developmental mechanisms involved.

*Sprouty* null-mutant (*Spry*$^{-/-}$) mice have an abnormally wide ureteric bud at embryonic day 11 (E11), compared to their wild-type counterparts, and can also have supernumerary ectopic ureteric buds that remain attached to the mesonephric duct after implantation into the cloaca (Basson et al. 2005). These features manifest as the presence of blind-ending ureters (female) or ureters that attach to the vas deferens (males), and multiple fused kidney primordia, as shown by the fact that nephrogenesis is not restricted to the cortex of the kidney. The forkhead transcription factors, Foxc1 and Foxc2, are expressed in the intermediate, mesonephric and metanephric mesenchyme at E8.5, E9.5 and E10.5 (a time when the ureteric bud arises), respectively. *Foxc1*$^{-/-}$ mutant mice have anteriorly located ectopic ureteric buds, double ureters and duplex kidneys, either bilaterally or unilaterally, and with incomplete penetrance (Kume et al. 2000). Finally, *Bmp4*$^{+/-}$ mice form an ectopic ureteric bud opposite somite 25, rather than somite 26, leading to an ectopic

vesicoureteric junction (the junction between the bladder and ureter) (Ichikawa et al. 2002).

Glial cell derived neurotrophic factor (Gdnf) and its receptor tyrosine kinase, Ret, lie at the heart of these defects, playing a central role in specifying the position of ureteric bud formation on the mesonephric duct (Ichikawa et al. 2002). Gdnf and Ret are expressed widely throughout the metanephric mesenchyme and mesonephric duct, respectively, and stimulate the initial budding (as well as subsequent branching) of the ureteric bud (Schuchardt et al. 1996). Because of this wide distribution of Gdnf/Ret throughout the metanephric mesenchyme/mesonephric duct it has been suggested (Ichikawa et al. 2002) that this signalling pathway provides the potential for budding, while other molecules regulate the location of this budding. In support of this idea, *Spry*$^{+/-}$ mesonephric duct explants (that are phenotypically normal *in vivo*) could be induced to undergo ectopic branching by treatment with exogeneous Gdnf in a dose-dependent manner, while *Spry*$^{-/-}$ mesonephric ducts could be induced to bud ectopically using only very low concentrations of Gdnf (Basson et al. 2005). Indeed, Bmp4 is expressed throughout the mesonephric duct, except at the site of ureteric bud formation, and antagonises Gdnf/Ret signalling (Ichikawa et al. 2002). In the *Foxc1*$^{-/-}$ mouse model (Kume et al. 2000), Gdnf expression was expanded anteriorly, corresponding to the site of ectopia, suggesting that this transcription factor defines the normal limit of Gdnf expression. The expression domain of Gdnf is also under the control of the hox11 gene paralogues, since *hoxa11*$^{-/-}$; *hoxd11*$^{-/-}$ double mutant mice have renal hypoplasia, and *hoxa11*$^{-/-}$; *hoxc11*$^{-/-}$; *hoxd11*$^{-/-}$ mice have bilateral renal aplasia since no ureteric bud is ever formed; these triple null-

mutants never express Gdnf (Grieshammer et al. 2004). As indicated by mouse models, other early branching molecules include WT1, LIM1, PAX2, SIX1, SALL1, EYA1 and Hs2st (Shah et al. 2004).

### 1-4-2 Branching morphogenesis of the ureteric bud

Ureteric bud growth *in vitro* is dependent on the presence of the metanephric mesenchyme (Grobstein 1953; Saxen 1987; Maizels & Simpson 1983). This mesenchyme produces growth factors that bind to various receptors on the ureteric bud epithelium through which signals are transduced that instruct the behaviour of the ureteric bud epithelial cells. As well as regulating ureteric bud formation, the receptor tyrosine kinase, RET, has additional roles in the continued branching morphogenesis of renal epithelia, being expressed in the branching tips of the ureteric bud, but being down-regulated as the collecting ducts mature (Towers et al. 1998); its expression is enhanced by signals from adjacent stroma initiated by activation of retinoic acid receptors (Batourina et al. 2001). Its ligand, GDNF, is expressed in metanephric mesenchyme adjacent to the ureteric bud ampullae (Towers et al. 1998). As discussed above, null-mutation of *Gdnf* in mice prevents initial outgrowth of the ureteric bud causing renal agenesis.

HGF is expressed in a number of organs that branch during their development, and the addition of HGF to epithelial cysts in culture has been shown to induce branching that resembles the morphogenesis of collecting ducts (Montesano et al. 1991). Within the developing metanephros itself, HGF is secreted by mesenchymal cells and its receptor

tyrosine kinase, MET, is expressed by the adjacent ureteric bud. Furthermore, the addition of antisera that prevent the binding of HGF to its receptor also prevent the branching of the ureteric bud in organ culture (Woolf et al. 1995), offering some functional evidence in support of a role for HGF in renal branching morphogenesis. In contrast, other growth factors, such as BMP4 (Miyazaki et al. 2000) and TGFβ (Rogers et al. 1993), can actually inhibit branching of epithelia in the kidney, the latter of which is expressed strongly in human dysplastic kidneys. Extracellular matrix proteins are also important for the regulation of branching morphogenesis with some, such as collagen I, allowing branching and with others, such as those in the mature basement membrane, inhibiting branching (Santos & Nigam 1993). Extracellular matrix molecules such as these might instruct branching via integrin receptors on the cell surface of the ureteric bud and collecting ducts (Zent et al. 2001).

Branching morphogenesis essentially serves the purpose of setting up the basic structure of the collecting system, following which the stems of the system must differentiate to form the mature collecting ducts that will essentially contain three cell types; principal cells (that secrete potassium), α intercalated cells (that transport protons into the tubule lumen) and β intercalated cells (that secrete bicarbonate) (Evan et al, 1991). In cell culture, it appears that certain molecules, such as corticosteroids, can enhance the differentiation of collecting ducts (Slotkin et al, 1992), while galectin-3, a cell-surface molecule which is expressed by maturing collecting ducts, acts as a brake on branching morphogenesis (Winyard et al. 1997; Bullock et al. 2001) and is critical for the terminal

differentiation of intercalated cells by polymerizing the extracellular matrix protein hensin (Hikita et al, 2000).

### 1-4-3 Molecular control of survival and induction of the metanephric mesenchyme

In his classic embryological studies, Grobstein established that signals secreted from the ureteric bud are essential for the survival and differentiation of metanephric mesenchymal cells (Grobstein 1953). When he cultured newly-formed metanephric mesenchyme from mice in the absence of the ureteric bud, it failed to survive; likewise, the ureteric bud failed to branch when cultured alone. Remarkably, when both tissues were cultured together, the mesenchymal cells underwent an epithelial transition to form nephrons and the ureteric bud branched to form collecting ducts. In contrast, it was reported that no other embryonic mesenchymal cells could be induced to produce nephron epithelia by either the ureteric bud or heterologous inducers such as the spinal cord; thus the metanephric mesenchyme is specified to form nephrons, although it requires inductive signals from the ureteric bud to permit its survival and to determine its fate. Similarly, the metanephric mesenchyme instructs the ureteric bud to branch, grow and differentiate in a co-ordinated manner.

When the metanephric mesenchyme is cultured in isolation, its subsequent death is a programmed event, requiring the synthesis of mRNA and protein, and thus proceeding by apoptosis (Koseki et al. 1992). In mice, addition of TNFα to metanephric explants in culture increases apoptosis (Cale et al. 1998), showing that apoptosis is co-ordinated by molecular signals, while FGF2 can prevent excess apoptosis of metanephric mesenchyme

(Perantoni et al. 1995), although it is not sufficient, on its own, to induce differentiation of the nephron lineage; other metanephric growth factors, such as BMP7, HGF and TGFα, may act as a brake preventing excessive cellular death (Koseki et al. 1992; Woolf et al. 1995; Dudley et al. 1999). Signalling to promote the survival of the metanephric mesenchyme may be mediated by WNT proteins; one such molecule is WNT1 that is expressed in the embryonic spinal cord, a heterologous inducer, although it is not expressed by the ureteric bud itself (Herzlinger et al. 1994). Other members of the WNT family are expressed in the metanephros, and mutant mouse phenotypes suggest that they do indeed play a role in promoting the survival and differentiation of the rudimentary kidney; in particular, WNT11, expressed by ureteric bud ampullae, enhances GDNF signalling and null mutation causes mice to have small kidneys (Majumdar et al. 2003), while the renal mesenchyme in mice lacking WNT4 begins to differentiate but then fails to form tubules (Stark et al. 1994) - thus loss of each of these molecules alone is not sufficient to prevent formation of the kidney.

In contrast, homozygous null mutation of the *Wt1* gene in mice causes accelerated death in the intermediate mesoderm which would normally form the metanephric mesenchyme, and hence produces a 'renal agenesis' phenotype (Kreidberg et al. 1991). WT1 is expressed at low levels in the newly formed metanephric mesenchyme and is subsequently upregulated during differentiation into nephron precursors. The *WT1* gene generates a number of different transcripts, some of which encode transcription factors, while others encode proteins that regulate mRNA splicing (Scholz & Kirschner 2005). A reduction in WT1 expression by exposure to teratogens is associated with increased

apoptosis in the metanephric mesenchyme (Tse et al. 1995). Further studies will be necessary in the future to understand the precise role of WT1 during normal kidney development. Similar 'renal agenesis' phenotypes can be generated in mice with a homozygous null-mutation of one of several genes encoding transcription factors including *Lim1* (Shawlot & Behringer 1995; Tsang et al. 2000), *Pax2* (Torres et al. 1995), *Sall1* (Nishinakamura et al. 2001) and *Six1* (Xu et al. 2003). Each of these transcription factors is expressed in a precise temporal and spatial pattern, and while *LIM1* upregulates *PAX2* in the intermediate mesoderm, *SIX1* is expressed upstream of *PAX2* and *SALL1* (Nishinakamura et al. 2001) and downstream of *EYA1*, a phosphatase expressed in both induced and uninduced metanephric mesenchyme that activates *SIX1* – these observations show that a complex transcriptional network regulates kidney development precisely.

### 1-4-4 Nephron tubule formation from metanephric mesenchyme

Metanephric precursor cells which differentiate into nephrons are said to undergo a mesenchymal-to-epithelial transition. First the mesenchymal cells aggregate to form a condensation, and this process is stimulated by growth factors, such as FGF2, secreted by the metanephros (Perantoni et al. 1995). During normal human development these aggregated cells up-regulate their expression of WT1, BCL2 and PAX2 (Winyard et al. 1996a); indeed, a reduction in the expression of these proteins *in vitro* in metanephric organ culture (PAX2) or *in vivo* by null-mutation in mice (BCL2) can prevent nephron formation (Rothenpieler & Dressler 1993) and cause renal hypoplasia (Sorenson et al. 1995), respectively. Expression studies of these genes in cystic dysplastic kidneys taken from human foetal/postnatal autopsy samples have also suggested that there is little

expression in the poorly differentiated tissues surrounding dysplastic tubules where many cells are undergoing apoptotic cell death (Winyard et al. 1996b), perhaps explaining the tendency for such organs to involute before or shortly after birth (John et al. 1998; Kuwertz-Broeking et al. 2004). Thus as the mesenchymal precursors transition from loosely packed and non-polarized cells to form a tightly-packed monolayer with specialized luminal, basal and lateral plasma membrane domains, it appears that WT1 is necessary for the survival and induction of renal mesenchyme, and that BCL2 and PAX2 protect the nephron precursors from their default instruction of dying during the earliest stage of morphogenesis.

The progression of each of these condensates from a hollow vesicle to a comma and then S-shaped body, is associated with down-regulation of mesenchymal cell-cell adhesion molecules, such as NCAM (Klein et al. 1998), and their replacement with the expression of molecules that characteristically mediate the contact of neighbouring epithelial cells in the primitive nephrons, such as E-cadherin (Vestweber et al. 1985). This acquisition of such adhesion molecules characteristic of epithelia further reinforces the transition to an epithelial phenotype; for example, $Na^+$-$K^+$-ATPase is redistributed to sites of cell-cell contact, as is found in epithelia in fibroblasts induced to express E-cadherin (McNeill et al. 1990), while conversely, the integrity of cell-cell junctions in epithelial cells in which E-cadherin has been blocked is compromised (Gumbiner et al. 1988).

The extracellular matrix proteins surrounding a cell also change during the mesenchymal-to-epithelial transition with, for example, renal mesenchymal cells being surrounded by

fibronectin and collagen I, but with these molecules being lost during the transition and with their replacement in primitive tubular epithelia by collagen IV, laminin, heparan sulphate and nidogen in the basement membrane. Indeed, interaction of laminin-1 with integrin α6, a cell-surface receptor, is essential for the formation of a lumen during early nephrogenesis (Klein et al. 1988; Sorokin et al. 1990), as shown in metanephric explants. Furthermore, the interaction of integrin α6 with the α-dystroglycan complex (Durbeej et al. 1995), present on the surface of nascent epithelial cells, and with nidogen (Ekblom et al. 1994), a matrix protein derived from mesenchymal cells, is also important in nephron tubulogenesis. Integrin α8 is also expressed in induced metanephric mesenchyme, and interaction of this receptor with its ligand nephronectin, expressed on the adjacent ureteric bud branches, is important for mesenchymal-to-epithelial transition since *integrin α8* null-mutant mice fail to undergo this transition (Muller et al. 1997; Brandenberger et al. 2001). Later in nephrogenesis, as glomerular epithelial podocytes mature, their basement membranes become depleted of laminin β1 (Noakes et al. 1995), and mice with *laminin β2* deleted suffer from an infantile nephrotic syndrome despite the appearance of grossly structurally normal glomeruli at birth. In addition, as nephron tubules form from condensates, while receptors and matrix proteins interact extracellularly, within cells the cytoskeleton becomes reorganized (Baccallao 1995; Musch 2004). For example, while microtubules form an array radiating from the centrosome in the undifferentiated metanephric mesenchyme, during the mesenchymal-to-epithelial transition a tubulin axoneme protrudes from the apical cell surface of the epithelial cells into the lumen of the tubule forming what is known as the primary cilium, a structure that is thought to

transduce differentiation signals into the epithelial cell, perhaps stimulated by urine flow (Nauli et al. 2003).

## 1-5 MOLECULAR CONTROL OF CLOACAL DEVELOPMENT

A number of murine genetic models that describe a phenotype of cloacal malformation have been described. These include mice null-mutant for the Sonic hedgehog (SHH) pathway genes, as well as for *GATA5*, *ephrinB2/ephB2* and *hoxa13/hoxd13*. It is worth describing the lower urinary tract phenotypes of these mice in detail with a view to their being candidates for genes that might cause similar malformations in humans when mutated. These mouse models of cloacal malformation are summarised in Table 2.

### 1-5-1 Sonic hedgehog pathway genes

SHH signalling is important for the development of a variety of organs in both vertebrates and invertebrates. The morphogen SHH signals by binding the two large extracellular loops of its receptor PTCH; this induces the de-repression of a second transmembrane receptor, SMO, and results in the activation of the GLI family of transcription factors (GLI2, GLI3) by inducing their conversion from transcriptional repressors to transcriptional activators. This then leads to the transcription of various genes that can induce important cellular events, including *BMP4* and the *HOX* genes.

Scanning electron microscopic analysis of the caudal end of *shh* null-mutant mice ($shh^{-/-}$), carrying a homozygous deletion of most of the protein coding region of the gene (Chiang et al. 1996), revealed defects in the perineal area of the embryo; whereas wild-type

***Table 2. Cloacal malformations in defined genetic mouse models.***

| Genotype | Phenotype |
|---|---|
| *shh*$^{-/-}$ | *Persistent cloaca* |
| *gli2*$^{-/-}$ | Recto-urethral (M)/recto-vaginal (F) fistula |
| *gli3*$^{-/-}$ | Anal stenosis; ectopic anus (30%) |
| *gli2*$^{+/-}$;*gli3*$^{-/-}$ , *gli2*$^{-/-}$;*gli3*$^{+/-}$ , *gli2*$^{-/-}$;*gli3*$^{-/-}$ | *Persistent cloaca* |
| *GATA5*$^{-/-}$ | Abnormal vaginal orifice/perineum; fistulas; splayed urethra |
| *hoxa13*$^{+/-}$;*hoxd13*$^{-/-}$ | Abnormal genitalia (F); recto-vaginal (F)/recto-urethral (M) fistula; reduced anogenital distance |
| *hoxa13*$^{-/-}$;*hoxd13*$^{-/-}$ | *Persistent cloaca* |
| *ephrinB2*$^{lacZ/+}$ | Hypospadias/unfused perineum (M) |
| *ephrinB2*$^{lacZ/lacZ}$ | Anal atresia; hypospadias/recto-urethral fistula (M); *persistent cloaca*/splayed clitoris (F) |
| *ephB2*$^{-/-}$;*ephB3*$^{-/-}$ , *ephB2*$^{ki/ki}$;*ephB3*$^{-/-}$ | Hypospadias (M)/reduced perineum (F) (25%) |

M, male phenotype; F, female phenotype. Data is taken from the following references: *Shh* and *gli2/gli3*, Mo et al. (2001); *eph/ephrin*, Dravis et al. (2004); *hoxa13/hoxd13*, Warot et al. (1997); *GATA5*, Molkentin et al. (2000). The phenotype of persistent cloaca is italicised.

embryos had distinct genital tubercle and rectal openings to the amnion at E18.5, *shh*$^{-/-}$ animals at the same stage of development had a single perineal opening (Mo et al. 2001). At E14.5, mid-sagittal tissue sections showed that the bladder and hindgut of *shh*$^{-/-}$ mice shared a single common opening, representing a persistent cloaca, and the bladder of such animals was hypoplastic and their ureters shortened.

In the same study, Mo et al. (2001) also analysed mice with null-mutations in both *gli2* and *gli3*; the *gli2* mutation was generated by targeted deletion of the DNA-binding zinc-finger motifs of the gene (Ming et al. 1998), whereas the *gli3* mutation arose spontaneously and represented a large deletion of the 3' region of the gene (Goodrich 1998), a region that carries the transcriptional activator domain that is cleaved following the receipt of a shh signal. All *gli2*$^{-/-}$ mutant mice had recto-urethral (males) or recto-vaginal (females) fistula that could be seen on histological sections as well as by radiographic dye injection. The *gli3*$^{-/-}$ mutants had anal stenosis, and a third of these mice also presented with an ectopic anus, located more ventrally at the junction between the lower abdomen and tail. Since both *gli2* and *gli3* mutants exhibited abnormal development of the caudal region, the authors investigated possible functional redundancy between the two genes by breeding compound mutants. While compound heterozygous mice (*gli2*$^{+/-}$; *gli3*$^{+/-}$) developed normally, animals with three or more mutant alleles in the two genes (*gli2*$^{+/-}$; *gli3*$^{-/-}$ or *gli2*$^{-/-}$; *gli3*$^{+/-}$ or *gli2*$^{-/-}$; *gli3*$^{-/-}$) had persistent cloaca with rectum, vagina and bladder opening into a common channel, and their single peritoneal opening was covered by a bulging cloacal membrane. These compound mutant mice phenotypes demonstrate functional redundancy between *gli2* and

*gli3* as well as a gene dosage effect, with the number of null-alleles determining the severity of the phenotype, and with a threshold of three being necessary to generate the most severe phenotype, persistent cloaca. The authors commented that the persistent cloaca phenotype of these compound *gli2*; *gli3* mutants was not as severe as in *shh* null-mutants.

These results indicate that sonic hedgehog signalling is necessary for the cellular events that result in septation of the cloaca into separate urinary, reproductive and digestive tracts. More generally, they also demonstrate that anorectal malformations (ARM), such as anal stenosis, ectopic anus, recto-urethral fistula, and persistent cloaca are part of the same spectrum of malformations in genetic terms, with anal stenosis representing the most mild and persistent cloaca the most severe manifestations of abnormal cloacal development, both in terms of clinical severity (for humans) and the number of *gli* mutations required to generate the phenotype.

### 1-5-2 GATA5

The GATA family of transcription factors play important roles in specifying cell fate, cellular differentiation and morphogenesis, sharing two zinc finger domains that mediate binding to DNA. GATA5 is expressed in the urogenital ridge, epithelial cells of the UGS, in the bladder and in the gut epithelium (Molkentin et al. 2000). By generating *GATA5* null-mutant mice with a targeted replacement of exon 1 with a neomycin cassette (similar mutation of *GATA4* or *GATA6* generates a null-phenotype, while disruption of the N-terminus of *GATA* genes had no effect), Molkentin et al. (2000) demonstrated that

homozygous null-mutant female mice displayed fully penetrant defects of their external genitalia and were also sub-fertile, since only 1/20 such females became pregnant. In contrast, heterozygotes for the null-allele were normal, as were homozygous null-mutant males. The *GATA5*$^{-/-}$ females had a reduced anogenital distance and an enlarged clitoris. Their vaginal orifice was abnormal in shape, with the vaginal epithelium extending laterally over the perineum, resulting in inflammation of the mucosa in some individuals. The authors commented that fistulas were commonly observed in these animals and, although it is not clear from their report, these were presumably recto-vaginal fistulas. Histological analyses showed that the *GATA5*$^{-/-}$ females lacked a distinct urethral tube, but instead had a "trough" along the surface of the vaginal wall; although it was not stated explicitly, this is reminiscent of hypospadias, perhaps representing a splayed clitoris. The pelvi-urethral glands and erectile tissue were normal, although the mice lacked a bone comparable to the os penis, and the sebaceous gland was hypoplastic. All the main internal visceral organs were examined and appeared normal.

### 1-5-3 Hox genes

Hox13 cluster genes are the 5' most of the Hox gene cluster that encode transcription factors. Expression of these genes is restricted to distal limbs and the most posterior regions of the embryo. Hoxa13 and hoxd13 transcripts have been found in the mesenchyme of the mouse genital tubercle at E12.5, and in the mesenchyme and epithelium of the UGS; later, at E14.5, transcripts of these genes can be found in the genital tubercle, around the caudal Wolffian and Mullerian ducts and in the wall of the urinary bladder (Warot et al. 1997). Homozygous null-mutation of *hoxa13* in mice gave

rise to a phenotype of abnormally located ureter extremities due to a failure of the ureter/mesonephric duct junction to reach the bladder at the normal stage of development, absence of the caudal paramesonephric ducts and hypoplasia of the UGS, particularly in the cranial portion that gives rise to the urinary bladder (Warot et al. 1997). In the same study, generation of *hoxa13*$^{+/-}$; *hoxd13*$^{-/-}$ compound mutant mice generated a phenotype of seminal vesicle and corpus cavernosum hypoplasia, coagulating gland and bulbourethral/preputial gland aplasia, and hydronephrosis in the males, while some of the females had abnormal external genitalia with a reduced anogenital distance owing to urethral-vaginal/recto-vaginal fistula, as well as agenesis of the uterine horn, cervix and cranial vagina. *hoxa13*$^{-/-}$; *hoxd13*$^{+/-}$ mice had a rudimentary UGS and the paramesonephric ducts and ureters had an abnormally rostral location. Strikingly, when *hoxa13*$^{-/-}$; *hoxd13*$^{-/-}$ compound homozygous null-mutant mice were bred, they exhibited a persistent cloaca: they lacked a separate hindgut and UGS, but instead the mesonephric ducts entered a single cavity attached directly to the mid-gut rostrally. These observations show that the *hoxa* and *hoxd* genes function redundantly to pattern the caudal end of the mouse embryo and demonstrate that four null-alleles of these two genes are required to generate a persistent cloaca. They also suggest that a fistula, either between the rectum/vagina or vagina/urethra (*hoxa13*$^{+/-}$; *hoxd13*$^{-/-}$) may represent a less severe defect in the same genetic spectrum as persistent cloaca (*hoxa13*$^{-/-}$; *hoxd13*$^{-/-}$) in females.

### 1-5-4 Eph/ephrin signalling

The eph family of receptor tyrosine kinases and their ephrin ligands are involved in a variety of developmental processes. A key feature of the ephs and ephrins is their ability

to transduce bidirectional signals into both the eph- and ephrin-expressing cell. Dravis et al. (2004) generated mice that were mutant for *ephrin-B2*. They targeted the C-terminus of the protein, after the transmembrane domain, disrupting the cytoplasmic region that undergoes phosphorylation upon binding to an eph receptor to mediate reverse signalling. Through homologous recombination they were able to generate mice that had lacZ in place of the C-terminal cytoplasmic domain (the ephrin-B2$^{lacZ}$ allele), and by cre-mediated recombination they could then ablate the lacZ portion to generate a truncated protein with no cytoplasmic domain (ephrin-B2$^{T}$). These alleles differed according to the genetic mechanism by which they operated: treatment of COS-7 cells co-transfected with ephrin-B2$^{lacZ}$ and wild-type ephrin-B2 cDNA with soluble eph-B2 protein failed to activate reverse signalling via the wild-type molecule, as evidenced by phosphorylation of the protein, whereas reverse signalling was activated following treatment of singly transfected cells with wild-type cDNA alone, showing that the ephrin-B2$^{lacZ}$ protein functions as a dominant-negative with respect to reverse signalling. In contrast, the *ephrin-B2*$^{T}$ mutation is a loss-of-function allele since the protein it encodes becomes trapped within the trans-Golgi network and does not correctly localise to the plasma membrane (Cowan et al 2004).

Mice carrying at least one copy of the dominant-negative mutation had developmental anomalies. Approximately one quarter of *ephrin-B2*$^{lacZ/+}$ males presented with hypospadias and an unfused perineum of varying severity, while 100% of *ephrin-B2*$^{lacZ/lacZ}$ males and females had anal atresia, with recto-urethral fistula in males and persistent cloaca in females. In addition, the males had hypospadias, while the females

had a splayed clitoris. Embryologically, the defect of cloacal septation was apparent at the earliest stage of this process, at E11, when wild-type mice had just initiated midline fusion of the cloaca; no such fusion event could be observed in the *ephrin-B2*$^{lacZ/lacZ}$ mice.

Mice heterozygous or homozygous for a mutation of *eph-B1*, *-B2*, *-B3*, *-A4* or *ephrin-B3* did not have hypospadias or any other anomaly similar to those observed in *ephrin-B2*$^{lacZ/lacZ}$ mice. However, when *eph-B2*$^{-/-}$; *eph-B3*$^{-/-}$ animals were generated, 25% had severe hypospadias and a reduced perineum, showing that the two eph receptors have overlapping and redundant roles in urethral development. Similarly, approximately one third of *eph-B2*$^{ki/ki}$; *eph-B3*$^{-/-}$ mice had this phenotype; *eph-B2*$^{ki}$ is an eph receptor allele that has β-gal in its cytoplasmic domain, such that forward, but not reverse, signalling is ablated. Taken together, these results indicate that both forward (*eph-B2*$^{ki/ki}$; *eph-B3*$^{-/-}$) and reverse (*ephrin-B2*$^{lacZ/-}$) eph/ephrin signalling is important for closure of the urethra and also indicate that hypospadias and perineal development is intimately related to cloacal septation.

Expression analyses in wild-type (using specific antibodies) and mutant (using X-gal staining procedures) mice showed that ephrin-B2 is expressed specifically at the apical surface of cells in the urethral/cloacal endoderm. Eph-B2 is also expressed in the endoderm, at the point where the urethral folds/cloaca are in contact, while at a more cranial level where the cloaca is septate, eph-B2 expression is refined to the anorectal epithelium. As well as the endoderm, eph-B2 expression was detected in the underlying mesenchyme immediately beneath the endodermal folds in which eph-B2 and ephrin-B2

co-localise. These expression data further support a role for eph/ephrin signalling in mediating the midline fusion events during urethral development and cloacal septation. Furthermore, these genetic data strongly suggest that a "male-version" of persistent cloaca may exist, since *ephrin-B2*$^{lacZ/lacZ}$ male mice had recto-urethral fistula, while female mice of the same genotype had persistent cloaca. Although persistent cloaca only occurs in females by definition, fistulae may represent the equivalent male clinical presentation.

### 1-5-5 Summary

In summary, these transgenic studies in mice have clearly demonstrated: (*i*) that persistent cloaca can have a genetic basis; (*ii*) that a range of anorectal malformations can be caused by abnormal cloacal development, including anal stenosis/ectopia and perineal/urethral malformation; and (*iii*) persistent cloaca is the most severe of this spectrum of malformations according to gene dosage.

# Part II. UROPLAKINS AND UROTHELIAL CELLS

Research into the Uroplakins (UPs) is a relatively new field of study, and so the purpose of Part II of the *Introduction* is to review the work that forms the basis for our understanding of these proteins.

## 1-6 UROPLAKIN BIOCHEMISTRY

### 1-6-1 Background: The "Asymmetric Unit Membrane"

The luminal surface of the mammalian urothelium is covered by plaques, 2-dimensional crystalline structures interconnected by smooth, flexible membrane domains, the so-called hinge regions (Figure 6); these plaques are also present in the membranes of cytoplasmic fusiform vesicles, the vesicles located toward the apical cell membrane (Porter & Bonneville 1963; Hicks 1965; Porter et al. 1967). Freeze fracture and electron microscopy has shown that these urothelial plaques are composed of hexagonal arrays of smaller particles, 12 nm in size, with a distance of 16 nm between the centre of each particle (Hicks & Ketterer 1969, 1970; Vergara et al. 1969; Staehelin et al 1972; Knutton & Robertson 1976; Severs & Hicks 1979). Remarkably, such studies have shown that the luminal aspect of the urothelial membrane is twice as thick (8 nm) as the cytoplasmic aspect (4 nm; Hicks 1965; Koss 1969), and so the term "asymmetric unit membrane" (AUM) was coined. This asymmetry can be accounted for, at least in part, by protein, since treatment of the AUM with trypsin results in a loss of asymmetry, with the treated luminal AUM leaflet adopting a thickness similar to that of the untreated cytoplasmic leaflet (4nm; Caruthers & Bonneville 1980). Ultra-thin sections of the AUM have also identified an array of cytoskeletal elements within urothelial cells that are approximately

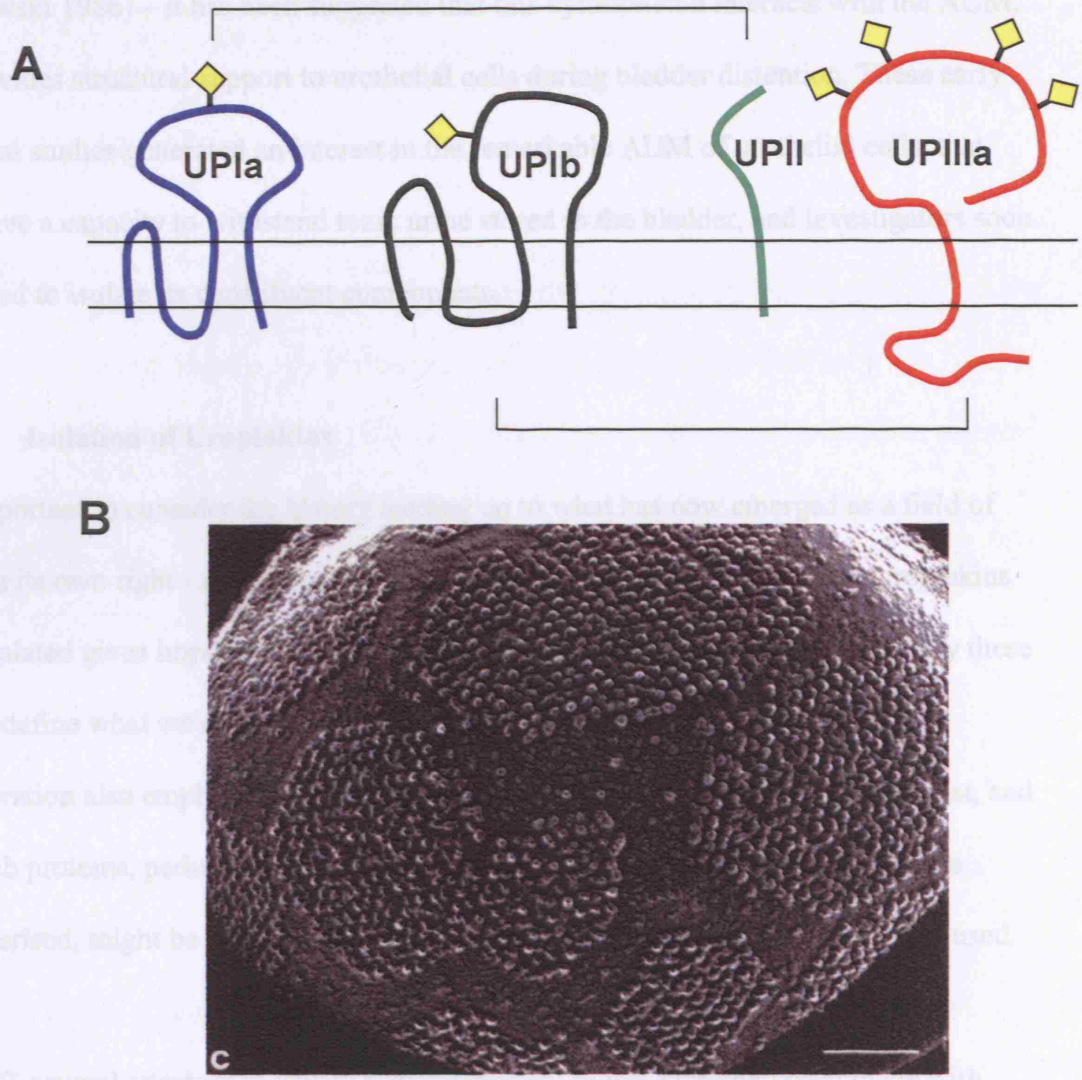


**Figure 6. The Uroplakins and the 'Asymmetric Unit Membrane'.** (**A**) Schematic of the Uroplakin proteins. UPIa and UPIb are four-pass tetraspanins and UPII and UPIIIa are single-pass Type I transmembrane proteins. Glycosylation sites are indicated by yellow diamonds. Specific UPIa/UPII and UPIb/UPIIIa heterodimeric pairings are indicated by the brackets. (**B**) Scanning electron micrograph of the 'Asymmetric Unit Membrane' viewed form the luminal aspect showing hexagonal arrays of 16nm particles, 'Urothelial Plaques', composed of Uroplakins, with intervening 'Hinge Regions'. Figure taken from Liang et al. (1999) with permission from Prof. Tung-Tien Sun (New York University Medical Center).

6-10 nm in diameter and in close proximity to the cytoplasmic aspect of the AUM (Chlapowski et al. 1972; Staehelin et al. 1972; Minsky & Chlapowski 1978; Sarikas & Chlapowski 1986) – it has been suggested that this cytoskeleton interacts with the AUM, and provides structural support to urothelial cells during bladder distention. These early structural studies generated an interest in the remarkable AUM of urothelial cells, that must have a capacity to withstand toxic urine stored in the bladder, and investigators soon attempted to isolate its constituent components.

### 1-6-2 Isolation of Uroplakins

It is important to consider the history leading up to what has now emerged as a field of study in its own right - uroplakin biology. In particular, the way in which the uroplakins were isolated gives important clues as to the nature of these proteins, and ultimately these studies define what we currently consider to be a "uroplakin". Such an historical consideration also emphasises that other, as yet undiscovered, uroplakins might exist, and that such proteins, perhaps with different physical properties to those that have been characterised, might be unveiled in the future if different extraction procedures are used.

By 1990, several attempts to isolate proteins present in the AUM had been made with little success. These attempts had resulted in a range of protein products of different sizes on SDS-PAGE, and the resulting smear of protein products were thought to be the result of protein degradation. Yu et al. (1990) succeeded by first isolating crude fractions of bovine AUM, simply by scraping the urothelial layer with a blunt scalpel, injecting them into mice and generating monoclonal antibodies. By screening for those antibodies which

specifically labelled superficial cells of the AUM, one such antibody (AE31) was deemed specific. The first major breakthrough in the identification of the uroplakins (constituents of *uro*thelial *plaq*ues) came by affinity-purifying the detergent-soluble fraction of the AUM using an AE31-column – this procedure resolved equimolar 27 and 15 kDa protein bands after SDS-PAGE, and also lower levels of a 47 kDa protein. In fact, the AE31 antigen(s) could also be extracted by discontinuous sucrose density gradient fractionation of crude AUM (Wu et al. 1990), and as further validation of successful extraction, electron microscopy of the positive fractions showed intact plaques with no contaminating organelles. Thus, the key to the isolation of these proteins was that plaques were isolated intact (Yu et al. 1990; Wu et al. 1990), whereas earlier attempts had employed harsh treatment with reducing agents at an early step in the extraction process, and the use of protease inhibitors. Evidence was also generated to suggest that these uroplakins were likely to be integral membrane proteins since they partitioned in the detergent phase after Triton X-114 (Yu et al. 1990) or deoxycholate (Wu et al. 1990) solution phase-separation, indicating that they were hydrophobic in nature. Indeed, the immunologically distinct uroplakin components were deemed likely to interact (as evidenced by the affinity purification of at least three major products using the mono-specific antibody, AE31) non-covalently, rather than by disulphide bonds for instance, since these separation procedures were shown to leave the AUM plaques intact (as assessed by electron microscopy), and the plaques could be disrupted by exposure to high temperature prior to SDS-PAGE (Wu et al. 1990).

These initial isolation procedures and analyses gave important clues as to the nature of the uroplakin proteins, identifying at least three species; 27 kDa (uroplakin "I"; UP"I"), 15 kDa (UPII) and 47 kDa (UPIII). These were deemed to be distinct species according to the following pieces of evidence (Yu et al. 1990; Wu et al. 1990): *i*) generation of distinct products on SDS-PAGE following cleavage with cyanogen bromide (CNBr) and peptide mapping; *ii*) the distinct sequences of some of the N-termini of these CNBr-generated fragments; and *iii*) the preparation of specific antibodies to each of these protein species, demonstrating that they were immunologically distinct. Ultimately the uroplakins were finally cloned and characterised using these studies as a foundation: partial peptide sequences of CNBr fragments were used to design degenerate PCR primers to amplify uroplakin cDNA, and those PCR products that were specific to bovine urothelial cDNA were then used to screen a bovine urothelial λgt10 cDNA library to identify single or overlapping clones that allowed the isolation of near full-length uroplakin cDNA sequences (Wu & Sun 1993; Lin et al. 1994; Yu et al. 1994).

### 1-6-3 Uroplakin IIIa

Wu & Sun (1993) first cloned bovine UPIIIa (originally called UPIII), the 47 kDa protein. By sequencing four overlapping clones from the λgt10 bovine urothelial cDNA library, they determined that it was encoded by a 1.7 kbp transcript consisting of 40 bp of 5' untranslated region (UTR), an 861 bp open reading frame and a substantial 3' UTR of 800 bp. Although no polyadenylation signal was identified in the 3' UTR, this was likely to represent a near full-length cDNA since the transcript identified in urothelial cells was also approximately 1.7 kbp in length.

The open reading frame of (mammalian) UPIIIa encodes 287 amino acids. Two stretches of hydrophobic amino acids were evident: the stretch at the N-terminus, consisting of 18 amino acid residues, is a signal peptide, consistent with the "-1/-3" rule (von Heijne 1986), i.e. residues -1 and -3 into the pre-sequence are alanines; a second stretch of 28 residues is long enough to span the lipid bilayer, and would split the molecule into a long extracellular domain of 189 amino acids, and a short cytoplasmic domain of 52 residues. In support of this structure, treatment of total AUM with chymotrypsin resulted in the loss of the cytoplasmic, but not extracellular, epitopes of UPIIIa (Liang et al. 2001), supporting the existence of a loosely packed cytoplasmic domain, and an extracellular domain that is tightly packed into 16 nm particles.

All polyclonal rabbit and chicken antisera that Wu & Sun (1993) raised against a number of synthetic peptides selected from the cDNA sequence recognised the 47 kDa protein species by immunoblotting. Curiously, however, the predicted molecular weight of UPIIIa according to its cDNA sequence was only 29 kDa. The discrepancy of 18 kDa could theoretically be explained if the three N-linked glycosylation consensus sites predicted from the cDNA sequence carried sugar moieties. Indeed, treatment of bovine AUM extracts with the enzyme Endo-F (endoglycosidase F - that cleaves N-linked sugars) resulted in a shift from 47 to 30 kDa, whereas treatment with Endo-H (an enzyme that cleaves high mannose sugars) or O-glycosidase (with or without neuraminidase pre-treatment) did not alter the electrophoretic mobility of the protein (Wu & Sun 1993; Sakakibara et al. 2005; Tu et al. 2002), indicating that UPIIIa is heavily glycosylated with

N-linked complex sugars. As discussed in more detail below, by transfecting UPIIIa into 293T cells with or without UPIb, Tu et al. (2002) demonstrated that while UPIIIa present in the endoplasmic reticulum (37 kDa) is Endo-H sensitive, UPIIIa present in the Golgi compartment (~40 kDa) is Endo-H resistant but Endo-F sensitive. Furthermore, UPIIIa isolated from bovine AUM is of greater molecular weight still (47 kDa, and Endo-F sensitive), demonstrating that additional post-translational modification of sugar moieties occur in urothelial cells. The urothelium is sugar coated, and this glycocalyx has been suggested to prevent binding of bacteria (Parsons et al. 1980; Pauli et al. 1983; Ruggieri et al. 1992) – these results clearly demonstrate that UPIIIa is a major constituent of the urothelial glycocalyx.

### 1-6-4 Uroplakin II

Partial sequencing of the CNBr fragments of the 15 kDa major AUM product, degenerate PCR and Northern blot identified a 1.2 kb cDNA present in urothelial, but not oesophageal, cDNA libraries, and screening of a urothelial cell λgt10 cDNA library identified four positive clones representing a 1061 bp product (Lin et al. 1994). This message encodes a single open reading frame of 185 amino acid residues encoding a 19.6 kDa protein. At the N-terminus is a prepro-sequence of 85 amino acids (the "pre-" signal peptide followed the "-1/-3" rule; von Heijne 1986), and the start of the mature protein is defined by a furin-cleavage site, RGRR. Cleavage of pro-UPII at this site has subsequently been proven by demonstrating that mutation of the RGRR consensus sequence ablates processing of the protein, that processing can be blocked by furin-inhibitors and that processing can be restored in furin-deficient cell lines by the addition

of exogeneous furin (Hu et al. 2005a). As well as the hydrophobic signal peptide, a stretch of 25 hydrophobic amino acids is present in the C-terminus of the protein, long enough to span the membrane (Lin et al. 1994). Furthermore, virtually all of the mature protein is predicted to protrude extracellularly, and a high serine/threonine content in this domain (25%) is suggestive of β-sheet formation. Analysis of the amino acid sequence of UPII also indicates the presence of three N-linked sugars in the pro-sequence, but none in the mature UPII protein, explaining why mature UPII isolated from the AUM is Endo-H resistant; as expected from this model, pro-UPII is both Endo-F and Endo-H sensitive (resulting in a shift from 27 to 18 kDa, i.e. the pro-sequence is 3 kDa), indicating that the pro-sequence does indeed harbour high-mannose glycans, and mutation of the three glycosylation sites singly and in combination indicates that all are glycosylated and carry equal amounts of sugar (mutation of all three sites in combination generates the same size product as Endo-F treatment) (Hu et al. 2005a). The fact that prepro-UPII inserts into the membrane via the signal peptide was elegantly demonstrated by the *in vitro* translation of UPII cDNA in the presence of canine microsomes coupled with trypsin/chymotryspin or glycosidase treatment, and that the N-glycosylated precursor peptide faces into the lumen of the endoplasmic reticulum was evidenced by its Endo-H resistance in the presence of microsomes (Lin et al. 1994).

Originally, the AE31 antigen was thought to be "UPI" (Yu et al. 1990; Wu et al. 1990). In fact, recently, protein sequencing of an AE31-positive protein band has shown that this antibody recognises the UPII pro-peptide (Hu et al. 2005a). Interestingly, when the uroplakins were first isolated, the 15 kDa and 27 kDa proteins were resolved in

equimolar amounts, whereas the 47 kDa protein (UPIIIa) was present at much lower levels (Yu et al. 1990; Wu et al. 1990). This makes sense in light of the observation that the 27 kDa AE31 antigen is pro-UPII (Hu et al. 2005a) and the 15 kDa protein is mature UPII (Lin et al. 1994). Extensive analysis of AE31 immunoreactivity by transfecting various recombinant UPII protein fragments into COS-1 cells demonstrated that this antibody recognises two sites in pro-UPII, one in the pro-sequence (residues -50 to -40) and another in the mature peptide (+40 to +60) (Hu et al. 2005a). In contrast, specific antibodies raised against peptides present in mature UPII only recognised the mature protein, but not the pro-protein. Since pro-UPII must also contain these antigens of the mature protein, lack of reactivity with the pro-protein must indicate that the antigens are masked and that the conformation of pro-UPII is profoundly different from that of the mature protein, possibly involving a hairpin structure involving interaction between both AE31 antigens (Hu et al. 2005a). Mature UPII is a type I transmembrane protein the precursor of which undergoes an intricate processing that substantially alters its conformation. The resulting mature protein, present in the AUM, is not glycosylated and further demonstrates the substantial contribution of UPIIIa to the glycocalyx.

### 1-6-5 Uroplakin IIIb

UPIIIb is the most recently discovered uroplakin, reported by Deng et al. (2002). Although the original papers described the extraction of only three major 47, 27 and 15 kDa AUM products (Yu et al. 1990; Wu et al. 1990), Deng et al (2002) described another minor SDS-PAGE band of molecular weight 35 kDa. This result raises the general possibility that further uroplakins may exist that have so far escaped immediate

identification with the extraction procedures currently in use (Yu et al. 1990; Wu et al. 1990) and emphasises the importance of understanding the technical context and history in which we currently understand the AUM and the "uroplakin system", especially since "uroplakin biology" is a relatively young and growing field of investigation.

The minor band of 35 kDa was CNBr digested, partially sequenced and cloned by bovine urothelial cDNA library screening. UPIIIb is present at <10% the levels of UPIIIa in purified plaques; Deng et al (2002) suggested that this low stoichiometry shows UPIIIb to be present only in a sub-set of plaques. The cDNA sequence predicts a protein that is 34% similar to UPIIIa with a very similar structure (a 200 amino acid extracellular domain, a transmembrane domain of 25 hydrophobic residues and a cytoplasmic tail of 47 residues, similar to that of UPIIIa), although the extracellular domains are more conserved than the cytoplasmic domains (36% *vs.* 18%). Of particular significance, however, is the fact that the UPIIIb residue equivalent to the tyrosine residue in the UPIIIa C-terminus that is phosphorylated upon *X. laevis* oocyte fertilisation (Sakakibara et al. 2005) is not conserved as tyrosine in UPIIIb, suggesting that at least one difference in the roles of the two proteins is that UPIIIb is not a transducer of extracellular signals into cells. Another difference is that while the extracellular domain of UPIIIa has 4 glycosylation sites, that of UPIIIb has only one such site (glycosylation being confirmed since UPIIIb singly transfected into COS-1 cells is Endo-H sensitive). Taken together, these observations emphasise the uniqueness of UPIIIa, being the only uroplakin to possess a (functional) cytoplasmic domain (Deng et al. 2002; Sakakibara et al. 2005; Hasan et al. 2005), and being the major contributor to the glycocalyx (Lin et al. 1994).

### 1-6-6 Uroplakins Ia and Ib

In Wu & Sun (1993), Figure 1a (lane 1) shows a silver nitrate stain of total bovine AUM, and a double protein band can be clearly seen in the size range of 27 kDa, the size of one of the three major AUM products originally thought to be a single protein species, "UPI" (Yu et al. 1990; Wu et al. 1990). Protein sequencing of the N-terminus of this protein band revealed a mixture of two sequences, and degenerate PCR of bovine bladder epithelium and liver cDNA identified a 270 bp probe that detected a 1.5 kbp product in bovine bladder (but not liver) mRNA (Yu et al. 1994). Sequencing of overlapping clones revealed a 1,363 bp cDNA, encoding UPIa. This cDNA encodes a 5' UTR of 18 bp, an open reading frame of 774 bp (258 amino acids) and a 3' UTR of 571 bp that included a polyadenylation signal. Similarly, UPIb was cloned, and a 1,965 bp cDNA molecule encoding a 61 bp 5' UTR, a 260 amino acid open reading frame and 1,124 bp 3' UTR, also containing a canonical polyadenylation signal indicating that a full-length 3' sequence had been cloned.

Both UPIa and UPIb have four stretches of hydrophobic amino acid residues long-enough to be transmembrane domains, and the location of these transmembrane domains was almost identical in both proteins, with the 1$^{st}$ and 4$^{th}$ being present in the N- and C-termini, respectively, the 1$^{st}$ and 2$^{nd}$ being connected by a short region of ~30 residues, and the 3$^{rd}$ and 4$^{th}$ domains being connected by long (~120 residues) hydrophilic loops. The long hydrophilic loop of both proteins contains 6 highly conserved cysteine residues and a single N-glycosylation consensus site; the presence of a sugar moiety at this residue

was confirmed since treatment of bovine AUM with Endo-H produces a reduction in the size of these two proteins (Yu et al. 1994; Tu et al. 2002) (as do UPIa/UPIb singly transfected into 293T cells that are endoplasmic reticulum confined, Tu et al. 2002) - this result is somewhat surprising since most N-linked oligosaccharides attached to plasma membrane proteins are modified in post-endoplasmic reticulum compartments such that they can not be removed by Endo-H (although they are Endo-F sensitive; Dong et al 1998), indicating that the processing of UPIa/UPIb is peculiar in this respect.

*In vitro* translation of UPIa/UPIb cDNA resulted in proteins equal in size to unglycosylated UPIa/UPIb, but these proteins increased in molecular weight to 27 kDa when microsomes were included in the reaction, indicating that glycosylation occurs in the endoplasmic reticulum; furthermore, these 27 kDa products were Endo-H sensitive, indicating that UPIa/UPIb are co-translationally inserted into pancreatic canine microsomes via their signal-peptide. Treatment of these microsome-inserted *in vitro* translation products with trypsin/chymotrypsin yielded core 26 kDa proteins, while the same treatment after detergent-permeabilisation of the microsomes resulted in extensive digestion of the proteins, indicating that the small cytoplasmic N-/C-termini had been cleaved, and showing that the glycosylated large hydrophilic loops face the lumen of the endoplasmic reticulum (Yu et al. 1994) – the highly charged short linker region between transmembrane domains 2 and 3, that must face intracellularly, were likely resistant to trypsin digestion owing to steric hinderence. UPIa and UPIb are therefore members of the tetraspanin family of proteins, defined as four-transmembrane domain proteins with one

large and one small extracellular domain (Hemler 2001), with the bulk of the proteins protruding into the lumen.

### 1-6-7 Uroplakin proteins: Summary

The cloning and characterisation of the UPs provided the molecular basis for the asymmetry of the AUM – the UPs are integral transmembrane proteins with large extracellular domains, and only UPIIIa/UPIIIb have significant, yet short, cytoplasmic domains. Furthermore, UPIIIa is unique in both its substantial contribution of sugars to the urothelial glycocalyx and in its possession of a "functional" cytoplasmic domain that is relatively free from the tight packaging that the extracellular domains of the UPs experience in forming urothelial plaques. UPII is also unique in its complex processing that involves a precursor protein with a complex conformation. The UP proteins are shown in Figure 6.

### 1-6-8 Cellular transport of uroplakin proteins

The first indication that the UP proteins might form higher-order pairings came when specific antibodies were raised against UPIa and (what were assumed to be) 54 kDa UPIa homodimers, that could be eliminated by SDS reduction, were observed in preparations of bovine, human, pig and rat AUM. Homodimer formation seemed to be specific to UPIa, of the UP tetraspanin pair, since no such bands were observed in AUM preparations probed with specific UPIb antisera (Yu et al. 1994; Wu et al. 1994). As an extension of this work, a more general analysis of UP protein-protein interactions was done by performing chemical cross-linking of crude bovine AUM preparations followed

by immunoblotting using monospecific antibodies to UPIa/Ib/II/IIIa; common bands representing protein-complexes were detected by probing (individually) with both UPIa and UPII antibodies or UPIb and UPIIIa antibodies. These common complexes suggested the possibility that specific UPIa/UPII and UPIb/UPIIIa heterodimers were formed, and this was confirmed when the complexes were stripped from their Western blot membranes and treated with hydroxylamine to relieve the cross-links – both of the individual UPs of each pair were retrieved (Wu et al. 1995).

UPIa/UPII and UPIb/UPIII(a/b) specific heterodimer formation was further confirmed by Tu et al. (2002) and, for UPIIIb, by Deng et al. (2002) by transfecting full-length bovine cDNA constructs into 293T cells, and assessing the transport of each UP. As discussed above, all five UPs are N-glycosylated, and so the authors' criteria for the cellular localisation of each protein was two-fold: *i*) conversion of N-linked oligosaccharides from an Endo-H sensitive to and Endo-H resistant form indicates that they have been processed by enzymes present in the Golgi apparatus, and so Endo-H resistance was the first criterion to determine proteins present in a post-endoplasmic reticulum compartment (however, even mature UPIa and UPIb isolated from the AUM are Endo-H sensitive and so this criterion was not informative as to the cellular localisation of these two uroplakins); *ii*) immunofluorescence was used to directly assess cellular localisation.

The single transfection of a UPII or UPIIIa construct into 293T cells demonstrated that each protein was Endo-H sensitive, and thus present in the endoplasmic reticulum. Furthermore, Endo-H treated total cell lysates of UPII single transfectants identified UPII

to be of molecular weight 18 kDa (Tu et al. 2002), that we now know corresponds to pro-UPII rather than the 15kDa protein extracted from AUM (Yu et al. 1990; Wu et al. 1990; Lin et al. 1994), showing that it had not been processed by furins present in the Golgi apparatus (Hu et al. 2005a) and further confirming its confinement to the endoplasmic reticulum. Immunofluorescence also showed that UPIa, UPII, UPIIIa and UPIIIb were confined to the endoplasmic reticulum, since expression co-localised with the endoplasmic reticulum marker ribophorin I-GFP, whereas none of the UPs (including UPIb) co-localised with the Golgi localisation marker, galactosyl transferase (Deng et al. 2002; Tu et al. 2002) – UPIb was the only singly transfected uroplakin that was able to reach the cell surface, as evidenced by staining of non-permeabilised cells (Tu et al. 2002).

It was only when co-transfected with UPIb that UPIIIa and UPIIIb were able to escape the endoplasmic reticulum and reach the cell surface, and this co-transfection also allowed UPIb to be correctly glycosylated (Deng et al. 2002; Tu et al. 2002). Similarly, UPIa and UPII were only Endo-H resistant and present at the cell surface when co-transfected together – correct transport of each UP was only observed when co-transfected with its correct partner, but not with other UPs, thus confirming the formation of specific UP heterodimers (UPIa/UPII, UPIb/UPIIIa and UPIb/UPIIIa) as predicted by nearest neighbour analysis (Wu et al. 1995). These results not only demonstrated that these heterodimers form, but also indicated that formation of these specific heterodimers is essential for the correct transport of the UPs out of the endoplasmic reticulum and onward to the cell surface, and also for the correct processing of the UPs. These results

are not just relevant to UPs transfected into 293T cells, but also to UPs expressed endogenously *in vivo* in urothelial cells. In *UPIIIa* null-mutant mice, transport of UPIa and UPII remain largely intact, with both being specifically targeted to the AUM; in contrast, UPIb is mistargeted to the baso-lateral membrane and is incompletely glycosylated (suggesting that it is transported to the cell surface via a different route), similar to singly transfected 293T cells (Hu et al. 2000). In *UPII* null-mutant mice, UPIa was localised diffusely in urothelial cell cytoplasm, while UPIb and UPIIIa were expressed at the AUM (Kong et al. 2004). These results indicate that loss of either UPIIIa or UPII specifically leads to perturbed transport of the heterodimeric partner of the disrupted gene, and does not overtly alter the transport of the UPs forming different pairings, demonstrating the specificity of these functional interactions of UPs in urothelial cells and its importance for cellular transport.

UPs are thought to be specific differentiation products of urothelial cells (Yu et al. 1990; Wu et al 1990; Wu & Sun 1993; Lin et al. 1994; Yu et al. 1994; discussed further below) and a particularly conspicuous urothelial cell compartment is the aforementioned fusiform vesicles that are present toward the AUM. In the first studies that extracted the major UP proteins and raised specific antisera to each of them, electron microscopy was used to analyse the distribution of each UP as it travelled along the secretory pathway. Unsurprisingly, the UPs were detected in fusiform vesicles, consistent with the presence of plaques in their membranes (Yu et al. 1990; Wu et al 1990; Wu & Sun 1993; Lin et al. 1994; Yu et al. 1994), but intriguingly, whether the staining pattern was observed on the

cytoplasmic or luminal leaflet of these vesicles varied according to the maturity of the vesicles (as determined by their vicinity to the AUM).

We now know that the UPs are processed as they pass along the secretory pathway by glycosylation (Yu et al. 1990; Wu et al 1990; Wu & Sun 1993; Lin et al. 1994; Yu et al. 1994; Hu et al. 2005a; Tu et al. 2002) and, in the case of pro-UPII, by furin cleavage (Hu et al. 2005a). Through the analysis of a panel of conformation-sensitive antibodies specific to each UP, Hu et al (2005a) have also shown that various antigens within each UP become masked or unmasked owing to heterodimer formation as they are transported, demonstrating that heterodimer formation induces global conformational changes in the UPs; furthermore, by forming a heterodimer with their tetraspanin partner, the single-pass UPs (UPII, UPIIIa, UPIIIb) become stabilised by virtue of escaping the proteasome that resides in the endoplasmic reticulum. These observations offer an explanation as to why the detection of cytoplasmic *versus* luminal UP antigens can be favoured at different stages of their transport, but it remains to be shown whether or not other cellular transport proteins have specific roles in the processing and distribution of the UPs in urothelial cells.

Recent work has shed some light on this possibility. The Rab family proteins are key regulators of vesicular transport, playing important roles in the targeting, docking and fusion of vesicular carriers with their acceptor compartments (Simons & Zerial 1993; Pfeffer et al. 1995; Pfeffer 1999; Pfeffer 2001). By performing degenerate PCR using primers targeted against the conserved Rab protein domains, Chen et al. (2003) identified

sequences corresponding to a number of Rab and Rab-related proteins by probing bovine urothelial cDNA, confirming that a range of cellular transport machinery is likely required for the transport of UPs to the AUM. With the exception of Rab27b, all identified proteins are expressed and function commonly in all cell types (Bao et al. 2002). Rab27b transcripts, however, were found to be specific to urothelial cells, and at the protein level, the Rab27b isoform (but not Rab27a) was specific to urothelium. Rab27b expression is differentiation-dependent, since Rab27b was found to be expressed at very much lower levels in cultured urothelial cells that lack fusiform vesicles and express low levels of UP (Surya et al. 1990), whereas it was expressed strongly in intact urothelium. Centrifugation demonstrated that Rab27b was present in the membrane fraction, where it co-localises with UPIIIa in the subplasmalemma (but not at the AUM, as shown by immunofluorescence), and electron microscopy showed that it is only present in fusiform vesicles, at the cytoplasmic aspect, but not at the AUM.

These findings clearly demonstrate that urothelium-specific proteins, as well as the UPs themselves, are likely to be essential for the correct targeting of the uroplakins to the cell surface. The "uroplakin system" (the system of molecules involved specifically in uroplakin cell biology) thus extends to transport proteins such as Rab27b. An excellent summary of UP protein modification at different stages of cellular transport is shown in Figure 7 of Hu et al. 2005a.

## 1-7 UROPLAKIN BIOLOGY: HUMAN GENETICS, DEVELOPMENT & DISEASE

### 1-7-1 The human *Uroplakin* genes

Fluorescent *in situ* hybridisation studies using human metaphase chromosome spreads (Wu et al 1998) and human genomics (Jiang et al. 2004) have assigned *UPIa*, *UPIb*, *UPII* and *UPIIIa* to chromosomes 19q13.1, 3q13.3-q21, 11q23 and 22q13.2-13.3 respectively. *UPIIIb* has been assigned to chromosome 7q11.23 (Deng et al. 2002). The genomic location of *UPIIIb* is particularly interesting; *UPIIIb* lies 0.5 Mbp centromeric to the gene *PMSR6* that encodes a mismatch repair enzyme (Horii et al. 1994; Nicolaides et al. 1995) – *UPIIIb* and *PMSR6* are >90% identical over several regions of each gene (both coding and non-coding), suggesting that one may have given rise to the other by gene duplication. Deng et al. (2002) have reasoned that the mismatch repair gene, *PMSR6*, gave rise to *UPIIIb* (and not *vice versa*), because it has a more primitive function, although this remains to be proven by phylogenetic and other analyses.

Jiang et al. (2004), Hall et al. (2005) and Olsburgh et al. (2002) determined the genomic structure of the human *UPIa*, *UPIb*, *UPII* and *UPIIIa* genes by employing a search of the human genome sequence using the four human cDNA sequences (generated by 5' RACE for UPIa and UPIb; Hall et al. 2005; Olsburgh et al. 2002) to determine the intron/exon boundaries, all of which follow the gt/ag splice donor/acceptor rule. Both *UPIa* and *UPIb* have 8 exons including a non-coding first exon, whereas *UPII* and *UPIIIa* have 5 and 6 exons, respectively (Jiang et al. 2004), and *UPIIIb* has 6 exons (Deng et al. 2002).

Jiang et al. (2004) also determined the sequence variation of the *UPIa/Ib/II/IIIa* genes by sequencing the complete coding sequence and surrounding 100-200 bp of intronic/UTR

sequence in 76 patients with primary non-syndromic VUR, and typing these single nucleotide polymorphisms (SNPs) in control DNA samples. *UPIa* has 4, *UPIIIa* 2 and *UPIb* just 1 non-synonymous SNP (Jiang et al. 2004; Hu et al. 2000), while *UPII* has none, although it did have a polymorphism changing the termination codon from TAA to TGA which might conceivably be functionally relevant owing to the fact that different termination codons can have different "strengths" depending on the sequence context surrounding them (Poole et al. 1995; Williams et al. 2004). *UPIIIa* had the greatest number of SNPs (n=9), including 5 common SNPs (minor allele frequency >25%; most synonymous) in exons, making it almost ten times more variable than the exonic regions of the average gene in the human genome, that has 5.28 SNPs per 10 kbp (Zhoa et al. 2003; the *UPIIIa* human transcript is 1050 kbp).

### 1-7-2 Uroplakins and urothelial differentiation

One of the major criteria for the successful isolation of the UPs in the original studies was that antisera raised against the extracted proteins could stain the AUM *in situ* (Yu et al. 1990; Wu et al. 1990); indeed, the first anti-UP antibody ever raised (AE31) and used to affinity purify the UPs was chosen by virtue of the fact that it stained the AUM (Yu et al. 1990). Furthermore, immunofluorescence studies using specific antisera to the UPs demonstrated the presence of each UP only in the superficial umbrella cell layer of bovine urothelium (Yu et al. 1990; Wu et al 1990; Wu & Sun 1993; Lin et al. 1994; Yu et al. 1994), and these (and subsequent) studies also reported that the UPs are urothelium-specific, leading to the current view that UPs are specific differentiation products of the urothelium. The UPs are also expressed in the superficial cells of the urothelium of a

variety of other adult organisms, including pigs, rats, mice, rabbits, humans and several other species (Wu et al. 1994), suggesting that their role might be evolutionarily conserved, and a homologue of UPIIIa is even expressed (at the protein level) in the ovaries, oocytes, urinary tract and kidney (pronephros) of the frog, *X. laevis* (Sakakibara et al. 2005). The main difference in UP expression between species is whether or not intermediate, as well as superficial, cells are UP positive; while UP expression is restricted to the superficial umbrella cells of the bovine urothelium (Yu et al. 1990; Wu et al 1990; Wu & Sun 1993; Lin et al. 1994; Yu et al. 1994) the intermediate cells of the mouse urothelium also express UPs (Lin et al. 1995; Romih et al. 2005).

In-depth histological and ultra-structural analyses of adult mouse renal tract epithelia has enabled the differentiation specificity of UP expression to be delineated since although the epithelium lining the length of the renal tract is continuous, different domains represent a group of diverse and distinct epithelial cells; for example, even the urothelium can vary depending on its location in the urinary tract, with the urothelium lining the mouse bladder trigone being twice as thick (7-8 cells) as the urothelium located elsewhere (3-4 cells) (Lin et al. 1995). Romih et al. (2005) noted that adult murine renal tract epithelia can be grouped into renal cortex, outer medulla, inner medulla and papillae, urothelium (lining the renal tract from renal pelvis to bladder neck), pelvic urethra, and penile urethra, from the proximal to distal regions of the renal tract; the female system is identical to that of the male except that the female urethra is much shorter, stretching from the bladder neck to the external ostium. The superficial cells of the urothelium, from the outer medulla to the bladder neck were positive for all UP

antibodies as well as cytokeratin 20 (CK20), a urothelial cell differentiation marker that is only expressed in superficial cells (Romih et al. 1998), with CK20 organised into an ordered network. The intermediate cells were also positive, although more weakly, and fusiform vesicles were the only positive compartment within the cells.

The papilla epithelium is simple, consisting of one layer of cells with microvilli, and does not express any of the UPs, or CK20 (Romih et al. 2005). The inner to outer bands of the outer medulla represent a transition from a simple epithelium to a differentiated urothelial epithelium. There is a gradual transition from a simple single-celled epithelium to a pseudostratified epithelium, in which the upper of two layers of cells are still attached to the basal lamina via narrow stalks, and these cells still have microvilli, but no fusiform vesicles and no AUM, characteristic of immature epithelial cells; no UPs or CK20 was expressed in either of these epithelia. In the outer medulla, the superficial cells have no contact with the basal lamina, have fusiform vesicles and are UP positive, with intermediate cells expressing UPs more weakly than the superficial umbrella cells that are also CK20 positive and have a scalloped AUM. The other region involving epithelial transition is at the neck of the bladder, where the urothelium ends. In contrast to the UP and CK20 positive superficial umbrella cells of the urothelium, there is a sharp transition to an epithelium with columnar superficial cells that are UP and CK20 negative, and that also have microvilli characteristic of a more immature state. The correlation of UP expression with CK20 expression and an absence of microvilli shows that the UPs are differentiation products of renal tract epithelia. Urothelial differentiation occurs at the

earliest stages of human development, since the human bladder primordium (UGS) is UP positive from 9-10 weeks gestation (Jiang et al. 2004; Shapiro et al. 2000).

This association of UP expression with epithelial differentiation is further supported by its loss following experimentally-induced or clinically-related urothelial damage. Romih et al. (1998) induced damage of the urothelium by feeding rats with sodium saccharin that is thought to be cytotoxic by inducing the formation of microcrystals; the damaged urothelium had sites of exfoliation, the size of which increased according to the duration of treatment. The urothelium underwent simple regenerative hyperplasia at the sites of damage, characterised by areas with 5-8 layers of cells. The exfoliated sites specifically lost the superficial umbrella cell-specific differentiation marker, CK20, although they maintained the expression of CK17 that specifically labels the intermediate and basal cell layers. UP expression was specifically down-regulated in the focal regions of regeneration, suggesting that expression of these proteins is specifically limited to terminally differentiated urothelial cells. In a study of fifteen men between 58-80 years old with bladder outflow obstruction secondary to benign prostatic hyperplasia, Romih et al. (2002) described a mildly dysplastic urothelial phenotype with a significantly different state of urothelial differentiation – although an AUM and UP positive cells were indeed found in all patients, a mixture of undifferentiated and normal cells were found in the majority of patients with only 10-90% of the superficial urothelial cells staining positive for uroplakins. Collectively, these results suggest that disruption of the terminal differentiation programme of the urothelium is accompanied by a loss of UP expression.

The urothelial-specificity of UP expression was largely upheld in a hybridisation-based screen of *UPIa*, *UPIb*, *UPII* and *UPIIIa* expression in 43 adult human tissues; all four were expressed in the bladder, although UPIb and UPII transcripts were additionally identified in the trachea, UPIb and UPIIIa transcripts in the prostate, and UPIb transcripts in the placenta, pancreas and kidney - the presence of transcripts was confirmed by *in situ* hybridisation and immunohistochemistry (Olsburgh et al. 2003). UPIb message was actually first extracted from a mink lung epithelial cell line as TI-1, a gene encoding a protein 93% identical in amino acid sequence to bovine UPIb (Kallin et al. 1992; discussed in Yu et al. 1994), and UPIb transcripts and protein have subsequently been identified in the wing cells of the corneal epithelium and, consistent with an absence of UPIIIa or UPIIIb, it was not present at the apical cell surface of superficial cells (Adachi et al. 2000). As for many genes, the expression of the UPs in a tissue and differentiation specific pattern is under the control of their promoters, which have been cloned by urothelial cDNA library screening, 5'RACE, database search and ribonuclease protection assay, together with studies that investigated their ability to drive reporter gene expression (Hall et al. 2005; Lin et al. 1995; Olsburgh et al. 2002).

Transfection of luciferase reporter constructs into cells showed that the UPIa promoter only drives expression in the urothelial cell line VMCUB-1, but not in the non-urothelial cell line HepG2 (Hall et al. 2005). Furthermore, Hall et al. (2005) were able to show that specific regions of the UPIa promoter are responsible for regulating urothelial cell-specific expression – maximal expression levels were achieved by using a construct that included the first 2147 bp of DNA sequence 5' upstream of the translational start site,

with progressively lower luciferase activity as the length of 5' sequence included was reduced. The UPIb promoter lacks a TATA box but contains a number of predicted transcription factor binding sites, consistent with the identification of multiple ribonuclease protected fragments of variable size (Olsburgh et al. 2002). Olsburgh et al. (2002) showed that the greatest reporter gene expression was achieved by using a construct that included only 235 bp of 5' upstream sequence, but negligible induction of transcription with constructs that included more than 388 bp, or less than 154 bp of 5' upstream sequence; they interpreted these results as showing that there exists a transcriptional repressor in the region -388 to -235 bp and a transcriptional activator in the region -235 to -154 bp. Finally, by generating a transgenic mouse in which lacZ is under the control of 3.6 kb of sequence 5' to the UPII translation start site, Lin et al. (1995) were able to show that the UPII promoter specifically drives expression in the urothelium, as evidenced by β-gal expression in the suprabasal cell layer. Collectively these data demonstrate that the expression of the UP genes is specific to terminally differentiated urothelial cells, and that this specificity is under strict genetic control.

### 1-7-3 *Uroplakin* genes and renal tract malformations

Hu et al. (2000) generated *UPIIIa* null-mutant mice by using a targeting vector to delete the first three exons of the gene and to create a frameshift mutation in its remaining exons. As discussed above, they observed that the transport and glycosylation of UPIb was abnormal. Two litters of homozygous *UPIIIa*$^{-/-}$ mice were small and perished within 2 weeks following birth, but four other litters survived and were relatively normal (Hu et al. 2000). However, their bladders were larger than normal and could be stretched more

easily, suggestive of elevated compliance, and the water permeability of the mutant bladders was increased, although the expression of water channels was not altered; trans-epithelial resistance, thought to be a property conferred by tight junctions rather than the AUM, remained normal (Hu et al. 2002). These animals showed abnormal urothelia: light microscopy and scanning electron microscopy showed that urothelia of mutant animals were thickened and the superficial cells had changed from a squamous to cuboidal phenotype. Quick-freeze deep-etch methodology demonstrated that the apical cells of the mutant urothelium were only one tenth the normal size (according to diameter; normally ~150 μm) and some were detached. The fusiform vesicles of *UPIIIa* null-mutant urothelial cells were replaced by the immature discoidal vesicles, the plaques were small (~1/30 normal size with respect to the number of 16 nm particles) and the hinge-regions were larger, all indicative of abnormal UP transport, consistent with the mis-targeting of UPIb to the basolateral membrane of the cells. The *UPIIIa*$^{-/-}$ AUM was unusually smooth and the diameter of the vesicoureteric junction, the point at which the ureter enters the bladder, was increased 3-fold. The vesicoureteric junction is thought to act as a passive valve that resists the reflux of urine as the bladder pressure increases, and in line with its abnormal morphology, Indian ink injection into the bladder showed that *UPIIIa*$^{-/-}$ mice display VUR at lower pressures (almost 50% less) than their wild-type counterparts; this manifested itself as hydronephrosis in some animals. The key phenotypes of *UPIIIa*$^{-/-}$ mice are summarised in Figure 7.

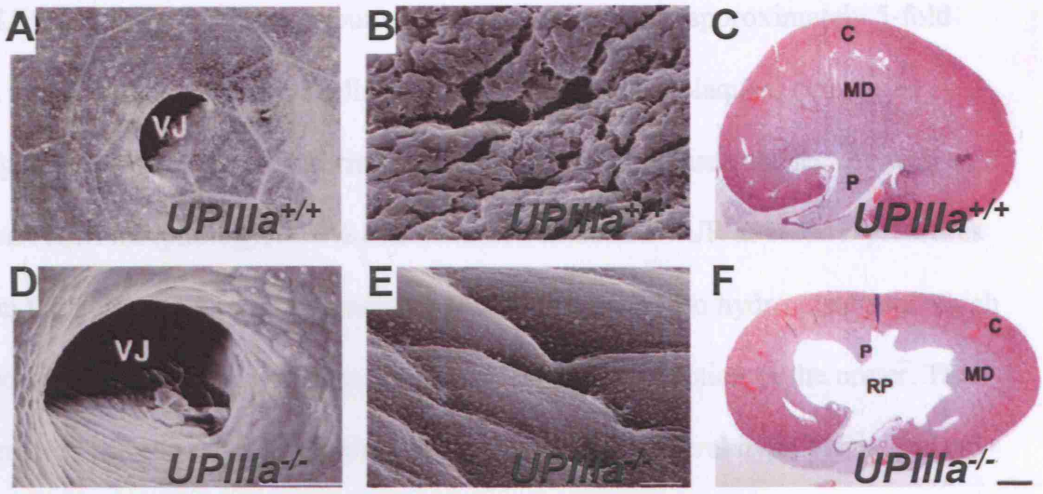


**Figure 7. Phenotype of *UPIIIa*-null mutant mice.**
(**A-C**) Renal tract in wild-type (WT) mice, showing normal vesicoureteric junction (VJ) (**A**), urothelial cell surface (**B**) and kidney (**C**) in the adult. In contrast in *UPIIIa*$^{-/-}$ mice the VJ is enlarged, showing an abnormal morphology (**D**), the urothelial cell surface is smooth (**E**) and mice display hydronephrosis secondary to vesicoureteric reflux (**F**). Figure taken from Hu et al. (2000) with permission from Prof. Tung-Tien Sun (New York University Medical Center).

In an analogous experiment, Kong et al. (2004) deleted the first four exons of the *UPII* gene in mice, and part of the fifth. *UPII*$^{-/-}$ mouse urothelium lacked a superficial umbrella cell layer, as shown by histology, and BrdU incorporation analyses showed that urothelial cell proliferation was elevated 100-fold and resulted in a thickening of the epithelium. Like the *UPIIIa*$^{-/-}$ mice, *UPII* knockout was accompanied by an approximately 5-fold reduction in the size of superficial cells, and a complete loss of plaques, perhaps explaining the replacement of fusiform vesicles by small immature vesicles. As well as this altered AUM morphology, >50% of these mice exhibited VUR at bladder pressures lower than the normal micturation pressure. These mice were also hydronephrotic, which was shown, by intravenous pyelogram, to be the result of obstruction of the ureter. This obstruction was presumably a consequence of the observed ureteral hyperplasia; indeed, serial sectioning revealed areas of the *UPII* null-mutant ureters that were occluded, and polyps were also observed. These congenital defects impair renal function in the mice, as evidenced by a doubling of the blood urea nitrogen concentration.

It is interesting that while the *UPII* null-mutant mice completely lacked plaques (Kong et al. 2004), *UPIIIa* null-mutants did have plaques, although they were significantly reduced in size (Hu et al. 2000). Together with the ureteral occlusion and renal function impairment reported in *UPII*, but not *UPIIIa*, null-mutants (although it is not clear whether ureters of *UPIIIa*$^{-/-}$ mice were assessed for occlusion by serial sectioning), this raises the possibility that UPIIIb may partially rescue the UPIIIa deficiency. Indeed, Deng et al. (2002) showed in *UPIIIa* null-mutant mice that while UPIb, UPIa and UPII are down-regulated at the protein level, UPIIIb is not, and, in contrast to the situation in

wild-type mice where it is only a minor component of AUM plaques, UPIIIb is the most strongly expressed UP in the homozygous *UPIIIa* null-mutants. In the same study, Deng et al. (2002) also showed that UPIIIb was able to heterodimerise with UPIb, each facilitating the transport of the other, and functional redundancy may explain why some plaques were present in *UPIIIa*$^{-/-}$ (Hu et al. 2000), but not in *UPII*$^{-/-}$ (Kong et al. 2004) mice. UPIIIb may indeed partially rescue a loss of UPIIIa. As further independent evidence in support of a role for UPIIIa in renal tract malformation, Okazaki et al. (2005) have recently shown that autoimmune hydronephrosis in BALB/c-*Fcgr2b*$^{-/-}$ *Pdcd1*$^{-/-}$ double-mutant mice is associated with the production of autoantibodies that specifically recognise UPIIIa protein *in situ*, suggesting that perhaps it is not the absence of UPIIIa, or urothelial plaques, *per se* that leads to renal tract malformations in *UPIIIa* null-mutant mice, but instead that malformation might arise by disruption of its normal functions during urothelial development.

*UPIIIb* resides in a region of chromosome 7 telomeric to the distal break-point associated with Williams-Beuren syndrome (OMIM 194050), a syndrome that includes bladder diverticulae, uninhibited bladder detrusor contraction and renal abnormalities in some patients and, less commonly, urethral stenosis, VUR and recurrent urinary tract infection. This raises the possibility that disruption of *UPIIIb* is involved in causing these renal tract anomalies (Deng et al. 2002), although large-scale chromosomal rearrangements can disrupt several genes, as well as non-coding genetic elements, and so the precise role of UPIIIb in the aetiology of these defects requires further investigation. In response to the phenotype observed in the *UPIIIa* null-mutant mice, especially the malformed

vesicoureteric junction, VUR and hydronephrosis that resemble defects sometimes observed in children, Jiang et al. (2004) recently sequenced *UPIa*, *UPIb*, *UPII* and *UPIIIa* in 76 patients with primary non-syndromic VUR (*UPIIIa* was also sequenced in an additional group of 25 patients, Giltay et al. 2004), but no mutations were found. As mentioned above, a well as defining the genomic structure of the human *UP* genes, Jiang et al. (2004) identified a number of common polymorphisms, and those of minor allele frequency >5% were chosen (because of statistical power considerations) to compare the frequency in an expanded cohort of 243 patients with primary non-syndromic VUR, and 150 control samples. One significant association was identified: the variant encoding a Pro154Ala change in exon 3 of *UPIIIa* was significantly more frequent in patients than in controls (25% *vs.* 15%). This is the first evidence directly implicating the *UP* genes in human disease.

On a cautionary note, however, while a true-positive association can be achieved owing to a genetic link with disease, misleading associations can also be detected if the case and control populations under study are differentially composed of a recent admixture of ethnic groups that have different marker and disease allele frequencies, a phenomenon known as population stratification. The case group of patients with VUR was composed of 76 patients from Pittsburgh, New York and London that were initially screened for mutations, 59 of whom had a positive family history, and an additional 167 patients from Boston and Newcastle-Upon-Tyne. The control group were composed of Caucasian individuals of European descent, and so it is not entirely clear whether or not the group is properly race-matched. Furthermore, the criteria for a diagnosis of "VUR" often rely on

the secondary consequences of reflux, since VUR often regresses with age and direct tests are invasive. The criteria used in the study of Jiang et al. (2004) were rather good, with all patients directly diagnosed as having reflux using a cystogram except for the Newcastle group who were assessed as adults; these patients were diagnosed as having typical features of reflux nephropathy.

# Part III. HEDGEHOG SIGNALLING

## 1-8 MOLECULAR COMPONENTS OF THE PATHWAY

The hedgehog signalling pathway was first delineated in the fruit fly, *Drosophila melanogaster*, through the discovery that the mutation of a group of genes, subsequently shown to encode the main hedgehog pathway components, caused defects in segment polarity that altered bristle pattern (Nusslein-Volhard & Wieschaus 1980). The hedgehog signalling pathway genes were discovered more than a quarter-of-a-century ago in *Drosophila*, and the vertebrate genes were cloned a decade ago. Hedgehog signalling plays an important role in many tissues in vertebrates as shown by genetic studies in mice, for example; this pathway is also important for human disease, with germ-line mutations in pathway components causing a range of congenital malformations and with signalling being disrupted in up to 25% of somatic cell cancers. Many excellent reviews have been published covering a vast body of literature, and the following description of the pathway is based on a number of texts, namely Hahn et al. (1999), Ingham & McMahon (2001), Ho & Scott (2002), Mullor et al. (2002), Bale (2002), Nybakken & Perrimon (2002), Roesller & Muenke (2003), Cohen (2003) and Lum & Beachy (2004). Recently, key differences in hedgehog signalling between vertebrates and invertebrates have been identified, and so the vertebrate pathway will be discussed here. The hedgehog signalling pathway is summarised in Figure 8.

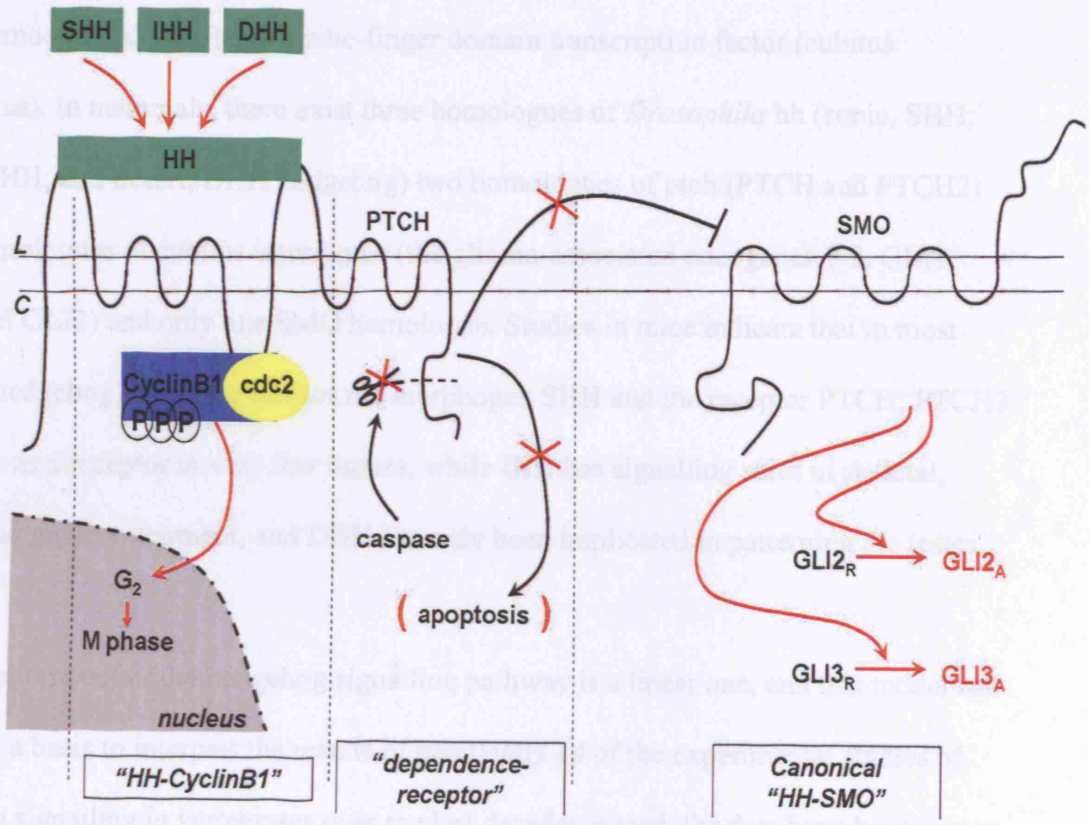


**Figure 8. The Hedgehog signalling pathway.**
Key: black lines/proteins/processes indicate the biochemical operations in a cell in the absence of morphogen; actions induced by binding of HH to the two large extracellular domains of PTCH are indicated in red. Three pathways involving PTCH are recognised, the canonical "HH-SMO" pathway, the action of PTCH as a "dependence-receptor" and the "HH-CyclinB1" pathway. *Canonical pathway:* Binding of a morphogen to PTCH leads to de-repression of SMO and the conversion of GLI2/GLI3 from their repressor ($GLI_R$) to their activator ($GLI_A$) forms. *Dependence-receptor pathway:* In the absence of morphogen, the C-terminal tail of PTCH is cleaved by a process involving caspases, revealing a death domain in PTCH and inducing cellular apoptosis. This process is inhibited by binding of HH morphogen to PTCH, generating a state of cellular dependence on morphogen. *HH-CyclinB1 pathway:* In $G_2$ phase of the cell cycle, the mitosis promoting factor (MPF) composed of phosphorylated (activate) CyclinB1 and cdc2 is bound by the large intracellular loop of PTCH and sequestered at the cell surface. Binding of HH to PTCH reverses this sequestration, allowing the MPF to translocate to the nucleus where it promotes $G_2$/M phase progression, thus elevating cellular proliferation. PTCH, patched; SMO, smoothened; HH, hedgehog; C, cytoplasmic face; L, luminal face of the cell membrane.

### 1-8-1 Core components of the canonical pathway

Four key components make up the hedgehog signalling pathway in flies; a hedgehog (hh) morphogen, its integral membrane receptor patched (ptch), a seven-pass transmembrane protein smoothened (smo) and a zinc-finger domain transcription factor (cubitus interruptus). In mammals, there exist three homologues of *Drosophila* hh (sonic, SHH; Indian, IHH; and desert, DHH hedgehog) two homologues of ptch (PTCH and PTCH2) three homologues of cubitus interruptus (the glioma-associated oncogenes 1-3, GLI1, GLI2 and GLI3) and only one SMO homologue. Studies in mice indicate that in most tissues, hedgehog signalling utilises the morphogen SHH and the receptor PTCH; PTCH2 only acts as a receptor in very few tissues, while IHH has signalling roles in skeletal, neural and gut development, and DHH has only been implicated in patterning the testes.

The current model of the hedgehog signalling pathway is a linear one, and this model has served as a basis to interpret the results of practically all of the experimental studies of hedgehog signalling in vertebrates over the last decade; indeed, the data have been largely consistent with this model, although some variations have been reported as will be discussed later. Cells that are responsive to a HH morphogen express PTCH. In the absence of a morphogen, this unbound receptor represses SMO, a member of the Frizzled family of proteins. In this cellular context, GLI2 and GLI3 undergo proteolytic cleavage to remove their C-termini that contain a transcriptional activator domain; the resultant truncated 89 kDa protein still possesses its zinc-finger domain, which ends just N-terminal to the cleavage site, and thus retains its ability to bind DNA, and in this context GLI2/GLI3 act as transcriptional repressors owing to an N-terminal transcriptional

repressor domain. HH binds to its receptor, and when a cell is stimulated in this way PTCH is altered, presumably owing to conformational change, such that SMO is de-repressed. De-repression of SMO activates a series of cellular processes that prevent the cleavage of GLI2/GLI3; in their full-length 190 kDa form, GLI2/GLI3 possess C-terminal transcriptional activator domains in combination with their zinc-finger domains and actively transcribe target genes. Both the mouse and human *GLI2/GLI3* genes possess an N-terminal repressor and C-terminal activator domain (Roessler et al. 2005) and so are responsible for mediating the hedgehog response. Studies in mice have suggested that GLI2 acts primarily as a transcriptional activator while GLI3 is primarily a transcriptional repressor (Bai et al. 2002; Mo et al. 1997; Park et al. 2000). In contrast, the GLI1 protein of both mice and men does not possess an N-terminal transcriptional repressor domain and is not responsive to signalling; while GLI2/GLI3 mediate the response to hedgehog in most developmental contexts, the *GLI1* gene is dispensable for development although it does compensate for a loss of transcriptional activation in mice lacking GLI2/GLI3 (Bai and Joyner 2001; Bai et al. 2002; Ding et al. 1998; Motoyama et al. 1998; Park et al. 2000), suggesting that GLI1-mediated transcriptional activation serves to 'top-up' the response to positive hedgehog signalling mediated by GLI2/GLI3.

In addition to this simple binary decision – *transcriptional repressor versus transcriptional activator* – the cellular location – *cytoplasm versus nucleus* – is also under the regulation of hedgehog signalling, with cubitus interruptus containing one nuclear localisation and two nuclear export signals; in the absence of sufficient morphogen, a scaffold of proteins will tether any uncleaved, potentially transcriptionally

active GLI protein to the cytoskeleton, preventing its entry into the nucleus, and this scaffold has been shown to involve a number of proteins in *Drosophila* cells. One such molecule is Costal-2, and although two vertebrate homologues, Kif7 and Kif27, have been identified as negative regulators of hedgehog signalling in zebrafish by morpholino knock-down (Tay et al. 2005), the role of these proteins in mammals is unknown. A "three-response" model has been proposed for the hedgehog response (Hooper & Scott 2005): in the absence of a HH morphogen GLI-repressor represses hedgehog target genes; in the presence of low concentrations of HH, the processing of GLI-repressor is blocked, but a fully functional GLI-activator is either not synthesized, or it is sequestered in the cell cytoplasm, and some target genes are derepressed; when a responsive cell is subject to high HH concentrations, GLI-activator enters the cell nucleus and actively transcribes target genes.

By definition, a morphogen is a secreted molecule that acts at long-range, and SHH and IHH have been elegantly shown to travel at a distance of many cell diameters from their source in mouse tissues using immunohistochemistry on tissues fixed in such a way that preserves proteoglycans/glycosaminoglycans and proteins in insoluble form (Gritli-Linde et al. 2001). Thus, one can imagine an intricate regulation of cellular processes within a tissue according to the spatial relationship relative to a source of HH according to a response mediated by GLI2/GLI3. Indeed, different genes respond differently to these changes in the balance of GLI activator:repressor forms; in the fly wing imaginal disc, loss of cubitus interruptus repressor alone suffices to activate *decapentaplegic* expression, whereas for other genes such as *ptch* itself, a so-called 'universal HH

pathway target' (Lum & Beachy 2004), expression requires the extra step of cubitus interruptus transcriptional activation (Methot & Basler 1999, 2001). Thus it is conceivable that hedgehog signalling according to the current model can pattern tissues according to a graded cellular response determined by morphogen concentration.

### 1-8-2 The hedgehog morphogens

One difference between HH signalling in the fly and in mammals is that while morphogen activity is mediated by only one fly *hh* gene, three mammalian HH morphogens exist; while each homologue may play the role of morphogen in different tissues, in other tissues, such as the gut, both SHH and IHH operate in tandem during development. This choice of morphogen represents another 'opportunity' for tissues to fine-tune HH signalling in developmental contexts since while SHH, IHH and DHH bind their receptor with equal affinity, in certain assays the concentration of each morphogen required to elicit a response can be very different (up to 60-fold); SHH is usually of greatest potency in most scenarios, with IHH and then DHH having a progressively reduced effect, although in some contexts, such as the inhibition of chondrocyte differentiation, DHH can be more potent than IHH (Pathi et al. 2001; this last observation might be somewhat surprising given the crucial role that IHH has to play in skeletal development, St-Jacques et al. 1999).

Each HH morphogen is expressed as a precursor protein of 52 kDa that is proteolytically cleaved to generate an N-terminal 19 kDa protein that fulfils all patterning activities both at short and long-range, and a C-terminal 25 kDa species (Lee et al. 1994; Porter et al.

1995); the C-terminal domain of the unprocessed precursor acts as an autocatalytic domain, serving to cleave the precursor protein at a highly conserved cysteine residue by an intramolecular mechanism, as evidenced by the concentration-independent cleavage kinetics (Porter et al. 1995). HH processing to generate an active N-terminal morphogen requires normal cholesterol metabolism; treatment of cells with inhibitors of cholesterol biosynthesis inhibits precursor processing into the two smaller fragments (Guy 2000), although it must be noted that these experiments employed a very severe inhibition of sterol metabolism. In a more recent study, Cooper et al. (2003) presented evidence to suggest that autoproteolysis of SHH precursor proceeds normally in *Dhcr7*$^{-/-}$ and *Sc5d*$^{-/-}$ mouse embryonic fibroblasts, that have a more mild defect in cholesterol biosynthesis owing to mutation of these metabolic enzymes. NIH3T3 cells transfected with SMO display low but significant levels of pathway activity, as assessed by a responsive reporter assay; treatment of these cells with cyclodextrin (an oligosaccharide that complexes with sterols) inhibited this response in a dose-dependent manner, however, the response in cells transfected with a constitutively active oncogenic form of SMO (SMOA1) was unaffected by cyclodextrin, suggesting that proper cholesterol biosynthesis is required for normal SMO activity rather than morphogen autoprocessing (Cooper et al. 2003). These results are also important for human disease, with mutations in *7-dehydrocholesterol reductase* (*DHCR7*) causing the Smith-Lemli-Opitz syndrome, the first inborn error of metabolism found that manifests itself as a malformation syndrome, with the range of malformations resembling those of patients with mutations in other hedgehog pathway components (Kelley et al. 2000).

It is now known that HH morphogens are modified by the addition of cholesterol following autoproteolysis of the precursor; the newly made N-terminus of the 19 kDa morphogen becomes covalently modified by the addition of cholesterol and its C-terminus becomes palmytoylated at the same time. It is thought that addition of cholesterol is important in determining the range over which HH signals. By harbouring a cholesterol moiety, HH has the tendency to remain at the surface of cells that have synthesized it, owing to hydrophobic interaction between the cholesterol group and cell surface lipids. In some tissues however, the HH-producing cell also expresses Dispatched (DISP), and HH signalling is long-range when expressed with DISP but juxtacrine/autocrine when DISP is absent. It is thought that DISP serves to mask the cholesterol motif of HH, reducing its affinity for the cell membrane and allowing its diffusion over many cell diameters, perhaps also promoting HH oligomerisation.

Thus it is evident that processing to generate an active morphogen is also involved in the tight regulation of hedgehog signalling. This process requires many fundamental cellular processes that might not be immediately obvious as patterning embryonic tissues.

### 1-8-3 Evidence for non-canonical signalling pathways

The hedgehog signalling pathway that has been described thus far is a widely accepted linear model, and has largely been adhered to in studies of the pathway. However, a handful of studies have suggested that variations from this dogma might exist. The first suggestion that hedgehog signalling components might operate differently came from a study of *Drosophila* head capsule development (Shyamala & Bhat 2002). In a screen for

mutations that cause head capsule maldevelopment, a new mutation of *ptch* (*ptch*$^{headless}$) was identified, and while loss-of-function *hh* mutants were phenotypically normal, the head capsule defects could be replicated in *hh* gain-of-function mutants. Cell proliferation in *ptch*$^{headless}$ mutants was reduced suggesting a model whereby PTCH permits cell proliferation by inhibiting SMO, under the canonical pathway. However, halving the *smo* copy number in the *ptch* mutant background increased the penetrance of the defects, rather than suppressing them. These results, the authors suggested, indicated a non-canonical relationship between PTCH and SMO in head development whereby PTCH and SMO act in concert to promote cell proliferation. Flies mutant for *babo*, the Activin type I receptor, also displayed the head capsule defects; indeed, *ptch*; *babo* transheterozygous flies were also malformed and flies with two mutant *ptch* alleles and one mutant *babo* allele displayed the defects with even higher penetrance. Thus the genetic data suggest that PTCH and SMO cooperate to promote cell proliferation in eye-antennal discs, and that this synergistic action is inhibited by binding of HH. Since Babo expression in *ptch*$^{headless}$ fly eye discs was not altered it is most likely that this PTCH-SMO interaction serves to activate the babo receptor at the protein, rather than transcriptional, level.

The second example of non-canonical hedgehog signalling involves the regulation of cellular apoptosis. The neural tube is patterned along the dorso-ventral axis by SHH which is secreted from the notochord and floor plate; the high levels of SHH in the ventral neural tube causes ventral neurons to differentiate. Withdrawal of SHH leads to a loss of ventral neuronal differentiation (Chiang et al. 1996) but it also leads to massive

apoptosis that can be rescued by the exogeneous addition of morphogen (Charrier et al. 2001; Litingtung et al. 2000). Some receptors (such as RET) act as so-called dependence-receptors by virtue of the fact that, in the absence of their ligand, they induce apoptosis of the cells in which they are expressed, generating a state of dependency on the ligand for survival. Thibert et al. (2003) found that transfection of full-length PTCH into 293T cells induced cell death to the same extent as transfection of the death inducer Bax, an effect that could be reversed by the addition of SHH in a dose-dependent manner, but which was unaffected by the co-expression of SMO, suggesting non-canonical signalling; similarly, over-expression of PTCH in chick neural tube induced apoptosis *in vivo*. Other known dependence receptors undergo cleavage of intracellular domains by caspases as a first step in apoptotic induction; indeed, transfection of only the large intracellular C-terminal tail of PTCH into 293T cells was sufficient to cause cell death. Addition of the caspase inhibitor, zVAD, to cells transfected with PTCH inhibited apoptosis to near-control levels, and the C-terminus could be cleaved *in vitro* by the addition of caspase-3, -7 or -8. Caspases cleave Asp residues at a consensus site, and mutation of $Asp^{1392}$ (mouse PTCH, equivalent to residue 1405 of the human protein) in the cytoplasmic tail of PTCH prevented this cleavage. Furthermore, PTCH-D1392N mutant proteins did not induce apoptosis when expressed in 293T cells, chick neural tube or in soft-agar assays. Finally, transfection of a PTCH protein truncated at this caspase cleavage site (that mimicked the cleaved form) induced apoptosis even in the presence of SHH. Thibert et al. (2001) proposed a mechanism for dependency whereby, in the absence of HH, PTCH is cleaved in its C-terminus by caspase-3, exposing a C-terminal proapoptotic domain and inducing cell death independently of SMO/GLI.

Another example of a non-canonical pathway involving PTCH and SHH, but independent of SMO-GLI, has been described by Barnes et al. (2001; 2005) involving the regulation of cell proliferation. In a search for factors that might regulate the activity of CyclinB1 during the cell cycle, a yeast two-hybrid screen of a mouse whole-embryonic cDNA library was undertaken using, as bait, a CyclinB1 protein that was mutated at four Ser sites (each Ser→Ala) to mimic the phosphorylated form of the protein. Surprisingly, PTCH was identified as an interacting partner, and further analyses confirmed that the interaction also occurred *in vivo* and demonstrated that it is actually the large intracellular loop of PTCH that interacts with CyclinB1; this domain is encoded by exons 13 and 14 of the human gene (residues 599-750).

Entry into mitosis requires the activation of M-phase promoting factor (MPF) which translocates into the cell nucleus at late $G_2$ where it induces mitosis by phosphorylating a number of nuclear factors. The MPF consists of cdc2, a Ser/Thr kinase, and CyclinB1. CyclinB1 is first expressed in cells at S phase and gradually accumulates until $G_2$ phase. CyclinB1 possesses a nuclear export signal (NES) that contains four Ser residues; when these residues are unphosphorylated, the NES mediates rapid export of CyclinB1 from the nucleus such that it accumulates cytoplasmically (Yang et al. 1998; Yang & Kornbluth 1999). At late $G_2$, these Ser residues within CyclinB1 undergo phosphorylation, disrupting NES function, allowing nuclear entry and initiating mitosis (Yang et al. 1998). Thus the phosphorylated form of the MPF is the active form. Immunoprecipitation of cdc2 in 293T cells transfected with PTCH showed that PTCH

also interacted with this partner of CyclinB1; it remains to be determined whether this interaction is direct or indirect, by virtue of the fact that both PTCH and cdc2 interact with CyclinB1, but these results clearly demonstrated that PTCH does interact with the active MPF.

In order to assess the significance of this interaction, 293T cells were transfected with PTCH, CyclinB1$^{Ala}$ (to mimic the unphosphorylated inactive form) and CyclinB1$^{Glu}$ (to mimic the phosphorylated active form), in combination or alone, and the cellular localization in cells singly transfected with CyclinB1 was consistent with the state of phosphorylation. Strikingly, in cells transfected with a CyclinB1 construct including a nuclear localization signal that constitutively localised the protein to the nucleus, co-transfection of PTCH reversed this nuclear localisation of the 'phosphorylated', but not 'unphosphorylated', form, sequestering the protein at the cell surface and increasing the proliferation index. This sequestration was partially reversed by exogeneous treatment of the cells with SHH, and this treatment reversed the effect on proliferation. Thus non-canonical hedgehog signalling can regulate cell proliferation, directly influencing the balance of nuclear *versus* cytoplasmic MPF localization at late $G_2$ phase, and regulating cell cycle progression through the $G_2$/M checkpoint. Indeed, the authors also demonstrated that a mutant form of PTCH found in patients with basal cell carcinoma that disrupts its large intracellular loop similarly resulted in elevated cell proliferation in transfection studies, offering a potential mechanism for oncogenesis (Barnes et al. 2005). Indeed, conditional null-mutation of *PTCH* (*Keratin6/Cre*, *Ptch*$^{cn/cn}$) specifically in the epidermis in mice causes elevated cell proliferation and basal-cell carcinoma, correlating

with an increased proportion of cell nuclei staining positive for CyclinB1 (as well as CyclinD1) (Adolphe et al. 2006).

These studies by Thibert et al. (2001) and Barnes et al. (2001; 2005) would suggest that the hedgehog signalling pathway can bifurcate at PTCH (Figure 8). Taken together with what we know about the canonical pathway, these observations indicate that HH and PTCH can have a number of distinct signalling roles, and show that the different operations conducted by PTCH are subdivided into distinct functional domains: while its large intracellular loop regulates the cellular localisation of CyclinB1 and its cytoplasmic C-terminal tail regulates apoptosis, the domain responsible for the repression/de-repression of SMO is not yet known but might also involve a different part of the protein. However, all of these processes are coordinated by the interaction of HH with the two large extracellular loops of PTCH.

Finally, evidence to suggest that SHH can also act independently of PTCH, SMO and GLI to regulate neural crest cell migration has also been reported (Jarov et al. 2003; Testaz et al. 2001). During neurulation, the flat neural plate bends to form a tube (the neural tube). SHH is secreted from the floor plate of the neural tube, generating a ventro-dorsal concentration gradient of this morphogen. Neural crest cells delaminate from the most dorsal region of the neural tube that experiences the lowest concentration of SHH, and Jarov et al. (2003) and Testaz et al. (2001) investigated whether SHH itself acts to maintain cell-cell interactions, thereby restricting the ventral-most cells within their neuroepithelium but permitting the delamination of the dorsal-most cells. By culturing

chick neural plates on fibronectin or laminin-1 coated plates *in vitro*, these investigators observed the adhesion of these neural progenitor cells over the first six hours, and then their migration until 72 hours of culture. By treating these explants with SHH in the culture medium, the cells similarly adhered and migrated, although between 48-72 hours of culture some cells began to differentiate, as shown by their extending neurites. Interestingly, the cells of explants cultured on plates onto which SHH had been adsorbed largely failed to adhere and the area of the explant shrank over the first 24 hours, and after 48 hours many cells began to differentiate and extend neurites; this effect was specific to adsorbed SHH, rather than secondary to depleting fibronectin/laminin-1 levels, since migration was normal when explants were cultured in medium supplemented with blocking-antibodies that specifically recognise SHH. Explants electroporated with SHH also displayed impeded cell migration. Furthermore, in explants that had only a small proportion of their cells electroporated, as evidenced by co-electroporation of a GFP construct, only nonelectroporated cells were migratory whereas cells overexpressing SHH did not contribute to this cell population.

These results suggest that SHH present in the extracellular matrix of neuroepithelial cells serves to stabilize the cells in an epithelium, while also inducing their differentiation. Indeed, these effects on migration were accompanied by a loss of concentration of the cell adhesion molecule integrin-β1 at focal adhesions, and addition of $Mn^{2+}$ to culture medium served to restore cell migration: $Mn^{2+}$ is known to induce highly active conformations of integrins, another class of cell adhesion molecules. Furthermore,

addition of N-cadherin blocking antibodies to explants also induced cellular dissociation and migration, and this effect was complete by 24 hours.

Interestingly, immunostaining of cells with markers of neuronal differentiation indicated that the presentation of SHH to explants, both in soluble form in culture medium and when adsorbed to culture plates, induced differentiation of neural precursors by 48 hours in a dose-dependent manner, consistent with the observation of neurite production by this time. Treatment of explants with cyclopamine, a plant-derived alkaloid that inhibits hedgehog signalling at the level of SMO, inhibited this differentiation of neurons, consistent with the mediation of this process by the canonical pathway. However, cyclopamine treatment did not alter the effect of adsorbed SHH on neural cell migration, indicating that this process is regulated via a non-canonical signalling pathway that involves components of the extracellular matrix, but not PTCH/SMO/GLI. These experiments also indicated that the observed differentiation and migration are independent processes, since blocking of differentiation had no effect of cell movement.

Taken as a whole, the studies described in this section indicate that hedgehog signalling does not necessary proceed via a linear pathway according to the canonical model (Figure 8). SHH can most likely act as ligand for extracellular matrix components, including integrin-β1 and N-cadherin, to restrict cell movement (Jarov et al. 2003; Testaz et al. 2001); PTCH regulates at least three distinct pathways, comprising signalling via SMO/GLI, the regulation of cell cycle progression by determining the cellular localisation of CyclinB1 (Barnes et al. 2001; 2005), and the regulation of cell survival by

virtue of a C-terminal death domain (Thibert et al. 2003) – all of these processes are also regulated according to the state of HH ligand binding to PTCH. It will be of great importance to evaluate the role of each of these non-canonical pathways *in vivo*.

All of these non-canonical pathways, other than the HH-CyclinB1 pathway, were identified in studies of the neural tube, an extensively studied system involving the patterning of cells according to a morphogen gradient. A recent study has shown that canonical hedgehog signalling controls the patterning, proliferation and survival of neuroepithelial cells independently, with each of these processes most likely being regulated by different transcriptional targets of the GLI proteins (Cayuso et al. 2005). It is therefore interesting to speculate that these independent outputs of hedgehog signalling are also intricately regulated by the integration of canonical and non-canonical responses. Recent studies of the regulation of cell proliferation are informative in this regard: elegant studies of the development of the hair follicle (Mill et al. 2005) and kidney (Hu et al. 2005b) using chromatin immunoprecipitation and gene expression analyses in mice with different combinations of *Shh* and *Gli3* null-alleles have shown that cell proliferation is regulated by canonical hedgehog signalling by the transcriptional regulation of CyclinD1, CyclinD2 and N-Myc, and that disruption of the balance of this regulation can cause maldevelopment. Perhaps regulation of these fundamental cell cycle components by the canonical pathway is integrated with the regulation of cell proliferation according to HH-CyclinB1 signalling: indeed, evidence has recently emerged that the $G_2$/M transition protein CDC25B is transcriptionally regulated by the canonical pathway in both mouse and chick (Benazeraf et al. 2006), and so a complex

interplay between both types of signalling might occur in some tissues. It is also interesting to note in this regard that mice homozygous null-mutant for *Gli3* do not display altered cellular proliferation or malformation of the hair follicle or kidney, although ablation of *Gli3* can rescue these proliferation defects in mice also null-mutant for *Shh*, and so it is possible that the canonical and non-canonical signalling pathways are functionally redundant in some tissues. This may make development more robust to mutational insults.

It is interesting that these non-canonical pathways directly regulate fundamental cellular processes, acting directly on the most basic of cellular machinery, in contrast to canonical signalling that involves a complicated pathway of hedgehog-specific components. An intriguing observation made following completion of the sequencing of the genome of the nematode worm, *C. elegans*, was that while the genome of this invertebrate contains many *hh*-related genes and many *ptch* and *ptch*-related homologues, the genome contains no *smo* gene (Kuwabara et al. 2000). Nonetheless, hedgehog signalling does operate in worms, with RNAi studies targeting PTCH homologues causing sterility (Kuwabara et al. 2000). Thus hedgehog signalling in worms must be non-canonical. This observation raises important questions regarding the evolution of the hedgehog signalling pathway, and it is interesting to speculate that the canonical components of the pathway were later additions to HH-PTCH signalling that perhaps regulated basic cell biological processes only through non-canonical means early in the evolution of the pathway; this possibility remains to be proven. Certainly the hedgehog signalling pathway holds many secrets, and

it is important to bear this in mind when interpreting the results of studies of hedgehog signalling in development and disease.

## 1-9 HEDGEHOG SIGNALLING IN RENAL TRACT DEVELOPMENT

Very little is known about the role of hedgehog signalling in renal tract development, although recent studies in mice suggest that it might indeed have a role to play (Yu et al. 2002; Hu et al. 2005b). In humans, mutations in *SHH* are occasionally associated with renal hypoplasia (Dubourg et al. 2004), urogenital malformation (Dubourg et al. 2004) and polyuria/enuresis (Heussler et al. 2002), suggesting that SHH signalling is important. *In situ* hybridisation studies have shown that SHH is expressed in the epithelium of the human cloaca (Odent et al. 1999), as well as in the urothelium of the UGS, urinary bladder and ureter, and in the renal pelvis and medullary collecting duct epithelia in mice (Bitgood & McMahon 1995; Nakashima et al. 2002; Yu et al. 2002). IHH is expressed in the outer medullary/cortical collecting duct epithelia (Nakashima et al. 2002; Yu et al. 2002) and GLI2 and GLI3 are expressed in the nephrogenic zone (Hu et al. 2005b; Nakashima et al. 2002; Yu et al. 2002), which is somewhat surprising since the HH receptor PTCH, expressed in cells responding to HH, has only been reported to be expressed in collecting ducts (both medullary and cortical; Yu et al. 2002). Expression of the serpentine protein SMO, which is compulsory for canonical hedgehog signalling, has never been investigated in the renal tract to my knowledge.

A total of four studies have investigated the function of (sonic) hedgehog signalling during renal tract development by the generation and analysis of mice null-mutant for *Shh* and/or *Gli2* and/or *Gli3*.

### 1-9-1 Cloacal development

As discussed in detail in *Section 1-5-2*, Mo et al. (2001) showed that the $Shh^{-/-}$ mouse is the only 'single-gene' animal model of persistent cloaca, and while $Gli2^{-/-}$ and $Gli3^{-/-}$ mice have anorectal amlformations (ARMs) including ectopic anus and anal stenosis, the persistent cloaca phenotype is recapitulated in mice with three null-alleles of *Gli2*/*Gli3*, indicating that gene-dosage is important in determining the severity of the malformation.

### 1-9-2 Development of the ureter

SHH is also important for the formation of muscle surrounding the ureter. By generating a mouse strain that drives Cre recombinase under the control of the *HoxB7* promoter in the mesonephric duct and its derivatives, including the epithelium of the ureter and kidney collecting ducts (i.e. the ureteric bud lineage), Yu et al. (2002) were able to create a conditional null-mutant of *Shh*, specifically ablating the gene in the developing kidney and ureter; this resulted in hypoplasia of the ureteric musculature that manifested itself as hydroureter owing to a functional obstruction to urine flow. In wild-type mice, PTCH and BMP4, a putative downstream target of hedgehog signalling (Bitgood & McMahon 1995), are expressed in the mesenchyme underlying the urothelium, indicating that SHH signals to the underling mesenchyme to regulate muscle formation. Analysis of the muscle cell differentiation marker, αSMA, showed that there were fewer differentiated

cells in mutant ureters. This might suggest that SHH induces muscle differentiation, however the culture of so-called 'sub-ureteral mesenchymal cells' dissected from E12.5 ureters in the presence of SHH-N actually inhibited αSMA expression in the cells, and the extent of this effect increased according to dose. In fact, mesenchymal cell proliferation in mutant ureters was reduced, and treatment of mesenchymal cells in culture increased their mitotic index. These data suggested a model whereby mesenchymal cells of the ureter have two possible fates, to proliferate or to differentiate terminally; SHH promotes proliferation and delays differentiation, allowing sufficient cells to populate the ureter before they differentiate. In the absence of SHH, insufficient cells are generated and the ureter is hypoplastic.

### 1-9-3 Kidney development

SHH signalling is also necessary for the normal formation of the metanephric kidney. Mice homozygous null-mutant for *Shh* or homozygous for a dominant-negative C-terminally truncated *Gli3* allele ($Gli3^{\Delta 699}$), similar to those carried (in heterozygous state) by patients with Pallister-Hall syndrome (Johnston et al. 2005), commonly display renal aplasia, while rare kidneys that are present are located ectopically ($Shh^{-/-}$; Hu et al. 2005b; Figure 9) or with a mislocated pelvis and lacking subdivision into cortex and medulla ($Gli3^{\Delta 699/\Delta 699}$; Bose et al.2002). As mentioned above, the *HoxB7/Cre*, $Shh^{c/n}$ ablated SHH specifically in the ureteric bud lineage (Yu et al. 2002). This strategy was necessary because the kidney primordia of conventional $Shh^{-/-}$ mice are fused secondary to midline defects of early somite stage embryos (unpublished observation in Yu et al. 2002) and kidneys are ectopic (Hu et al. 2005b). It is therefore important to interpret the phenotype

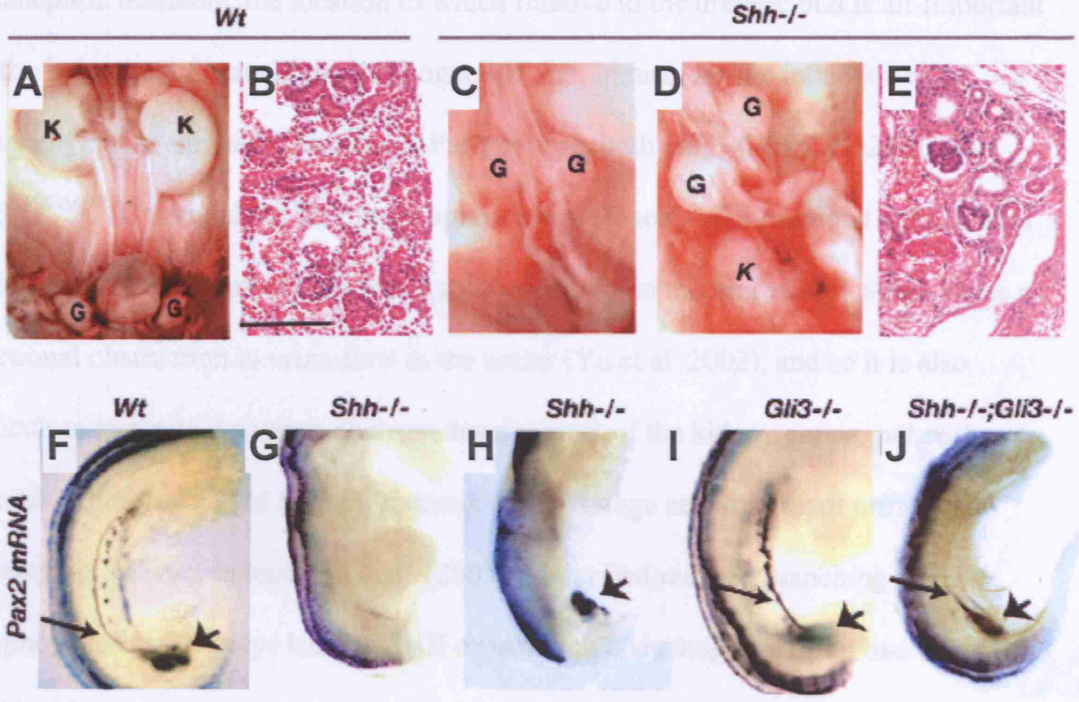


**Figure 9. Renal phenotype of *Shh* null-mutant mice.**
(**A,C,D**) Gross anatomical features of kidney development in wild-type (WT) and *Shh*$^{-/-}$ mice at E18.5. In contrast to WT mice (**A**), *Shh*$^{-/-}$ mice exhibited either absence of both kidneys (**C**) or the presence of a single ectopic kidney located in the pelvis (**D**). (**B,E**) Renal histological phenotype in E18.5 mice. In contrast to the organised appearance of glomeruli and tubules in the renal cortex of WT mice (**B**), the single kidney found in ~50% of *Shh*$^{-/-}$ mice (**E**) was characterised by a paucity of glomeruli and the presence of dilated tubules. (**F-J**) *Pax-2* mRNA expression in E11.5 mouse embryos. In WT and *Gli3*$^{-/-}$ embryos, *Pax-2* mRNA is expressed in the Wolffian duct (long arrow) and metanephros (short arrow). *Pax-2* mRNA was barely detectable in the Wolffian duct in ~50% of *Shh*$^{-/-}$ embryos (compare **G** with **F**). *Pax-2* mRNA was rescued to WT levels in all *Shh*$^{-/-}$; *Gli3*$^{-/-}$ embryos. Figure adapted from Hu et al. (2006) with permission from Prof. Norman D. Rosenblum (University of Toronto).

of *Shh*$^{-/-}$ and *Gli3*$^{\Delta 699/\Delta 699}$ mice with great caution since it is difficult to attribute malformations to defective hedgehog signalling, rather than to misplacement of the metanephric blastema, the location of which relative to the ureteric bud is all-important for the induction of branching morphogenesis and, in turn, for the induction of a mesenchymal-to-epithelial transition. Furthermore, both *Shh*$^{-/-}$ (Mo et al. 2001) and *Gli3*$^{\Delta 699/\Delta 699}$ (Bose et al. 2002) mice display severe cloacal malformations indicative of perturbed bladder development, while ablation of *Shh* in the urothelium would cause a functional obstruction to urine flow in the ureter (Yu et al. 2002), and so it is also difficult to attribute defects to aberrant development of the kidney *per se*, rather than to secondary defects caused by perturbations of the storage and voiding of urine in the developing embryo. Indeed, Hu et al. (2005b) described reduced branching morphogenesis in kidneys lacking SHH or in which hedgehog signalling had been inhibited by treatment with cyclopamine, as well as cystic dysplasia, both *in vivo* and in explant cultures of E11.5 organs, and this was also accompanied by reduced *Gli1* and *Gli2* expression. Moreover, *Pax-2*, *Sall1*, *CyclinD1* and *N-Myc* were downregulated in *Shh*$^{-/-}$ kidneys (Figure 9), and chromatin immunoprecipitation studies suggested that this was due to inhibition of the expression of these genes by excess Gli3-repressor; consistent with this possibility, *Shh*$^{-/-}$;*Gli3*$^{-/-}$ kidneys expressed these important kidney-patterning molecules and cell-cycle proteins normally, and the reduced cellular proliferation observed in both the ureteric bud and metanephric mesenchyme lineage of *Shh*$^{-/-}$ kidneys was rescued to normal levels by ablation of *Gli3* as well. These data show that sonic hedgehog signalling is necessary for the normal placement of the metanephric blastema and the correct interaction of the ureteric bud with this mesenchyme; in these

misplaced kidneys, excess Gli3 transcriptional repressor might cause the inhibition of proteins normally required for kidney development, however whether these perturbations occur during kidney development itself or during formation of the ureteric bud remains to be shown (Pax-2 expression was lost both in the mesonephric duct before ureteric bud formation as well as in the ureteric bud lineage), and the contribution of renal ectopia and/or obstructed urine flow to these defects raises many doubts over these observations.

Analyses of the conditional-null *Shh* mice are informative as to the role of SHH in the renal tract, independent of any potentially secondary defects (Yu et al. 2002). The kidneys of these mice were hypoplastic, as indicated by a 52% reduction in kidney volume standardized to body weight, and although this was accompanied by a 40% reduction in glomerular number, the glomerular density was actually increased by 26% in the mutants suggesting that it is not nephron formation *per se* that is perturbed. However, these organs were otherwise grossly normal, and they were not ectopically placed or absent in any of the animals (Figure 10). Taken together with the data in ureters showing that SHH regulates mesenchymal proliferation, Yu et al. (2002) suggested that these defects might arise from altered mesenchymal growth of the kidneys, rather than because of perturbed nephron formation; thus they concluded that sonic hedgehog signalling regulates development of the distal kidney, including collecting ducts, renal pelvis and ureter. Indeed, while BMP4 was downregulated in the ureteric mesenchyme of *Shh* mice, its expression was normal in glomeruli. The *Gli* genes are expressed exclusively in the nephrogenic zone of the metanephros (Nakashima et al. 2002; Yu et al. 2002) and so many questions remain about the role of the Gli transcription factors in kidney

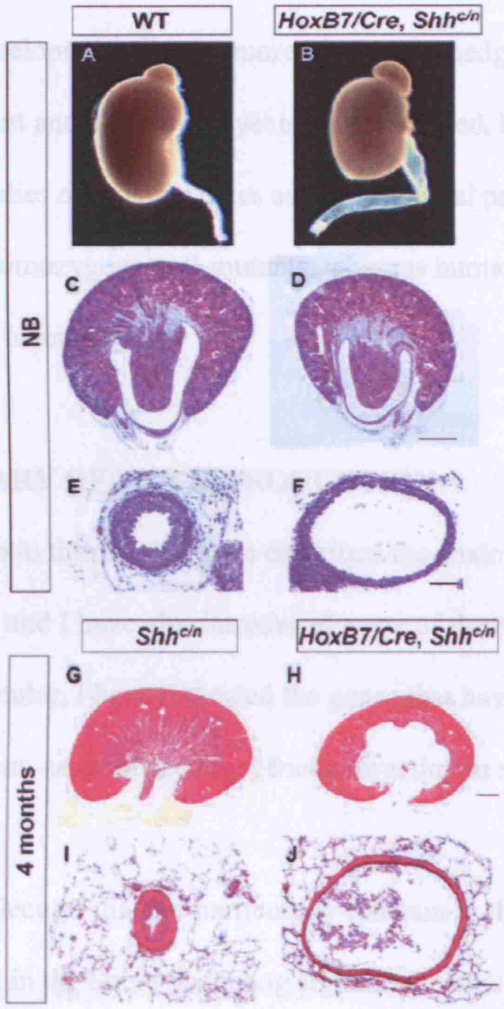


**Figure 10. Renal phenotype of *HoxB7/Cre*; *Shh* conditional null-mutant mice.**

Conditional removal of *Shh* activity from the urothelium with HoxB7/Cre results in hypoplasia, hydroureter and hydronephrosis. (**A,B**) Whole-mount view of the newborn kidney and ureter of wild-type (WT) and HoxB7/*Cre*, *Shh*$^{c/n}$ mice. (**C-J**) Hematoxylin and Eosin staining of coronal sections (**C,D**) and parasagittal sections (**G,H**) of the kidney (**C,D,G,H**) and cross-sections of the ureter (**E,F,I,J**) at stages indicated. Reproduced from Yu et al. (2002) with permission from Prof. Andrew P. McMahon (Harvard University).

development. The lack of a phenotype in *Gli3*$^{-/-}$ mouse kidneys (versus the anorectal malformations seen in these mice) raises further questions as to the importance of this gene in kidney development. Furthermore, the role of hedgehog signalling in human kidney development and disease has yet to be considered, because although these developmental studies offer some clues as to the general processes governed by SHH, the mice studied are homozygous null-mutants, whereas humans with mutations in *SHH* and *GLI2*/*GLI3* are all heterozygotes.

## 1-10 SUMMARY OF THE INTRODUCTION

In the *Introduction* to this thesis I have described the anatomical development of the human renal tract, and I have also introduced some of the molecules that regulate these processes. In particular, I have reviewed the genes that have been implicated in altered cloacal development, as evidenced by genetic targeting in mice.

Two groups of molecules that are particularly relevant to this thesis are the Uroplakins and those involved in the Sonic hedgehog signalling pathway, and so *Parts II* and *III* of the *Introduction* serve to introduce these proteins and their relevance to renal tract development, as well as to consider them as candidates in the genetic determination of human renal tract malformations. In *Part II* I have paid particular attention to the studies that founded the relatively new field of study that is 'Uroplakin biology', since I believe that these works have shaped our current view of the Uroplakins - while we need to embrace the conceptual basis that these studies have provided, we must also be aware of their limitations. In *Part III* I have described the Hedgehog signalling pathway, focusing

on recent studies suggesting that a number of non-canonical pathways might exist – this will serve as a basis to understand some of the work presented in *Study IV* of the *Results*. Once again, understanding the limitations of the accepted model is important to fully understand the biology of this group of proteins.

I have arranged the *Results* chapter into four sections as follows:

*Study I. Mutational analyses of* UPIIIa *and* UPIb *in patients with renal adysplasia.*
Hypothesis - Mutations in *UPIIIa* and *UPIb* cause human renal tract malformations;
Aim - To seek *UPIIIa* and *UPIb* mutations in patients with bilateral renal adysplasia.

*Study II. Mutational analyses of* UPII *in patients with renal adysplasia.*
Hypothesis - Mutations in *UPII* cause human renal tract malformations;
Aim - To seek *UPII* mutations in patients with bilateral renal adysplasia.

*Study III. Mutational analyses of* UPIIIa *and* SHH *in persistent cloaca and associated malformations.*
Hypothesis - Mutations in *UPIIIa* and *SHH* cause persistent cloaca;
Aim - To seek *UPIIIa* and *SHH* mutations in patients with persistent cloaca.

*Study IV. Expression analyses of Sonic hedgehog pathway proteins in human renal tract tissues.*

Hypothesis - Sonic hedgehog signalling proteins are expressed at key stages during human renal tract development;

Aim - To immunolocalise the core SHH signalling proteins during human renal tract development.

Some of the human developmental descriptions presented in the *Introduction* have been published in the form of a book chapter (Woolf & Jenkins 2006). The work described in *Studies I* and *III* of the *Results* have also been accepted for publication in peer-reviewed journals (Jenkins et al. 2005; Jenkins et al. 2006), while the work described in *Study II* is under review – copies of the published works are provided in the sleeve at the back of this thesis.

# Chapter 2. MATERIALS & METHODS

## 2-1 MATERIALS

### 2-1-1 Patients

The research project was approved by the Local Ethical Committees and leukocyte DNA collected after informed consent and extracted by the salt-precipitation method. Four groups of patients were studied:

*Group 1* was 17 children with renal failure associated with bilateral renal adysplasia without overt urinary tract obstruction;

*Group 2* was six children (boys) with PUV, and consequently bilateral renal dysplasia and ESRF secondary to urinary tract obstruction;

*Group 3* was 19 patients with unilateral MCDK without renal failure, who have previously been reported by Belk et al. (2002);

*Group 4* was 20 girls with persistent cloaca, many of whom also had malformations of other organs including their kidneys (Table 5 below), one of whom was also in *Group 1*. In addition to these patients with persistent cloaca, 2 girls with ectopic anus and 1 with cloacal extrophy were also screened.

### 2-1-2 Human tissues

The following tissues were examined: First trimester tissue sections from embryos at 4 weeks (n=2), 7 (n=2), 9 (n=2), 11 (n=2) and 13 (n=2) weeks. Second trimester kidney sections were available from 16 (n=1), 18 (n=1), 20 (n=1), 23 (n=2), 25 (n=1), 26 (n=1) and 28 (n=1) week embryos. All embryos were apparently normal. Tissues were aged by Carnegie Staging (first-trimester samples) or by the time since the last period (second trimester), which occurs 2 weeks before conception on average. In addition, key histological features were used to stage tissues; for example, metanephroi at 7 weeks contain their first layer of glomeruli and nephrogenesis ceases after 36 weeks gestation (Woolf & Jenkins 2006).

*Ethical approval*

Human tissues were collected from two sources during this thesis. Ethical approval for the collection and use of this material was obtained in each case from the appropriate Ethical committee. The embryonic tissues were obtained from the Wellcome Trust and Medical Research Council funded Human Developmental Biology Resource (HDBR) at the Institute of Child Health (Lindsay et al. 2005). Later antenatal samples were obtained by Dr. Paul Winyard from University College London Medical School. Use of this material was approved by the Joint University College London/University College Hospital Committee on the Ethics of Human Research.

*First trimester samples (before 13 weeks gestation)*

Normal human foetuses from the first trimester (donated by the HDBR) were obtained from chemically induced terminations of pregnancy. The foetus was collected immediately after delivery, fixed intact in cold 4% paraformaldehyde/phosphate buffered saline (pH 7.0) overnight at 4°C and processed for histology as below, by the HDBR technicians. All samples were processed within 2 hours of collection.

*Second trimester samples (13-28 weeks gestation)*

The kidney samples in this group comprised normal kidneys from spontaneous miscarriages. The designation of these kidneys as normal was classified by a trained pathologist. The foetus was stored at 4°C until autopsy when organs were fixed in 10% formalin. All specimens were processed using routine laboratory procedures within 24 hours.

### 2-1-3 Reagents

Restriction enzymes and their buffer (Buffers 1, 2, 3 and 4) were purchased from New England Biolabs; other enzymes were from Qiagen; deoxy-nucleotide triphosphates (dNTPs) were from Promega; oligonucleotides (PCR primers) were from Sigma Aldrich (*Appendix I*); primers for genotyping of microsatellite markers were Set 2 from Research Genetics; chemicals were from Sigma; all commercial antibodies were from Santa Cruz, except for anti-BMP4 that was from Novocastra, alkaline phosphatase conjugated anti-α smooth muscle actin (αSMA) was from DAKO and PCNA that was from Oncogene

Science (Table 3); anti-UPIIIa, -UPIb and -AUM primary antibodies were gifts from Prof. Tung-Tien Sun, New York University Medical Center and anti-UPII was a gift from Prof. Jennifer Southgate, York University (Table 3); secondary antibodies/polymers were from DAKO, as were peroxidase block, serum-free protein block and diaminobenzidine (DAB)/DAB-substrate buffer; COS-1 cells (88031701; Monkey African green kidney, SV40 transformed) and Madine-Darby Canine Kidney cells (84121903; Canine Cocker Spaniel kidney) were from ECACC; chemically competent DH5α *E. coli* cells were from Invitrogen; all cell culture media were from Gibco BRL and plastics were from Nunc; proteasome inhibitor was from Calbiochem; cycloheximide was from Sigma; and recombinant mouse SHH-N, corresponding to the N-terminal portion of the sonic hedgehog protein that performs all signalling functions at both long- and short-range (Lee et al. 1994; Porter et al. 1995), was purchased from R&D Systems. Light and fluorescent microscopy was performed on a Zeiss Axiophot microscope (Carl Zeiss) using lenses of 4x, 10x, 20x, 40x and 63x (oil immersion) magnification. Dark field microscopy was examined on an Olympus BH-2 microscope (Olympus) using lenses of 4x, 10x, 20x, and 40x magnification, and digital photographs were taken using a Canon digital camera. Confocal fluorescent microscopy used a Leica Aristoplan microscope and computer confocal laser scanning system (Aristoplan-Leica) with oil immersion lenses of 4x, 10x, 25x, 40x, 63x and 100x and software interpolation of intermediate magnifications. Images were saved as tagged image format files and imported, for labelling, into Adobe Photoshop (Version 3; Adobe Systems) or Microsoft Powerpoint (Version 4; Microsoft Corporation). DNA sequencing and microsatellite genotyping products were separated

***Table 3. Details of antibodies.***

| **Name** [Dilution] | **Source** | **Species (type)** | **Epitope** | **Specificity** |
|---|---|---|---|---|
| AU1 [1/50] | [1]T-T Sun | Mouse (monoclonal; IgG1[3]) | (b) | Monoclonal; only UPIIIa recognised on Western blot of bovine urothelium[3] |
| AUM [1/200] | [1]T-T Sun | Rabbit (polyclonal) | Total UPs of highly purified AUM (b) | Recognises UPIa, UPIb, UPII and UPIIIa, but no other species, on Western blot[4] |
| BMP4 [1/10] | Novocastra; NCL-BMP4 | Mouse (monoclonal; IgG) | (h) | Monoclonal; IgG control[6]; (Figure 11) |
| CyclinB1 (H-20) [1/100] | Santa Cruz; sc-594 | Rabbit (polyclonal) | C-terminus, 20 amino acids (h) | Pre-immune control using blocking peptide (Figure 11) |
| Patched (C-20) [1/200] | Santa Cruz; sc-6147 | Goat (polyclonal) | C-terminus, 20 amino acids (h) | Serum control[6] (Figure 11) |
| Shh (N-19) [1/50] | Santa Cruz; sc-1194 | Goat (polyclonal) | N-terminus, 19 amino acids (h) | Pre-immune control using blocking peptide (Figure 11); Recognises only the 52kDa Shh precursor in mouse gut by Western blot[5] |
| Smo (H-300) [1/100] | Santa Cruz; sc-13943 | Rabbit (polyclonal) | Amino acids 488-787 (h) | Serum control[6] (Figure 11) |
| αSMA [1/200] | Sigma; A5691 | Mouse (monoclonal; IgG) | (h) | Monoclonal |
| UPIb [1/200] | [1]T-T. Sun | Rabbit (polyclonal) | Amino acids 130-149 (b) | Recognises only UPIb on Western blot of bovine AUM[3] |
| [7]UPII [1/5] | [2]J. Southgate | Mouse (IgG) | Amino acids 124-140 (h) | Monoclonal[6] |

[1] Sackler Institute, New York University Medical Center, USA
[2] Jack Birch Unit of Molecular Carcinogenesis, University of York, UK
[3] Liang et al. (2001), and references therein
[4] Wu et al. (1994)
[5] van den Brink et al. (2001)
[6] Replacing primary antibody with same concentration of IgG (monoclonal antibodies) or serum (polycloncal) taken from the same species of animal as that in which the antibody was raised
[7] Clone JBU14.7; Pettit et al. (*in preparation*)
(h), raised against human protein; (b), raised against bovine protein.

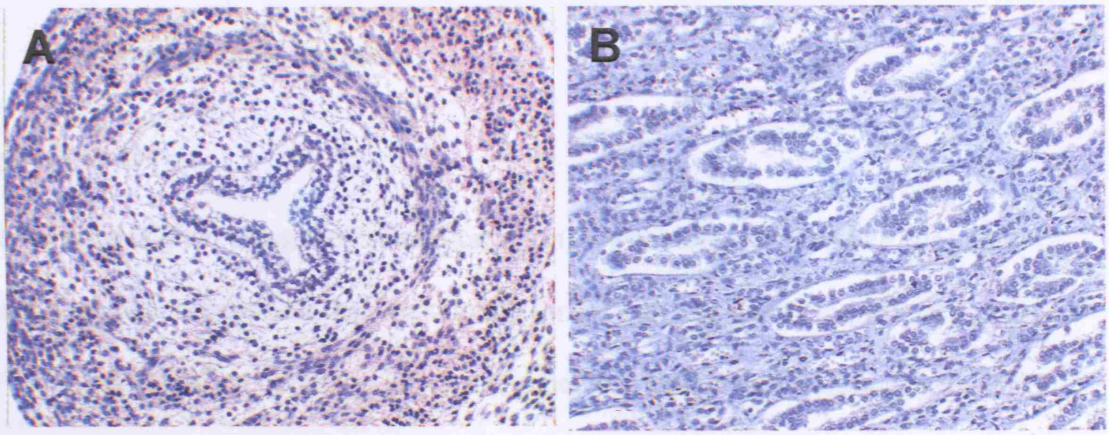


**Figure 11.** **Negative controls**
Examples of negative controls for immunohistochemistry. (**A**) Antibody (anti-SHH) preincubated with ten-fold excess of immunising peptide. (**B**) Pre-immune IgG substituted for primary antibody.

using the MegaBACE DNA analyser (Amersham). The source of other reagents are indicated in the text where necessary.

## 2-2 MOLECULAR GENETICS

### 2-2-1 Polymerase chain reaction

*Design of primers*

Primers were designed using the Primer3 program (www.biologyworkbench.sdsc.edu). This software chooses primers that are suitable for PCR in a target region primarily based on G/C content (which is optimally 50%) and annealing temperature (optimally 55-70°C and equal for both forward and reverse primer) within a desired region; the software also chooses primers that are less likely to form secondary structures that might disrupt annealing to template.

*Amplification of template*

The primers used for PCR in this thesis are listed in *Appendix I.* I used a hot-start DNA polymerase (Hotstart Taq polymerase), an enzyme that is inactive at room temperature and only becomes active once heated to 95°C, thus preventing non-specific amplification at sub-optimal/-stringent annealing temperatures. A typical PCR mix used was 4 µl DNA (20 ng/µl), 2.5 µl $MgCl_2$ (25 nM), 2.5 µl Buffer II, 0.1 µl dNTPs (20mM), 1 µl each primer (10 µM), 0.1 µl Hotstart Taq polymerase and 13.8 µl $ddH_2O$, making a total reaction volume of 25 µl. If required, Buffer Q (dimethylsulfoxide, DMSO) was also incorporated at a final concentration of 10% to prevent non-specific primer annealing, for

example in templates that are G/C rich; this was used for *SHH* exon 3c, and *UPIIIa* exon 1. Cycle conditions were: 94°C, 8 min; 30 cycles of 94°C for 30 sec, A°C for 30 sec, 72°C for 1 min; 72°C for 10 min – A is the annealing temperature (*Appendix I*).

### 2-2-2 DNA sequencing

*'Exo/SAP' treatment*

PCR products were first treated with exonuclease I (Exo I) and shrimp alkaline phosphatase (SAP) to remove any residual primer and to inactivate any remaining dNTPs, respectively, that may interfere with the sequencing reaction. A mix of 15 µl of Exo I (10 U/µl), 30 µl of SAP (1 U/µl), 7.5 µl of SAP dilution buffer and 22.5 µl of $ddH_2O$ was made (or multiples thereof), and 5 µl of the mix was added to between 5-17 µl of template DNA. This was incubated in a PCR machine at 37°C for 30 min, followed by 85 °C for 15 min to inactivate the enzymes.

*Sequencing reaction*

For each sequencing reaction 2 µl of terminator ready reaction mix (2.5X), 3 µl of sequencing buffer (5X), 1 µl of forward *or* reverse primer (3.2 *p*mol/µl), 2 µl of template DNA and 12 µl of $ddH_2O$ were mixed in a tube. The mix was incubated at 96 °C for 1 min. This was followed by 30 cycles of 96 °C for 10 sec, 50 °C for 5 sec and 60 °C for 4 min. Following the 30 cycles the products were stored at 4 °C.

*Desalting of sequence products*

Salt was removed by centrifugation, allowing the high-throughput handling of samples. A spin column plate was set up that has G-50 Sephadex applied to each column using an applicator. 150 µl of $ddH_2O$ was added to each column, and the plate was wrapped in cling-film and left at 50°C for 3 hours. The plate was then centrifuged for 5 min at 911 g. A further 150 µl was added to each column and the plate was spun again at 911 g for 5 min. Each sample for desalting was added to a separate column and centrifuged into a clean 96-well PCR plate at 911 g for 5 min. The resulting samples were desalted and suitable for running on a sequencing gel.

*Separation of sequence products*

Sequence products were run using the MegaBACE system. The sequence products were denatured at 95°C for 1 min on a hot plate and loaded into the MegaBACE following prompts from the computer to rinse the capillary tips, load buffer and load matrix. They were then injected into the gel by a capillary-based system at 3 KV for 60 sec, and then run out for 100 min at 9 KV. The data were then visualised using Sequencher v4.1 software. Chromatograms were scanned thoroughly by eye and edited so as to aid in the identification of double peaks that may represent heterozygotes that the analysis software often overlooks.

### 2-2-3 Amplification of genomic DNA samples

Whole genomic DNA from patients was amplified using the Genomiphi DNA amplification kit (Amersham Biosciences). 1 µl of patient DNA (a minimum of 1 ng is required) was mixed with 9 µl of sample buffer in a PCR tube. This was heated to 95°C for 3 min and then placed on ice, so as to denature the DNA. A mix of 9 µl of reaction buffer and 1 µl of Genomiphi enzyme (or a master mix in these proportions for multiple samples) was made on ice and added to the 10 µl of DNA/sample buffer mix. This was incubated at 30°C for 18 hours to amplify the DNA. After 18 hours, the sample was heated to 65°C for 10 min to denature the Genomiphi enzyme, after which the sample was stored at 4°C.

### 2-2-4 Restriction fragment length polymorphism assays

*UPIIIa Pro273Leu (818C/T)*

An enzyme digest was designed to seek the specific mutation found in exon 6 of *UPIIIa*, a change in nucleotide 818 (C/T) leading to a P273L missense change. A 322 bp PCR product was generated using the HaeIII primers (*Appendix I*). Following amplification 20 µl of template, 5 µl of Buffer 2, 10 µl of ddH20 and 2.5 µl HaeIII were incubated at 37°C. The PCR product from a wild-type allele has four HaeIII restriction sites, whereas the mutation abolishes one of these: digestion of wild-type DNA yielded bands of sizes 159 and 88 bp (as well as smaller bands of 35, 28 and 12 bp), while digestion of mutant DNA yielded bands of size 159 and 123 bp (as well as 28 and 12 bp).

*UPII L60fsX68*

A restriction digest was used to confirm the sequence change at nucleotide 215 of UPII, an insertion of the bases CACT producing a frameshifted allele, L60fsX68: following amplification of exon 2, 20 µl of template, 5 µl of Buffer 3, 10 µl of ddH20 and 2.5 µl MslI were incubated at 37°C, giving wild-type products of 244 and 66 bp, or a 314 bp product from the mutant allele.

## 2-3 CELL BIOLOGY

### 2-3-1 Preparation of Uroplakin cDNA constructs for transfection

Bovine cDNA encoding full-length UP protein was cloned into the multiple cloning site of a pcDNA3 plasmid to generate a construct encoding wild-type UPIIIa as well as one each encoding wildtype UPIb and UPIa. In brief, full length bovine UP cDNA was generated by PCR using primers that contained EcoR1 and Xho1 restriction endonuclease recognition sequences at their 5' end and, following digestion of both the cDNA and plasmid with these enzymes, the cDNA was ligated into the multiple cloning site of the pcDNA3 vector by virtue of the resulting overhang ends. Site directed mutagenesis (Stratagene) was then used to create 273Leu and 154Ala UPIIIa constructs. These constructs were kindly generated and provided by collaborators at New York University Medical Center (see acknowledgements).

### 2-3-2 Transformation and amplification of competent bacteria

To amplify the UP construct DNA, they were transformed into chemically competent DH5α *E.coli*; 5-10 µl of DNA construct was added to 100 µl of competent cells that had

been defrosted from storage at -80°C slowly on ice. This mix was vortexed very quickly (to mix the two but to avoid damage to the cells) and then placed on ice for 1 hr. Following this time, the bacteria were heat-shocked by incubating at 42°C for 90 sec, and then placed on ice for 2-5 min. 400 µl of LB broth was added to the cells in a 50 ml Falcon tube and incubated at 37°C for 45 min, shaking at 250 rpm.

250 µl of the bacteria were spread on 10 cm Ampicillin (50 µg/ml) plates (made by setting LB broth with agar in a mix containing the appropriate concentration of ampicillin), spreading the bacteria, drying by placing the inverted plate near a Bunsen burner, spreading and drying until all moisture had evaporated from the plate. The plates were then inverted and incubated at 37°C for 12-15 hrs; incubation for longer than this time was not done so as to avoid the growth of satellite colonies that do not carry a plasmid but grow once the Ampicillin has been depleted owing to metabolism by the resistant cells.

Three well-separated colonies were selected for each construct - they were picked using a sterile wire loop and inoculated into 250 ml of LB broth and incubated overnight at 37°C, shaking at 250 rpm. After this time, the cultures were centrifuged at 6,000 rpm for 15 min at 4°C. DNA was then extracted using the QIAgen High Speed Plasmid Maxi Kit according to the manufacturer's instructions.

### 2-3-3 Preparation of glycerol stocks of bacteria for long-term storage

To make a glycerol stock, a colony was picked and inoculated into 2-5 ml LB broth with Ampicillin (50 μg/ml) in a 50 ml Falcon tube. This was cultured for 8 hrs at 37°C and shaking at 300 rpm. After 8 hours, this was diluted into 100 ml (high-copy plasmids) or 250 ml (low-copy plasmids) LB broth in a large conical flask and cultured under the same conditions for a further 12-15 hrs. 300 μl of sterile (autoclaved) 50% glycerol (v/v) was added to a screw-cap 1.5 ml tube. 700 μl of culture medium containing transformed bacteria were added to the tube, and the two were mixed by vortexing and the tube was then stored at –80°C. To make a fresh culture from the stock, a small amount was scraped from the surface of the stock, ensuring that the stock did not thaw, inoculated into LB broth and cultured as described previously.

### 2-3-4 Re-ligation into new vector

So as to ensure that the vector DNA sequence itself had not been altered during its replication in bacteria, the insert was digested out of the vector, and re-ligated into new vector. The constructs were digested using EcoR1 and Xho1 restriction enzymes as follows: 10 μl DNA, 2 μl 10x Buffer 2, 1 μl EcoR1, 1 μl Xho1, 2 μl 10x bovine serum albumin (BSA) and 4 μl $ddH_2O$ were combined in an eppendorf tube and incubated at 37°C for 2 hrs. The resulting 20 μl product was run on a 1% agarose gel and gel purified using the Qiagen gel purification kit according to the manufacturer's instructions.

Gel purified insert was then re-ligated into new vector by mixing 1 μl of 10x ligation buffer, 1 μl of fresh (linearised) vector, 1 (or 2) μl of insert, 1 μl of DNA ligase and 6 (or 5) μl of $ddH_2O$, and incubating at 14°C. Following preparation of the desired construct, it

was amplified after transformation into competent DH5α bacteria, and gel-purified. Inserts were sequenced at each step of this preparation procedure using Sp6 and T7 primers so as to ensure sequence fidelity.

### 2-3-5 Cell culture

*Freezing cells*

Cells growing well or in log phase were pelleted by centrifugation at 1,000 rpm for 2 min in a 15 ml Falcon tube. The cells were then resuspended in cold freezing media (90% foetal calf serum, 10% DMSO) so that the concentration was no more than $5x10^6$ cells/ml. 1 ml of cells were transferred to screw cap cryovials and maintain on ice for approximately 30 minutes. The vials were transferred to -80°C for 24hrs, and then transferred to -140°C in liquid nitrogen for long-term storage.

*Thawing cells*

To thaw the cells, vials were removed from liquid nitrogen and immediately transferred to a 37°C water bath; while holding the tip of the vial, it was gently agitated, being careful not to allow water to penetrate the cap or seal. When completely thawed, the contents were transferred to a 15 ml test tube, and 10 ml of warm Dulbecco's Modified Eagles Medium containing 10% foetal calf serum with 1X antibiotics (DMEM/10% FCS/1X ABs) was slowly added to dilute the DMSO that is toxic to cells. This was centrifuged at 1000g for 2 min, and then the pellet of cells were resuspended in

DMEM/10% FCS (including antibiotics), and cells were transferred to fibronectin-coated tissue culture plates and incubated at 37°C in 5% $CO_2$.

*Propagation of a cell line*

Cells were grown by incubating them at 37°C in a humidified incubator until 90% confluent, at which point they were passaged again. The culture medium was drawn off the cells, and the cells were washed by adding and then removing 2 ml of PBS. Cations, that inhibit trypsin activity, are quenched by washing the cells in 5 mM EDTA in 1x PBS. 0.25% trypsin was then added to the cells in Hank's buffered salt solution to digest their contact to the fibronectin-coated plates mediated by extracellular matrix components. Having added the trypsin, the plate was agitated for 5 mins until cells were clearly seen free in the solution. Then, in order to bring tryspin activity to a halt, DMEM containing FCS was added (same volume of DMEM as trypsin). The cells in DMEM were then added to a 50 ml Falcon tube and repeatedly pipetted against the side of the tube to 'break' cell-cell interactions to make a cell suspension. The cells were pelleted by centrifugation at 1600 rpm for 5 min, the supernatant removed and fresh DMEM/10% FCS added. The cell suspension was then pipetted carefully and evenly onto new fibronectin-coated plates.

### 2-3-6 Transfection of cells

The method of transfection that I have used in this thesis is lipofection. Transfection was performed using the FuGENE 6 Transfection Reagent (Roche). The FuGENE 6 reagent

must be diluted directly in serum-free medium, avoiding contact of the undiluted reagent with plastics. 4 µl of FuGENE 6 was added to a volume of serum-free medium such that after adding 1 µg of DNA construct the total volume would be 100 µl. If a co-transfection was being performed, an extra 4 µl of FuGENE 6 was added per 1 µg of other construct(s) and the volume of serum-free medium reduced accordingly. Once the FuGENE 6 had been added to the serum-free medium, the eppendorf tube containing the mix was tapped 50 times to allow the combination of DNA and lipofectamine. Then the DNA was added and again the mix tapped. The mix was then incubated at room temperature for 15-45 min.

Before the transfection, the cells were grown until 40-60% confluent. When this was achieved, the medium was replaced with fresh medium that had been warmed to 37°C. The cells were allowed to adjust to their new medium by incubating for another 1 hr at 37°C. Following this time the 100 µl of transfection mix was then added, drop-wise, evenly over the surface of the cells/medium and gently swirled to allow an even distribution.

Once the cells had grown to ~90% confluence, they were processed as required for immunocytochemistry, Western blot etc.

### 2-3-7 Treatment of cells

*SHH-N*

Recombinant mouse SHH morphogen (SHH-N), purchased conjugated with carrier, was reconstituted in 0.5 ml of sterile FCS giving a concentration of 50 μg/ml (2680 nM). 15 μl were added to each ml of DMEM/10% FCS and 1X antibiotics, giving a final concentration of 40 nM in medium (equivalent to 750 ng/ml); this concentration is middle of the range that is typically used in experimental studies (for example, Yu et al. 2002). As a negative control, 15 μl of FCS was added to medium. Cells were plated to low confluence (~50-60 %), so as to avoid effects on cell proliferation secondary to contact inhibition and terminal differentiation of the cell monolayer, for 24 hours.

### 2-3-8 Western blotting

Western blotting involves the separation of different protein species by electrophoresis. For detection, the proteins are immobilised and detected using specific antibodies.

*Protein extraction*

Tissue samples were combined with 200 μl of RIPA buffer (150 mM NaCl, 50 mM Tris pH8, 1% NP40, 0.5% DOC, 0.1% SDS), to which proteinase inhibitors had just been added (30 ml / l Aprotonin, 1 mM sodium orthovanadate, 0.1 g / l phenoxymethyl sulphoxide (PMSF)), in an eppendorf. This was left on ice for 30 min, homogenising the tissue with a glass homogeniser. When the tissue was completely homogenised and after the 30 min, the sample was centrifuged at 12,000 rpm for 20 min at 4°C. The supernatant was removed to a fresh 200 μl PCR tube, to which 200 μl of 2X sample buffer (2% SDS, 10% glycerol, 0.01% bromophenol blue, 62.5 mM Tris-HCl, pH 6.8, 100 mM DTT) was added. This was mixed thoroughly and heated to 95°C in a PCR machine for 10 min.

To make total cell lysates from cell monolayers, medium was aspirated and washed twice in ice cold PBS. Cells were scraped and transferred in PBS to a 15 ml Falcon tube. The cells were then pelleted by centrifugation at 2,000 rpm for 5 min; the supernatant was removed and the cells resuspended in 1-2 ml of sample buffer. Cells were homogenised by repeated syringing through needles of decreasing calibre; this was also important for electrophoresis so as to shear genomic DNA that might impede the separation of samples. Samples were either run immediately or stored at -20°C.

*Protein electrophoresis*

Proteins were separated on denaturing polyacrylamide gels (SDS-PAGE). Gels (8 or 12.5% to resolve proteins of 50-100 kDa or 14-66 kDa, respectively) were cast and run in Mini-PROTEAN gel apparatus (Bio-Rad). The gel contained $ddH_2O$, a variable percentage of Protogel (37.5:1 acrylamide to bisacrylamide stabilized solution), 0.25 M Tris pH 8.8, 0.1% SDS, 0.02% fresh ammonium persulfate and 1% N,N,N',N' tetramethylethylenediamine (TEMED); TEMED catalyses free radical formation from ammonium persulfate which accelerates the polymerisation of acrylamide and bisacrylamide. After the resolving gel was poured it was covered with water-saturated butanol to flatten the top surface of the gel and prevent the diffusion of oxygen into the gel which would inhibit polymerisation. The gels were left at room temperature for 30-60 min to set. The overlaid water was poured off, and the upper surface of the gel was washed with $ddH_2O$ and blotted dry with Whatman 3MM filter paper.

Next a stacking gel was poured on top of the resolving gel. This aligns the proteins in a very thin layer on the surface of the resolving gel which increases protein resolution. A 5% gel was used: each 2 ml mix comprised 1.4 ml deionised water, 0.33 ml Protogel, 0.25 ml 1.0 M Tris pH 6.8, 0.02 ml 10% SDS, 0.02 ml 10% ammonium persulfate, and 2 µl TEMED. This was poured on top of the resolving gel until it reached the top of the smaller glass plate and a 10 well comb was inserted carefully to avoid bubbles. This was left to set for 30 minutes at room temperature and then immersed in tris-glycine buffer (diluted 5x stock: 25 mM Tris, 250 mM glycine pH 8.3, 0.1% SDS) in the running tanks. The Laemmli discontinuous buffer system was used (Laemmli et al. 1970) with part of the buffer between the gels and the rest in the running tank.

Gels were run at 40 V until the bromophenol blue reached the interface with the resolving gel. Voltage was then increased to 70 V until the bromophenol blue ran off the bottom of the gel.

The glass plates were removed from the gel tank and the resolving gel was placed in transfer buffer (48 mM Tris, 39 mM glycine, 0.037% SDS, 20% methanol) for 10 minutes. One piece of nitrocellulose membrane and six pieces of Whatman 3 mm filter paper were cut to the exact size of the gel and floated on transfer buffer at the same time.

Next the proteins were transferred from the gels to the nitrocellulose membrane with a semi-dry electroblotter (Bio-Rad). A sandwich of gels and filter paper were placed on the anode in the following order: three pieces of filter paper, nitrocellulose membrane,

resolving gel and three more pieces of filter paper. Air bubbles were rolled out with a 1 ml pipette. The lid which contained the cathode was then fitted and the proteins were blotted at 5 V for 30 minutes.

Protein transfer was initially assessed by colour transfer of the marker proteins and further blotting was performed if these had not transferred completely. Further assessment used red Ponceau S solution which binds proteins. The filter was marked by cutting off one corner to allow orientation of the proteins. It was then placed in a solution of Ponceau S for 5 min followed by several washes in $ddH_2O$. As the stain washed out the proteins were visualised as pink bands.

*Detection of protein*

Membranes were incubated in blocking solution (5% non-fat milk in PBS) for 1-2 hrs at room temperature. All subsequent procedures, until the final washes, were done in this blocking solution to reduce non specific background. The primary antibody was applied for 1 hr at room temperature on a shaker. The membrane was washed thoroughly three times for 10 minutes in PBS. Primary antibodies were detected using horseradish peroxidase-conjugated secondary antibodies (Dako Cytomation). Membranes were incubated with appropriate horse radish peroxidase conjugated secondary antibodies diluted 1:2000 for 30 min at room temperature. They were then washed three times in PBS.

Excess PBS was drained off the membranes and enhanced chemiluminescence (ECL) reagent was applied for exactly 1 minute. This was, in turn, drained off and the membrane was wrapped in cling film. This was exposed to X-ray film under safelight conditions in an X-ray cassette. Exposure times were varied depending on intensity of the signal. The size of the proteins which were detected was then assessed by reference to size markers.

### 2-3-9 Immunohistochemistry

*Peroxidase-based staining*

Paraffin sections were de-paraffinised twice in histoclear for 10 min each. Following this, sections were rehydrated by placing twice in 100% alcohol for 5 min each, followed by 5 min each in 90%, 80%, 70% and 50% alcohol. Following this, the slides were placed in PBS for 15 min to completely rehydrate the tissue. Sections were circled on glass slides using a PAP (wax) pen.

To make the antigens available for binding by the primary antibody, antigen retrieval was performed by microwaving the slides in citric acid (2.1g in 1 litre $ddH_2O$, pH 6.0) on full power for 6 min (for UPII immunohistochemistry no antigen retrieval was performed). The tissue sections were then treated with mild detergent (0.02% NP40 in PBS) for 1 hr to permeabilise the cells.

To avoid background staining caused by the antibody binding to the glass slide, the slides were blocked using serum-free protein block for 30 min. The primary antibody diluted in

PBS was then added to the section (dilutions for individual antibodies used are given in Table 3) and left overnight at 4°C. Endogeneous peroxidase activity may give a background signal after application of DAB (di-amino-benzidine), and so endogenous peroxidase activity was saturated by applying peroxidase block for 30 min at room temperature.

The sections were washed three times for 10 min each in mild detergent (PBS/0.02% NP40, as before), following which the secondary antibody was applied for 30 min at room temperature (either anti-rabbit IgG or anti-mouse IgG polymer neat, or anti-Goat IgG secondary antibody diluted 1 in 200 in PBS). The secondary antibody was removed by washing three times for 10 min each in PBS/0.02% NP40, followed by 5 min in PBS. Then DAB substrate solution (Dako Cytomation) was applied to the sections (one drop, approximately 45 µl, per ml of DAB substrate solution) for 5-10 min.

Following this, the slides were put into $ddH_2O$ to stop the peroxidase reaction, and then into Meyer's haematoxylin solution for 3-5 min (1.5 min for a light counterstain) to stain nuclei and thus give an overall representation of histology. The slides were then de-hydrated by running sequentially through the alcohol series (50%, 70%, 80%, 90%, 100% twice) for 5 min each, including 10 min twice in histoclear. Then the slides were mounted in DPX mounting medium.

*Amplification of signal using the avidin/biotin system*

In some cases, the signals generated by binding of specific primary antibodies were amplified to generate a more intense signal using the avidin/biotin kit (Vector Laboratories, Peterborough, UK). Using this method, immunohistochemistry was performed as described above, however two additional steps were incorporated into the protocol. First, blocking of endogenous biotin was performed as an additional step after the blocking of endogenous peroxidase, following which the sections were washed in PBS as normal. Second, instead of HRP-conjugated secondary antibodies, the anti-IgG secondary antibodies used were biotinylated; then a streptavidin/HRP ABC complex (DAKO) was added with washing between each step according to the manufacturer's instructions. Signal was then generated using DAB as described previously.

*Peroxidase/alkaline phosphatase double staining*

In order to stain a tissue section for two different antigens such that they could both be distinguished by light microscopy, it is possible to detect one bound primary antibody by a peroxidase-based method that gives a brown signal, and a second primary antibody that is conjugated to alkaline phosphatase and thus gives a red signal. First, immunohistochemistry was performed as described above using the primary antibody to be detected using the peroxidase method. However, before the slides were dehydrated following generation of the signal using DAB, a primary antibody conjugated to alkaline phosphatase was added to the sections for 1 hr at room temperature. After this time, the section was washed three times in PBS for 10 min each. Signal was then generated using the Fast Red system (Sigma) according to the manufacturer's instructions; briefly, one Tris buffer tablet and one Napthol tablet were dissolved in 1ml of $ddH_2O$ and then added

to the probed sections for between 5-10 mins. Using this method, slides must be mounted in an aqueous mounting medium (Citifluor), since the signal generated by this method is soluble in alcohol so that dehydration and mounting in DPX was not possible.

*Negative controls*

A number of controls were performed for the antibody staining (Figure 11). These consisted of: *i*) Omission of the primary antibody and substitution with PBS, allowing assessment of the background levels of peroxidase activity or autofluorescence; *ii*) Pre-incubation of the primary antibody with the immunizing peptide (available for SHH and CyclinB1 immunohistochemistry) at ten fold excess (g for g), allowing assessment of primary antibody specificity; and *iii*) The use of preimmune serum or IgG in place of the primary antibody, from the same species as that in which the primary antibody was raised.

### 2-3-10 Immunocytochemistry

*Fluorescent antibody staining*

Cells were aspirated and washed three times in cold PBS for 1 min each. The cells were then fixed by addition of 4% paraformaldehyde at room temperature for 10-20 minutes, following which they were washed three times for 10 min each in PBS. If the cells were to be permeabilised so as to assess the intracellular localisation of a protein, then 0.02% NP40 (MDCK cells) or 0.1% Triton-X (COS-1 cells) was included with the PBS during these washing steps. Then primary antibody was added to the cells for 1 hr at room temperature, and then Alexa fluorophore- (MDCK cells) or FITC- (COS-1 cells)

conjugated secondary antibodies were added to the cells in the dark for 30 min also at room temperature; washing three times for 10 min each in PBS was performed between each of these steps. The cells were then mounted in aqueous mounting medium (Citifluor).

*Staining of nuclei with Hoescht*

If cell nuclei were also to be visualized, then Hoescht 33342 dye (Sigma) was included at a concentration of 50 ng/ml with secondary antibody (i.e. this was added to cells for 30 min at room temperature).

# Chapter 3. RESULTS

## 3-1 Study I. Mutational analysis of *UPIIIa* and *UPIb* in patients with renal adysplasia

Hypothesis - Mutations in *UPIIIa* and *UPIb* cause human renal tract malformations;

Aim - To seek *UPIIIa* and *UPIb* mutations in patients with bilateral renal adysplasia.

### 3-1-1 Background

Around 1000 UK children have ESRF and, in approximately half of these individuals, the cause is a congenital abnormality of both kidneys (Lewis 2003), usually renal dysplasia, in which kidneys begin to form but contain undifferentiated and metaplastic tissues, sometimes with cysts (Woolf et al. 2004). On occasion, renal adysplasia exists as one part of a multiorgan syndrome (Woolf et al. 2004) caused by mutation of a gene expressed during kidney development, including branchio-oto-renal (*EYA1* and *SIX1* mutations; Abdelhak et al. 1997; Ruf et al. 2004), Fraser (*FRAS1*; McGregor et al. 2003), hypoparathyroidism-deafness-renal (*GATA3*; van Esch et al. 2000), and renal-cysts-diabetes (*HNF1β*; Bingham et al. 2002) syndromes. However, in clinical practice, most children with renal adysplasia and renal failure do not have an overt syndrome affecting organs beyond the genitourinary tract.

At the time that this project began, the observation that *UPIIIa* null mutant mice have high grade VUR and hydronephrosis, and that some of these mutants die soon after birth with renal failure, established an important role for this gene in renal tract development

(Hu et al. 2000), and the absence of pathogenic mutations in patients with primary non-syndromic VUR raised the possibility that mutations might be involved in the pathogenesis of more severe renal tract malformations. In mammals *UPIIIa* is expressed specifically in the renal tract (Wu et al. 1994), and this led me to hypothesise that *UPIIIa* (or its partner, *UPIb*) might therefore be mutated in humans with severe non-syndromic renal tract malformations.

### 3-1-2 Results

At seven weeks gestation the nascent tube-like bladder has recently formed from the cloaca and surrounding mesenchyme has begun to differentiate, as evidenced by αSMA expression (Figure 12A). At this time-point, UPIIIa was immunolocalised in the luminal epithelial layer of the UGS (Figure 12B) and a similar pattern was noted for UPIb (Figure 12C). At the same stage, the ureter and metanephric kidney has begun to form but the UPs were not detected in these structures (not shown). In the bladder at 13 weeks, the UPs were also detected in the urothelium (Figure 12K). At 13 weeks, unlike the bladder at this stage, mesenchyme surrounding the ureter has not yet formed muscle bundles (Figure 12D; the ureter was negative for αSMA, data not shown). At this stage, UPIIIa and UPIb were expressed in urothelium of the ureters and also the renal pelvis (Figure 12D-I). Expression of UPIIIa (and UPIb) always appeared apical (Figure 12G), consistent with the formation of urothelial plaques. By contrast, mesenchymal/stromal cells adjacent to the ureteric and pelvic urothelium did not express UPs. UPIb was immunolocalised in collecting duct epithelium of the kidney at 25 weeks (Figure 12L), however it was localised to the basolateral membrane, consistent with the absence of UPIIIa that is

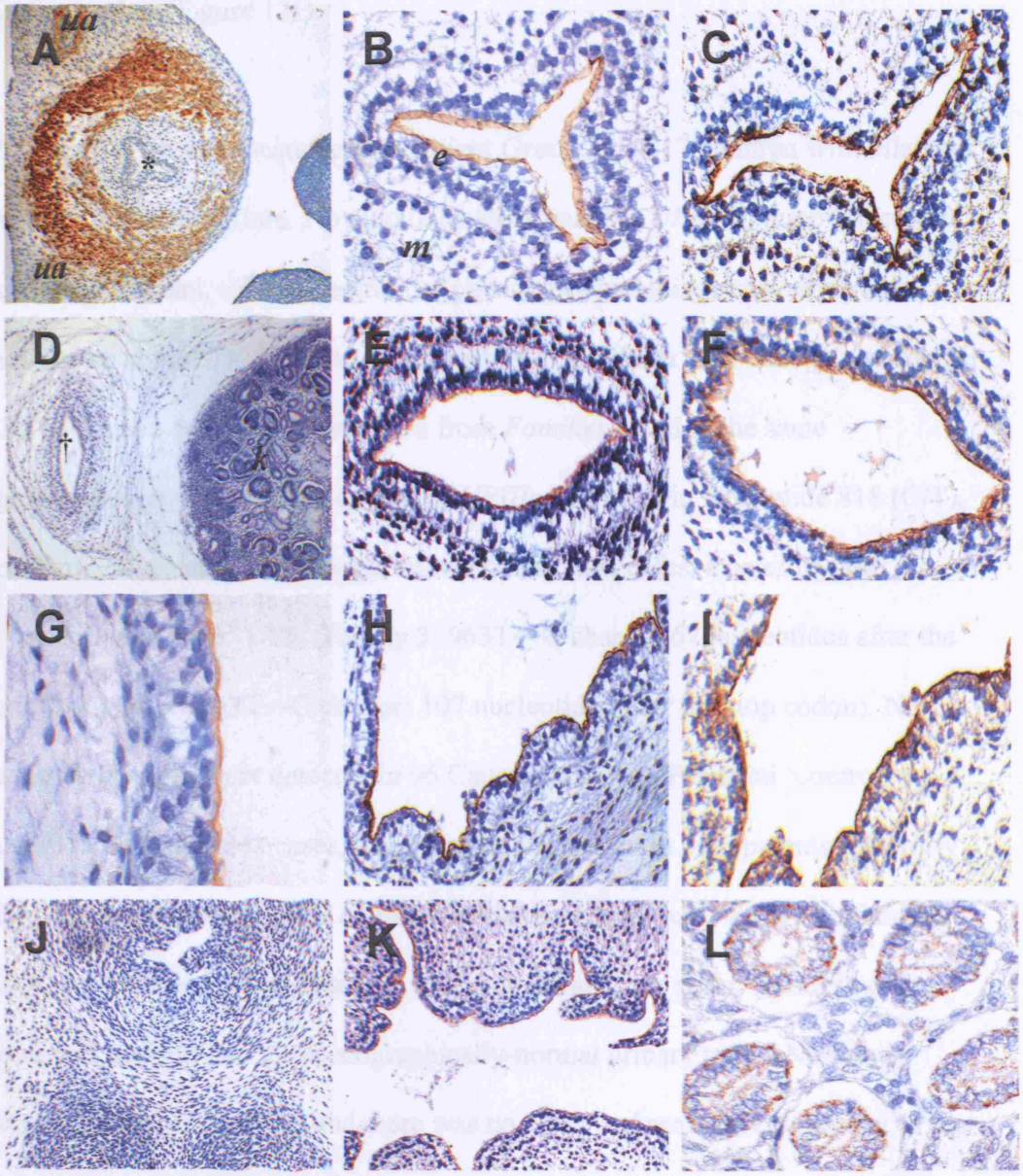


**Figure 12. UPIIIa immunohistochemistry.**

Normal human embryos were studied by immunohistochemistry using antibodies specific for either αSMA (*A*), UPIIIa (*B, D, E, G* and *H*) or UPIb (*C, F, I, J, K, L*). In the seven weeks gestation urogenital sinus (*, in which αSMA was expressed in the differentiating, surrounding mesenchyme; *A*), both UPIIIa and UPIb proteins immunolocalized (brown signal) to urothelial epithelia (*e*) (*B* and *C*). From 13 weeks (*D*), expression was also detected in the forming ureter (†, tangential sections; *E, F*) and renal pelvis (*H, I*) of the kidney (*k*). Surrounding mesenchyme/stroma (*m*) did not express UPs. UPIIIa protein localised to the apical surface of urothelium (*G*). UPIb was also detected in the bladder at 13 weeks (K) but not in the urethra (J). At 25 weeks UPIb was also detected in medullary collecting ducts and, consistent with an absence of UPIIIa, was localised to the basolateral membrane (L). Sections counterstained with hematoxylin. Magnifications: *A, D* – x12.5; *H, I* – x50; *B, C, E, F* – x100; *G* – x157.5. Abbreviation: *ua* – umbilical artery.

required for its transport to the apical membrane (Tu et al. 2002). The UPs were not detected in the urethra (Figure 12J).

Next, *UPIIIa* and *UPIb* were sequenced in patient *Group 1*, the 17 children with bilateral renal adysplasia and renal failure. No mutations were found in *UPIb*. In three Caucasian patients and one Pakistani, with a spectrum of phenotypes including renal adysplasia, cloacal malformation and VUR (Table 4), a heterozygous *UPIIIa* base change was found (Figure 13). In the two unrelated index cases from *Families 1* and *2*, the same heterozygous mutation was found in exon 6 of *UPIIIa*, a change in nucleotide 818 (C/T), leading to a Pro273Leu missense change. In two other index cases, a heterozygous mutation was found in the 3' UTR (Family 3: 963T→G change; 67 nucleotides after the stop codon: Family 4: a 1003T→C change; 107 nucleotides after the stop codon). No similar sequence changes were detected in 96 Caucasian and 96 Pakistani 'control' individuals. In these four index cases, the mutation was absent in both parents (paternity was confirmed using seven unlinked autosomal microsatellites) and, in the two families with siblings, the mutations were absent in two brothers and one sister. Furthermore, these parents and siblings had ultrasonographically-normal urinary tracts. No family reported consanguineous marriage and there was no history of renal disease in any of the extended families. These were heterozygous *de novo* mutations and correlated with the new occurrence of renal adysplasia within each of the four families.

The detailed clinical descriptions of these patients are as follows, courtesy of Prof. Adrian Woolf (ICH).

*Table 4. Clinical features of index patients with heterozygous UPIIIa mutations.*

| Family | Renal Phenotype | VUR | Bladder | Other Malformations |
|---|---|---|---|---|
| 1 | Right aplasia<br>Left dysplasia | Severe | Diverticula | Cloaca<br>Ventricular septal defect<br>Hemivertebrae |
| 2 | Bilateral dysplasia | Severe | Normal | No |
| 3 | Bilateral dysplasia | Absent | Normal | No |
| 4 | Bilateral dysplasia and cortical cysts | Absent | Small volume | Simple external right ear |

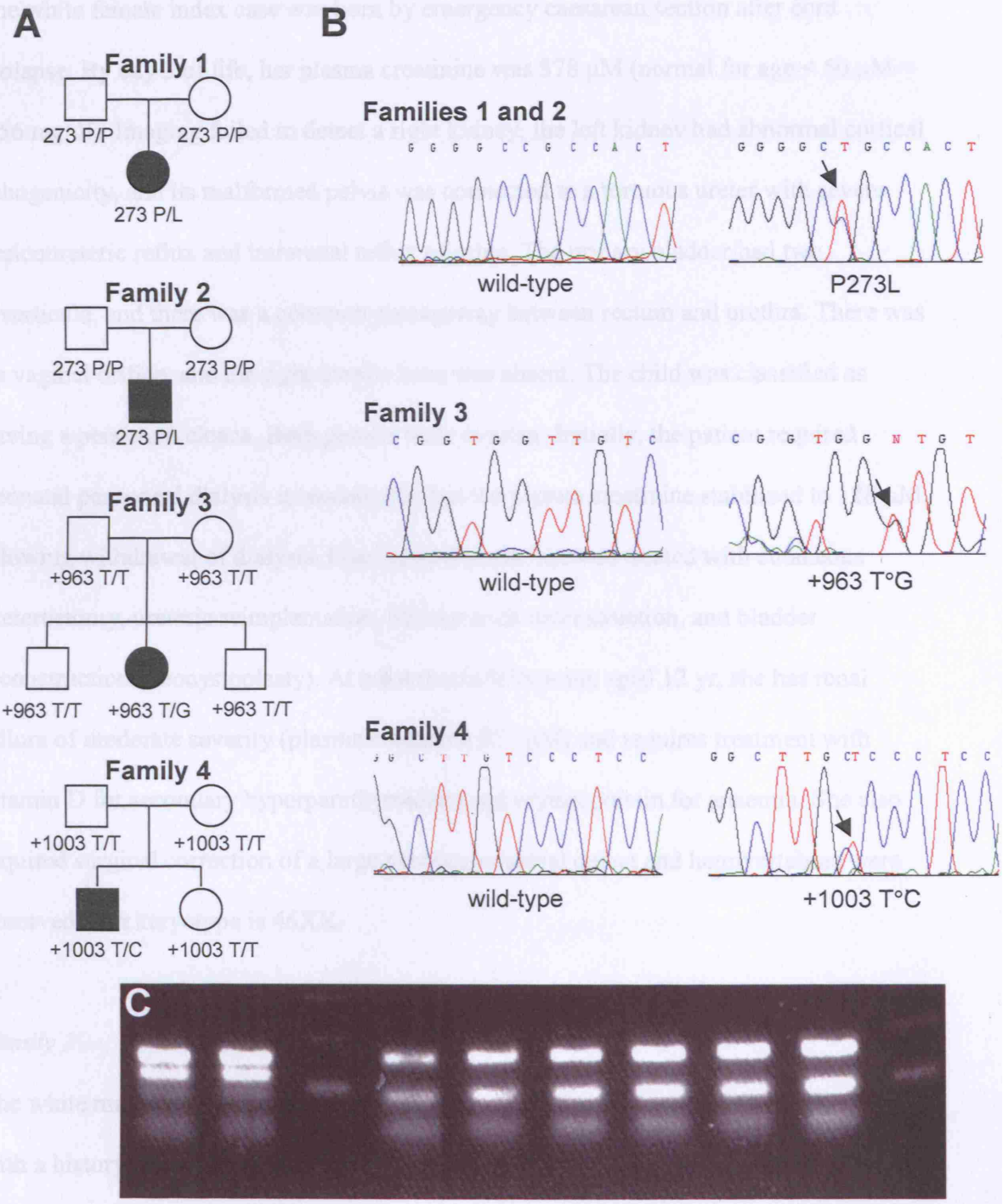


**Figure 13.** ***UPIIIa*** **mutations.**

(**A,B**) Three heterozygous *de novo* mutations were identified in *UPIIIa* in index cases. Two unrelated patients (*Families 1* and *2*) carried the same missense mutation (Pro273Leu) in the cytoplasmic domain of UPIIIa, and two other patients had a mutation in the 3' untranslated region; 963 T→G (*Family 3*) and 1003 T→C (*Family 4*). *Families 1*, *2* and *4* were white-Caucasians; *Family 3* was of Pakistani origin. (**C**) HaeIII restriction digest confirming heterozygosity for the Pro273Leu mutation in index cases from *Families 1* and *2* (lanes 1,2) but its absence in patients with persistent cloaca (lanes 4-9). Lanes 3 and 10, 100bp DNA ladder.

*Family 1*

The white female index case was born by emergency caesarean section after cord prolapse. By day 3 of life, her plasma creatinine was 378 μM (normal for age < 50 μM = 0.56 mg/dl). Imaging failed to detect a right kidney; the left kidney had abnormal cortical echogenicity, and its malformed pelvis was connected to a tortuous ureter with severe vesicoureteric reflux and intrarenal reflux of urine. The urinary bladder had two diverticula, and there was a common passageway between rectum and urethra. There was no vaginal orifice, and the right uterine horn was absent. The child was classified as having a persistent cloaca. Both gonads were ovarian. Initially, the patient required neonatal peritoneal dialysis to sustain life, but the plasma creatinine stabilized to 128 μM, allowing withdrawal of dialysis. Over several years, she was treated with cutaneous ureterostomy, ureteric reimplantation, bladder neck reconstruction, and bladder reconstruction (ileocystoplasty). At most recent follow-up, aged 12 yr, she has renal failure of moderate severity (plasma creatinine 267 μM) and requires treatment with vitamin D for secondary hyperparathyroidism and erythropoietin for anaemia. She also required surgical correction of a large ventricular septal defect and hemivertebrae were observed. Her karyotype is 46XX.

*Family 2*

The white male index case was born at 41 weeks gestation. He presented at 2 yr of age, with a history of being "unwell" for >3 months. He had severe anaemia (haemoglobin 6.3 g/dl) and renal failure (plasma creatinine 285 μM). On imaging, both kidneys were present, but they had abnormally increased cortical echogenicity and thinned

parenchyma. There was bilateral hydronephrosis (dilated renal pelvis) with severe vesicoureteric reflux into tortuous ureters. The urethra was normal. Now aged 15 years, he has progressive chronic renal failure (creatinine 345 μM) and requires treatment with vitamin D for secondary hyperparathyroidism and erythropoietin treatment for anaemia. It is considered that he will require renal transplantation in the next few years.

*Family 3*

The Pakistani female index case presented with intrauterine growth retardation at 34 weeks gestation, with induction of labour at 37 weeks. She was admitted as a neonate with a history of vomiting and found to have renal failure (plasma creatinine 176 μM). Both kidneys were small (<2 standard deviations below the mean for age) and had increased cortical echogenicity with no evidence of obstruction or vesicoureteric reflux. Subsequently, her renal excretory function slowly deteriorated, and she received a cadaveric renal transplant at age 9 years.

*Family 4*

The white male index was delivered at 42 weeks gestation by emergency caesarean section because of foetal distress. By day 4 of life, he was noted to have severe renal failure (plasma creatinine 411 μM). Subsequent assessment showed a "simple right ear" and evidence of short stature. Imaging showed two small highly echogenic kidneys 2 and 3 cm long, each with cortical cysts. Cystogram revealed a small-volume, irritable bladder with no VUR and a normal urethra. His karyotype is 46XY. He was initially treated with

alkali for acidosis and erythropoietin for anaemia, but renal excretory function deteriorated and he received a cadaveric renal transplant at age 3 years.

The specificity of the above mutations for bilateral renal adysplasia was established when two other groups of patients with different types of malformation were genotyped; the first set comprised 6 cases with PUV (*Group 2*), most of whom had secondary VUR and renal failure, and the second comprised 19 patients with unilateral MCDK (*Group 3*), none of whom had renal failure. In both conditions, impairment of foetal urine flow, at the level of obstructed urethras and ureters respectively, is thought to cause renal dysplasia (Woolf et al. 2004; Nyirady et al. 2002). No mutations in *UPIIIa* or *UPIb* were found, suggesting that *UPIIIa* and *UPIb* are not major causes of these varieties of renal dysplasia.

Residue 273 of UPIIIa is conserved as proline in man, mouse, rat and cow (Figure 14) and the change would significantly alter the secondary structure of the UPIIIa cytoplasmic C-terminus. In order to test the hypothesis that the Pro273Leu mutation would interfere with normal transport of UPIIIa to the cell surface, bovine UP pcDNA3 constructs were transfected into COS-1 cells. As well as the wild-type and 273Leu variants, transport of the 154Ala variant of UPIIIa, that has been significantly associated with primary non-syndromic VUR (Jiang et al. 2004), was also assessed, allowing the effect of two distinct disease-associated amino acid substitutions to be compared, one present in the cytoplasmic (273Leu) and another in the extracellular (154Ala) domain of UPIIIa.


**Figure 14. Alignment of UPIIIa protein sequences in different species.** Alignment of UPIIIa amino acid sequence in four different species. Using Boxshade (http://bioweb.pasteur.fr/seqanal/interfaces/boxshade.html) human (*Homo sapiens* - OR75631), mouse (*Mus musculis* - Q9JKX8), bovine (*Bos taurus* - P38574) and rat (*Rattus norvegicus* –gi:34867511) UPIIIa amino acid sequences were aligned showing conserved residues with a black background (Swiss-Prot accession numbers in brackets). The cytoplasmic domain is underlined in red according to the human entry in Swiss-Prot (http://us.expasy.org/sprot/) and the residue at which the missense change was identified is conserved as proline in all four species (as indicated by the arrow).

Western blotting of whole cell lysates allows endoplasmic reticulum localised UPIIIa (of size 37 kDa) to be discerned from UPIIIa that has entered the Golgi apparatus (these glycosylated products give a smear between 37-40 kDa). Western blot analysis of whole cell lysates of COS-1 cells transfected with a wild-type, 273Leu or 154Ala UPIIIa construct identified a band of size 37 kDa, showing that each of these constructs can drive expression of UPIIIa in COS-1 cells (Figure 15A, lanes 1-6; UPIIIa is not endogenously expressed in these cells, lane 19), and that the protein is present in the endoplasmic reticulum. In singly-transfected cells treated with proteasome inhibitor, a (more intense) band was also observed at 37 kDa, and several shorter bands were also observed; these shorter bands represent de-glycosylated degradation products (UPIIIa has three glycosylation sites; endoH treatment of UPIIIa to remove all sugar moieties results in a single band the same size as the smallest band observed in that 'ladder', Hu et al. 2005a). This further demonstrates that UPIIIa is present in the endoplasmic reticulum, since proteasomal degradation only occurs in this cellular compartment, and were the protein located outside of the endoplasmic reticulum, these bands would not have been observed. In cells co-transfected with each of the UPIIIa constructs as well as a wild-type UPIb construct (lanes 7-12), '37-40' kDa UPIIIa was observed, indicating that UPIIIa has been transported out of the endoplasmic reticulum and has entered the Golgi apparatus, where it becomes glycosylated. In contrast, co-transfection of cells with a UPIIIa construct as well as the wild-type UPIa construct, yielded only the 37 kDa UPIIIa protein, but not the '37-40' kDa Golgi-located species (lanes 13-18). Degradation of the proteins was also observed by treating cells with cycloheximide following their transfection, a chemical that inhibits protein synthesis allowing protein degradation to be observed by

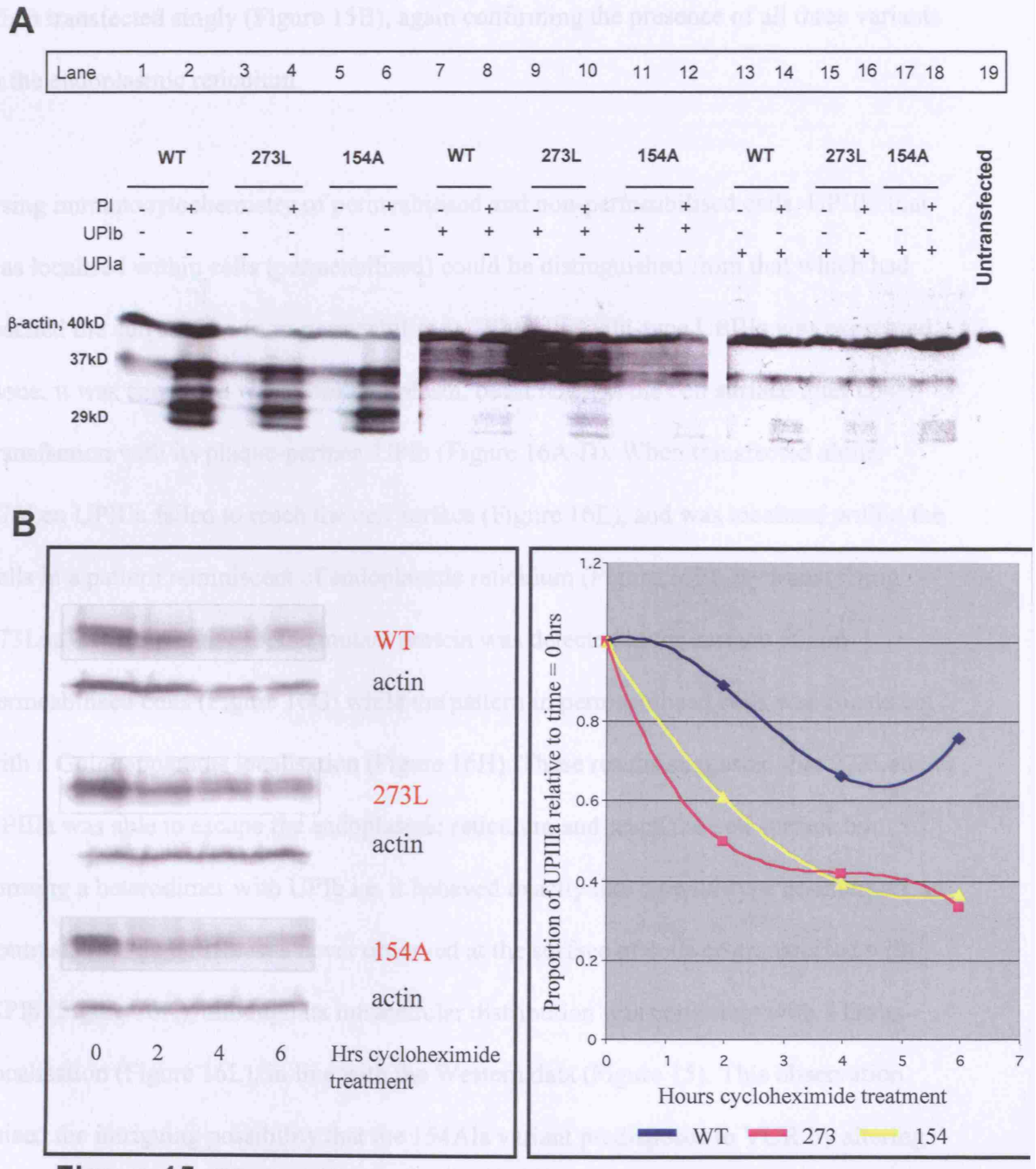


**Figure 15. Western blot analysis of UPIIIa protein transport.**
(**A**) Western blot of COS-1 whole-cell lysates using a monoclonal anti-UPIIIa antibody. Lanes 1-6, cells transfected with UPIIIa alone; lanes 7-12, cell transfected with UPIIIa and UPIb; lanes 13-18, cells transfected with UPIIIa and UPIa; lane 19, cells transfected with empty vector. Even-numbered lanes, cells treated with proteasone inhibitor (PI). Cells transfected with wild-type (WT), 273Leu or 154Ala UPIIIa constructs as indicated. 37kDa, endoplasmic reticulum-localised UPIIIa; 37-40kDa smear in lanes 7-12, UPIIIa localised in the Golgi apparatus; 40kDa, membranes also probed using anti-βactin antibody as loading control. (**B**) Cells transfected with each UPIIIa construct and treated with cycloheximide for 0-6 hours. Left, Western blot detecting UPIIIa; Right, plot of UPIIIa band quantification relative to βactin relative to time 0hr showing protein degradation. Number of replicates = 1.

Western blotting; all three variants underwent similar protein degradation over 6 hrs when transfected singly (Figure 15B), again confirming the presence of all three variants in the endoplasmic reticulum.

Using immunocytochemistry of permeabilised and non-permeabilised cells, UPIIIa that was localised within cells (permeabilised) could be distinguished from that which had reached the cell surface (non-permeabilised). When the wild-type UPIIIa was expressed alone, it was contained within the cytoplasm, but it reached the cell surface after co-transfection with its plaque-partner, UPIb (Figure 16A-D). When transfected alone, 273Leu UPIIIa failed to reach the cell surface (Figure 16E), and was localized within the cells in a pattern reminiscent of endoplasmic reticulum (Figure 16F). By transfecting 273Leu UPIIIa with UPIb, the mutant protein was detected at the surface of non-permeabilised cells (Figure 16G) while the pattern in permeabilised cells was consistent with a Golgi apparatus localisation (Figure 16H). These results suggested that 273Leu UPIIIa was able to escape the endoplasmic reticulum and reach the cell surface by forming a heterodimer with UPIb i.e. it behaved exactly like its wild-type counterpart. In contrast, 154Ala UPIIIa was never observed at the surface of cells co-transfected with UPIb (Figure 16K), although its intracellular distribution was consistent with a Golgi-localisation (Figure 16L), in line with the Western data (Figure 15). This observation raised the intriguing possibility that the 154Ala variant predisposes to VUR by altering normal transport of the protein at a post-Golgi point in the secretory pathway.

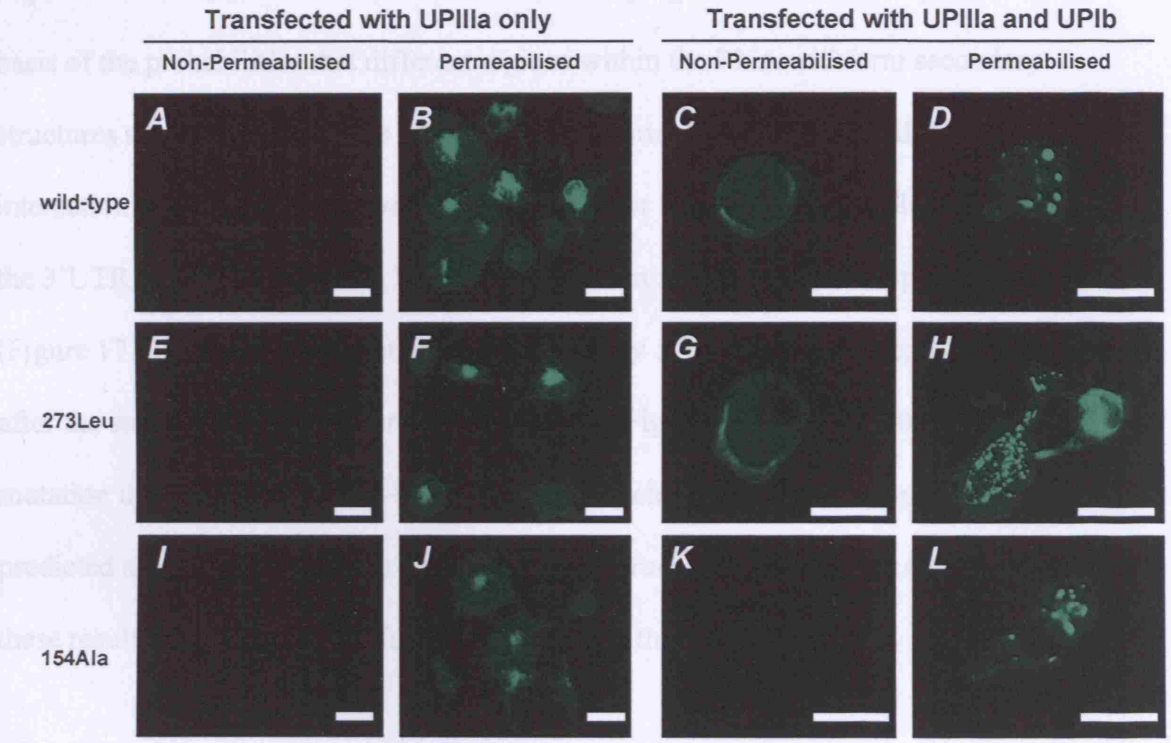


**Figure 16.** **Missense UPIIIa expression *in vitro***

UPIIIa immunocytochemistry in non-permeabilised (**A**, **C**, **E** and **G**) and permeabilised (**B**, **D**, **F** and **H**) COS-1 cells transfected with: wildtype UPIIIa alone (**A** and **B**); wild-type UPIIIa and wildtype UPIb (**C** and **D**); Pro273Leu UPIIIa alone (**E** and **F**); Pro273Leu UPIIIa and wild-type UPIb (**G** and **H**); Pro154Ala UPIIIa alone (**I** and **J**); Pro154Ala UPIIIa and wild-type UPIb (**K** and **L**). No variant of UPIIIa reached the cell surface when transfected alone (**A**, **E** and **I**) but all were immunodetected (green) in a pattern reminiscent of endoplasmic reticulum in permeabilised cells (**B**, **F** and **J**). When cotransfected with UPIb, both wild-type and mutant UPIIIa reached the cell surface (**C** and **G**) and, in permeabilised cells, UPs were detected in a Golgi-like pattern (**D** and **H**). In contrast, 154Ala UPIIIa was never detected at the cell surface when co-transfected with UPIb (**K**), although it was present within cells in a pattern reminscent of the Golgi apparatus (**L**). Note that untransfected COS-1 cells do not express UPs. Bars are 20 microns.

Next, the possible effect of the genetic changes found in the 3'UTR were interrogated using the program RNAfold (Knudsen et al. 2003; http://www.daimi.au.dk/~compbio/rnafold/). This program folds RNA sequences on the basis of the probabilities that different regions within the RNA will form secondary structures such as hairpin-loops that might be important for mRNA stability and/or interaction with proteins involved in transcription or translation. RNAfold predicted that the 3'UTR of wild-type human UPIIIa folds to form a single hairpin-loop structure (Figure 17A), but that the mutation found in *Family 3* (963T→G change; 67 nucleotides after the stop codon) would disrupt this structure (Figure 17B). The +1003 *UPIIIa* mutation in *Family 4* (a 1003T→C change; 107 nucleotides after the stop codon) predicted a more global change in the secondary structure of the mRNA (Figure 17C); these results support potential functional effects of these mutations.

### 3-1-3 Interpretation and interim discussion

Here, I have shown for the first time using specific antibodies that UPIIIa and UPIb proteins are expressed in the developing human ureter and renal pelvis and report *de novo UPIIIa* mutations in children with severe renal adysplasia with kidney failure. In fact, this is the first report of *UP* mutations in a human renal disease and I believe that this report also constitutes the first *de novo* genetic changes associated with non-syndromic urinary tract malformations. The genetic findings also have potentially considerable clinical implications. The occurrence of *de novo UP* mutations in children with adysplasia and with severe renal failure leads to the possibility that, because it is now possible to save the lives of such children with medications, dialysis and transplantation (Rees 2002), a

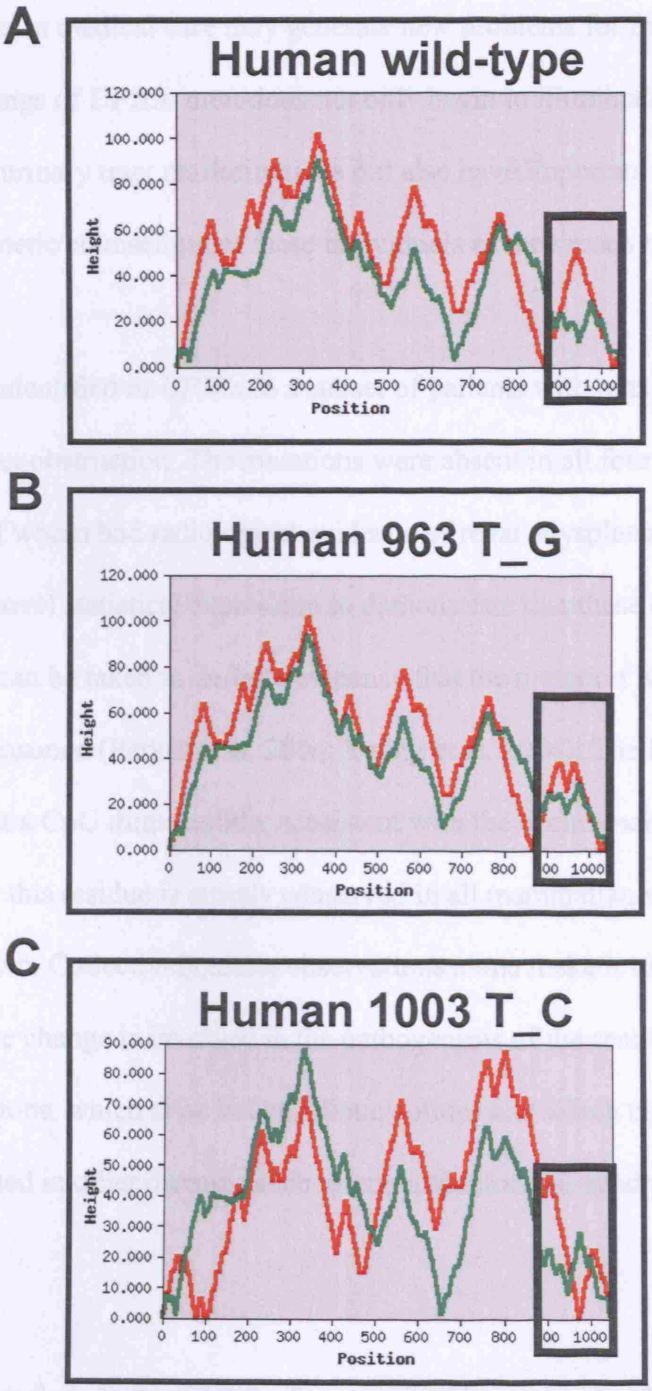


**Figure 17. RNAfold analysis of 3'untranslated region mutations.**
Full-length UPIIIa mRNA analysed by RNAfold. Predicted structures are indicated in red; peaks represent hair-pin loop structures, with the apex representing the loop and paired upward and downward slopes representing paired hairpin structures. Green line represents the predicted free energy of the most stable structure (**A**) The 3'UTR (black box) of wild-type mRNA forms a hairpin-loop structure. (**B**) The 963 T>G mutation would disrupt the loop of this structure, (**C**) The 1003T>C mutation would globally alter the structure of the mRNA, with the first half of the 3'UTR predicted to pair with the 5'UTR

new generation inheriting dominant mutations may arise; furthermore, this next generation may be at risk of suffering from severe congenital renal disease. In this manner, advances in medical care may generate new problems for future generations. Thus, these findings of *UPIIIa* mutations not only begin to illuminate the pathogenesis of human sporadic urinary tract malformations but also have important implications regarding the genetic counselling of these individuals as they reach reproductive age.

Mutations were identified in *UPIIIa* in a subset of patients with renal adysplasia with no overt urinary tract obstruction. The mutations were absent in all four sets of parents, and siblings, none of whom had radiological evidence of renal adysplasia. In *Appendix II*, I have derived a novel statistical expression to demonstrate that these observations of *de novo* mutations can be taken as definite evidence that the mutation is causative, as others have cogently reasoned (Parker et al. 2004; Twigg et al. 2004). The Pro273Leu missense mutation arose at a CpG dinucleotide, consistent with the occurrence in two unrelated index cases, and this residue is strictly conserved in all mammalian species whose *UPIIIa* sequence is known. Collectively, these observations alone make it highly likely that the *de novo* missense change is involved in the pathogenesis of the renal malformation. Recurrent mutations, which arise in CpG dinucleotides and which can occur *de novo*, have been reported in other diseases such as craniofrontonasal syndrome (Twigg et al. 2004).

Two cases of mutations in the 3'UTR of a gene, *UPIIIa*, were also found. Using the (purely theoretical) RNAfold analyses, it was noted that the *de novo* changes found in the

*UPIIIa* 3'UTR would be predicted to alter secondary structure of the mRNA, giving some credence to possible functional effects of the 3'UTR nucleotide changes. It is also interesting to note that the sequence TGT, altered by the 1003T→C mutation in *Family 4*, is the most common sequence found in the 3'UTRs of genes other than the polyadenylation signal (Louie et al. 2003). Although 3'UTR mutations have rarely been recognised, they have been reported to cause human disease, as described for α-globin in thalassemia (Waggoner et al 2003). There is considerable evidence that the 3'UTRs of many genes are critical in controlling the amount of proteins finally made (Waggoner et al. 2003; Erlitzki et al. 2002; Kakoki et al. 2004), and it is conceivable that the UPIIIa 3'UTR mutations operate in this manner. It is known that in *UPIIIa* null-mutant mice, UPIb is upregulated and incompletely glycosylated suggesting that the expression of *UPIIIa* and *UPIb* is interactive (Hu et al. 2000) and so altered *UPIIIa* expression levels may influence the expression of *UPIb* as well. Alternatively the effect of a 3'UTR mutation may be more complex. For example, microinjection of wild-type Prohibitin 3'UTR RNA can suppress cellular growth and proliferation, while an allelic variant associated with an increased risk of breast cancer and differing, like the *UPIIIa* mutations, by only one nucleotide, can not (Manjeshwar et al. 2003). Thus it is also possible that the 3'UTR RNA of UPIIIa has independent effects on the biology of the cell. Clearly, additional studies are needed to test hypotheses about how these *de novo* mutations may lead to disease.

Urothelial cells undergo endo/exocytosis to modulate urothelial surface area in response to changes in bladder pressure (Lewis et al. 1984) and binding of the *E. coli* FimH

receptor to UPIa mediates urothelial invasion of this bacterium (Zhou et al. 2001); unlike UPIa, UPIb or UPII, UPIIIa has a significant cytoplasmic tail, and it has been suggested that this region interacts with cytoplasmic proteins to mediate membrane/cytoplasmic interactions (Yu et al. 1994). I have shown in COS-1 cells that wild-type UPIIIa protein can only escape the endoplasmic reticulum and reach the cell surface in the presence of UPIb, as was shown previously in 293T cells (Tu et al. 2002). Although I hypothesised that the Pro273Leu mutation in the cytoplasmic domain of UPIIIa might prevent UPIIIa from reaching the cell surface, I showed that it was possible for the missense mutant protein to reach the cell surface in COS-1 cells when co-transfected with UPIb. In contrast, experiments in these COS-1 cells suggested that a variant in the extracellular domain that is associated with VUR (Pro154Ala) might negatively influence transport of the protein. On the other hand, it must be acknowledged that COS-1 cells might not be the ideal system with which to study targeting of an 'epithelial-cell protein' such as UP because polarised monolayer formation is not a characteristic of these cells. Mindful of this, I have performed preliminary experiments co-transfecting UPIIIa (either the wild-type or missense mutant) with wild-type UPIb into Madine-Darby Canine Kidney (MDCK) cells, a prototypical renal epithelial line. The results firstly demonstrate that these cells have no endogeneous expression of UPIIIa, at least as assessed by antibodies which detect human and bovine UPIIIa. Second, neither the wild-type nor the missense protein appears to reach the cell membrane i.e. the UPIIIa protein is only immunodetected in permeabilised, but not non-permeabilised, cells (data not shown). Difficulties with both the COS-1 and MDCK models may reflect lack of appropriate polarity and/or molecular machinery used for cellular transport of UPs. Moreover, even if

a mutant UPIIIa protein was targeted to the apical surface, following on from the hypothesis that the missense mutation may act in a 'dominant-negative' manner, one would need to measure relatively subtle biological readouts of plaque structure and epithelial function. The appropriate cell to study will be the human urothelial cell itself. Not only are these cells polarised, but they are known to have specific machinery to deliver UPs to the apical membrane, for example Rab27b (Chen et al. 2003). In addition, urothelial cells have the theoretical capacity to assemble plaques at the asymmetric unit membrane, and they also have specific physiological properties such as high transepithelial resistance (Hu et al. 2002). In future, the function of these mutations may be unravelled by expression of mutant UP proteins in 'Normal Human Urothelial' cells which can be propagated, and also induced to differentiate, in culture (Varley et al. 2004). These cells are susceptible to high efficiency retroviral transduction when proliferative (personal observation, J. Southgate) and, when differentiated, display physiological and biochemical characteristics of human urothelium found *in vivo*.

It is notable that the two patients with the Pro273Leu mutation also had severe primary VUR in combination with renal adysplasia; in contrast the individuals with a 3'UTR mutation had no bladder/ureteric phenotype, and the effect of these mutations may be a 'loss of function'. With regard to primary VUR, it is interesting that the missense mutation was not detected in two studies which screened *UPIIIa* in a total of 101 individuals with the condition (Giltay et al. 2004; Jiang et al. 2004); perhaps this can be explained by the facts that only a minor subset of primary VUR patients have bilateral renal adysplasia and the Pro273Leu mutation is probably lethal without intensive therapy

in early life. Furthermore, it has already been established, using a whole-genome search based on families with several affected members, that the condition called 'primary VUR' is in fact genetically heterogeneous (Feather et al. 2000).

To study the cellular basis of renal adysplasia, I studied the expression of UPIIIa and its partner, UPIb, during human development. The metanephros forms 28 days after fertilisation when the ureteric bud penetrates the renal mesenchyme (Potter 1972). Ultimately, the ureteric bud lineage forms urothelium, from the renal pelvis to bladder trigone, and kidney collecting ducts. The first 6-10 bud branch generations remodel, generating the renal pelvis and calyces, while the subsequent generations form collecting ducts; nephron tubules form as branch tips induce adjacent renal mesenchyme. Using micro-dissection studies of dysplastic kidneys, Potter (1972) reasoned that the primitive tubules found in some human dysplastic kidneys represent early ureteric bud branches which fail to remodel into a normal renal pelvis and which also fail to produce further, nephron-inducing branches. As kidneys and ureters form, the UGS demarcates from the cloaca to form the bladder, and stroma around primitive urothelia forms smooth muscle; clearly, these developmental events have gone wrong in congenital malformations such as persistent cloaca. UPs are expressed in postnatal human urothelia (Olsburgh et al. 2003) and UPIb has been detected in human bladder urothelia at 10 weeks gestation (Jiang et al. 2004). The data that I have presented here, using for the first time a UPIIIa-specific antibody, shows that expression of both UPIIIa and UPIb plaque-partner proteins also occurs in the early stages of human organogenesis. UPIIIa and UPIb are expressed at 13 weeks in the urothelium of the bladder, ureters and renal pelvis and at 7 weeks in the

UGS, evagination of which is a crucial event in distal female genital tract formation (Shapiro et al. 2000), and which is relevant to the cloacal malformation seen in the proband in *Family 1*. These findings therefore put UPIIIa in place to affect kidney development in its earliest stages. Furthermore, the fact that UPIIIa is expressed in the renal pelvis, but not in the kidney itself, suggests the observed *UPIIIa* mutations might cause renal adysplasia by affecting the pelvicalyceal system, or by disrupting metanephric development secondary to impaired urine flow.

## 3-2 Study II. Mutational analyses of *UPII* in patients with renal adysplasia

Hypothesis - Mutations in *UPII* cause human renal tract malformations;

Aim - To seek *UPII* mutations in patients with bilateral renal adysplasia.

### 3-2-1 Background

As I have described in the previous section, the discovery of *UPIIIa* mutations established a role for the UPs in human renal tract development and disease. Shortly after I had identified these mutations and established their pathogenicity, it was reported that mice with null mutation of another member of the UP family, *UPII*, lack urothelial plaques and often have congenital hydronephrosis associated with either primary VUR or with urothelial cell overgrowth, the latter causing ureteric obstruction (Kong et al. 2004). These observations led to the hypothesis, tested in the current study, that *UPII* mutations may be present in humans with renal tract malformations.

### 3-2-2 Results

Mutations of the gene *UPII* were sought in *Groups 1*, *2* and *3* (of 42 children with renal tract anomalies) by directly sequencing all five exons of the gene as well as the surrounding sequences. All but one had normal *UPII* sequencing; the clinical history of this one patient in whom a heterozygous genetic change was found in *UPII* is as follows.

*Family 5*

A Caucasian female presented at the age of eight years to her local Paediatric Department with a one year history suggestive of symptomatic lower urinary tract infections, at least

one of which had been confirmed by a positive culture from a mid-stream urine specimen. She also reported a tendency to poor bladder emptying and had experienced nocturia (x1 per night) for several years. A micturating cystourethrogram showed marked (grade IV) VUR bilaterally (Figure 18A). Ultrasonography revealed dilated distal ureters bilaterally (Figure 18B) and both left and right kidneys were 'small' and hydronephrotic (Figure 18C, D). A scan, following intravenous administration of $^{99m}$Technetium-diethylenetriaminepentaacetic acid (an isotope undergoing glomerular filtration and tubular secretion), showed poor uptake bilaterally, with 71% of total function in the left system. Plasma creatinine was 227 μM (2.55 mg/dl), and creatinine clearance, based on 24 hour urine collection, was 22 ml/min/1.73 $m^2$. She received treatment with 1α vitamin D for biochemical hyperparathyroidism and prophylaxis against urinary tract infection with low dose Trimethoprim.

The subject had been born at 36 weeks gestation by normal vaginal delivery following a pregnancy that had been uneventful, apart from the fact that the mother had chicken pox at the time of the patient's delivery; the patient was treated with immunoglobulin and had the disease mildly. The subject has two sisters (aged 15 and 22 years) and there was no definite family history of renal disease, although the father had complained of having a 'weak bladder' and the mother's sister had a history of systemic hypertension. Subsequently, the parents and both sisters underwent renal ultrasonography with normal findings; both the mother's parents were deceased at this point.

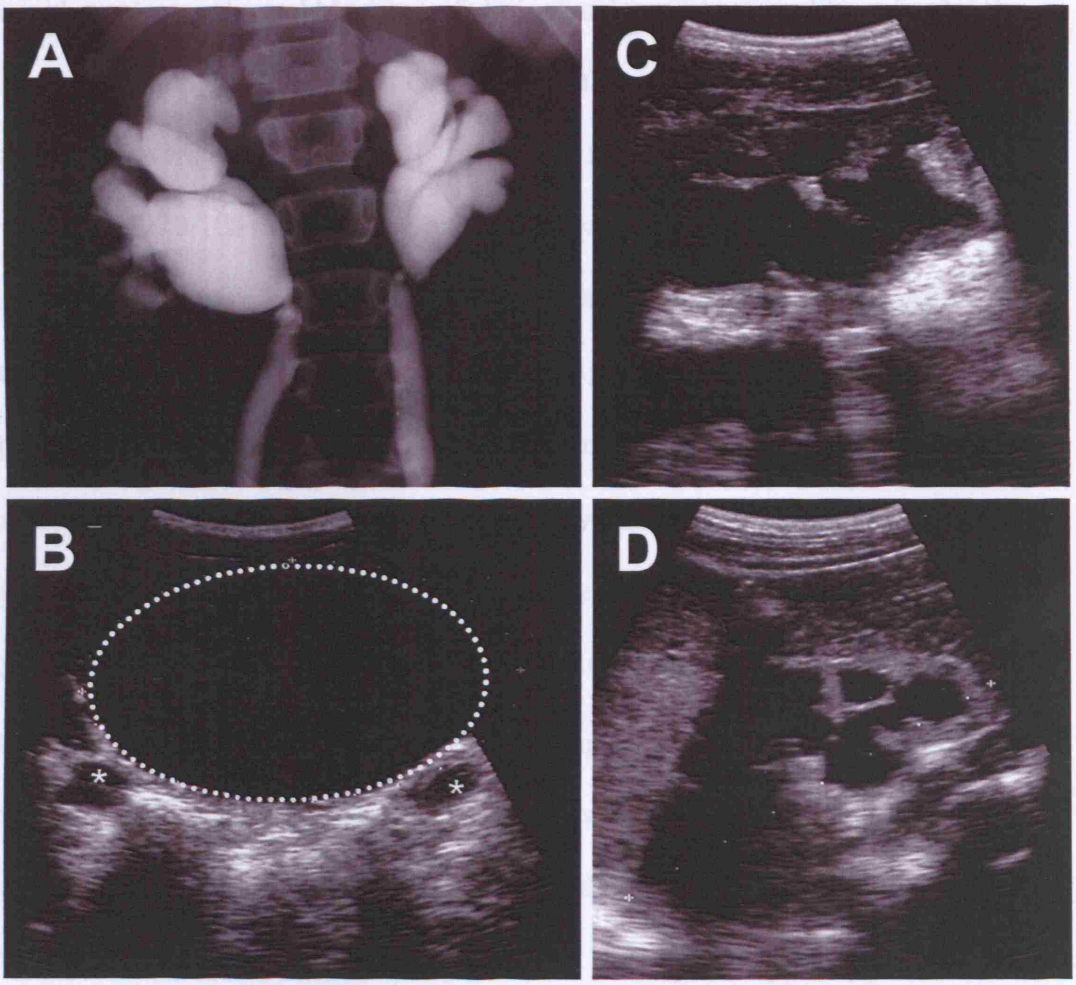


**Figure 18. Radiology of index patient with a *UPII* mutation.**
(**A**) Bilateral VUR on micturating cystogram. (**B-D**) Ultrasonography showed: **B** dilated ureters (*) behind bladder (dotted line); **C** and **D** are hydronephrotic right and left kidneys, respectively.

One year after presentation, the subject complained of a three month history of headaches. She was found to be hypertensive (170/110 mmHg) and commenced on treatment with a calcium channel blocker (nifedipine) and was transferred from her local hospital to the Nephrology Unit at Great Ormond Street Hospital. Her height (123 cm) and weight (22 kg) were both below the $10^{th}$ percentile for age and sex. Her admission blood pressure was 140/100 mmHg and electrocardiogram showed left ventricular hypertrophy, consistent with a long-term history of high blood pressure and suggestive of chronic renal disease that may therefore have had a congenital basis. She was in renal failure (plasma creatinine 255 μM), and was also acidotic (plasma bicarbonate 16 mM) with a mildly raised parathyroid hormone level. Oral hydralazine, frusemide, sodium bicarbonate and calcium carbonate were added to her regimen. A midstream urine showed plentiful white cells but without growth on culture, and she had proteinuria (3+ on dip-stick testing). A renal scan with $^{99m}$Tc-dimercaptosuccinic acid, an isotope concentrated only in normally-functioning tubules, showed poor uptake bilaterally, with 94% of total uptake on the left. Ultrasound scan showed two bright kidneys with loss of corticomedullary differentiation (right 47 mm long and left 81 mm long; median for age 90 mm); the urinary bladder contained 638 ml but failed to empty completely, with a post-micturition residue of 107 ml. Because of the apparently incomplete bladder emptying, she underwent a trial of continuous urinary catheter drainage, but her plasma creatinine level failed to fall over one week.

Subsequently, the level of renal failure progressed and continuous ambulatory peritoneal dialysis (CAPD) was commenced, followed by a cadaveric renal transplant at the age of

11 years. After a series of rejection episodes, followed by post-transplant lymphoproliferative disease associated with Esptein Barr virus infection, a transplant nephrectomy was performed four months later and CAPD was recommenced. Visualisation of her optic discs and retina by a Consultant Ophthalmologist (performed during investigations for headaches) revealed no abnormality. A second cadaveric renal transplant was performed when she was 13 years old; function was compromised by chronic allograft nephropathy several years later, necessitating the return to the dialysis programme. At 15 years of age the patient had failed to undergo menarche and an ultrasound, performed as part of the investigations showed a bicornuate uterus. Menstruation finally started at the age of 17 years.

Four bases (CACT) were inserted at nucleotide position 215 (Figure 19B). This results in a frameshift predicted to affect the UPII protein at codon 60, altering the seven amino acid residues encoded by codons 61 to 67 and inserting a premature termination codon at 68; this change was therefore designated L60fsX68. The final postulated effect on the UPII protein is shown in Figure 19C and D i.e. the UPII pre- and pro-sequences fused to a short, novel peptide. The same genetic change was also detected in leukocyte DNA from the mother, but not in the father, both of whom had normal renal ultrasounds. The renal tracts of the two sisters of the index case were also deemed normal as assessed by ultrasound scanning, although DNA samples from them were unavailable for analysis because permission for venesection was not granted; DNA was also unavailable for the two maternal grandparents because they were deceased. This genetic change was absent in 96 Caucasian control individuals (192 chromosomes), as assessed by direct sequencing

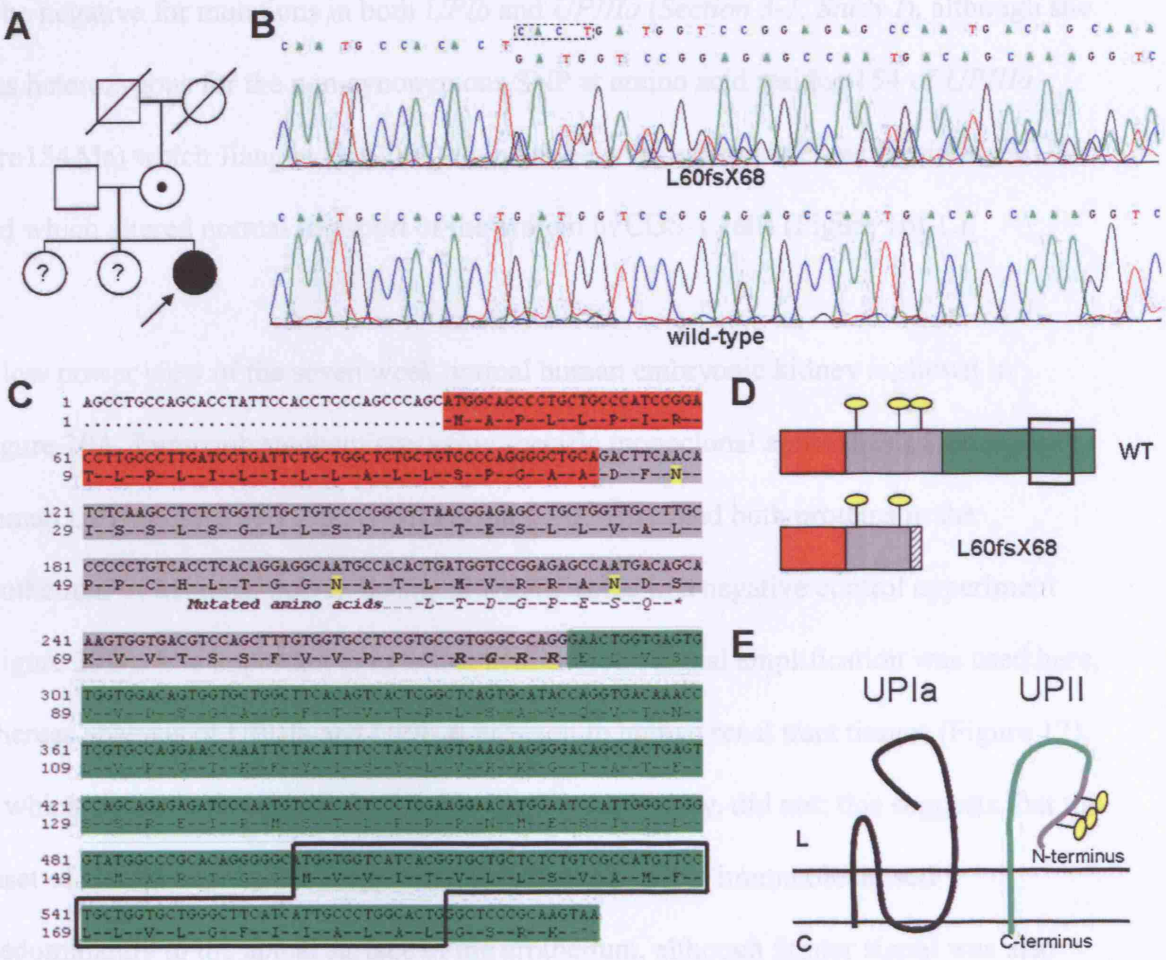


**Figure 19. Genetic analysis of UPII.**

(**A**) Pedigree of *Family 5*. Index case (arrow), with sisters and both parents having normal ultrasonography: the mother's parents were deceased at the time of this study. The UPII heterozygous change was found in the index case and her mother. ? indicates that genetic analysis was not done (venesection declined in siblings). (**B**) Upper panel shows heterozygous frameshift change of UPII, with wild-type sequence in lower panel; the inserted nucleotides, CACT, are indicated by the box. (**C**) Nucleotide and protein sequence, with the pre-sequence of the protein in red, the pro-sequence in grey and the mature protein in green; potential glycosylation sites shown as yellow ellipses; furin-cleavage site (RGRR) is underlined in yellow. (**D**). The wild-type (upper panel) and postulated variant (lower panels) proteins. Boxes in **C** and **D** indicate transmembrane sequence. (**E**) Wild-type UPII associated with its plaque-partner UPIa in the endoplasmic reticulum; the glycosylated pro-sequence of UPII (grey) will be removed in the trans-Golgi network (Hu et al. 2005a).

of *UPII* exon 2, and an additional 54 controls (108 chromosomes) were also genotyped as homozygous wild-type by *Ms1*I restriction digest. The index case was previously shown to be negative for mutations in both *UPIb* and *UPIIIa* (*Section 3-1, Study I*), although she was heterozygous for the non-synonymous SNP at amino acid residue 154 of *UPIIIa* (Pro154Ala) which Jiang et al. (2004) found to be weakly associated with primary VUR and which altered normal transport of the protein in COS-1 cells (Figure 16I-L).

A low power view of the seven week normal human embryonic kidney is shown in Figure 20A. Immunohistochemistry using specific monoclonal antibodies raised against human UPII (Figure 20B) and UPIIIa (Figure 20C) detected both proteins in the urothelium of the renal pelvis: no signal was detected in a negative control experiment (Figure 20D). It is important to note that avidin-biotin signal amplification was used here, whereas analysis of UPIIIa and UPIb expression in human renal tract tissues (Figure 12), in which UPIIIa could not be detected in the 7 week kidney, did not; this suggests that the onset of UPIIIa expression is approximately 7 weeks. UPII immunolocalised predominantly to the apical surface of the urothelium, although fainter signal was also detected apparently on other urothelial cell surfaces: by contrast, UPIIIa was exclusively detected in an apical location.

### 3-2-3 Interpretation and interim discussion

This study, the first to examine *UPII* in human congenital renal diseases, offers no definitive support for *UPII* mutations causing these conditions. In particular, no *de novo* mutations were detected in 42 index cases. I did, however, immunolocalise UPII in the

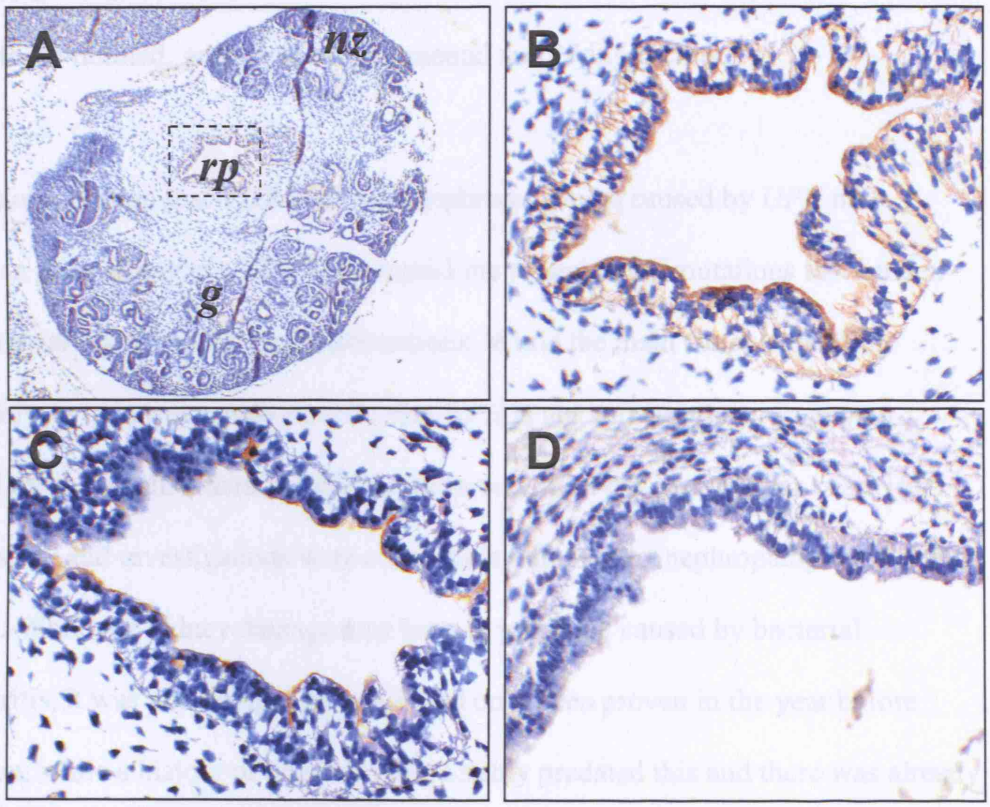


**Figure 20. UP immunohistochemistry in a seven week metanephros.**
(**A**) Low power view shows whole kidney with nephrogenic zone (nz), first glomeruli (g) and renal pelvis (rp). **B** and **C**, respectively, show UPII most prominently, and UPIIIa exclusively, localised to the apical zone of the urothelium. (**D**) No signal with preimmune IgG.

urothelium of the developing normal human renal tract in a pattern similar to UPIIIa, and also found a heterozygous frameshift change of *UPII* in a single index case who had VUR, nephropathy and renal failure. I would postulate that *UPII* mutations may occasionally predispose individuals to renal tract malformations in conjunction with other, yet-to-be-defined, genetic or environmental modifying factors.

The recent observation that VUR and hydronephrosis can be caused by *UPII* null-mutations in mice (Kong et al. 2004) prompted me to seek *UPII* mutations in 42 index cases with a variety of renal tract malformations. While the main conclusion to the genetic analyses in current study must be that *UPII* is not a major player in human congenital renal tract disorders, a *UPII* insertion was observed in one index case. Her clinical history and investigations were compatible with 'reflux nephropathy' associated with VUR. While the kidney damage may have in part been caused by bacterial pyelonephritis, it was notable that urosepsis had only been proven in the year before presentation, while a history of nocturia considerably predated this and there was already marked somatic growth impairment at presentation: this is consistent with a long history of established renal failure. Perhaps her nephropathy had a congenital basis (hypoplasia/dysplasia), as has been increasingly recognised in the primary VUR population with renal failure (Woolf & Wilcox 2004). Could the frameshift change found in *UPII* have contributed to the pathogenesis of renal disease in the current index case? Here I examine evidence 'for' and 'against' this contention.

Several observations would support a role in pathogenesis. First, it was absent in 150 healthy Caucasian control individuals (96 assessed by direct sequencing and another 54 by restriction digests), making it rather unlikely that it was a 'chance occurrence', unrelated to the renal disease. Second, the genetic change would have major functional implications with regard to the UPII protein. The frameshift might encode a transcript that undergoes accelerated decay or, if such a transcript were to be translated, it would lead to a radical truncation of the wild-type sequence to generate a protein lacking relevant domains for interaction of pro-UPII with its plaque partner, UPIa, a process essential for exit of the complex from the endoplasmic reticulum: insertion of UPII into cell membranes would also be prevented (Hu et al. 2005a; Lin et al. 1994). One can postulate that in such a case, the human renal tract malformation in the current case results from 'haploinsufficiency' because the genetic change only affects one of the two *UPII* alleles. On the other hand, because the glycosylated pro-sequence may regulate formation of UP heterotetramers (Hu et al. 2005a), it is conceivable that the frameshift mutation is 'dominant-negative', interfering with the function of UPII protein generated by the wild-type allele. Third, as demonstrated for the first time in this study, UPII protein, like UPIIIa, is immunolocalised to the nascent human urothelium at seven weeks gestation: therefore, it could begin to have a critical function at a very early stage of human renal tract development.

Other observations, however, question whether the insertion does contribute to pathogenesis. First, an insertion-deletion polymorphism ('indel') of *UPII* has been reported in dbSNP (www.ncbi.nlm.nih.gov/SNP; rs5795154), and this would cause a

frameshift at amino acid residue 56 leading to a premature termination at residue 60, thus generating a truncated protein similar to the L60fsX68 protein. However, this database entry is unvalidated, and neither this, nor any other, 'indel' was observed by direct sequencing of exon 2 in either 96 controls (this study) or by sequencing of the entire gene in either 41 additional patients (this study) or in 76 patients with primary VUR (Jiang et al. 2004); also, no clinical information is available regarding the individual in whom this variant was apparently detected. Second, our index case's mother had a normal renal ultrasonography but carried the same heterozygous *UPII* change as her affected daughter. In this regard, it should be noted that ultrasonography will not detect all structural defects and, in the mother's case, it was not considered clinically-justified to perform cystography (to seek VUR) or intravenous urography/isotope scanning (to seek renal parenchymal/calyceal defects). It could also be postulated that this family exhibits 'incomplete penetrance' for renal tract anomalies. In this regard, inheritance in some humans with non-syndromic renal anomalies has been considered autosomal dominant with incomplete penetrance, with carriers having only a 50-90% chance of displaying a phenotype (McPherson et al. 1987). Furthermore, in several human malformation syndromes, the occurrence and severity of renal anomalies varies strikingly between individuals carrying the same mutations e.g. in the renal-cysts-and diabetes (*HNF1*β mutations; Edghill et al. 2005) and the renal-coloboma (*paired box 2* mutations; Schimmenti et al. 1997) syndromes. Additionally, mice carrying *UPII* null mutations (in homozygous state) only display hydronephrosis with a penetrance of 80% and the mutation only reproducibly causes juvenile renal failure in the progeny of certain breeding pairs (129/SvEv x Swiss Webster) (Kong et al. 2004).

Perhaps, rare alleles of *UPII* encoding a truncated protein are present in the general population and these variants predispose to renal malformation. Congenital renal disease would only result, however, when a heterozygous *UPII* change was present with other factors which could perturb renal differentiation. Such a factor might be a 'modifying gene' and, in this regard, it is noteworthy that the index case was also heterozygous for the Pro154Ala *UPIIIa* variant significantly associated with primary non-syndromic VUR (Jiang et al. 2004); unfortunately insufficient DNA from the mother remained following analysis of *UPII* to genotype her for this variant in *UPIIIa*. It is increasingly evident that diverse environmental factors can alter the trajectory of kidney and urinary tract differentiation (Welham et al. 2005; Tse et al. 2005). As a neonate, the index case was exposed to varicella infection because the mother had chicken pox at the time of delivery. Exposure of foetuses to this virus, especially in midgestation, can cause severe neuropathic bladder associated with VUR (Fujita et al. 2004; Koren et al. 2005). Even though the current case lacked other classical features of the full-blown congenital varicella syndrome (developmental delay, microphthalmia/microcornea, limb hypoplasia and gut dysfunction), the large bladder capacity together with incomplete emptying is suggestive of an accompanying neural component. It is possible to postulate that her renal tract disease could have been generated by a (mild) viral infection in an individual who was genetically-predisposed to renal tract anomalies by virtue of carrying a variant of *UPII*, a gene expressed in the maturing renal tract.

## 3-3 Study III. Mutational analyses of *UPIIIa* and *SHH* in persistent cloaca and associated malformations

Hypothesis - Mutations in *UPIIIa* and *SHH* cause persistent cloaca;

Aim - To seek *UPIIIa* and *SHH* mutations in patients with persistent cloaca.

### 3-3-1 Background

Concurrent with the genetic analyses presented above, a DNA collection of girls with persistent cloaca was being undertaken by Louise Thomasson, Duncan Wilcox and Adrian Woolf at the Institute of Child Health, London. This malformation of the urinary tract commonly coexists with renal anomalies (see Table 5 below). Persistent cloaca has been associated with chromosome 7q rearrangements (Miller et al. 1979), and mutations that disrupt a single gene, *DHCR7*, can cause persistent cloaca in combination with renal aplasia/hypoplasia/ectopia as part of the Smith-Lemli-Opitz syndrome (Kelley et al. 2000), demonstrating that this malformation can have a genetic basis, at least in some individuals. Indeed, one patient in whom a *de novo* Pro273Leu *UPIIIa* mutation was identified presented with this malformation (Index case from *Family 2*). This led me to investigate the general contribution of *UPIIIa* mutations to the pathogenesis of persistent cloaca in a group of patients typically presenting to Nephrologist/Urologists. I also screened a second candidate gene, *SHH*, mutations of which have been associated with upper and lower renal tract malformations in man (Dubourg et al.2004 ; Hehr et al. 2004; Heussler et al. 2002) and persistent cloaca in mice (Mo et al. 2001).

### 3-3-2 Results

20 patients with persistent cloaca and associated malformations were screened for mutations in *UPIIIa* (Table 5). Previously-reported *UPIIIa* coding region SNPs (Jiang et al. 2004) were found at nucleotide residues 402 (C/T), 460 (C/G), 549 (A/G), 858 (A/G): in particular, the exon 3 variant affecting a C/G conversion and a Pro154Ala change, reported to be associated with primary VUR (Jiang et al. 2004), was found in a heterozygous state in five patients; this is equivalent to an allele frequency of 12.5% that is slightly lower than the frequency previously reported in controls (16%) and individuals with primary VUR (25%) (Jiang et al. 2004), although no statistical inference can be made in this small, ethnically diverse group. The three *UPIIIa* mutations that I identified in patients with severe bilateral renal adysplasia were not observed in this cohort, and a PCR restriction fragment length polymorphism assay for the 818 C/T mutation showed that while the previously reported *Patient 6* (this study) was a heterozygote, all other patients were homozygous for the wild-type allele.

In *Study IV*, I have established *SHH* as a candidate gene for persistent cloaca, it being expressed in the cloaca of a 4 week gestation embryo, a stage when septation of the cloaca is in progress (Nievelstein et al. 1998; Pennington & Hutson 2002a; Qi et al. 2000; Sasaki et al. 2004a). In the *SHH* gene, one variant was observed in patients with persistent cloaca, a known SNP in intron 2 (rs1233555).

*Table 5. Clinical features of individuals with persistent cloaca.*

| Patient | Kidney malformations | Kidney function | Associated local/other organ malformations |
|---|---|---|---|
| 1 | DYSK (L and R) VUR (L and R) | CRF (11 yrs) | SVD, UM |
| 2 | SNK | NRF (3 yr) | ASD, SVD, UM, VSD |
| 3 | Hydronephrosis (L and R) | CRF (3yr) | SVD, UM |
| 4 | RE, VUR | CRF (6 yr) | Dextrocardia, SVD, UM |
| 5 | DUPK, DYSK, VUR (L and R) | CRF (8 yr) | AG, SVD, UM |
| 6 | SOK, VUR (L) | ESRF (16 yr) | AG, OVD, UD, UM, VSD |
| 7 | SNK | NRF (3 yr) | Caudal regression, SVD, UM |
| 8 | DYSK, VUR (L) | NRF (4 yr) | OVD, SVD |
| 9 | RE | CRF (2 yr) | SVD |
| 10 | DYSK, VUR (L) | NRF (6 yr) | SVD, TOF |
| 11 | DYSK (R), VUR (L and R) | CRF (6 yr) | ASD, SVD |
| 12 | RE | ESRF (9 yr) | Bladder atresia, OVD VACTERL |
| 13 | VUR (L) | CRF (6 yr) | SVD, UM |
| 14 | SOK (R) | NRF (1 yr) | UM |
| 15 | DYSK (L and R) | CRF (3yr) | UM, VSD |
| 16 | VUR (L and R) | NA | SVD, UM |
| 17 | VUR (L and R) | CRF (5 yr) | SVD, UM |
| 18 | DYSK (L and R) | ESRF (14 yr) | AG, SVD, TOF, UM, VACTERL |
| 19 | DUPK (L and R) | NRF (13 yr) | UM |
| 20 | SNK | NRF (4yr) | SI, SVD, VSD |

*Patient 2* had a mother with diabetes mellitus and *Patient 6* is the patient with a *UPIIIa* mutation (Pro273Leu).

Key: AG, ambiguous genitalia; ASD, atrial septal defect; CRF, chronic renal failure (i.e. either a plasma creatinine concentration above the normal range for age and/or a $^{51}$chromium EDTA GFR below 80 ml/min/1.73m$^2$; age in years at last measurement in parentheses); DUPK, duplex kidney and DYSK, dysplastic kidney (i.e. as assessed by radiological findings); ESRF, end-stage renal failure (i.e. long-term dialysis or functioning renal transplant); L, left; NA, not available/not assessed; NRF, normal renal function (i.e. not CRF or ESRF); R, right; RE, renal ectopia; SVD, sacral vertebral defect; OVD, other (i.e. non-sacral) vertebral defect; SI, situs inversus; SNK, structurally normal kidneys (i.e. assessed by radiology); SOK, solitary kidney; TOF, tracheoesophageal fistula; UD, urethral duplication; UM, uterus malformation (i.e. hydrocolpos and/or bicornuate/unicornuate uterus); VACTERL is the VACTERL association; VSD, ventricular septal defect; VUR, vesicoureteric reflux.

### 3-3-3 Interpretation and interim discussion

This study is the first to search for mutations that cause persistent cloaca in a cohort of patients typically presenting to Nephrologists and Urologists and, although the results are negative, it offers a contribution to the genetics of persistent cloaca and associated renal malformations. This study shows that persistent cloaca is only rarely associated with *UPIIIa* mutation and offers no support for an involvement of *SHH* mutations.

In this study direct sequencing was used, the "gold-standard" for mutation screening; this investigation can therefore reliably exclude any missense, nonsense, frameshift or splice-site mutations in *SHH*, or additional mutations in *UPIIIa*, in persistent cloaca patients. However, the strategy of direct sequencing would not detect large heterozygous deletions or mutations in regulatory sequences, and so these alterations are not excluded as causes of this birth defect.

Apart from these caveats, the simplest explanation as to why no pathogenic mutations were identified is that they simply haven't happened to occur in these genes in these particular patients and so it will be interesting to screen for mutations in other genes in these patients in the future. Obvious candidates would include other genes in the same molecular signalling pathways as the four analysed in this study (e.g. *GLI* genes in the *SHH* pathway). Mutations of the *HLXB9* homeobox transcription factor gene have been reported in the Currarino triad (Hagan et al. 2000), a disorder which consists of partial sacral agenesis, anorectal anomalies (imperforate anus, ectopic anal position or rectovaginal fistula), and a presacral mass (anterior meningocoele or teratoma). On

occasion, the triad can be associated with neurogenic bladder, VUR and bicornuate uterus. Mutations of another homeobox transcription factor gene, *HOXA13*, occur in the hand-foot-genital syndrome (Goodman et al. 2000), a condition which can be associated with paramesonephric duct fusion disorders and ureteric malformations. Furthermore, mutations in mouse homologous and orthologous genes cause a spectrum of anomalies in female genital, urinary and alimentary tracts reminiscent of human persistent cloaca (Warot et al. 1997). Although none of the current set of patients met the criteria for either the Currarino triad or the hand-foot-genital syndrome, it may in future be informative to seek *HLXB9* and *HOXA13* mutations in patients with persistent cloaca. Other disorders in which renal tract and uterine anomalies can coexist include: Mayer-Rokitanski-Kuster-Hauser syndrome (absent structures derived from paramesonephric ducts; a case with unilateral renal agenesis and *WNT4* mutation has been described) (Biason-Lauber et al. 2004); and the McKusick-Kaufman and Bardet-Biedl syndromes (vaginal atresia, urogenital sinus, ectopic urethra, no urethral opening, no vaginal opening, gut fistulae) (Slavotinek et al. 2000).

Finally, it should be noted that persistent cloaca could be considered as but one phenotype of a broader spectrum of malformations. Evidence for this contention derives from genetic studies in mice because animals with genotypes $Gli2^{+/-}/Gli3^{-/-}$, $Gli2^{-/-}/Gli3^{+/-}$ (Mo et al. 2001), $Efnb2^{lacZ/lacZ}$ (Dravis et al. 2004) and $Hoxa13^{-/-}/Hoxd13^{-/-}$ (Warot et al. 1997) have persistent cloaca, whereas mice with other combinations of mutations in these pathways have recto-vaginal/recto-urethral fistula ($Gli2^{-/-}$) (Mo et al. 2001), anal stenosis/ectopic anus ($Gli3^{-/-}$) (Mo et al. 2001), hypospadias

(*Efnb2*$^{+/lacZ}$, *Ephb2*$^{-/-}$/*Ephb3*$^{-/-}$) (Dravis et al. 2004) and urethral-vaginal/recto-vaginal fistula with uterine malformations (*Hoxa13*$^{+/-}$/*Hoxd13*$^{-/-}$) (Warot et al. 1997), showing that, in genetic terms, persistent cloaca lies within the same spectrum of malformations as these more mild urethral/ARMs. If this can be taken as a paradigm for human disease, then it would be logical to seek mutations of *UPIIIa* and *SHH* in a similar, wider spectrum of malformations.

All index cases in the current study have had routine karotyping performed, with confirmation of XX status and no major cytogenetic anomalies found. On the other hand, perhaps 'submicroscopic deletion(s)' may be present in some cases. In future, new technologies such as microarray comparative genomic hybridisation (Snijders et al. 2003) could be used to seek small deletions and chromosomal amplifications and may give clues with regard to other candidate genes in humans with persistent cloaca.

## 3-4 Study IV. Expression analyses of Sonic hedgehog pathway proteins in human renal tract tissues

Hypothesis - Sonic hedgehog signalling proteins are expressed at key stages during human renal tract development;

Aim - To immunolocalise the core SHH signalling proteins during human renal tract development.

### 3-4-1 Background

It has been shown that *UPIIIa* mutations (*3-1, Study I*), and a polymorphism (Jiang et al. 2004) that alters protein transport (*3-1, Study I*), can cause/predispose to malformations of the upper (renal adysplasia) and lower (VUR, persistent cloaca) renal tract. Indeed, UPIIIa is expressed throughout the renal tract, from the renal pelvis to the bladder neck, although the precise functions of UPIIIa in renal tract development and disease will require future biochemical and functional analyses. Other molecules/pathways also have dual roles in upper and lower tract development, an example recently of interest being vitamin A signalling (Batourina et al. 2001).

Genetic disruption of SHH signalling is associated with many of the renal tract malformations studied in this thesis. Specifically, defective cholesterol metabolism, caused by *7-dehydrocholesterol reductase* (*DHCR7*) mutations, is thought to disrupt autoprocessing of SHH (Guy 2000) and signal transduction by SMO (Cooper et al. 2003), and is associated with hypoplasia/aplasia/cortical cysts/foetal lobation of the kidney, bladder/ureter hypoplasia, ureteric duplication, hypospadias and persistent cloaca in

patients with the Smith-Lemli-Opitz syndrome (reviewed in Kelley & Hennekam 2000). Furthermore, heterozygous mutations in *SHH* itself are associated with renal hypoplasia (Dubourg et al. 2004), urogenital malformation (Dubourg et al. 2004), polyuria/eneuresis (Heussler et al. 2002) and hypospadias (Hehr et al. 2004). Mutation of *GLI3* is also associated with urinary tract/cloacal malformations in humans as part of the Pallister-Hall syndrome, including UGS, VUR and hypospadias (Johnston et al. 2005). This suggested that the SHH pathway might provide an interesting paradigm to understand the variety of independent roles that a group of molecules can conduct in different tissues within the human renal tract, especially given the detailed understanding of this pathway at the biochemical level (Lum & Beachy 2004; Bitgood & McMahon 1995).

Mice carrying a targeted mutation of *Shh* also display kidney (Yu et al. 2002; Hu et al. 2005b) and cloacal (Mo et al. 2001) malformations, showing that SHH signalling is involved in a number of aspects of renal tract development. However, while cloacal development in mice of genotype $gli2^{-/-}$ or $gli3^{-/-}$ is aberrant, resulting in ARM or persistent cloaca (Mo et al. 2001), the kidneys of these mice are normal (Hu et al. 2005b). This led to the hypothesis that the hedgehog signalling machinery is implemented differently in the development of the upper versus lower renal tract. To investigate this possibility, and to determine whether studies in mice can be extended to the human condition, the spatio-temporal distribution of the core SHH signalling molecules were carefully analysed in human embryonic tissues with respect to markers of cellular proliferation or differentiation. This has allowed hypotheses stemming from biochemical and animal genetic studies to be tested, serving to identify precise molecular mechanisms

defining the differential susceptibility of human tissues within the renal tract to genetic insults on SHH signalling.

### 3-4-2 Results

In order to explore the role of SHH signalling during septation of the human cloaca, immunohistochemistry was performed using specific antibodies raised against SHH, PTCH and SMO on transverse sections of a 4 week gestation embryo (Figure 21A-C). At this stage, all three proteins were detected in the cloacal epithelium at a level slightly cranial to the urorectal septum. Furthermore, BMP4, a putative downstream target of hedgehog signalling (Lum & Beachy 2004; Bitgood & McMahon 1995), was also expressed in this epithelium at an axial level marking the caudal border of the urorectal septum (Figure 21D). These results show that SHH signalling, that is essential for normal partition of the cloaca into distinct urogenital and digestive tracts in mice (Bose et al. 2002; Mo et al. 2001), regulates signalling within epithelial, rather than mesenchymal, cells during this process.

Next the newly formed UGS was investigated at 7 weeks gestation. I first sought to describe differentiation of this nascent bladder in detail in order to implicate SHH signalling in this process, as has been demonstrated in the mouse ureter (Airik et al. 2005; Yu et al. 2002). The series of sections in Figure 22 shows that, while the UGS and rectal epithelia are distinct, the mesenchyme of each of these tracts becomes progressively separated at more cranial levels by the formation of the peritoneal cavity and its expansion around the future anorectum, and with situation of the

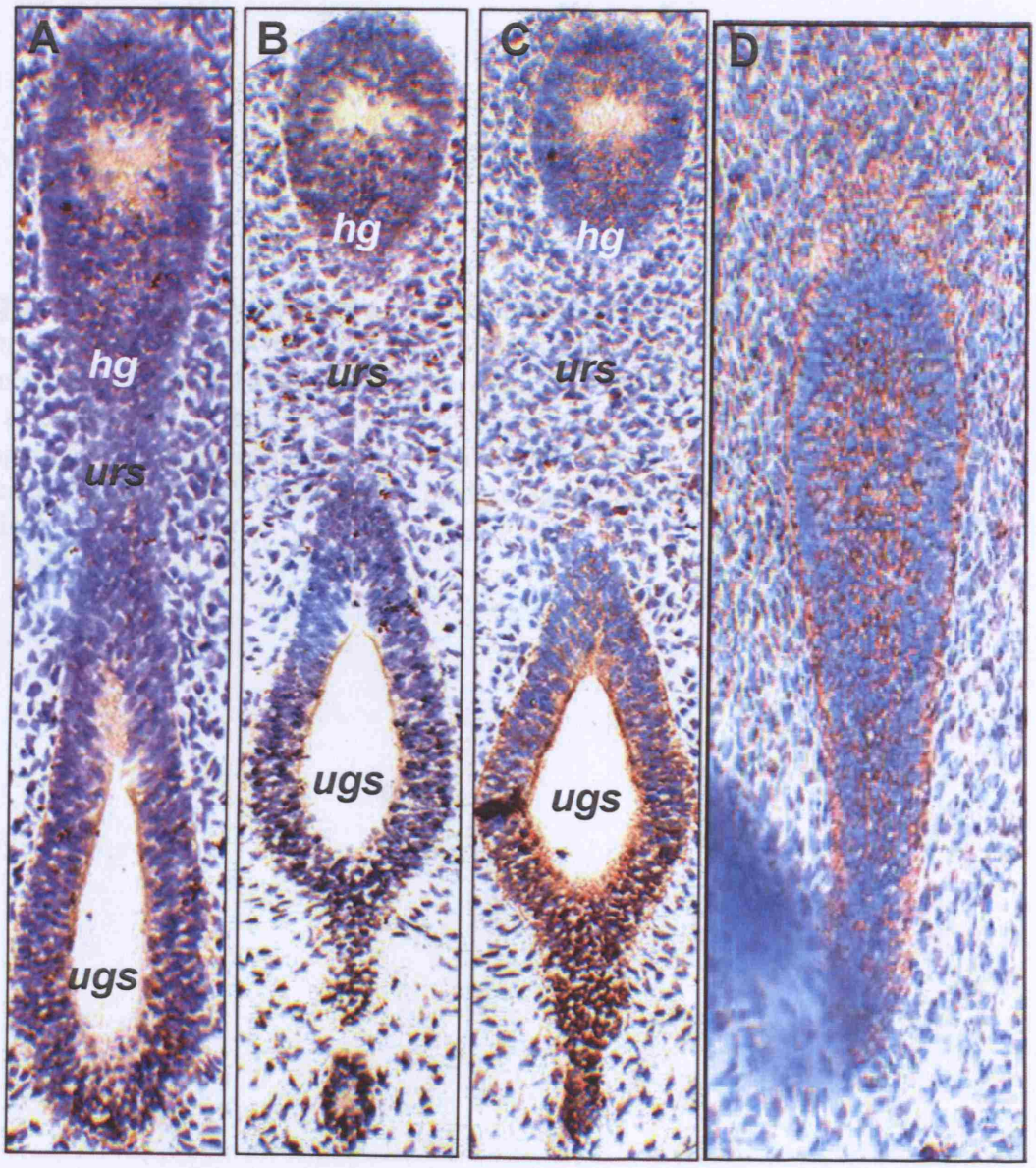


**Figure 21. SHH immunohistochemistry in a 4 week cloaca**
Immunolocalisation of SHH (A) PTCH (B) SMO (C) and BMP4 (D) in epithelia of the urogenital sinus (*ugs*) and (*hg*) of the cloaca that is undergoing septation. *urs*, urorectal septum.

**Figure 22. Differentiation of a 7 week urogenital sinus.**
Expression of 'UP' (brown signal) and αSMA (pink/red signal) in a series of transverse sections of the urogenital sinus (ugs) from most caudal (A) to most cranial (E) axial level. A'-E', high-power view of the urothelial membrane. Note in A'-E' images have been rotated 60° anti-clockwise relative to A-E to allow larger images to be captured. V, ventral; D, dorsal; hg, hindgut; ugs, urogenital sinus; pc, peritoneal cavity.

*Figure 22*

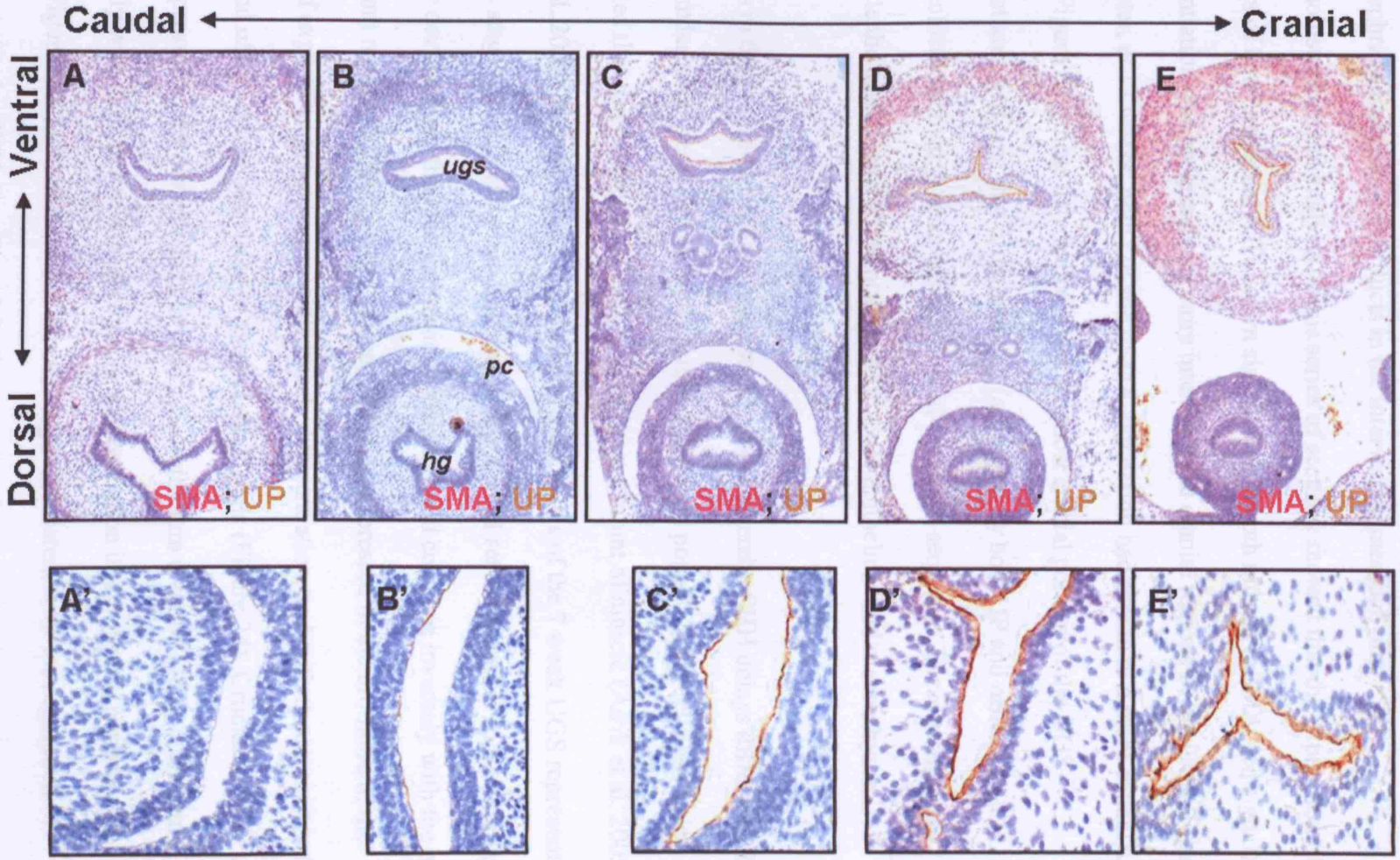
Caudal
Cranial
Ventral
Dorsal
A
B
C
D
E
ugs
pc
hg
SMA; UP
SMA; UP
SMA; UP
SMA; UP
SMA; UP
A'
B'
C'
D'
E'

mesonephric/paramesonephric ducts in the intervening mesenchyme. Immunohistochemical analysis of this series of sections showed that the expression of markers of both urothelial (UP, brown signal) and smooth muscle (αSMA, red signal) differentiation was progressively more intense in the cranial regions of the UGS (Figure 22). Later, at 13 weeks, both UP and αSMA expression had spread to a more caudal axial level (Figure 23); these data indicate that the most cranial portion of the UGS differentiates first, and that differentiation (as judged by both UP and αSMA immunohistochemistry) proceeds in a cranial-to-caudal sequence. These results also illustrate the co-ordinate differentiation of bladder epithelium and mesenchyme.

Studies in the mouse ureter have suggested a model whereby SHH delays differentiation of the underlying mesenchyme until a sufficiently large population of cells has been generated that can differentiate to form the correct amount of muscle (Airik et al. 2005; Yu et al. 2002). Having shown that different axial levels of the 7 week UGS represent distinct stages of differentiation, I predicted that if SHH served a similar role in human bladder development then the expression of SHH would correlate inversely with the onset of smooth muscle differentiation. Indeed, SHH was expressed in the urothelium, the onset of expression preceding smooth muscle differentiation, and with the intensity of SHH and αSMA being correlated at more cranial levels (Figure 24). Crucially, SHH was first expressed in the dorsal aspect of the UGS urothelium (Figure 24C'), correlating inversely with the onset of smooth muscle differentiation in the ventral portion of the UGS (Figure 24D) at a later (more cranial) stage. Consistent with the regulation of differentiation by SHH signalling, PTCH, SMO and BMP4 were expressed in a very

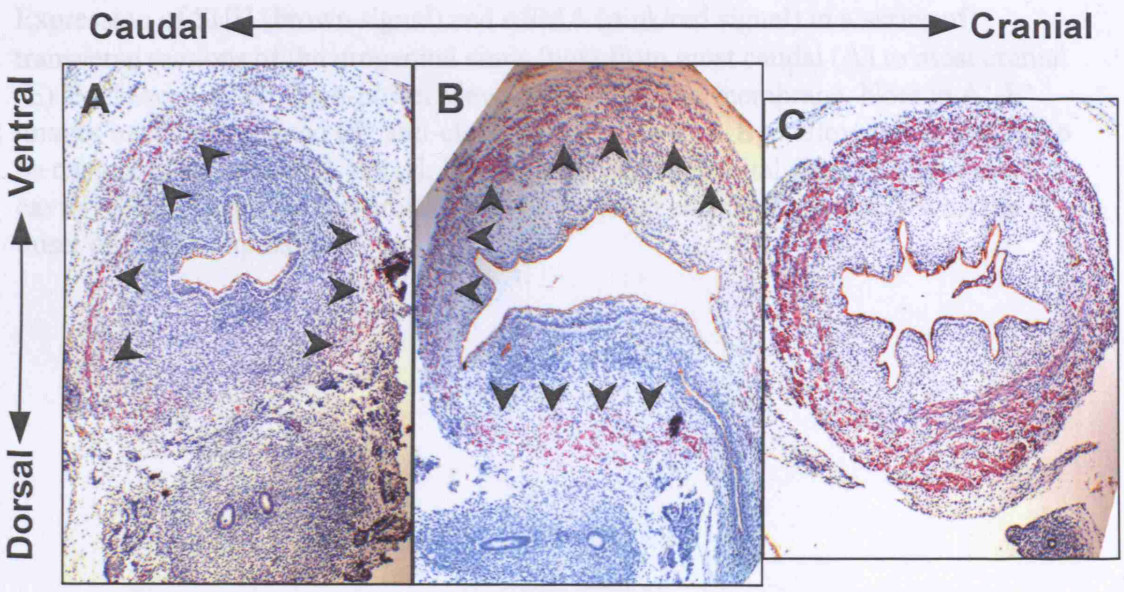


**Figure 23. Differentiation of a 13 week bladder.**
Expression of 'UP' (brown signal) and αSMA (pink/red signal) in a series of transverse sections of the 13 week bladder. (**A**) corresponds to an axial level between B-C in *Figure 19* while (**B**) and (**C**) represent axial levels equivalent to D and E in *Figure 19*. Arrowheads indicate αSMA expression; note that both differentiation markers are now expressed at all axial levels, both ventrally and dorsally, and that αSMA expression has resolved into muscle bundles

**Figure 24. SHH expression in a 7 week urogenital sinus**
Expression of SHH (brown signal) and αSMA (pink/red signal) in a series of transverse sections of the urogenital sinus (ugs) from most caudal (A) to most cranial (E) axial level. A'-E', high-power view of the urothelial membrane. Note in A'-E' images have been rotated 60° anti-clockwise relative to A-E to allow larger images to be captured. V, ventral; D, dorsal; hg, hindgut; ugs, urogenital sinus; pc, peritoneal cavity. SHH is expressed in urothelium and its onset correlates inversely with the onset of _SMA expression.

*Figure 24*

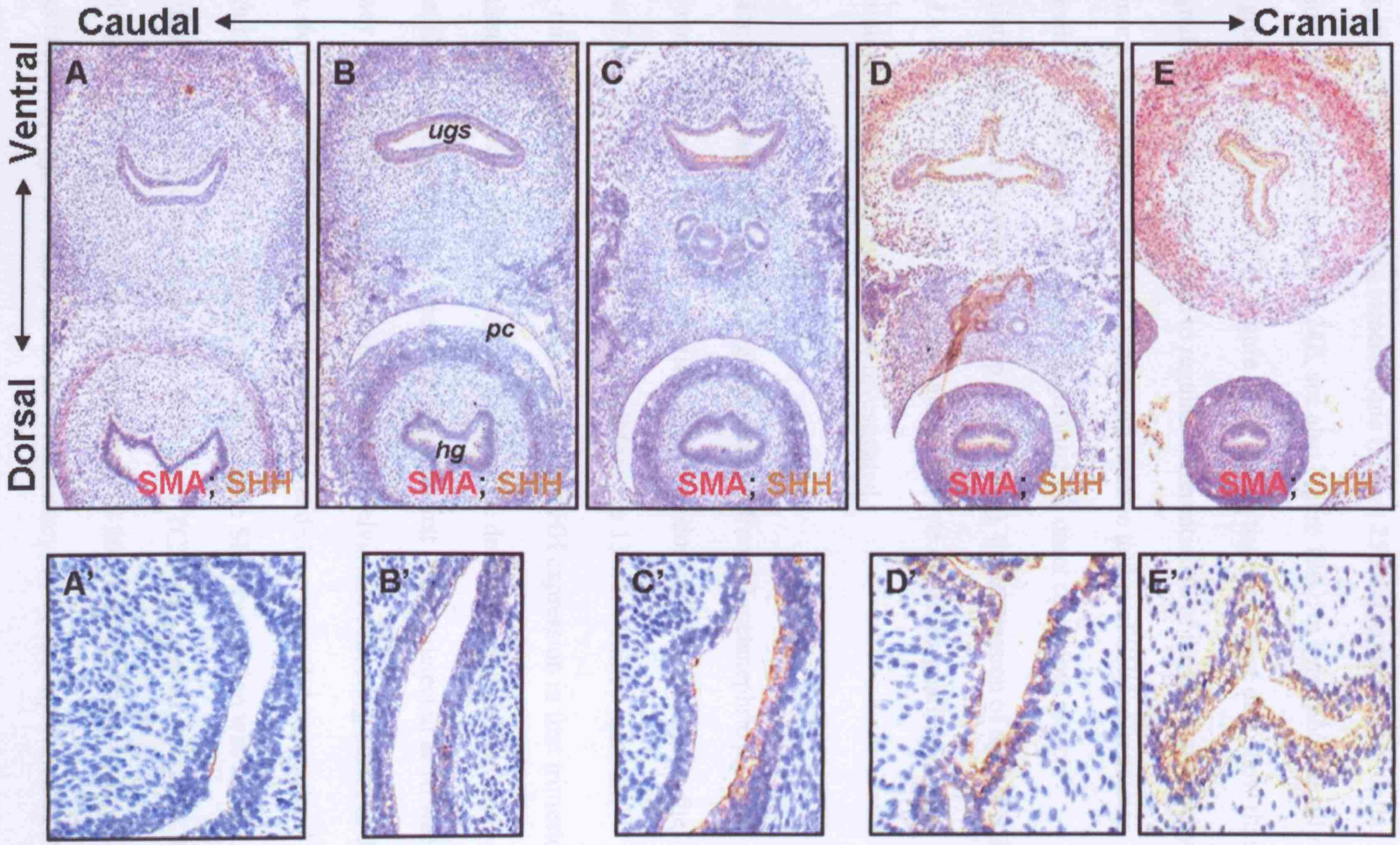
Caudal
Cranial
Ventral
Dorsal
A
B
C
D
E
ugs
pc
hg
SMA; SHH
SMA; SHH
SMA; SHH
SMA; SHH
SMA; SHH
A'
B'
C'
D'
E'

similar pattern in the surrounding mesenchyme (Figure 25B-D), coinciding with the expression of αSMA (Figure 22E & 24E, see also Figure 12A), in a morphologically distinct group of cells in the UGS (Figure 25A). Taken together, these data show that SHH signalling proteins are in place to regulate differentiation of the UGS mesenchyme. Furthermore, the initiation of αSMA expression relative to that of SHH is in precise accord with a role for SHH signalling in regulating the onset of smooth muscle differentiation. In the available tissues (up to 13 weeks), the expression of neither SHH nor αSMA could be detected in the ureter, and so the role of SHH signalling during differentiation of this tissue could not be investigated.

Expression of SHH and PTCH was sought in sections from 10 metanephric kidney samples ranging from 7-28 weeks gestation. No expression could be detected in the kidney at 7 weeks, and expression was negligible in the 13 week kidney (data not shown); this is consistent with a previous analysis of SHH expression in first trimester human tissue samples in which transcripts could not be detected in kidney sections (Odent et al. 1999). Expression of these proteins was first reliably detected at 16 weeks, where they were found in the epithelium of the renal pelvis and collecting ducts; in these sections, expression of PTCH in collecting ducts extended out toward the capsule (although it was absent in the nephrogenic zone), while SHH expression was limited to the medullary collecting ducts (Figure 26). SHH and PTCH were also expressed in the renal pelvis and medullary collecting ducts between 18-26 weeks gestation (only data for 26 weeks is shown, Figure 27A,B). In the 28 week kidney, while the expression of PTCH remained in medullary collecting duct epithelia, SHH was no longer detectable (Figure

**Figure 25. SHH signalling in the 7 week urogenital sinus.**
Immunolocalisation of PTCH (**B**), SMO (**C**) and BMP4 (**D**) in the peripheral mesenchyme of the 7 week urogenital sinus. (**A**) Negative control; antibody replaced with anti-rabbit IgG. **A'-D'** High power view corresponding to the inset dashed box in **A-D**. Note expression of all three proteins overlaps very closely in these adjacent sections, and that expression also corresponds to a morphologically distinct group of cells that express αSMA (*Figures 12A, 22E* and *24E*).

*Figure 25*

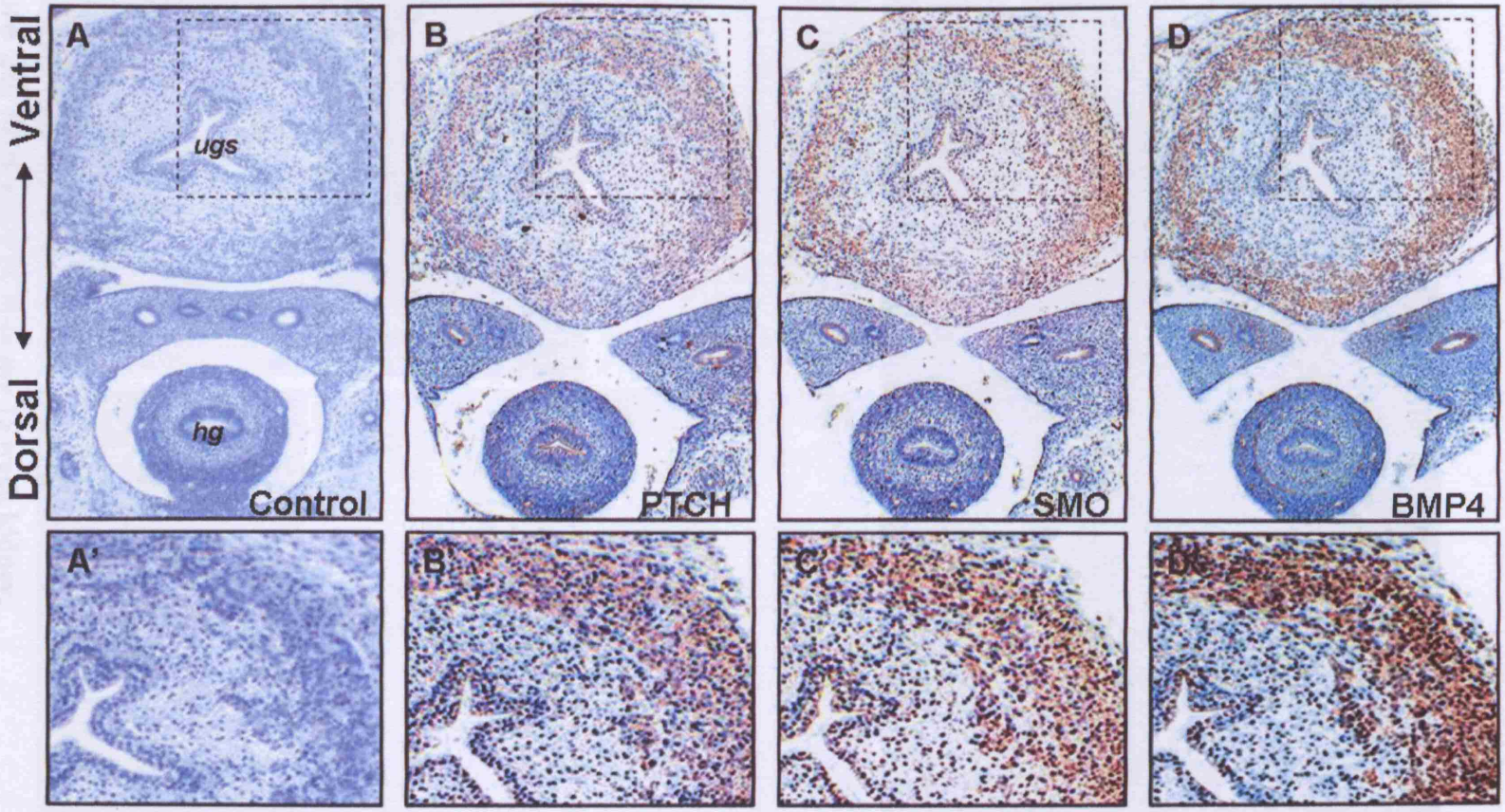

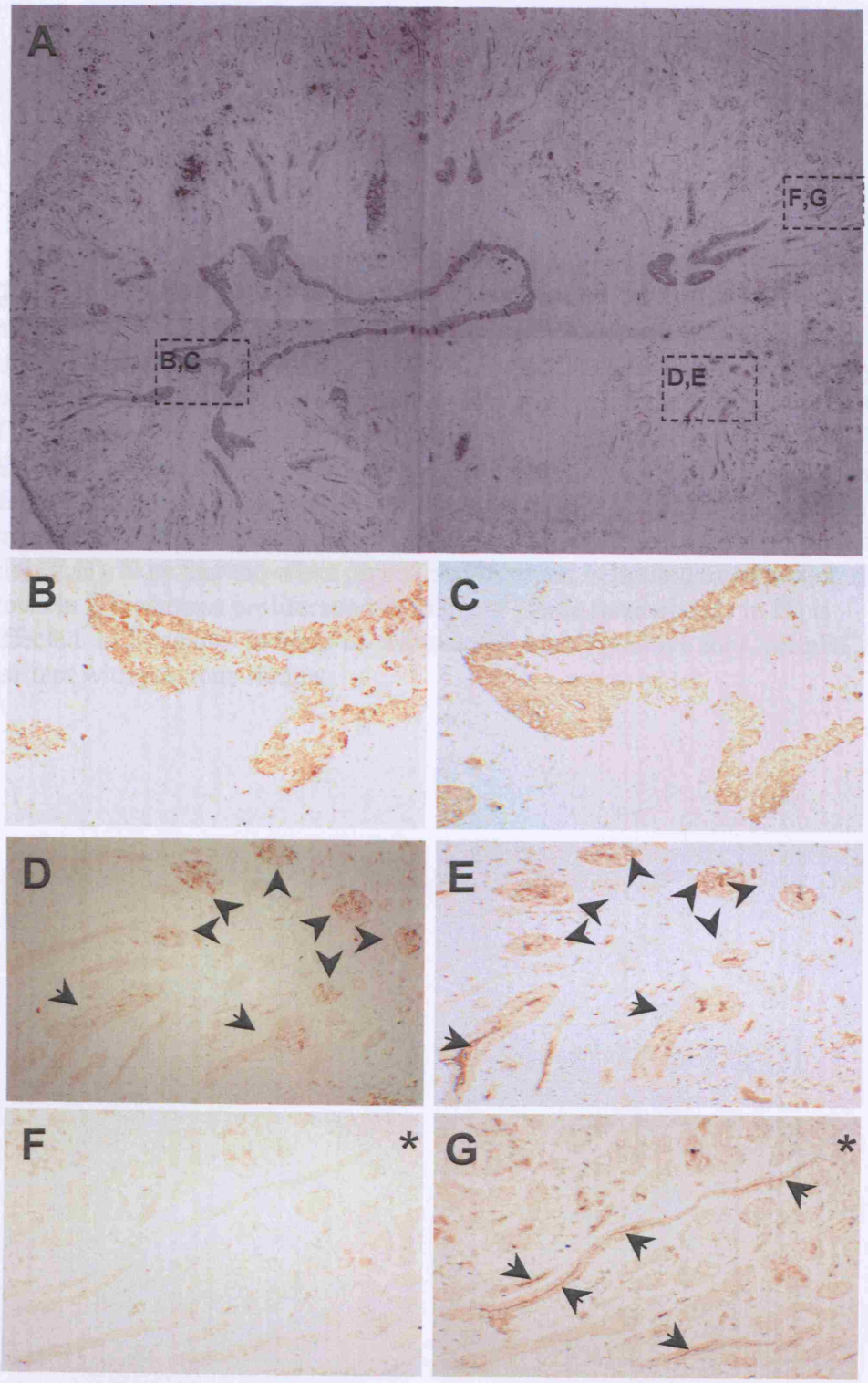


**Figure 26. SHH and PTCH in the 16 week kidney.**

(**A**) Greyscale view of PTCH expression in the 16 week kidney showing overall morphology. Inset dashed boxes refer to fields of view shown in **B-G**. **B,D,F** – expression of SHH; **C,E,G** – expression of PTCH. SHH and PTCH are expressed in the renal pelvis (**B,C**), and medullary collecting ducts (**D,E**). PTCH (**G**), but not SHH (**F**), is also expressed in collecting ducts extending out to the capsule (*) of the kidney, but not in the nephrogenic zone. Note that PTCH is localised predominantly at the apical surface of collecting ducts. Arrowheads and arrows indicate collecting ducts sectioned transversely and longitudinally, respectively.

**Figure 27. SHH-CyclinB1 signalling in the second trimester kidney.** Expression of SHH (**A,C**), PTCH (**B,D**), CyclinB1 (**E,G**) and PCNA (**F,H**) in medullary collecting ducts of the 26 (**A,B,E,F**) and 28 (**C,D,G,H**) week kidney. SHH is expressed in medullary collecting ducts at 26 weeks, but not a 28 weeks (**A,C**). PTCH is expressed at both ages and is localised to the apical cell surface (**B,D**). Loss of SHH at 28 weeks corresponds with a redistribution of CyclinB1 to the apical cell surface (**E,G**) similar to the pattern observed for PTCH. This also corresponds with decreased cellular proliferation, as evidence by the proportion of PCNA-positive nuclei (**F,H**). Note that the effect on cell proliferation is limited to collecting ducts (arrows in **H**), whereas proliferation in loops of Henle (arrowheads in **H**) is unaffected. In **E**, arrows indicate occasional cell nuceli positive for CyclinB1, consistent with previous studies.

*Figure 27*

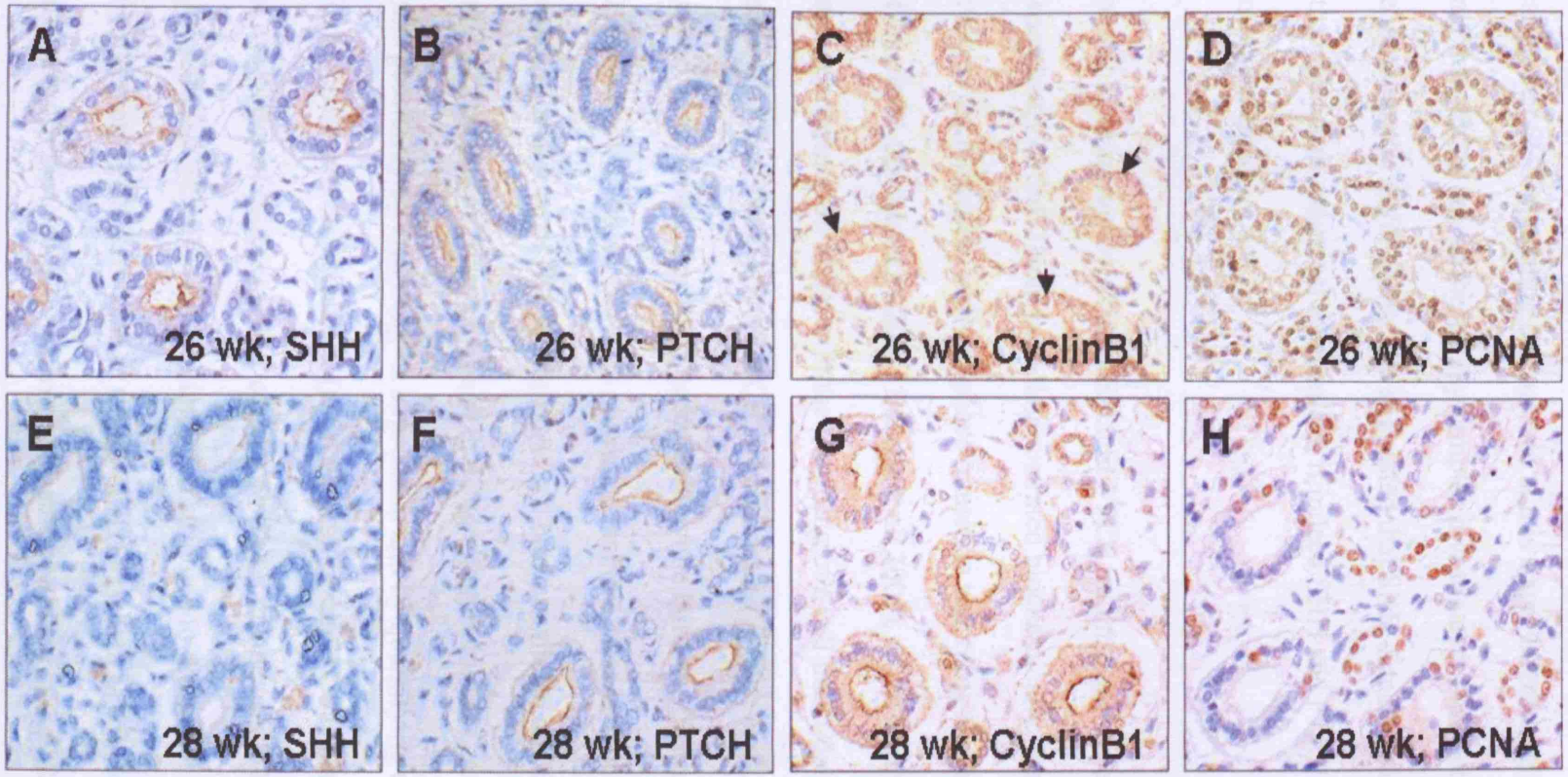
A
26 wk; SHH
B
26 wk; PTCH
C
26 wk; CyclinB1
D
26 wk; PCNA
E
28 wk; SHH
F
28 wk; PTCH
G
28 wk; CyclinB1
H
28 wk; PCNA

27C,D), indicating that SHH signalling is repressed at this stage. Interestingly, expression of SMO was not detected in any of the kidney samples investigated (data not shown); since only one paralogue of *SMO* exists, this suggested that SHH signalling in the kidney must operate through a non-canonical mechanism, if indeed SHH and PTCH were transducing any signal at all.

Two non-canonical mechanisms by which SHH and PTCH might regulate cellular processes independently of SMO have been demonstrated biochemically. One mechanism involves the regulation of $G_2$-M phase transition according to the subcellular distribution of CyclinB1 (Barnes et al. 2001; Barnes et al. 2005), while another generates a state of cellular dependency on SHH, with the unveiling of a cell death-domain by proteolytic cleavage of the C-terminus of PTCH in its absence (Thibert et al. 2003). I reasoned that it was unlikely that signalling proceeded by the latter mechanism because the antibody that was used to detect PTCH is raised against this cleaved C-terminus, and no difference in the distribution of PTCH was observed between the 26 and 28 week kidneys (Figure 27B,D). Instead, I hypothesised that signalling involved CyclinB1, and sought to test this possibility by analysing its expression and by quantifying cell proliferation. In the SHH-expressing kidney (at 26 weeks), CyclinB1 was distributed diffusely in the cytoplasm of collecting duct cells as well as in the occasional cell nucleus (Figure 27E); in contrast, CyclinB1 was strikingly redistributed to the apical cell surface in the collecting ducts of the 28 week kidney (Figure 27G) in which SHH was absent. The proliferation index of these cells was also significantly reduced in the 28 week kidney, as compared to the 26 week kidney, as assessed by PCNA staining

(Figure 27F,H). These results are in precise accord with a model whereby SHH and PTCH regulate the proliferation of collecting duct cells according to the subcellular distribution of CyclinB1.

In order to further confirm these data, functional evidence was sought for this pathway *in vitro* using MDCK cells; these are archetypal kidney collecting duct (epithelial) cells derived from an adult female cocker spaniel. Like the collecting duct cells in the post-26 week kidney, the MDCK cells did not express SHH or SMO (data not shown), while PTCH and CyclinB1 proteins were both immunolocalised in a strikingly similar pattern to one another in optical sections at the apical cell surface, as determined by fluorescence confocal microscopy (Figure 28B,D); barely any cytoplasmic or nuclear CyclinB1 was detected in these cells (Figure 28C). When the cells were treated with 40nM recombinant mouse SHH protein (SHH-N) for 24 hours, a predominantly nuclear, but also cytoplasmic, pattern of CyclinB1 staining was observed in all cells (Figure 28H), but no protein was detected at the cell surface. This treatment also resulted in a significant increase in the proportion of mitotic cell nuclei (Figure 28J), as assessed by staining nuclei with Hoescht, elevating the mitotic index from 3.5% in controls to 4.7% in the treated cells (*p*-value $1.5 \times 10^{-8}$; n=3). Taken together, these results confirm that SHH-CyclinB1 signalling acts at short range to regulate collecting duct cell proliferation, both *in vitro* and *in vivo*, using endogenous cellular machinery, and extend the results of Barnes et al. (2001; 2005) using transfected cells, showing that SHH-CyclinB1 signalling can regulate proliferation using the endogeneous molecular machinery of epithelial cells.

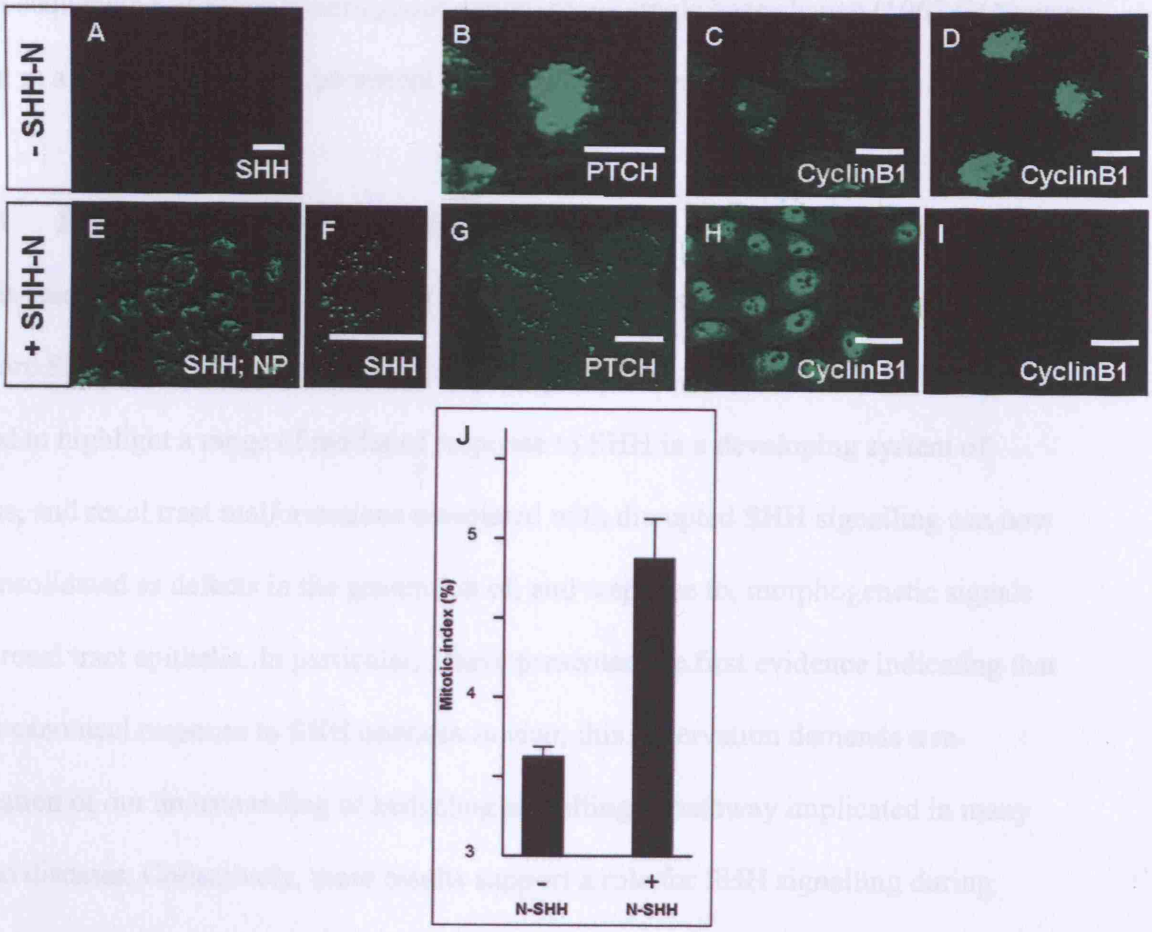


**Figure 28. SHH-CyclinB1 signalling in Madine-Darby Canine Kidney Cells.** MDCK cells express PTCH at their apical cell surface (**B**), but not SHH (**A**) or SMO (data not shown). CyclinB1 is also detected in optical sections at the apical cell surface (**D** – note the strikingly similar pattern between **B** and **D**), but not in optical sections through cell nuclei (**C**). Recombinant-mouse SHH protein (SHH-N) added to cells in culture is detected at the apical surface of non-permeabilised (NP) cells (**E**) as well as internally in permeabilised cells in a vesicular pattern (**F**). PTCH is also detected internally in treated cells (**G**). In MDCK cells treated with SHH-N, CyclinB1 is redistributed to cell nuclei (**H**). In contrast, no CyclinB1 is detected in optical sections at the surface of cells (**I**). This redistribution of CyclinB1 correlates with an elevated proportion of mitotic cell nuclei (**J**), as evidenced by staining of cells with Hoescht. Cells were permeabilised before immunocytochemistry was performed, except in **E**. Bars are 20 microns.

PTCH interacts with CyclinB1 via its large intracellular loop, encoded by exons 13-14 of the gene (Barnes et al. 2001; 2005). While loss-of-function mutations in *PTCH* cause Gorlin syndrome, I hypothesised that mutations that specifically disrupt SHH-CyclinB1 signalling might result in kidney malformations. 61 patients with a range of kidney malformations (*Groups 1-4*) were screened for mutations in *PTCH* exons 13 and 14 by direct sequencing. While a heterozygous synonymous single base change (1962 G/A) was found in a single patient with persistent cloaca, no pathogenic mutations were found.

### 3-4-3 Interpretation and interim discussion

In this study I have presented a detailed description of the spatio-temporal distribution of the core SHH signalling molecules during human renal tract development. This has served to highlight a range of modes of response to SHH in a developing system of organs, and renal tract malformations associated with disrupted SHH signalling can now be consolidated as defects in the generation of, and response to, morphogenetic signals from renal tract epithelia. In particular, I have presented the first evidence indicating that a non-canonical response to SHH operates *in vivo*; this observation demands a re-evaluation of our understanding of hedgehog signalling, a pathway implicated in many human diseases. Collectively, these results support a role for SHH signalling during multiple steps of human renal tract development, and offer insight into the integration of developmental processes at the systems level, as well as that of the organism as a whole.

SHH was immunolocalised in epithelia throughout the renal tract, at various stages of development and with a distinct onset of expression in each, indicating the common

action of these cells as signalling centres. However, the key difference in SHH signalling in different tissues resides in their mode of response to morphogen, as evidenced by the expression of the proteins that transduce this signal (PTCH, SMO and CyclinB1). Specifically, while long-range signalling would operate during differentiation of the UGS, SHH would be predicted to act at short-range to regulate epithelial cell processes during septation of the cloaca and in the regulation of collecting duct cell proliferation. Furthermore, while SMO was detected in the cloaca and UGS, in a pattern overlapping with that of PTCH, no expression was detected in the kidney, suggesting that signalling involves SMO in the lower, but not upper, renal tract.

To investigate the precise roles of SHH signalling in bladder and kidney development, I carefully analysed the expression of these core SHH pathway components with respect to markers of cellular differentiation or proliferation. This purely genetic analysis allowed hypotheses stemming from previous biochemical (Barnes et al. 2001; Barnes et al. 2005) and mouse genetic studies (Hu et al. 2005b; Yu et al. 2002; Bose et al. 2002; Mo et al. 2001) to be tested *in vivo*, according to the correlated expression of the proteins analysed, as well as their subcellular distribution. I believe that such a precise correlation of the tissue/cellular distribution of numerous proteins in line with established molecular/developmental mechanisms represents strong genetic support for the operation of these mechanisms in a tissue, and further reinforces antibody specificity. In this latter regard, it must be noted that, while I detected PTCH protein in collecting duct epithelia, *ptch* transcripts have been reported to be expressed in the stroma surrounding collecting ducts at similar stages of development in the mouse (Yu et al. 2002). Whether this

difference can be attributed to 70 million years of divergent evolution, or to technical differences, is debatable. However, the collecting duct cell autonomous effect observed, together with the co-localisation of PTCH and CyclinB1 and the replication of these results using MDCK cells *in vitro* (independent of renal stroma) suggests that my immunolocalisation of PTCH is robust.

In the UGS, I have established that different tissue sections in the cranial-caudal axis represent different stages of differentiation, a fundamental property of bladder development that has been reported previously by morphological analysis of the human bladder from 7 weeks (Matsuno et al. 1984); an analogous phenomenon has also been demonstrated in mouse (Yu et al. 2002) and human (Tacciuoli et al. 1975; Matsuno et al. 1984) ureters, that differentiate in a proximal-to-distal sequence, albeit at a relatively later stage of development (from 12 weeks). The onset of expression of SHH in this temporal-spatial series, as well as the overlapping expression of PTCH, SMO, BMP4 and αSMA in the mesenchyme, are exactly in line with a model whereby SHH delays smooth muscle differentiation (Yu et al. 2002) and regulates its subsequent progression. Indeed, a role for SHH in bladder differentiation also matches the bladder/ureter malformations seen in patients with a mutation in *DHCR7*, *SHH*, *GLI2* or *GLI3*, including bladder/ureter hypoplasia, UGS, VUR and polyuria/eneuresis (Kelley et al. 2000; Heussler et al. 2002; Roessler et al. 2003; Johnston et al. 2005). While I detected PTCH in the peripheral mesenchyme of the UGS, transcripts have been previously described in the subureteral mesenchymal cells of the mouse ureter (Yu et al. 2002); again, whether this represents

species, tissue or technical differences remains to be shown, although the striking overlap of PTCH, SMO, BMP4 and αSMA that I observed gives credence to my result.

The down-regulation of SHH in medullary collecting ducts of the 28 week kidney, as compared to the 26 (and 18-25) week kidney(s), allowed the mechanism of metanephric SHH signalling to be interrogated in the presence or absence of SHH in two similarly aged organs. The absence of SMO protein in all of the kidneys assessed, together with the absence of other paralogues in the human genome, suggested the possibility of a non-canonical response to SHH in this tissue; indeed, the exact correlation between the subcellular distribution of CyclinB1, according to the presence or absence of SHH, with collecting duct cell proliferation represents compelling evidence that SHH-CyclinB1 signalling (Barnes et al. 2001; 2005) regulates growth of this ureteric bud lineage following the completion of branching morphogenesis. This may shed light on the mechanisms generating 'renal hypoplasia', as well as the developmental window in which this anomaly is generated, since this phenotype is found in patients with either *DHCR7* or *SHH* mutations (Kelley et al. 2000; Dubourg et al. 2004). Indeed, another study has shown that proliferation in post-branching collecting ducts is important in kidney development, implicating defective cell proliferation in cystogenesis (Fischer et al. 2006).

Other studies in mice have suggested that signalling in the kidney does indeed operate canonically, as evidenced by a phenotype of overt renal dysplasia in mice homozygous for a putative dominant-negative *gli3* mutation ($gli3^{\Delta 699}$/ $gli3^{\Delta 699}$; Bose et al. 2002), as

well as in those treated with cyclopamine (a specific SMO antagonist; Hu et al. 2005b), and the rescue of this phenotype in *Shh*$^{-/-}$;*Gli3*$^{-/-}$ double mutants (Hu et al. 2005b). However, these defects are most likely secondary to the observed renal ectopia (Hu et al. 2005b; Bose et al. 2002) owing to early embryonic midline defects (Yu et al. 2002), rather than an intrinsic defect in metanephric development itself, since although the metanephros of mice with a kidney-specific conditional null-mutation of *Shh*$^{-/-}$ is hypoplastic, it is otherwise histologically normal (Yu et al. 2002). Indeed, the ectopic kidneys in some patients with the Smith-Lemli-Opitz syndrome (caused by a severe defect in hedgehog signalling) can also be cystic and abnormally lobed (Kelley et al. 2000). Furthermore, the gli transcription factors are expressed in the nephrogenic zone of the kidney (Nakashima et al. 2002; Hu et al. 2005b), and so it is difficult to imagine how SHH expressed in collecting ducts (this study; Yu et al. 2002; Nakashima et al. 2002) could signal to these distant cells through many cell layers or in opposition to urine flow. These observations suggest that normal canonical SHH signalling is important for kidney development owing to a temporal dependency on the normal development of other tissues early in embryonic development, but that signalling in the metanephros itself operates non-canonically.

The results presented here demonstrate the diverse roles that a signalling pathway can have in a system of organs. The importance of human studies such as this are being increasingly recognised, since the differences between species is thought to result from the different expression of genes, rather than in their sequences (Lindsay et al. 2005). This study serves to define the tissues that are defective in the generation of, or response

to, SHH and the developmental time points for which this is important. This information will be useful in the generation of therapies in the future, not only for patients suffering disrupted hedgehog signalling, but also for patients with a range of congenital anomalies of the kidney and urinary tract. For example, the finding that the urothelium and muscle of the human bladder differentiate co-ordinately, together with a recent study showing that genetic disruption of murine ureteric mesenchyme development also disrupts that of the urothelium (Airik et al. 2005), suggests that the induction of a hedgehog response at an appropriate stage of development in one tissue (for example see Kusano et al. 2005) might also be beneficial for the other; in addition, the identification of a molecular mechanism that acts as a brake on collecting duct cell proliferation from an early stage of kidney development and possibly through into adulthood (as evidenced by the experiments in MDCK cells, an adult collecting duct cell line) might facilitate the manipulation of epithelia in cystic kidneys. Taken together, these findings offer insight into the range of molecular processes that sculpt the human renal tract in its entirety, providing a framework for understanding human pathology and offering a glimpse into the development of the human as a whole.

# Chapter 4. DISCUSSION

The identification of mechanisms by which congenital renal tract malformations arise is an important area of research given that these defects account for approximately half of all children who progress to end-stage renal failure (Lewis 2003). Understanding the genetic contribution to this pathogenesis is of particular value, facilitating the counselling of families with a history of disease, serving to highlight the critical window(s) during which the course of development is altered, and aiding in the identification of molecular pathways that might be amenable to therapy in the future. This thesis is focused on furthering our understanding of how non-syndromic renal tract malformations are genetically determined. Here I will discuss the implications of this work for human clinical and molecular genetics, the transduction of genetic information in human renal tract tissues and the ontogeny of this group of malformations.

The major findings of this thesis are as follows:

Study I. *UPIIIa*, a gene expressed in early human development, is mutated in a subset of patients with severe bilateral renal adysplasia.

Study II. No definitive evidence was found that *UPII* mutations cause renal tract malformations, although variants in this gene might be a rare predisposing factor.

Study III. No support was found for *SHH* mutations in human persistent cloaca, although *UPIIIa* mutations are occasionally associated with this condition.

Study IV. The expression patterns of SHH/PTCH/SMO in normal human renal tract development is consistent with a variety of signalling patterns: *i)* epithelial-to-epithelium

canonical signalling in the cloaca; *ii)* epithelial-to-mesenchyme canonical signalling in the UGS; and *iii)* epithelial-to-epithelium non-canonical signalling in kidney medullary collecting ducts.

A summary of the genes and patients screened for mutations is given in *Tables 6* and *7*.

## 4-1 HUMAN CLINICAL AND MOLECULAR GENETICS

The primary aim of this work was to identify mutations that cause severe non-syndromic renal tract malformations. Interest in the *UPs* stemmed from human linkage (Feather et al. 2000) and mouse genetic (Hu et al. 2000) studies that linked *UPIIIa* and VUR. Subsequently, mutational analyses excluded *UP* mutations in the pathogenesis of primary non-syndromic VUR in humans (Giltay et al. 2004; Jiang et al. 2004), and this generated an interest in more severe malformations.

I have found mutations of *UPIIIa* in almost one quarter of a group of patients with severe renal adysplasia, with or without VUR, all of whom were referred to the renal failure clinic at Great Ormond Street Hospital. Surprisingly, a follow-up study identified an additional mutation in only one patient out of 176 with non-obstructive 'renal dysgenesis' (Schonfelder et al. 2005). This discrepancy in pick-up rate suggests a specificity of *UPIIIa* mutations for a particular defect in renal development, one that was enriched in the 17 patients that I screened. In this regard it is interesting to note that this group represents a diverse spectrum of renal phenotypes, although the four mutation carriers

***Table 6. Novel variants identified in the patients screened.***

| Gene | Position | Protein | De novo? |
|---|---|---|---|
| *UPIb* | IVS1 +34 T/G | - | NA |
| | IVS2 +110 G/C | - | NA |
| | IVS3 +100 C/T | - | NA |
| | IVS4 +10 C/T | - | NA |
| | IVS4 +35 T/C | - | NA |
| | IVS5 +91 A/G | - | NA |
| | IVS6 +20 Cdel | - | NA |
| *UPII* | 5'UTR -26 A/G | - | NA |
| | c.179 CACTins | L60fsX68 | No |
| *UPIIIa* | IVS2 -78 A/G | - | NA |
| | c.818 C/T | P273L | Yes |
| | 3'UTR +963 T/G | - | Yes |
| | 3'UTR +973 C/G | - | Maternal* |
| | 3'UTR +1003 T/C | - | Yes |
| *PTCH* | c.1962 G/A | S | NA |

S, synonymous nucleotide substitution; NA, not assessed; Maternal*, variant identified in heterozygous state in an unaffected mother, but not in her affected child.

***Table 7. Summary of genes and patients screened for mutations.***

| **GENE** | **PATIENTS** | | | |
|---|---|---|---|---|
| | *Group1* | *Group 2* | *Group 3* | *Group 4* |
| | **Renal adysplasia (n=17)** | **PUV (n=6)** | **MCDK (n=19)** | **Persistent Cloaca (n=24)** |
| *UPIb* | Normal | Normal | Normal | NA |
| *UPII* | L60fsX68 | Normal | Normal | NA |
| *UPIIIa* | Pro273Leu; 963T→G; 1003T→C | Normal | Normal | Normal |
| *SHH* | NA | NA | NA | Normal |
| *PTCH* (exons 13 & 14) | Normal | Normal | Normal | Normal |

Key: NA, not assessed.

each had a similar disease, namely bilateral renal malformation severe enough to cause end-stage kidney failure; in contrast, less than 15% of patients in the study by Schonfelder et al. (2005) would fall into this category. In future it will be interesting to attempt to refine the phenotypes associated with *UPIIIa* mutation by analysing a large number of patients with severe bilateral disease and perhaps even through histological analyses of the kidneys of patients carrying a mutation in this gene. In contrast to syndromic disease, defining the affection status of patients with non-syndromic disease relies solely on an accurate assessment of their kidneys, and so I believe that refinement of the phenotype associated with *UPIIIa* mutation is crucial if these observations are to be taken forward into the clinic in the future.

The patient in whom Schonfelder et al. (2005) identified the Gly202Asp mutation had a phenotype of multicystic dysplastic kidney, unlike the four patients with either the Pro273Leu or 3'UTR mutations; indeed, I excluded mutations in 19 individuals with this phenotype. Furthermore, it is interesting that while the patients with Pro273Leu had high grade VUR, as well as renal adysplasia, those with a 3'UTR mutation did not. It is possible that the different types of mutation might have distinct consequences for renal tract development. While the Gly202Asp mutation affects the extracellular domain of UPIIIa, the Pro273Leu mutation most likely causes a major conformational change in the cytoplasmic domain of the protein by ablating a "proline-kink" (von Heijne 1991; Ceruso et al. 2002; Koshy et al. 1990). The surface area of urothelial cells is modulated by endo/exocytosis in response to changes in bladder pressure (Lewis et al. 1984) and binding of the *E. coli* FimH receptor to UPIa mediates urothelial invasion of this

bacterium (Zhou et al. 2001); unlike UPIa, UPIb or UPII, UPIIIa has a significant cytoplasmic tail, and it has been suggested that this region interacts with cytoplasmic proteins to mediate membrane/cytoplasmic interactions (Yu et al. 1994). Furthermore, recent studies have implicated this domain of UPIIIa in the relay of intracellular signals during the fertilisation of *Xenopus* oocytes (Hasan et al. 2005; Sakakibara et al. 2005). In this regard, the normal transport of the 273Leu UPIIIa to the surface of COS-1 cells is consistent with a dominant-negative effect, and so the mode of action of different classes of mutation might also explain the range of phenotypes presenting in different patients. In contrast, the 3'UTR mutations might be expected to alter mRNA stability (Waggoner et al. 2003; Erlitzki et al. 2002; Kakoki et al. 2004), perhaps resulting in haploinsufficiency. Of course, the number of patients carrying a *UPIIIa* mutation is currently too small to infer genotype-phenotype correlations, and so these possibilities remain to be assessed in the future. If they do exist, these specificities could be important for genetic counselling and patient management.

Another possibility is that modifying factors refine the phenotype of a mutation in different carriers. Lessons from syndromic renal malformations support this possibility, since patients with the renal coloboma and renal-cysts-and-diabetes syndrome, for example, exhibit incomplete penetrance and highly variable expressivity (van Esch et al. 2000; Bingham et al. 2002), and renal adysplasia is estimated to have a penetrance of only 50-80% (McPherson et al. 1987). Obviously, information from the phenotype of other organs is not available to supplement the genetic analysis of non-syndromic disease, as it is for multi-organ syndromes, and so the identification of variants that

predispose to this category of renal tract malformation is more difficult and will require systematic genome-wide screens to be undertaken (for example, Kelley et al. 2005). Nonetheless, some information is available implicating the *UPs* in predisposing to congenital renal tract anomalies in a non-Mendelian fashion.

Jiang et al. (2004) identified a significant, albeit weak, association of the 154Ala allele of *UPIIIa* with primary non-syndromic VUR, although this was not replicated in a genome-wide study (Kelley et al. 2005). However, the experiments that I performed in COS-1 cells gives credence to putative functional affects of this polymorphism, suggesting that it interferes with normal transport of the protein to the cell surface; the 154Ala variant of *UPIIIa* might therefore be important for VUR in the general population, approximately 1% of whom have this anomaly (Bailey 1975). One female carrying the Pro273Leu mutation, that can itself account for renal disease as evidenced by its *de novo* occurrence, had persistent cloaca, as well as heart and vertebral defects, tissues in which UPIIIa has not been found to be expressed. While persistent cloaca might be explained by defects in evagination of the dorsal wall of the UGS (Shapiro et al. 2000), it is difficult to reconcile these other malformations, and *UPIIIa* mutations were absent in an additional 19 girls with persistent cloaca; perhaps additional genetic insults independently encode these heart/vertebral defects, possibly also modulating the renal phenotype. I also identified a frameshifted allele of *UPII* (L60fsX68) in a patient with bilateral VUR and reflux nephropathy, a variant inherited from an overtly unaffected mother; here, the much clearer predicted functional effect of the genetic change constitutes the main evidence in favour of a role in pathogenicity. It is interesting to note that this patient also had bilateral

renal disease leading to renal failure, similar to those with a *UPIIIa* mutation, and this individual was also heterozygous for the Pro154Ala polymorphism. Thus rare *UP* variants in the general population might predispose individuals to renal malformations in combination with certain common variants in other *UP* genes. It is interesting to speculate that numerous variants collaborate to alter the course of development; if this is true, then it is possible that insults on multiple facets of the 'UP system' combine to surpass some threshold intrinsic to urothelial cells that determines whether development will be altered in such a way to manifest disease.

## 4-2 SIGNALLING PATHWAYS IN HUMAN TISSUES

Following their isolation (Wu et al. 1994; Yu et al. 1994), the UPs were generally considered to 'simply' confer important physical properties to the asymmetric unit membrane, decreasing its permeability to urine; this function was elegantly confirmed by demonstrating that the genetic ablation of UPIIIa in mice elevates urothelial permeability (Hu et al. 2000). However, the observation that *UPIIIa* null mutant mice also have congenital VUR and hydronephrosis (Hu et al. 2002) provided the first indication that the UP family might have additional roles in the differentiation of the renal tract itself. The finding of *de novo UPIIIa* mutations, together with its expression in human renal tract tissues at the earliest stages of their development, also implicates this gene in human development.

Missense mutations can be informative as to the function of specific domains within a protein. The Pro273Leu mutation is located in the cytoplasmic domain of UPIIIa, and it

has recently been demonstrated that a tyrosine residue in this domain of *Xenopus* UPIII (xUPIII; equivalent to mammalian residue 266Tyr) is phosphorylated by interacting with the protein Src when oocytes are fertilised (Hasan et al. 2005; Sakakibara et al. 2005); indeed, xUPIII is the receptor that mediates these sperm-egg interactions, as evidenced by a dose-dependent inhibition of fertilisation using an antibody that specifically recognises the extracellular domain of xUPIII. This is suggestive of a biological role for the cytoplasmic domain of human UPIIIa, possibly in transducing developmentally important signals into urothelial cells following ligand binding in the extracellular domain and its subsequent phosphorylation (Figure 29). It is interesting to note that the residue at which the Pro273Leu mutation was identified is in close proximity to this tyrosine residue, 266Tyr. It is, however, unlikely that 273Pro plays a direct role in mediating the phosphorylation of 266Tyr since residues 273-277 are absent from the equivalent *Xenopus* protein. Instead, the Pro273Leu mutation may alter the availability of 266Tyr for phosphorylation by proteins such as Src, thus impeding the transduction of a signal by UPIIIa into urothelial cells. The Gly202Asp mutation is located in the conserved GRR consensus sequence in the extracellular domain of UPIIIa which is proteolytically cleaved in the homologous protein found in *Xenopus* eggs following sperm-egg interaction (Hasan et al. 2005; Figure 29). This process is necessary for fertilisation and presumably, therefore, involves signal transduction by UPIIIa (Hasan et al. 2005). One of the most important outcomes of these human genetic findings, together with biochemical studies in the frog, is the possible identification of a novel signal transduction pathway important for urothelial development. Whether such signalling operates in urothelial

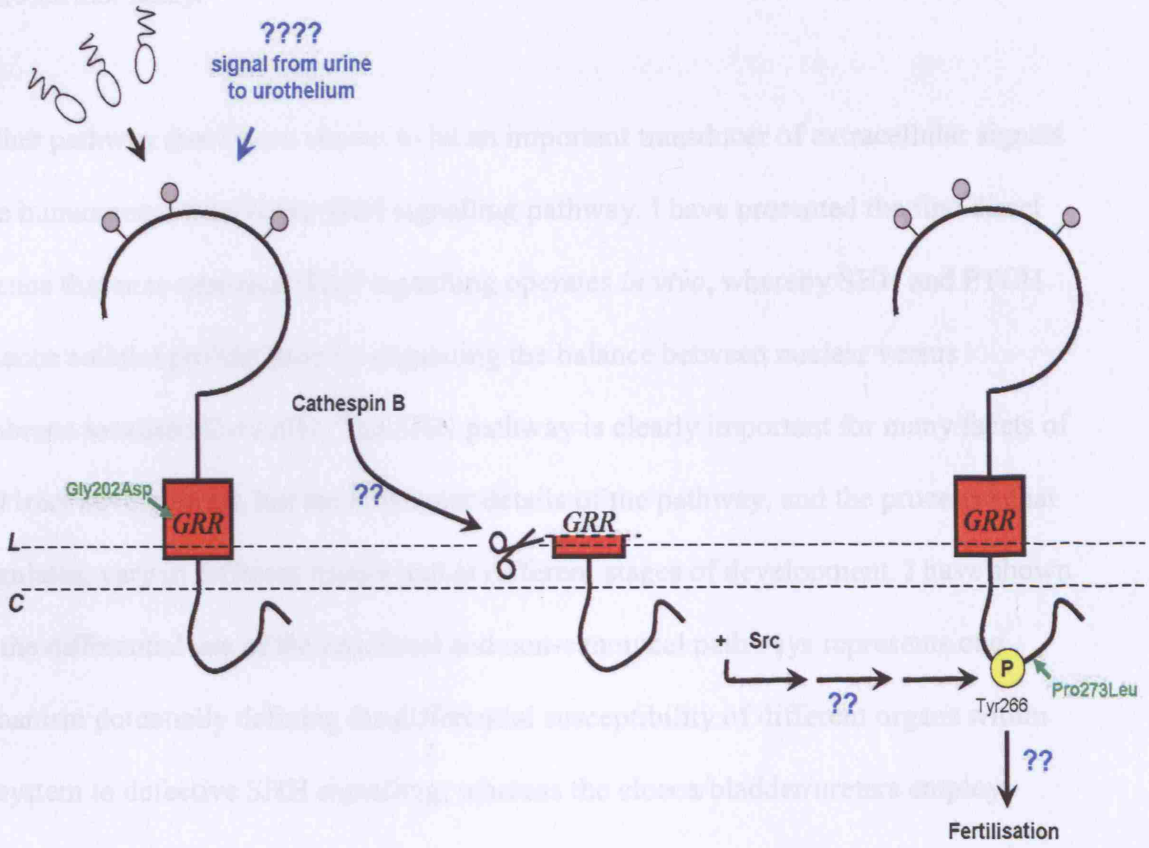


**Figure 29. A new signal transduction pathway involving UPIIIa.**
The biochemistry of signal transduction by UPIIIa based on the results of Hasan et al. (2005) and Sakakibara et al. (2005). UPIIIa is the receptor for sperm-egg interaction in *Xenopus* oocytes, since fertilisation is inhibited in a dose-dependent manner using an antibody that specifically recognises the extracellular domain of UPIIIa. Binding of sperm to UPIIIa causes the protein to be cleaved in the 'conserved domain' (red rectangle) that carries the '-GRR-' consensus site for the sperm protease, Cathepsin B; indeed a synthetic peptide corresponding to the conserved region can compete with native UPIIIa as substrate for this protease. Since full-length UPIIIa is the major product that is phosphorylated as a prerequisite for fertilisation, and activation of Src is also required, a model whereby cleaved UPIIIa interacts with active Src to phosphorylate the remaining uncleaved UPIIIa would fit the data, and this phosphorylated UPIIIa clearly transduces a 'fertilisation signal' into oocytes. The correspondence between the locations of *de novo UPIIIa* missense mutations identified in patients with severe renal dysplasia (shown in green) and the domains that are important for signal transduction would indicate that UPIIIa transduces signals into urothelial cells that are important for renal tract development. It remains to be shown whether signal transduction in human urothelia proceeds in a similar way to that in *Xenopus* oocytes (as indicated by the blue question marks), but it is interesting to speculate that UPIIIa might be the receptor for a secreted molecule(s) present in urine; the fact that the onset of UPIIIa expression in the human urothelium (~7 weeks) coincides with formation of the first glomeruli and production of the first embryonic urine would fit with this possibility.

cells, and whether mutations render the protein constitutively active or inactive, will require further study.

Another pathway that I have shown to be an important transducer of extracellular signals in the human renal tract is the SHH signalling pathway. I have presented the first direct evidence that non-canonical SHH signalling operates *in vivo*, whereby SHH and PTCH influence cellular proliferation by regulating the balance between nuclear versus membrane localised CyclinB1. The SHH pathway is clearly important for many facets of renal tract development, but the molecular details of the pathway, and the processes that it regulates, vary in different tissues and at different stages of development. I have shown that the differential use of the canonical and non-canonical pathways represents one mechanism potentially defining the differential susceptibility of different organs within this system to defective SHH signalling; whereas the cloaca/bladder/ureters employ canonical signalling, the kidney does not, and consistently, while mice null-mutant for *gli2* or *gli3* display urinary tract malformations (Mo et al. 2001), the kidneys of these mice are normal (Hu et al. 2005b). I believe that this mechanism may also hold for other tissues, perhaps even in all tissues in which the canonical pathway is known to operate, although the differential use of the two types of signalling might not always be so clear-cut; it is possible that the balance between the different modes of signalling in determining cell fate might be important.

In support of this possibility, a recent study of the neural tube has shown that regulation of cell proliferation and differentiation by SHH are regulated independently of one

another (Cayuso et al. 2005), and while this may represent the regulation of distinct transcriptional targets by GLI2/GLI3, it might also be the case that canonical and non-canonical pathways contribute differently to the regulation of these distinct cellular responses. For example, regulation of cell proliferation can utilise both types of signalling, involving both the non-canonical SHH-CyclinB1 pathway in the manner investigated in this study (Barnes et al. 2001; Barnes et al. 2005) as well as the canonical transcriptional regulation of the cell cycle components CyclinD2 and N-Myc, as shown in the hair follicle (Mill et al. 2005); in contrast, it seems intuitive to assume that SHH-CyclinB1 signalling is not directly involved in cellular differentiation. In fact, subdivision of the regulation of distinct cellular responses between canonical/non-canonical signalling has been demonstrated for another non-canonical pathway; in neural tube explants, SHH has been shown to regulate both neural precursor differentiation by canonical signalling, and neural crest cell migration by a non-canonical pathway whereby SHH interacts with extracellular matrix components independently of PTCH/SMO/GLI (Jarov et al. 2003; Testaz et al. 2001).

Similar principles might also serve as a paradigm to understand renal tract malformations caused by genetic disruption of other signalling pathways. Indeed, a range of upper and lower renal tract malformations are found in patients in whom pathogenic *UP* variants have been identified and, although the urothelium lines the entire renal tract, from the pelvis of the kidney to the bladder neck, the vagaries of putative UPIIIa signalling might be different in distinct urothelial subdomains. For example, signalling in urothelium of

the ureter versus the bladder, or that in the trigone and vesicoureteric junction. Differences such as these might account for the different effects of distinct *UP* variants.

## 4-3 ONTOGENY OF HUMAN RENAL TRACT MALFORMATIONS

Understanding the developmental origins of renal tract malformations is an important area of investigation to complement human genetic findings as well as to take this new-found information forward into the clinic. However, renal tract development proceeds via a series of intricately choreographed events.

Current concepts propose that human renal malformations arise from either a primary failure of metanephric mesenchymal induction by the ureteric bud or physical obstruction of urine flow (Woolf et al. 2004). Neither UPIIIa nor the SHH signalling proteins were found to be expressed within the metanephros itself, probably ruling out any direct role in nephrogenesis. Rather, the expression of these proteins would be consistent with roles in the development of epithelia within the collecting duct/pelvicalyceal system during the second trimester. For both sets of proteins, the likely onset of expression in the kidney was detected (7 weeks, UPIIIa; 13 weeks, SHH) also refuting possible roles in remodelling of the first 3-10 bud branches, a process that is complete by 7 weeks (Potter 1972). I have shown that SHH signalling, at least in collecting ducts, is important for regulating epithelial cell proliferation, and so this pathway is important for the ongoing regulation and maintenance of distal renal epithelia; it is possible that UPIIIa has similar roles.

Alternatively, it might be more reasonable to consider that the collecting ducts are distinct from the renal pelvis, with the latter simply being an extension of the ureter; indeed, *ptch* transcripts have been reported in the mesenchyme of the renal pelvis similar to the more distal ureter in mice (Yu et al. 2002), while I detected PTCH in collecting duct epithelia. In this regard, a more likely possibility is that human *UP* mutations cause an obstruction to foetal urine flow which perturbs kidney development. Indeed, it has been shown that *UPII* null-mutant mice die from obstructive congenital nephropathy (urothelial hyperproliferation within the ureter), although this was not formally assessed in the *UPIIIa* null-mutant mouse (Kong et al. 2004; Hu et al. 2000). Further support for this contention comes from the identification of a *de novo UPIIIa* mutation in a patient with multi-cystic dysplastic kidney (Schonfelder et al. 2005), a condition classically thought to be caused by obstructed urine flow at the level of an atretic ureter. It is also of note that the patient with a frameshifted *UPII* allele had reflux nephropathy.

In contrast, the patients in whom I detected different *UPIIIa* mutations had a distinct phenotype and obstructed ureters were not reported, raising the possibility that their disease is caused by an alternative mechanism. Perhaps a more likely scenario in these patients is that disease is caused by a 'functional obstruction' to urine flow. Indeed, mice with a conditional null-mutation of SHH specifically in the ureteric bud lineage have hydroureter and fewer glomeruli; in these mice differentiation of the ureteric mesenchyme is disrupted and the ureteric musculature is hypoplastic (Yu et al. 2002). It has also been demonstrated that urinary tract-specific deletion of *calcineurin subunit b1*, a gene expressed in mesenchyme near differentiating urothelia, reduced proliferation in

nascent smooth muscle cells accompanied by defective pyeloureteral peristalsis, progressive renal obstruction, and renal failure (Chang et al. 2004). Functional obstruction of the developing kidney also occurs in mice mutant for *AT1*, an angiotensin II receptor (Mendelsohn 2004). In fact, differentiation of the urothelium and its surrounding mesenchyme are not independent processes. I have shown that the sequence of differentiation of these two tissues mirrors one another closely, at least in the UGS. Furthermore, null-mutation of *Tbx18*, a gene expressed exclusively in the ureteric mesenchyme, disrupts differentiation of both the muscle and urothelium (Airik et al. 2005). I speculate that *UPIIIa* mutations would disrupt the nurturing relationship between urothelia of the ureter/renal pelvis and the surrounding mesenchyme. This might result from a loss of structural integrity within the epithelium or from a more subtle effect, namely altered epithelial/mesenchymal signalling.

Distinguishing between primary and secondary developmental defects is a major difficulty in understanding the ontogeny of renal tract malformations. A question of particular interest to this thesis is whether a kidney malformation is caused by defective signalling within the metanephros itself or secondary to alteration of another developmental process. One way of answering this question is through the generation of mutations specific to the kidney, and this strategy has proven useful in the study of SHH signalling (Yu et al. 2002). Interestingly, while *Shh*-null mice have renal aplasia, ectopia and cystic dysplasia (Hu et al. 2005b), the kidney in mice with a *HoxB7/Cre* conditional null-mutation of *Shh* are histologically normal (although glomeruli are fewer and more densely packed perhaps owing to hydroureter) (Yu et al. 2002). My studies offer

compelling evidence that SHH signalling in the kidney operates independently of SMO and therefore also the GLI proteins (Figure 30). Therefore the renal malformations seen in the kidneys of mice with a homozygous dominant-negative *gli3* mutation (Bose et al. 2002) must also be secondary effects. Thus the renal anomalies caused by disruption of the SHH pathway exemplify the complex interplay between primary and secondary developmental defects: while the gross histological defects seen in the kidney of these mice seem to be secondary to ectopia and fusion, abnormal development of the ureteric musculature might also contribute to more subtle defects seen in the kidney owing to perturbed urine flow; a role for SHH signalling in the continued growth of collecting ducts in the second trimester of human development might have even more subtle consequences, perhaps influencing the size of the kidney. In humans in whom both copies of the *DHCR7* gene is ablated (causing Smith-Lemli-Opitz syndrome), the ectopic kidneys can exhibit cystic dysplasia (Kelley et al. 2000), while patients with one missense loss-of-function allele of *SHH* have normally positioned kidneys that can occasionally be 'hypoplastic' (Dubourg et al. 2004). Thus, while a severe genetic insult on SHH signalling can significantly disrupt renal development secondary to altered positioning of the metanephros, a more mild insult has rare subtle consequences for the kidney via a more direct mechanism (Figure 30). Collectively, these observations suggest that disparate primary and secondary effects of a signalling pathway might therefore be hierarchical in genetic terms according to the immediacy of the different effects for kidney development.

**Figure 30. Modes of response to SHH in human renal tract tissues and the ontogeny of kidney malformations.**

At least three modes of response to SHH operate in human renal tract tissues. The KEY shows that the locations of the different proteins studied correspond to the colour of the hatching. Renal tract epithelia are a source of SHH, in the cloacal epithelium (**A**), urothelium of the urogenital sinus (**B**) and medullary collecting ducts of the kidney (**C**). SHH acts at short-range in the cloaca and kidney (**A,C**) whereas the molecules that would respond to SHH are expressed at a distance from the source in the urogenital sinus (**B**). While the data would be consistent with a canonical response to SHH in the lower renal tract (**A,B**), SMO is not expressed in the kidney (**C**); however, SHH would regulate collecting duct cell proliferation by a non-canonical mechanism involving CyclinB1. In the kidney, therefore, the molecular data would imply that signalling is also independent of the GLI transcription factors. This would suggest that the kidney malformations observed in *gli3*$^{\Delta 699/\Delta 699}$ mice are not caused by altered signalling within the metanephros *per se*, but are secondary to defective signalling during early embryonic development that disturbs formation of the kidney primordia, as evidenced by ectopia/aplasia. This is also supported by the combination of aplasia/ectopia with cystic dysplasia in the *shh*$^{-/-}$ kidneys, but the normal gross histology of *shh*$^{cn/cn}$ kidneys that form normally. In humans, kidney malformations associated with perturbed SHH signalling would have a skewed distribution as indicated by the hashed line in the stylised graph (**D**), since patients with the Smith-Lemli-Opitz syndrome (SLOS) have severe disease (indicated by the expressivity) with much higher penetrance than the occasional patient with a *SHH* mutation presenting with renal hypoplasia. The ectopia/aplasia and dysplasia in SLOS caused by homozygous *DHCR7* mutation, compared with the hypoplasia associated with heterozygous *SHH* mutation, would suggest that two populations of patient exist: the latter in whom a mild genetic insult on SHH signalling allows normal formation of the kidney but subtly disrupts subsequent development of the metanephros itself (red Gaussian curve); and the former in whom a more severe insult causes severe kidney malformations by disrupting its early formation (blue curve). This would indicate two distinct causes of kidney malformations associated with defective SHH signalling, and suggest that the effects on the kidney and the underlying causes can be judged according the severity of mutation.

**Figure 30.** **Modes of response to SHH in human renal tract tissues and the ontogeny of kidney malformations.**

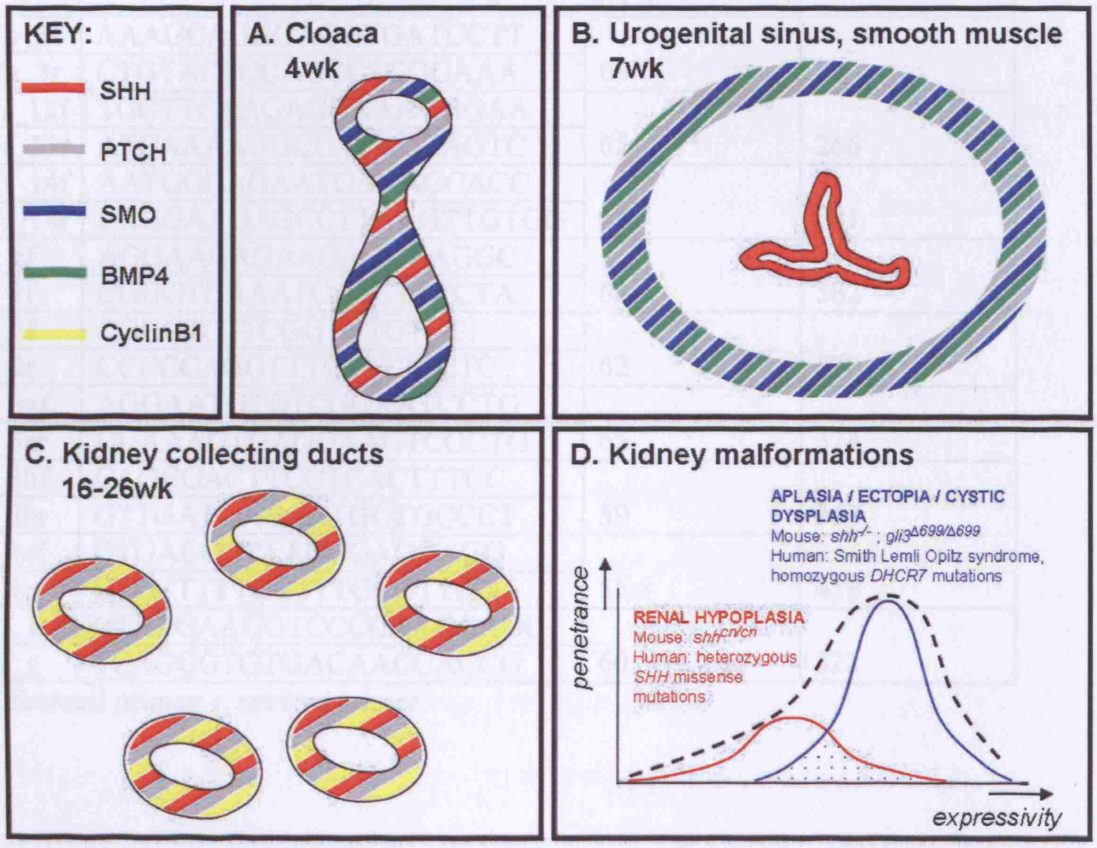

## Appendix I. PCR primers

Primer names and sequences, PCR annealing temperatures and product lengths for *UPIIIa*, *PTCH* and *SHH*. Other *Uroplakin* primers used were those previously published by Jiang et al. (2004).

| Primer | Primer sequence 5' to 3' | PCR annealing temperature (°C) | PCR product length (bp) |
|---|---|---|---|
| *UPIIIa*_3f | AAAGCAGGGAGGTGATCCTT | 68 | 749 |
| *UPIIIa*_3r | CTGTACTCCAGCCTGGGAAA | | |
| *PTCH*_13f | TGCTTCAAGAGGAAAGGGAA | 65 | 266 |
| *PTCH*_13r | ATCAAAAGGCCACAGCAGTC | | |
| *PTCH*_14f | AATGGCAGAATGAAAGCACC | 65 | 501 |
| *PTCH*_14r | CAGGAAGAGCCTTAAGTTGTGG | | |
| *SHH*_1f | AGGAAGAGAAGAGCGAGGC | 68 | 582 |
| *SHH*_1r | CGGGTGAAATCACCTTCCTA | | |
| *SHH*_2f | CGGCTCTTCGGTGTGTCT | 62 | 512 |
| *SHH*_2r | CCCCCAGGTTTCTTTTTCTC | | |
| *SHH*_3af | AGGAATGTGTCGGAATCCTG | 65 | 374 |
| *SHH*_3ar | GGAAAGTGAGGAAGTCGCTG | | |
| *SHH*_3bf | CAGCGACTTCCTCACTTTCC | 59 | 367 |
| *SHH*_3br | GTTGATGAGAATGGTGCCCT | | |
| *SHH*_3cf | GTGACCCTAAGCGAGGAGG | 55.5 | 459 |
| *SHH*_3cr | GTGTTTTTGCTTTGCGTTGC | | |
| *HaeIII*_f | GTATGAAGGTCCCCAAGCAGC | 60 | 322 |
| *HaeIII*_r | TCAGGGTGTGACAACCACCG | | |

Key: f, forward primer; r, reverse primer.

## Appendix II. Statistical genetic evidence in favour of a causative role for a *de novo* mutation

*De novo* mutations, acting in a dominant mode, have been reported in over 150 sporadically occurring human diseases according to a PubMed search (www.ncbi.nlm.nih.gov/entrez). Many of these diseases are genetically-lethal, with affected individuals failing to survive to adulthood, being reproductively sterile or not reproducing due to social stigma. One example is congenital central hypoventilation syndrome (OMIM_209880), with approximately 90% of such cases being caused by *de novo* mutations, usually polyalanine tract expansions in the gene *PHOX2B* (Amiel et al. 2003). Another example is Apert syndrome, with 99% of cases being caused by *de novo* mutations in one of two adjacent codons in *FGFR2* (Wilkie et al. 1995). An example involving X-linked dominant mutations is Rett syndrome, and it has been proposed that a preponderance of new mutations in the paternal germ-line coupled with 'genetic lethality' for both sexes can account for the *de novo* inheritance of *MECP2* mutations predominantly in females (Thomas 1996). These many reports suggest that *de novo* mutations constitute strong genetic evidence implicating a genetic variant in the causation of disease, although the strength of this evidence has not been evaluated in a formal statistical manner to my knowledge. The use of purely classical genetic evidence to implicate genetic variants in disease is particularly important here since two *de novo* mutations were identified in the non-coding 3' UTR of *UPIIIa*, and the following argument represents a purely abstract evaluation of the statistical evidence in favour of the hypothesis that a genetic change is causative of disease if it has arisen *de novo*, irrespective of putative functional effects.

*Probability of de novo mutation*

The statistical argument here hinges on the probability of observing a *de novo* mutation. Consider a two-generation family, each consisting of two unaffected parents and one affected child. Suppose that the disease is caused by a dominant gene, such that affected children have genotype *A*/- (*Aa* or *AA*; *A* is the disease-causing allele, that has population frequency $q$; *a* represents all other alleles, having frequency $p = 1-q$). The unaffected parents are of unknown genotype, but if they are of genotype *A*/-, they are unaffected with probability $1-f$; where $f$ is the penetrance. If a mutation ($A \rightarrow a$) is causative of disease, a proportion $I$ (Table 8) of patients will have inherited the mutation, while it will have arisen by *de novo* mutation in a proportion $p^4\mu$ of patients, where $\mu$ is the per nucleotide per generation mutation rate; in this latter scenario, it is assumed that their parents were of genotype *aa* (probability $p^4$), because although *de novo* mutations could occur in patients with a parent of genotype *Aa*, this is highly unlikely compared to the possibility that the variant was inherited. Thus the probability that affected individuals will have obtained a mutant allele by *de novo* mutation, assuming that it is causative of disease, is $\square = p^4\mu/(p^4\mu+I)$. In contrast the probability that a *de novo* mutation has occurred by chance alone and is unrelated to disease is simply $\mu$.

In calculating $\square$, as can be seen from Table 8, it is critical to be able to estimate the penetrance of the mutation. If we assume that for an autosomal dominant allele, the penetrance is related to the maximum frequency that it can take in controls ($q_{max}$), such

***Table 8. Probability of inheriting a mutation from unaffected parents***

| Mating | Prob. mating type | Prob. parents unaffected | Prob. meiosis →A- child | Total prob. |
|---|---|---|---|---|
| aa x aa | $p^4$ | 1 | 1 | ***0*** |
| Aa x aa | $2p^3q$ | $(1-f)$ | ½ | $\boldsymbol{p^3q(1-f)}$ |
| AA x aa | $p^2q^2$ | $(1-f)$ | 1 | $\boldsymbol{p^2q^2(1-f)}$ |
| Aa x Aa | $4p^2q^2$ | $(1-f)^2$ | ¾ | $\boldsymbol{3p^2q^2(1-f)^2}$ |
| AA x Aa | $2pq^3$ | $(1-f)^2$ | 1 | $\boldsymbol{2pq^3(1-f)^2}$ |
| AA x AA | $q^4$ | $(1-f)^2$ | 1 | $\boldsymbol{q^4(1-f)^2}$ |
| | | | Total | ***I*** |

All probabilities are derived under the assumption of Hardy-Weinberg equilibrium and Mendelian inheritance. $p$, population frequency of wild-type allele a; $q$, population frequency of mutant allele A; $f$, penetrance of allele A.

that $q_{max} = (1-f)e^{-f}$, since the greater the penetrance, the smaller that $q_{max}$ can be, then it is possible to estimate the penetrance from the frequency of the variant in a control population. Thus, for a fully penetrant disease allele, $f$=1, $I$=0 and □=1; all affected individuals will have arisen through *de novo* mutation

The alternative hypothesis ($H_1$) to be tested is that the mutation is causative of disease versus the null hypothesis ($H_0$) that the mutation is a chance event unrelated to disease status. A likelihood, $L$, is a conditional probability: specifically, the likelihood of $H_1$, $L(H_1)$, is the probability that the mutation is causative of disease given that it has arisen *de novo*; the likelihood of $H_0$, $L(H_0)$, is the probability of observing a *de novo* mutation given that it is not causative of disease. The likelihood ratio test of Haldane and Smith (1946) is based on the fact that the expected value of the ratio of $L(H_1)$:$L(H_0)$ is equal to 1 regardless of the alternative hypothesis (Wald 1947); as discussed by Morton (1955), if the likelihood ratio for a test of the null hypothesis against some alternative hypothesis is $\Lambda$, then $\Lambda > A$ (for $A>1$) can not occur with probability greater than $1/A$, since if it did this would itself raise the mean value of $\Lambda$ to 1, and so the occurrence of a value of $\Lambda$ greater than A would be significant evidence against the alternative hypothesis at the $1/A$ significance level. This general test also forms the basis of modern linkage analysis, adapted for sequential testing (Morton 1955).

*Statistical significance of identifying a de novo mutation*

□is the probability of a pathogenic *de novo* mutation occurring in a sporadically affected individual, whereas the probability of a *de novo* mutation occurring by chance

(unrelated to disease) is simply $\mu$; the odds in favour of an observed *de novo* mutation being pathogenic are therefore □$\mu$. The human genome consists of approximately $3x10^9$ base pairs, such that we are each born with, on average, $3\mu$ $x10^9$ *de novo* mutations. In sporadic index cases, therefore, the prior probability that a particular base pair, at which a *de novo* mutation occurs, is causative of disease is $(3\mu\ x10^9)^{-1}$. In addition, the greater the number of base pairs screened for mutations ($N$), the greater the chance that a *de novo* mutation that is unrelated to disease will be identified, such that the rate of false-positives is proportional to $N$. Therefore, a $p$-value of 5% (overall odds of 20:1 in favour of the alternative hypothesis) corresponds to an odds ratio of (20 x $3\mu$ $x10^9$ x $N$):1, equal to $60\mu N x10^9$:1, according to Bayes theorem.

Assuming that $\mu$ is of the order of $10^{-8}$ (Kondrashov 2003), if the entire genome ($N$=$3x10^9$) is screened for mutations odds of over $1.8x10^{13}$:1 (Lod=13.3) are required to provide significant evidence of pathogenicity, whereas if the coding region of an average size gene ($N$=$10^3$) is screened, odds of $6x10^6$:1 (Lod=6.8) are needed – as far as I am aware, this is the first rigorous evaluation of the statistical significance of observing a *de novo* mutation, and shows that such an observation can be a significant finding even if the 'mutant' allele is common in controls. For a fully penetrant autosomal dominant disease (□=1), observing a *de novo* mutation in one individual gives a Lod score of 8 (odds $10^8$:1), and two individuals with a *de novo* mutation at the same locus (Lod=16) are therefore needed for a genome-wide search, whereas only one such observation is required for a one-gene screen.

In the current situation, each independent occurrence of a *de novo* mutation in *UPIIIa* was observed after screening 1 kbp of DNA. Furthermore, the mutations were not detected in 96 control individuals. Let it be assumed, in the most conservative scenario, that if one further control allele had been screened, then the mutation would have been detected, giving a conservative population frequency of 1/193 chromosomes, or an allele frequency of 0.0052. This would give a minimum penetrance estimate of 0.986. From Table 8, therefore, this conservative penetrance gives a lod score of 3.8 for one observed *de novo* mutation, compared to a required score of 6.8 for significance. Two observed *de novo* mutations give a lod score of 7.6 and four give a lod score of 15.2. These four observed *de novo* mutations are therefore highly significant evidence in favour of a pathogenic role for these variants in causing disease.

## References

Abdelhak S, Kalatzis V, Heilig R, Compain S, Samson D, Vincent C, Weil D, Cruaud C, Sahly I, Leibovici M, Bitner-Glindzicz M, Francis M, Lacombe D, Vigneron J, Charachon R, Boven K, Bedbeder P, Van Regemorter N, Weissenbach J, Petit C. A human homologue of the Drosophila eyes absent gene underlies branchio-oto-renal syndrome and identifies and novel gene family. *Nat Genet* 15:157-164, 1997.

Adachi W, Okubo K, Kinoshita S. Human uroplakin Ib in ocular surface epithelium. *Invest Opthalmol Vis Sci* 41:2900-2905, 2000.

Adolphe C, Hetherington R, Ellis T, Wainwright B. Patched1 Functions as a Gatekeeper by Promoting Cell Cycle Progression. *Cancer Res* 66:2081-2088, 2006.

Airik R, Bussen M, Singh MK, Petry M, Kispert A. Tbx18 regulates the development of the ureteral mesenchyme. *J Clin Invest* 116:663-674, 2005.

Alcaraz A, Vinaixa F, Tejedo-Mateu A, Fores MM, Gotzens V, Mestres CA, Oliveira J, Caretero P: Obstruction and recanalization of the ureter during embryonic development. *J Urol* 145:410-461, 1991.

Amiel J, Laudier B, Attie-Bitach T, Trang H, de Pontial L, Gener B, Trochet D, Etchevers H, Ray P, Simonneau M, Vekemans M, Munnich A, Gaultier C, Lyonnet S. Polyalanine expansions and frameshift mutations of the paired-like homeobox gene PHOX2B in congenital central hypoventilation syndrome. *Nat Genet* 33:459-461, 2003.

Attar R, Quinn F, Winyard PJD, Mouriquand PDE, Foxall P, Hanson MA, Woolf AS. Short-term urinary flow impairment deregulates PAX2 and PCNA expression and cell survival in fetal sheep kidneys. *Am J Pathol* 152:1225-1235, 1998.

Baccallao R. The role of the cytoskeleton in renal development. *Semin Nephrol* 15:285-290, 1995.

Bai CB, Auerbach W, Lee JS, Stephen D, Joyner AL. Gli2, but not Gli1, is required for initial Shh signaling and ectopic activation of the Shh pathway. *Development* 129: 4753-4761, 2002.

Bai CB, Joyner AL. Gli1 can rescue the in vivo function of Gli2. *Development* 128:5161-5172, 2001.

Bailey RR. Vesicoureteric reflux in healthy infants and children. In: *Hodson J, Kincaid-Smith P (eds) Reflux nephropathy.* Masson, New York, pp 59-61, 1975.

Bale AE. Hedgehog signaling and human disease. *Annu Rev Genomics Hum Genet* 3:47-65, 2002.

Bao X, Faris AE, Jang EK, Haslam RJ. Molecular cloning, bacterial expression and properties of Rab31 and Rab32. *Eur J Biochem* 269:259-271, 2002.

Barnes EA, Heidtman KJ, Donoghue DJ. Constitutive activation of the shh-ptc1 pathway by a patched1 mutation indentified in BCC. *Oncogene* 24:902-915, 2005.

Barnes EA, Kong M, Ollendorff V, Donoghue DJ. Patched1 interacts with cyclin B1 to regulate cell cycle progression. *EMBO* 20:2214-2223, 2001.

Basson MA, Akbulut S, Watson-Johnson J, Simon R, Carroll TJ, Shakya R, Gross I, Martin GR, Lufkin T, McMahon AP, Wilson PD, Costantini FD, Mason IJ, Licht JD. Sprouty1 is a critical regulator of GDNF/RET-mediated kidney induction. *Dev Cell* 8:229-239, 2005

Batourina E, Gim S, Bello N, Shy M, Clagett-Dame M, Srinvas S, Costantini F, Mendelsohn C. Vitamin A controls epithelial/mesenchymal interactions through Ret expression. *Nat Genet* 27:74-78, 2001.

Battin J, Lacombe D, Leng JJ. Familial occurrence of hereditary renal adysplasia with mullerian anomalies. *Clin Genet* 43:23-24, 1993

Belk RA, Thomas DFM, Mueller RF, Godbole P, Markham AF, Weston MJ. A family study and the natural history of prenatally detected unilateral multicystic dysplastic kidney. *J Urol* 167:666-669, 2002.

Benazeraf B, Chen Q, Peco E, Lobjois V, Medevielle F, Ducommun B, Pituello F. Identificaion of an unexpected link between the Shh pathway and a G2/M regulator, the phosphatase CDC25B. *Dev Biol* 294:133-147, 2006.

Biason-Lauber A, Konrad D, Navratil F, Schoenle EJ. A WNT4 mutation associated with Mullerian-duct regression and virilization in a 46,XX woman. *New Engl J Med* 351:792-798, 2004.

Bingham C, Ellard S, Cole TRP, Jones KE, Allen LIS, Goodship JA, Goodship THJ, Bakalinova-Pugh D, Russell GI, Woolf AS, Nicholls AJ, Hattersley AT. Solitary functioning kidney and diverse genital tract malformations associated with hepatocyte nuclear factor-1β mutations. *Kidney Int* 61:1243-1251, 2002.

Bitgood, McMahon AP. Hedgehog and Bmp genes are expressed at many diverse sites of cell-cell interaction in mouse embryos. *Dev Biol* 172:126-138, 1995.

Bose J, Grotewold L, Ruther U. Pallister-Hall syndrome phenotype in mice mutant for *Gli3*. *Hum Mol Genet* 11:1129-1135, 2002.

Brandenberger R, Schmidt A, Linton J, Wang D, Backus C, Denda S, Muller U, Reichardt LF. Identification and characterization of a novel extracellular matrix protein

nephronectin that is associated with integrin α8β1 in the embryonic kidney. *J Cell Biol* 154:447-458, 2001.

Bullock SL, Johnson TM, Bao Q, Hughes RC, Winyard PJ, Woolf AS. Galectin-3 modulates ureteric bud branching in organ culture of the developing mouse kidney. *J Am Soc Nephrol* 12:515-23, 2001.

Cale CM, Klein NJ, Morgan G, Woolf AS. Tumour necrosis factor-α inhibits epithelial differentiation and morphogenesis in the mouse metanephric kidney in vitro. *Int J Dev Biol* 42:663-674, 1998.

Caruthers JM, Bonneville MA. The asymmetric unit membrane (AUM) structure in the luminal plasma membrane of urothelium: the effect of trypsin on the integrity of the plaques. *J Ultrastruct Res* 71:288-302, 1980.

Charrier JB, Lapointe F, Le Douarin NM, Teillet MA. Anti-apoptotic role of Sonic hedgehog protein at the early stages of nervous system organogenesis. *Development* 128:4011-4020, 2001.

Cayuso J, Ulloa F, Cox B, Briscoe J, Marti E: The Sonic hedgehog pathway independently controls the patterning, proliferation and survival of neuroepithelial cells by regulating Gli activity. *Development* 133:517-528, 2005.

Ceruso MA, Weinstein H. Structural mimicry of proline kinks. Tertiary packing interaction support local structural distortions. *J Mol Biol* 318:1237-1249, 2002.

Chang CP, McDill BW, Neilson JR, Joist HE, Epstein JA, Crabtree GR, Chen F. Calcineurin is required in urinary tract mesenchyme for the development of the pyeloureteral peristaltic machinery. *J Clin Invest* 113:1051-1058, 2004.

Chen Y, Guo X, Deng FM, Liang FX, Sun W, Ren M, Izumi T, Sabatini DD, Sun TT, Kreibich G. Rab27b is associated with fusiform vesicles and may be involved in targeting uroplakins to urothelial apical membranes. *Proc Natl Acad Sci USA* 100:14012-14017, 2003.

Chevalier RL, Goyal S, Kim A, Chang AY, Laudau D, LeRoith D. Renal tubulointerstitial injury from ureteral obstruction in the neonatal rat is attenuated by IGF-1. *Kidney Int* 57:882-890, 2000.

Chiang C, Litingtung Y, Lee E, Young KE, Corden JL, Westphal H, Beachy PA. Cyclopia and defective axial patterning in mice lacking Sonic hedgehog gene function. *Nature* 383: 407-413, 1996.

Chlapowski FJ, Bonneville MA, Staehelin LA. Lumenal plasma membrane of the urinary bladder. II. Isolation and structure of membrane components. *J Cell Biol* 53:92-104, 1972.

Cohen MM Jr. The hedgehog signaling network. *Am J Med Genet* 123:5-28, 2003.

Cooper MK, Wassif CA, Krakowiak PA, Taipale J, Gong R, Kelley RI, Porter FD, Beachy PA. A defective response to Hedgehog signaling in disorders of cholesterol biosynthesis. *Nat Genet* 33:508-513, 2003.

Cowan CA, Yokoyma N, Saxena A, Chumley MJ, Silvany RE, Baker LA, rivastava D, Henkemeyer M. Ephrin-B2 reverse signaling is required for axon pathfinding and cardiac valve formation but not early vascular development. *Dev Biol* 271:263-271, 2004.

Deng FM, Liang FX, Tu L, Resing KA, Hu P, Supino M, Hu CC, Zhou G, Ding M, Kreibich G, Sun TT. Uroplakin IIb, a urothelial differentiation marker, dimerizes with uroplakin Ib as an early step of urothelial plaque assembly. *J Cell Biol* 159:685-694, 2002.

Ding Q, Motoyama J, Gasca S, Mo R, Sasaki H, Rossant J, Hui CC. Diminished Sonic hedgehog signaling and lack of floor plate differentiation in Gli2 mutant mice. *Development* 125:2533-2543, 1998.

Dong JF, Gao S, Lopez JA. Synthesis, assembly, and intracellular transport of th platelet glycoprotein Ib-IX-V copmlex. *J Biol Chem* 273:31449-31454, 1998.

Dravis C, Yokoyama N, Chumley MJ. Bidirectional signaling mediated by ephrin-B2 and EphB2 controls urorectal development. *Dev Biol* 271:272-290, 2004.

Dubourg C, Lazaro L, Pasquier L, Bendavid C, Blayau M, Le Duff F, Durou MR, Odent S, David V. Molecular Screening of *SHH*, *ZIC2*, *SIX3* and *TGIF* Genes in Patients With Features of Holoprosencephaly Spectrum: Mutation Review and Genotype-Phenotype Correlations. *Hum Mutat* 24:43-51, 2004.

Dudley AT, Godin RE, Robertson EJ. Interaction between FGF and BMP signalling pathways regulates development of metanephric mesenchyme. *Genes Dev* 13:1601-1613, 1999.

Durbeej M, Larsson E, Ibraghimov-Beskrovnaya O, Roberds S L, Campbell KP, Ekblom P. Non-muscle α-dystroglycan is involved in epithelial development. *J Cell Biol* 130:79-91, 1995.

Edghill EL, Bingham C, Ellard S, Hattersley AT. Mutations in hepatocyte nuclear factor-1β and their related phenotypes. *J Med Genet* 43:84-90, 2006.

Edouga D, Hugueny B, Gasser B, Bussieres L, Laborde K. Recovery after relief of fetal urinary obstruction: morphological, functional and molecular aspects. *Am J Physiol* 281: F26-37, 2001.

Ekblom P, Ekblom M, Fecker L, Klein G, Zhang H-Y, Kadoya Y, Chu M-L, Mayer U, Timpl R. Role of mesenchymal nidogen for epithelial morphogenesis *in vitro*. *Development* 120:2004-2014, 1994.

Erlitzki R, Long JC, Theil EC. Multiple, conserved iron-responsive elements in the 3'-untranslated region of transferring receptor mRNA enhance binding of iron regulatory protein 2. *J Biol Chem* 277:42579-42587, 2002.

Evan AP, Satlin LM, Gattone II VH, Connors B, Schwartz GJ. Postnatal maturation of rabbit renal collecting duct. II. Morphological observations. *Am J Physiol* 261:F91-F107, 1991.

Forrester MB, Merz RD. Impact of excluding cases with known chromosomal abnormalities on the prevalence of structural birth defects, Hawaii, 1986-1999. *Am J Med Genet* 128A:383-388, 2004.

Feather SA, Malcolm S, Woolf AS, Wright V, Blaydon D, Reid CJD, Flinter FA, Proesmans W, Devriendt K, Carter J, Warwicker P, Goodship THJ, Goodship JA. Primary, non-syndromic vesicoureteric reflux and its nephropathy is genetically heterogeneous with a locus on chromosome 1. *Am J Hum Genet* 66:1420-1425, 2000.

Fischer E, Legue E, Doyen A, Nato F, Nicolas JF, Torres V, Yaniv M, Pontoglio M. Defective planar cell polarity in polycystic kidney disease. *Nat Genet* 38:21-23, 2006.

Fujita H, Yoshii A, Maeda J. Genitourinary anomaly in congenital varicella syndrome: case report and review. *Pediatr Nephrol* 19:554-557, 2004.

Gilbert S. *Developmental Biology*, 6th Edition. *Sinauer Associates, Inc. Massachussetts.* 2000.

Giltay JC, van de Meerakker J, van Amstel HK, de Jong TP. No pathogenic mutations in the ureoplakin III gene of 25 patients with primary vesicoureteral reflux. *J Urol* 171:931-932, 2004.

Glick PL, Harrison MR, Adzick NS, Noall RA, Villa RC. Correction of congenital hydronephrosis in utero IV: in utero decompression prevents renal dysplasia. *J Pediatr Surg* 19:649-657, 1984.

Goodman FR, Bachelli C, Brady AF, Brueton LA, Fryns JP, Mortlock DP, Innis JW, Holmes LB, Donnenfeld AE, Feingold M, Beemer FA, Hennekam RC, Scambler PJ. Novel HOXA13 mutations and the phenotypic spectrum of hand-foot-genital syndrome. *Hum Mol Genet* 67:197-202, 2000.

Goodrich LV, Scott MP. Hedgehog and patched in neural development and disease. *Neuron* 21:1243-1257, 1998.

Grieshammer U, Le Ma, Plump AS, Wang F, Tessier-Lavigne M, Martin GR. SLIT2-mediated ROBO2 signaling restricts kidney induction to a single site. *Dev Cell* 6:709-17, 2004.

Gritli-Linde A, Lewis P, McMahon AP, Linde A. The whereabouts of a morphogen: Direct evidence for short- and graded long-range activity of hedgehog signaling peptides. *Dev Biol* 236:364-386, 2001.

Grobstein C. Morphogenetic interaction between embryonic mouse tissues separated by a membrane filter. *Nature* 172:869-871, 1953.

Groenen PM, Vanderlinden G, Devriendt K, Fryns JP, Van de Ven WJ. Rearrangement of the human CDC5L gene by a t(6;19)(p21;q13.1) in a patient with multicystic renal dysplasia. *Genomics* 49:218-229, 1998.

Grutzner F, Graves JA. A platypus' eye view of the mammalian genome. *Curr Opin Genet Dev*14:642-649, 2004.

Gumbiner B, Stevenson B, Grimalfi A. The role of the cell adhesion molecule uvomorulin in the formation and maintenance of the epithelial junctional complex. *J Cell Biol* 107:1575-1587, 1988.

Guy RK. Inhibition of sonic hedgehog autoprocessing in cultured mammalian cells by sterol deprivation. *Proc Natl Acad Sci USA* 97:7303-7312, 2000.

Hagan DM, Ross AJ, Strachan Y. Mutation analysis and embryonic expression of the HLXB9 Currarino syndrome triad. *Am J Med Genet* 66:1504-1515, 2000.

Hahn H, Wojnowski L, Miller G, Zimmer A. The patched signaling pathway in tumorigenesis and development: lessons from animal models. *J Mol Med* 77:459-468, 1999.

Haldane JBS, Smith CAB. A new estimate of the linkage between the genes for colour-blindness and haemophilia in man. *Ann Eugen* 13:122-134, 1946.

Hall GD, Weeks RJ, Olsburgh J, Southgate J, Knowles MA, Selby PJ, Chester JD. Transcriptional control of the human urothelial-specific gene, uroplakin Ia. *Biochimica et Biophysica Acta* 1729:126-134, 2005.

Hardman P, Landels E, Woolf AS, Spooner BS. Transforming growth factor-β1 inhibits growth and branching morphogenesis in embryonic mouse submandibular and sublingual glands. *Dev Growth Differ* 36:567-577, 1994.

Hasan AK, Sato K, Sakakibara K, Ou Z, Iwasaki T, Ueda Y, Fukami Y. Uroplakin III, a novel Src substrate in Xenopus egg rafts, is a target for sperm protease essential for fertilization. *Dev Biol* 286:483-492, 2005.

Herzlinger D, Qiao J, Cohen D, Ramakrishna N, Brown AM. Induction of kidney epithelial morphogenesis by cells expressing Wnt-1. *Dev Biol* 166:815-818, 1994.

Hicks RM. The fine structure of the transitional epithelium of the rat ureter. *J Cell Biol* 26:25-48, 1965.

Hicks RM, Ketterer B. Hexagonal lattice of subunits in the thick luminal membrane of the rat urinary bladder. *Nature* 224:1304-1305, 1969.

Hicks RM, Ketterer B. Isolation of the plasma membrane of the luminal surface if rat bladder epithelium, and the occurrence of a hexagonal lattice of subunits both in negatively stained whole mounts and in sectioned membranes. *J Cell Biol* 45:542-553, 1970.

Hikita C, Vijayakumar S, Takito J, Erdjument-Bromage H, Tempst P, Al-Awqati Q. Induction of terminal differentiation in epithelial cells requires polymerization of hensin by galectin-3. *J Cell Biol* 151:1235-1246, 2000.

Hehr U, Gross C, Diebold U, Wahl D, Beudt U, Heidmann P, Hehr A, Mueller D. Wide phenotypic variability in families with holoprosencephaly and a sonic hedgehog mutation. *Eur J Pediatr* 163:347-352, 2004.

Hemler ME. Specific tetraspanin functions. *J Cell Biol* 155:1103-1107, 2001.

Hiraoka M, Taniguchi T, Nakai H, Kino M, Okada Y, Tanizawa A, Tsukahara H, Ohshima Y, Muramatsu I, Mayumi M. No evidence for AT2R gene derangement in human urinary tract anomalies. *Kidney Int* 59:1244-1249, 2001.

Huessler HS, Suri M, Young ID, Muenke M. Extreme variability of expression of a Sonic Hedgehog mutation: attention difficulties and holoprosencephaly. *Arch Dis Child* 86:293-296, 2002.

Ho KS, Scott MP. Sonic hedgehog in the nervous system: functions, modifications and mechanisms. *Curr Opin Neurobiol* 12:57-63, 2002.

Hooper JE, Scott MP. Communicating with Hedgehogs. *Nat Rev Mol Cell Biol* 6:306-317, 2005.

Horii A, Han HJ, Sasaki S, Shimada M, Nakamura Y. Cloning, characterization and chromosomal assignment of the human genes homologous to yeast PMS1, a member of mismatch repair genes. *Biochem Biophys Res Commun* 204:1257-1264, 1994.

Hu P, Deng FM, Laing FX, Hu Cm, Auerbach AB, Shapiro E, W XR, Kachar B, Sun TT. Ablation of Uroplakin III Gene Results in Small Urothelial Plaques, Urothelial Leakage, and Vesicoureteral Reflux. *J. Cell Biol* 151:961-971, 2000.

Hu CC, Liang FX, Zhou G, Tu L, Tang CH, Zhou J, Kreibich G, Sun TT. Assembly of Urothelial Plaques: Tetraspanin function in membrane protein trafficking. *Mol Biol Cell* 16:3937-3950, 2005a.

Hu MC, Mo R, Bhella S, Wilson CW, Chuang PT, Hui CC, Rosenblum ND. GLI3-dependent transcriptional repression of *Gli1*, *Gli2* and kidney patterning genes disrupts renal morphogenesis. *Development* 133:569-578, 2006.

Hynes PJ, Fraher JP. The development of the male genitourinary system: I. The origin of the urorectal septum and the formation of the perineum. *Br J Plast Surg* 57:27-36, 2004a.

Hynes PJ, Fraher JP. The development of the male genitourinary system: II. The origin and formation of the urethral plate. *Br J Plast Surg* 57:112-121, 2004b.

Ichikawa I, Kuwayama F, Pope IV JC, Stephens DF, and Miyazaki Y. Paradigm shift from classic anatomic theories to contemporary cell biological views of CAKUT. *Kidney International* 61:889-898, 2002.

Ingham PW, McMahon AP. Hedgehog signaling in animal development: paradigms and principles. *Genes Dev* 15:3059-3087, 2001.

Jadeja S, Smyth I, Pitera JE, Taylor MS, van Haelst M, Bentley E, McGregor L, Hopkins J, Chalepakis G, Philip N, Perez Aytes A, Watt FM, Darling SM, Jackson I, Woolf AS, Scambler PJ. Identification of a new gene mutated in Fraser syndrome and mouse myelencephalic blebs. *Nat Genet* 37:520-525, 2005.

Jarov A, Williams KP, Ling LE, Koteliansky VE, Duband JL, Fournier-Thibault C. A dual role for Sonic hedgehog in regulating adhesion and differentiation of neuroepithelial cells. *Dev. Biol.* 261:520-536, 2003.

Jenkins D, Bitner-Glindzicz M, Malcolm S, Hu CC, Allison J, Winyard PJ, Gullett AM, Thomas DF, Belk RA, Feather SA, Sun TT, Woolf AS. *De novo Uroplakin IIIa* heterozygous mutations cause human renal adysplasia leading to severe kidney failure. *J Am Soc Nephrol* 16:2141-2149, 2005.

Jenkins D, Bitner-Glindzicz M, Thomasson L, Malcolm S, Warne SA, Feather SA, Flanagan SE, Ellard S, Bingham C, Santos L, Henkemeyer M, Zinn A, Baker LA, Wilcox DT, Woolf AS. Mutational analyses of *UPIIIA*, *SHH*, *EFNB2*, and *HNF1*□in persistent cloaca and associated kidney malformations. *J Pediatr Urol*, 2006. *In press*.

Jiang S, Gitlin J, Deng FM, Liang FX, Lee A, Atala A, Bauer A, Ehrlich GD, Feather SA, Goldberg JD, Goodship JA, Goodship TH, Hermans M, Hu FZ, Jones KE, Malcolm S, Mendelsohn C, Preston RA, Retik AB, Schneck FX, Wright V, Ye XY, Woolf AS, Wu XR, Ostrer H, Shapiro E, Yu J, Sun TT. Lack of major involvement of human uroplakin

exons and flanking introns in primary vesicoureteral reflux: implications for disease heterogeneity. *Kidney Int* 66:10-19, 2004.

John U, Rudnik-Schoneborn S, Zerres K, Misselwitz J. Kidney growth and renal function in unilateral multicystic dysplastic kidney disease. *Pediatr Nephrol* 12:567-571, 1998.

Johnston JJ, Olivos-Glander I, Killoran C, Elson E, Turner JT, Peters KF, Abbott MH, Aughton DJ, Aylsworth DJ, Bamshad MJ, Booth C, Curry CJ, David A, Dinulos MB, Flannery DB, Fox MA, Graham JM, Grange DK, Guttmacher AE, Hannibal MC, Henn W, Hennekam RC, Holmes LB, Hoyme HE, Leppig KA, Lin AE, Macleod P, Manchester DK, Marcelis C, Mazzanti L, McCann E, McDOnald MT, Medndelsohn NJ, Moeschler JB, Moghaddam B, Neri G, Newbury-Ecob R, Pagon RA, Phillips JA, Sadler LS, Stoler JM, Tilstra D, Walsh Vockley CM, Zackai EH, Zadeh TM, Brueton L, Black GC, Biesecker LG. Molecular and clinical analyses of Grieg cephalopolysyndactyly and Pallister-Hall syndromes: robust phenotype prediction from the type and position of GLI3 mutations. *Am J Hum Genet* 76:609-622, 2005.

Kakoki M, Tsai YS, Kim HS, Hatada S, Ciavatta DJ, Takashashi N, Arnold LW, Maeda N, Smithies O. Altering expression in mice of genes by modifying their 3' regions. *Dev Cell* 6:597-606, 2004.

Kallin B, de Martin R, Etzold T, Sorrentino V, Philipson L. Cloning and growth arrest-specific and transforming growth factor beta-regulated gene, TI-1, from an epithelial cell line. *Mol Cell Biol* 11:5338-5345, 1991.

Keller SA, Jones Jm, Boyle A. Kidney and retinal defects (*Krd*), a transgene-induced mutation with a deletion of mouse chromosome 19 that includes the *Pax-2* locus. *Genomics* 23:309-320, 1994.

Kelley B, Ennis S, Yoneda A, Bermingham C, Shields DC, Molony C, Green AJ, Puri P, Barton DE. Uroplakin III is not a major candidate gene for primary vesicoureteral reflux. *Eur J Hum Genet* 13:500-502, 2005.

Kelley RI, Henekam RC. The Smith-Lemli-Opitz syndrome. *J Med Genet* 37:321-335, 2000.

Kim JH, Kim PCW, Hui CC. The VACTERL association: lessons from the Sonic hedgehog pathways. *Clin Genet* 59:306-315, 2001.

Klein G, Langegger M, Garidis C, Ekblom P. Neural cell adhesion molecules during embryonic induction and development of the kidney. *Development* 102:749-761, 1988.

Knudsen B, Hein J. Mfold: RNA secondary structure prediction using stochastic context-free grammars. *Nucleic Acids Res* 31:3423-3428, 2003.

Knutton S, Robertson JD. Regular structures in membranes. *J Cell Sci* 22:355-370, 1976.

Kolatsi-Joannou M, Bingham C, Ellard S, Bulman MP, Allen LI, Hettersley AT, Woolf AS. Hepatocyte nuclear factor-1beta: a new kindred with renal cysts and diabetes and gene expression in normal human development. *J Am Soc Nephrol* 12:2175-2180, 2001.

Koren G. Congenital varicella syndrome in the third trimester. *Lancet* 366:1591-1592, 2005.

Koshy TI, Luntz TL, Schejter A, Margoliash E. Changing the invariant proline-30 of rat and *Drosophila melanogaster* cytochromes c to alanine or valine destabilizes the heme crevice more than the overall conformation. *Proc Natl Acad Sci USA* 87:8697:8701, 1990.

Koss LG. The asymmetric unit membranes of the epithelium of the urinary bladder of the rat. An electron microscopic study of a mechanism of epithelial maturation and function. *Lab Invest* 21:154-168, 1969.

Kondrashov AS. Direct estimates of human per nucleotide mutation rate at 20 loci causing Mendelian diseases. *Hum Mutat* 21:12-27, 2003.

Kong XT, Deng FM, Hu P. Roles of uroplakins in plaque formation, umbrella cell enlargement, and urinary tract diseases. *J Cell Biol* 167:1195-1204, 2004.

Koseki C, Herzlinger D, Al-Awqati. Apoptosis in metanephric development. *J Cell Biol.* 119:1322-1333, 1992.

Kreidberg JA, Sariola H, Loring JM, Maeda M, Pelletier J, Housman D, Jaenisch R. WT-1 is required for early kidney development. *Cell* 74:679-691, 1991.

Kume T, Deng K, Hogan BL. Murine forkhead/winged helix genes Foxc1 (Mf1) and Foxc2 (Mfh1) are required for the early organogenesis of the kidney and urinary tract. *Development* 127 (7):1387-95, 2000.

Kusano KF, Pola R, Murayama T, Curry C, Kawamoto A, Iwakura A, Shintani S, Ii M, Asai J, Tkebuchava T, Thorne T, Takenaa H, Aikawa R, Goukassian D, von Samson, Hamada H, Yoon YS, Silver M, Eaton M Ma H, Heyd L, Kearney M, Munger W, Porter JA, Kishore R, Losordo DW. Sonic hedgehog myocardial gene therapy: tissue repair through transient reconstitution of embryonic signaling. *Nat Med* 11:1197-1204, 2005.

Kuwabara PE, Lee MH, Schedl T, Jefferis GSXE. A *C. elegans* patched gene, *ptc-1*, functions in germ-line cytokinesis. *Genes Dev* 14:1933-1944, 2000.

Kuwertz-Broeking E, Brinkmann OA, Von Lengerke HJ, Sciuke J, Fruend S, Bulla M, Harms E, Hertle L. Unilateral multicystic dysplastic kidney: experience in children. *BJU Int* 93:388-392, 2004.

Laemmli UK. Cleavage of structural proteins during the assembly of the head of bacteriophage T4. *Nature* 227:680-685, 1970.

Larsen WJ. *Human embryology*. New York, USA, Churchill Livingstone Inc. 1-540, 2001.

Liang FX, Riedel I, Deng FM, Zhou G, Xu C, Wu XR, Kong XP, Moll R, Sun TT. Organization of uroplakin subunits: transmembrane topology, pair formation and plaque composition. *Biochem J* 355:13-18, 2001.

Lee JJ, Ekker SC, von Kessler DP, Porter JA, Sun BI, Beachy PA. Autoproteolysis in hedgehog protein biogenesis. *Science* 266:1528-1537, 1994.

Lewis SA, de Moura JL. Apical membrane area of rabbit urinary bladder increases by fusion of intracellular vesicles: an electrophysiological study. *J Membr Biol* 82:123-136, 1984.

Lewis MA, Shaw J. Report from the paediatric renal registry. In The UK Renal Registry: the Fifth Annual Report. Eds. Ansell D, Burden R, Feest T, Newman D, Roderick P, Will E, Williams AJ. The Renal Association, Bristol, UK. 253-273, 2002.

Lin JH, Wu XR, Kreibich G, Sun TT. Precursor sequence, processing and urothelium-specific expression of a major 15-kDa protein subunit of asymmetric unit membrane. *J Biol Chem* 269:1775-1784, 1994.

Lin JH, Zhao H, Sun TT. A tissue-specific promoter that can drive a foreign gene to express in the suprabasal urothelial cells of transgenic mice. *Proc Natl Acad Sci USA* 92:679-683, 1995.

Lindsay S, Copp AJ. MRC-Wellcome Trust Human Developmental Biology Resource: enabling studies of human developmental gene expression. *Trends Genet* 21:586-590, 2005.

Litingtung Y, Chang C. Specification of ventral neuron types is mediated by an antagonistic interaction between Shh and Gli3. *Nature Neuroscience* 3:979-985, 2000.

Lopez-Casillas F, Cheifetz S, Doody J, Andres J, Lane W, Massague J. Structure and expression of the membrane proteoglycans betaglycan, a component of the TGF-beta complex..*Cell* 67:785-795, 1991.

Louie E, Ott J, Majewski J. Nucleotide frequency variation across Human Genes. *Genome Res.* 13:2594-2601, 2003.

Lum L, Beachy PA. The hedgehog response network: sensors, switches, and routers. *Science* 304:1755-1759, 2004.

Maizels M, Simpson SB. Primitive ducts of renal dysplasia induced by culturing ureteral buds denuded of condensed renal mesenchyme. *Science* 219:509-510, 1983.

Majumdar A, Vainio S, Kispert A, McMahon J, McMahon AP. Wnt11 and Ret/Gdnf pathways cooperate in regulating ureteric bud branching during metanpehric kidney development. *Development* 2003 130:3175-3185.

Manjeshwar S, Branam DE, Lerner MR, Brackett DJ, Jupe ER. Tumor suppression by the prohibitin gene 3'untranslated region RNA in human breast cancer. *Cancer Res* 63:5251-5256, 2003.

Matsuno T, Tokunaka S, Koyanagi T. Muscular development in the urinary tract. *J Urol* 132:148-152, 1984.

McNeill H, Ozawa M, Kemler R, Nelson WJ. Novel function of the cell adhesion molecule uvomorulin as an inducer of cell surface polarity. *Cell* 62:309-316, 1990.

McGregor L, Makela V, Darling SM, Vrontou S, Chalepakis G, Roberts C, Smart N, Rutland P, Prescott N, Hopkins J, Bentley E, Shaw A, Roberts E, Mueller R, Jadeja S, Philip N, Nelson J, Francannet C, Perez-Aytes A, Megarbane A, Kerr B, Wainwright B, Woolf AS, Winter RM, Scambler PJ. Fraser syndrome and mouse blebbed phenotype caused by mutations in FRAS1/Fras1 encoding a putative extracellular matrix protein. *Nat Genet* 34:203-208, 2003.

McPherson E, Carey J, Kramer A, Hall JG, Pauli RM, Schimke RN, Tasin MH. Dominantly inherited renal adysplasia. *Am J Med Genet* 26:863-872, 1987.

Minsky BD, Chlapowski FJ. Morphometric analysis of the translocation of luminal membrane between cytoplasm and cell surface of transitional epithelial cells during the expansion-contraction cycles of mammalian urinary bladder. *J Cell Biol* 77: 685-697, 1978.

Mendelsohn C. Functional obstruction: the renal pelvis rules. *J Clin Invest* 113:957-959, 2004.

Methot N, Basler K. Hedeghog controls limb development by regulating the activities fo distinct transcriptional activator and repressor forms of Cubitus interruptus. *Cell* 96: 819-831, 1999.

Methot N, Basler K. An absolute requirement for Cubitus interruptus in Hedgehog signaling. *Development* 128:733-742, 2001.

Mill P, Mo R, Hu MC, Dagnino L, Rosenblum ND, Hui CC. SHH Controls Epithelial Proliferation via Independent Pathways that Converge on N-Myc. *Dev. Cell* 9:293-303, 2005.

Miller M, Kaufman G, Reed G. Familial, balanced insertional translocation of chromosome 7 leading to offspring with deletion and duplication of the inserted segment, 7p15 leads to 7p21. *Am J Med Genet* 37:321-335, 1979.

Ming JE, Roessler E, Muenke M. Human developmental disorders and the Sonic hedgehog pathway. *Mol Med Today* 4:343-349, 1998.

Miyazaki Y, Oshima K, Fogo A, Hogan BL, Ichikawa I. Bone morphogenetic protein 4 regulates the budding site and elongation of the mouse ureter. *J Clin Invest* 105:863-873, 2000.

Mo R, Freer AM, Zinyk DL, Crackower MA, Michaud J, Heng HH, Chik KW, Shi XM, Tsui LC, Cheng SH. Specific and redundant functions of Gli2 and Gli3 zinc finger genes in skeletal patterning and development. *Development* 124: 113-123, 1997.

Mo R, Kim JH, Zhang J. Anorectal malformations caused by defects in sonic hedgehog signaling. *Am J Pathol* 159:765-774, 2001.

Molkentin JD, Tymitz KM, Richardson JA, Olson EN. Abnormalities of the Genotourinary Tract in Female Mice Lacking GATA5. *Mol Cell Biol* 20:5256-5260, 2000.

Montesano R, Matsumoto K, Nakamura T, Orci L. Identification of fibroblast-derived epithelial morphogen as hepatocyte growth factor. *Cell* 67:901-908, 1991.

Moore KL, Persaud TVN. *The developing human. Clinically oriented embryology.* Philadelphia, Pennsylvania, WB Saunders. 1-575, 2003.

Morton NE. Sequential tests for the detection of linkage. *Am J Hum Genet* 7:277-318, 1955.

Motoyama J, Liu J, Mo R, Ding Q, Post M, Hui CC. Essential function of Gli2 and Gli3 in the formation of lung, trachea and oesophagus. *Nat. Genet.* 20:54-57, 1998.

Muller U, Wang D, Denda S, Meneses JJ, Pedersen RA, Reichardt LF. Integrin $\alpha 8\beta 1$ is critically important for epithelial-mesenchymal interactions during kidney morphogenesis. *Cell* 88:603-613, 1997.

Mullor JL, Sanchez P, Altaba AR. Pathways and consequences: Hedgehog signaling in human disease. *Trends Cell Biol* 12:562-569, 2002.

Musch A. Microtubule organisation and function in epithelial cells. *Traffic* 5:1-9, 2004.

Nakashima M, Tanese N, Ito M, Auerbach W, Bai C, Furukawa T, Toyono T, Akamine A, Joyner AL. A novel gene, *GliH1*, with homology to the *Gli* zinc finger domain not required for mouse development. *Mech Dev* 119:21-34, 2002.

Nauli SM, Alenghat FJ, Luo Y, Williams E, Vassilev P, Li X, Elia AE, Lu W, Brown EM, Quinn SJ, Ingber DE, Zhou J. Polycystins 1 and 2 mediate mechanosensation in the primary cilium of kidney cells. *Nat Genet* 33:129-137, 2003.

Nicolaides NC, Carter KC, Shell BK, Papadpoulos N, Vogelstein B, Kinzler KW. Genomic organization of the human PMS2 gene family. *Genomics* 30:195-206, 1995.

Nievelstein RA, van der Werff JF, Verbeek FJ, Valk J, Vermeij-Keers C. Normal and abnormal embryonic development of the anorectum in human embryos. *Teratology* 57:70-78, 1998.

Nishimura H, Yerkes E, Hohefellner K, Miyazaki Y, Ma J, Hunley TE, Yoshida H, Ichiki T, Threadgill D, Phillips JA 3rd, Hogan BML, Fogo A, Brock JW 3rd, Inagami T, Ichikawa I. Role of the angiotensin type 2 receptor gene in congenital anomalies of the kidney and urinary tract, CAKUT, of mice and men. *Mol Cell* 3:1-10, 1999.

Nishinakamura R, Matsumoto Y, Nakao K, Nakamura K, Sato A, Copeland NG, Gilbert DJ, Jenkins NA, Scully S, Lacey DL, Katsuki M, Asashima M, Yokota T. Murine homologue of SALL1 is essential for ureteric bud invasion in kidney development. *Development* 128:3105-3115, 2001.

Noakes PG, Miner JH, Gautam M, Cunningham JM, Sanes J, Merlie JP. The renal glomerulus of mice lacking s-laminin/laminin β2: nephrosis despite molecular compensation by laminin β1. *Nat Genet* 10: 400-406, 1995.

Nusslein-Volhard C, Wieschaus E. Mutations affecting segment number and polarity in Drosophila. *Nature* 287:795-801, 1980.

Nybakken K, Perrimon N. Hedgehog signal transduction: recent findings. *Curr Opin Genet Dev* 12:503-511, 2002.

Nyirady P, Thiruchelvam N, Fry CH, Godley ML, Winyard PJD, Peebles DM, Woolf AS, Cuckow PM. Effects of in utero bladder outflow obstruction on fetal sheep detrusor contractility, compliance and innervation. *J Urol* 168:1615-1620, 2002.

Odent S, Atti-Bitach T, Blayau M. Expression of the Sonic hedgehog (SHH) gene during early human development and phenotypic expression of new mutations causing holoprosencephaly. *Hum Mol Genet* 8:1683-1689, 1999.

Okazaki T, Otaka Y, Wang J, Hiai H, Takai T, Ravetch JV, Honjo T. Hydronephrosis associated with antiurothelial and antinuclear autoantibodies in BALB/c-Fcgr2b-/-Pdcd1-/-mice. *J Exp Med* 19:1643-1648, 2005.

Olsburgh J, Weeks R, Selby P, Southgate J. Human uroplakin 1b gene structure and promoter analysis. *Biochimica et Biophysica Acta* 1576:163-170, 2002.

Olsburgh J, Harnden P, Weeks R, Smith B, Joyce A, Hall G, Poulsom R, Selby P Southgate J. Uroplakin gene expression in normal human tissues and locally advanced bladder cancer. *J Pathol* 199:41-49, 2003.

Osathanondh V, Potter EL. Development of kidneys as shown by microdissection. I. Preparation of tissues with reasons for possible misinterpretation of observations. *Arch Pathol* 76:271-276, 1963a.

Osathanondh V, Potter EL. Development of kidneys as shown by microdissection. II. Renal pelvis, calyces and papillae. *Arch Pathol* 76:277-289, 1963b.

Osathanondh V, Potter EL. Development of kidneys as shown by microdissection. III. Formation and interrelationship of collecting ducts and nephrons. *Arch Pathol* 76:290-302, 1963c.

Osathanondh V, Potter EL. Development of the human kidney as shown by microdissection: IV. Development of tubular portions of nephrons. *Arch Pathol* 82:391-402, 1966a.

Osathanondh V, Potter EL. Development of the human kidney as shown by microdissection. V. Development of vascular pattern of glomerulus. *Arch Pathol* 82:403-411, 1966b.

Park HL, Bai C, Platt KA, Matise MP, Beeghly A, Hui CC, Nakashima M, Joyner AL. Mouse Gli1 mutants are viable but have defects in SHH signaling in combination with a Gli2 mutation. *Development* 127: 1593-1605, 2000.

Parker M, Ashcroft R, Wilkie AO. Ethical review of research into rare genetic disorders. *BMJ* 329:288-289, 2004.

Parsons CF, Stauffer C, Schmidt JD. Bladder surface glycosaminoglycans: an efficient mechanism of environmental adaptation. *Science* 605-607, 1980.

Pauli BU, Alroy J, Weinstein RS. The ultrastructure and pathobiology of urinary bladder cancer. In *The Pathology of Bladder Cancer* (ed. Bryan GT, Cohen SM), CRC Press, Boca Raton, Florida, pp42-140, 1983.

Pathi S, Pagan-Westphal S, Baker DP, Garber EA, Rayhorn P, Bumcrot D, Tabin CJ, Pepinsky RB, Williams KP. Comparative biological responses to human Sonic, Indian and Desert Hedgehog. *Mech Dev* 106: 107-117, 2001.

Pennington EC, Hutson JM. The cloacal plate: the missing link in anorectal and urogenital development. *BJU International* 89:726-732, 2002a.

Pennington EC, Hutson JM. The urethral plate--does it grow into the genital tubercle or within it? *BJU International* 89:733-739, 2002b.

Perantoni AO, Dove LF, Karavanova I. Basic fibroblast growth factor can mediate the early inductive events in renal development. *Proc Natl Acad Sci USA* 92:4696-4700, 1995.

Pfeffer SR, Soldati T, Geissler H, Rancano C, Dirac-Svejstrup B. Selective membrane recruitment of Rab GTPases. *Cold Spring Harbor Symp Quant Biol* 60:221-227, 1995.

Pfeffer SR. Transport-vesicle targeting: tethers before SNAREs. *Nat Cell Biol* 1:E17-E22, 1999.

Pfeffer SR. Rab GTPases: specifying and deciphering organelle identity and function. *Trends Cell Biol* 11:487-491, 2001.

Poole ES, Brown CM, Tate WP. The identity of the base following the stop codon determines the efficiency of in vivo translational termination in Escherichia coli. *EMBO J* 14 (1):15-18, 1995.

Porter KR, Bonneville MA. *An Introduction to the Fine Structure of Cells and Tissues. Lea & Febiger, New York*, 1963.

Porter KR, Kenyon K, Badenhausen S. Specializations of the unit membrane. *Protoplasma* 63:262-274, 1967.

Porter JA, von Kessler DP, Ekker SC, Young KE, Lee JJ, Moses K, Beachy PA. The product of *hedgehog* autoproteolytic cleavage active in local and long-range signaling. *Nature* 374: 363-366, 1995.

Potter EL. *Normal and Abnormal Development of the Kidney*. Year Book Medical Publishers, Inc. Chicago. 1-305, 1972.

Qi BG, Beasley SW, Williams AK, Frizelle F. Does the urorectal septum fuse with the cloacal membrane?. *J Pediatric Surgery* 35 (12):1810-1816, 2000.

Rathke H. Abhandhungen zur Bildungs- und Entwicklungsgeschichte der Tier. Leipzig. 1832.

Rees L. Management of the infant with end-stage renal failure. *Nephrol Dial Transplant* 17:1564-1567, 2002.

Retterer E. Sur l'origine et l'evolution de la region ano-genitale des mammiferes. *J Anat Physiol* 26:126-216, 1890.

Rink RC, Herndon CD, Cain MP. Upper and lower urinary tract outcome after surgical repair of cloacal malformations: a three decade experience. *BJU Int* 96:131-134, 2005.

Ruggieri MR, Balagani RK, Rajter JJ, Hanno PM. Characterization of bovine bladder mucin fractions that inhibit Escerischia coli adherence to the mucin deficient rabbit bladder. *J Urol* 148:173-178, 1992.

Roessler E, Ermilov AN, Grange DK, Wang A, Grachtchouk M, Dlugosz AA, Muenke M. A previously unidentified amino-terminal domain regulates transcriptional activity of wild-type and disease-associated human GLI2. *Hum Mol Genet* 14:2181-2188, 2005.

Roessler E, Du YZ, Mullor JL, Casas E, Allen WP, Gillessen-Kaesbach G, Roeder ER, Ming JE, Altaba AR, Muenke M. Loss-of-function mutations in the human *GLI2* gene are associated with pituitary anomalies and holoprosencephaly-like features. *Proc Natl Acad Sci USA* 100:13424-13429, 2003.

Roesller E, Muenke M. How a Hedgehog might see holoprosencephaly. *Hum Mol Genet* 12:R15-R25, 2003.

Rogers SA, Ryan G, Purchio AF, Hammerman MR. Metanephric transforming growth factor-β1 regulates nephrogenesis in vitro. *Am J Physiol* 264:F996-F1002, 1993.

Romih R, Jezernik K, Masera A. Uroplakins and cytokeratins in the regenerating rat urothelium after sodium saccharin treatment. *Histochem Cell Biol* 109:263-269, 1998.

Romih R, Korosec P, Jezernik K, Sedmak B, Trsinar B, Deng FM, Liang FX, Sun TT. Inverse expression of uroplakins and inducible nitric oxide synthase in the urothelium of patients with bldder outlet obstruction. *BJU International* 91:507-512, 2003.

Romih R, Korosec P, de Mello W Jr, Jezernik K. Differentiation of epithelial cells within the urinary tract. *Cell Tissue Res* 320:259-268, 2005.

Roodhooft AM, Birnholz JC, Holmes LB. Familial nature of congenital absence and severe dysgenesis of both kidneys. *N Eng J Med* 310:1341-1345, 1984.

Rothenpieler UW, Dressler GR. *Pax-2* is required for mesenchyme-to-epithelium conversion during kidney development. *Development* 119:711-720, 1993.

Ruano-Gil D, Coca-Payeras A, Tejedo-Mateu A. Obstruction and normal recanalization of the ureter in the human embryo. Its relation to congenital ureteric obstruction. *Eur Urol* 1:287-293, 1975.

Ruf RG, Xu PX, Silvius D, Otto EA, Beekmann F, Muerb UT, Kumar S, Neuhaus TJ, Kemper MJ, Raymond Rm Jr, Brophy PD, Berkman J Gattas M, Hyland V, Ruf EM, Scwartz C, Chang EH, Smith RJ, Stratakis CA, Weil D, Petit C, Hildebrandt F. SIX1

mutations cause branchio-oto-renal syndrome by disruption of EYA1-SIX1-DNA complexes. *Proc Natl Acad Sci USA* 101:8090-8095, 2004.

Sakakibara K, Sato K, Yoshino K. Molecular identification and characterization of Xenopus egg uroplakin III, an egg raft-associated transmembrane protein that is tyrosine-phosphorylated upon fertilization. *J Biol Chem* 280:15029-15037, 2005.

Salerno A, Kolhase J, Kaplan BS. Townes-Brock syndrome and renal dysplasia: A novel mutation in the *SALL1* gene. *Pediatr Nephrol* 14:25-28, 2000.

Santos OFP, Nigam SK. HGF-induced tubulogenesis and branching of epithelial cells is modulated by extracellular matrix and TGF-β. *Dev Biol* 160:293-302, 1993.

Sanyanusin P, Schimmentil LA, McNoe LA, Ward TA, Pierpont ME, Sullivan MJ, Dobyns WB, Eccles MR. Mutations of the *PAX2* gene in a family with optic nerve colobomas, renal anomalies and vesicoureteral reflux. *Nat Genet* 9:358-364, 1995.

Sarikas SN, Chlapowski FJ. Effect of ATP inhibitors on the translocation of luminal membrane between cytoplasm and cell surface of transitional epithelial cells during the expansion-contraction cycle of the rat urinary bladder. *Cell Tissue Res* 246: 107-117, 1986.

Sasaki C, Yamaguchi K, Akita K. Spatiotemporal distribution of apoptosis during normal cloacal development in mice. *The Anatomical Record Part A* 279A:761-767, 2004a.

Sasaki Y, Iwai N, Tsuda T, Kimura O. Sonic hedgehog and bone morphogenetic protein 4 expressions in the hindgut region of murine embryo with anorectal malformation. *J Pediatr Surg* 39:170-173, 2004b.

Sase M, Tsukahara M, Oga A, Kaneko N, Nakata M, Saito T, Kato H. Diffuse cystic renal dysplasia: nonsyndromal familial case. *Am J Med Genet* 63:332-334, 1996.

Saxen L. Organogenesis of the kidney. Cambridge, UK: Cambridge Universisty Press, 1987, 1-184.

Scholz H, Kirschner KM. A role for the Wilms' tumor protein WT1 in organ development. *Physiology* (Bethesda) 20:54-59, 2005.

Schonfelder EM, Knuppel T, Tasic V, Milijkovic P, Konrad M, Wuhl E, Antignac C, Bakkaloglu A, Schaefer F, Weber S: ESCAPE Trial Group. Mutations in Uroplakin IIIA are a rare cause of renal hypodysplasia in humans. *Am J Kidney Dis* 47:1004-1012, 2006.

Schroeter S, Tosney KW. Spatial and temporal patterns of muscle cleavage in the chck thigh and their value as criteria for homology. *Am J Anat* 191:325-350, 1991.

Schuchardt A, D'Agati V, Pachnis V, Constantini F. Renal agenesis and hypodysplasia in ret-k- mutant mice result from defects in ureteric bud development. *Development* 122:1919-29, 1996.

Severs NJ, Hicks RM. Analysis of membrane structure in the transitional epithelium of rat urinary bladder. *J Ultrastruct Res* 69:279-296, 1979.

Shah MM, Sampogna RV, Sakurai H, Bush KT, Nigam SK. Branching morphogenesis and kidney disease. *Development* 131:1449-1462, 2004.

Shapiro E, Huang HY, Wu XR. Uroplakin and androgen receptor expression in the human fetal genital tract: insights into the development of the vagina. *J Urol* 164:1048-1051, 2000.

Shawlot W, Behringer RR. Requirement for Lim1 in head-organizer function. *Nature* 374:425-432, 1995.

Shyamala BV, Bhat KM. A positive role for Patched-Smoothened signaling in promoting cell proliferation during normal head development in *Drosophila*. *Development* 129:1839-1847, 2002.

Simons K, Zerial M. Rab proteins and the road maps for intracellular transport. *Neuron* 11:789-799, 1993.

Simpson JL. Genetics of the female reproductive tract. *Am J Med Genet* 89:224-239, 1999.

Slavotinek AM, Biesecker LG. Phenotypic overlap of McKusick-Kaufman syndrome with Bardet-Biedl syndrome: a literature review. *Am J Med Genet* 95:208-215, 2000.

Slotkin TA, Seidler FJ, Kavlock RJ, Gray JA. Fetal dexamethasone exposure accelerates development of renal function: relationship to dose, cell differentiation and growth inhibition. *J Dev Physiol* 17:55-61, 1992.

Sorenson CM, Rogers SA, Korsmeyer SJ, Hammerman MR. Fulminant metanephric apoptosis and abnormal kidney development in bcl-2-deficient mice. *Am J Physiol* 268: F73-81, 1995.

Sorokin L, Sonnenberg A, Aumailley M, Timpl R, Ekblom P. Recognition of the laminin E8 cell-binding site by and integrin possessing the alpha 6 subunit is essential for epithelial polarization in developing kidney tubules. *J Cell Biol* 111:1265-1273, 1990.

Squiers EC, Morden RS, Bernstein J. Renal multicystic dysplasia: an accasional manifestation of the hereditary renal adysplasia syndrome. *Am J Med Genet* 2"279-284, 1987.

Staehelin LA, Chlapowski FJ, Bonneville MA. Lumenal plasma membrane of the urinary bladder. I. *J Cell Biol* 53:73-91, 1972.

Stark K, Vainio S, Vassileva G, McMahon AP. Epithelial transformation of metanephric mesenchyme in the developing kidney regulated by *Wnt-4. Nature* 372:679-683, 1994.

Steinhardt GF, Lipais H, Phillips B, Volger G, Nag M, Yoon KW. Insulin-like growth factor improves renal architecture of fetal kidneys with complete ureteric obstruction. *J Urol* 154:690-693, 1995.

St-Jacques B, Hammerschmidt M, McMahon AP. Indian hedgehog signaling regulates proliferation and differentiation of chondrocytes and is essential for bone formation. *Genes Dev* 13:2072-2086, 1999.

Surya B, Yu J, Manabe M, Sun TT. Assessing the differentiation state of cultured bovine urothelial cells: elevated syndthesis of stratification-related K5 and K6 keratins and persistent expression of uroplakin I. *J Cell Sci* 97:419-432, 1990.

Tacciuoli M, Lotti T, de Matteis A, Laurenti C. Development of the smooth muscle of the ureter and vesical trigone: histological investigation in human fetus. *Eur Urol* 1:282-286, 1975.

Testaz S, Jarov A, Williams KP, Ling LE, Koteliansky VE, Fournier-Thibault C, Duband JL. Sonic hedgehog restricts adhesion and migration of neural crest cells independently of the Patched-Smoothened-Gli signaling pathway. *Proc Natl Acad Sci USA* 98:12521-12526, 2001.

Thibert C, Teillet MA, Lapointe F, Mazelin L, Le Douarin NM, Mehlen P. Inhibition of Neuroepithelial Patched-Induced Apoptosis by Sonic Hedgehog. *Science* 301:843-846, 2003.

Thiruchelvam N, Nyirady P, Peebles DM, Fry CH, Cuckow PM, Woolf AS. Urinary outflow obstruction increases apoptosis and degregulates Bcl-2 and Bax expression in the fetal ovine bladder. *Am J Pathol* 162:1271-1282, 2003.

Thomas GH. High male:female ratio of germ-line mutations: an alternative explanation for postulated gestational lethality in males in X-linked dominant disorders. *Am J Hum Genet* 58:1364-1368, 1996.

Torres M, Gomex-Pardo E, Dressler GR, Gruss P. *Pax-2* controls multiple steps of urogenital development. *Development* 121:4057-4065, 1995.

Torrey TW. The early development of the human nephros. *Contrib Embryol Carnegie Inst* 35:175, 1954.

Tourneaux F. Sur les premiers developpements du cloaque du tubercle genital et de l'anus chez l'embryon de mouton. *Anat Physiol* 24 :503-17, 1888.

Towers PR, Woolf AS, Hardman P. Glial cell line-derived neurotrophic factor stimulates ureteric bud outgrowth and enhances survival of ureteric bud cells in vitro. *Exp Nephrol* 6:337-351, 1998.

Tsang TE, Shawlot W, Kinder SJ, Kobayashi A, Kwan KM, Schughart K, Kania A, Jessell TM, Behringer RR, Tam PP. Lim1 activity is required for intermediate mesoderm differentiation in the mouse embryo. *Dev Biol* 223:77-90, 2000.

Tse HK, Leung MB, Woolf AS, Menke AL, Hastie ND, Gosling JA, Pang CP, Shum AS. Implication of Wt1 in the pathogenesis of nephrogenic failure in a mouse model of retinoic acid-induced caudal regression syndrome. *Am J Pathol* 37:520-525, 2005.

Tu L, Sun TT, Kreibich G. Specific heterodimers formation is a prerequisite for uroplakins to exit from the endoplasmic reticulum. *Mol Biol Cell* 13:4221-4230, 2002.

Twigg SR, Kan R, Babbs C, Bochukova EG, Robertson SP, Wall SA, Morriss-Kay GM, Wilkie AO. Mutations of ephrin-B1 (EFNB1), a marker of tissue boundary formation, cause craniofrontonasal syndrome. *Proc Natl Acad Sci USA* 101: 8652-8657, 2004.

Valasek P, Evans DJR, Maina F, Grim M, Patel K. A dual fate of the hindlimb muscle mass: cloacal/perineal musculature develops from leg muscle cells. *Development* 132:447-458, 2005.

Varley CL, Stahlschmidt J, Lee WC, Holder J, Diggle C, Selby PJ, Trejdosiewicz LK, Southgate J. Role of PPARgamma and EGFR signalling in the urothelial terminal differentiation programme. *J Cell Sci* 117:2029-2036, 2004.

Van den Brink GR, Hardwick JC, Tytgat GN, Brink MA, Ten Kate FJ, Van Deventer SJ, Pepelenbosch MP. Sonic hedgehog regulates gastric gland morphogenesis in man and mouse. *Gastroenterology* 121:317-328, 2001.

Van Esch, Groenen P, Nesbit MA, SChuffenhauer S, Lichter P, Vanderlinden G, Harding B, Beetz R, Bilous RW, Holdaway I, Shaw NJ, Fryns JP, Van de Ven W, Thakker RV, Devriendt K. GATA3 haplo-insufficiency causes human HDR syndrome. *Nature* 406:419-422, 2000.

Vergara J, Longley W, Robertson JD. A hexagonal arrangement of subunits in membrane of mouse urinary bladder. *J Mol Biol* 46:593-596, 1969.

Vestweber D, Kemler R, Ekblom P. Cell-adhesion molecule uvomorulin during kidney development. *Dev Biol* 112:213-221, 1985.

von Heijne. A new method for predicting signal sequence cleavage sites. *Nucleic Acids Res* 14:4683-4690, 1986.

von Heijne G. Proline kinks in transmembrane alpha-helices. *J Mol Biol* 218:499-503, 1991.

Waggoner SA, Liebhaber SA. Regulation of alpha-globin mRNA stability. *Exp Biol Med* 228:387-395, 2003.

Wald A. 1947. *Sequential Analysis*. New York: Wiley.

Warne SA, Wilcox DT, Ransley PG. Long-term urological outcome in patients presenting with persistent cloaca. *J Urol* 168:1859-1862, 2002a.

Warne SA, Wilcox DT, Ledermann SE, Ransley PG. Renal outcome in patients with cloaca. *J Urol* 167:2548-2551, 2002b.

Warne SA, Wilcox DT, Creighton S, Ransley PG. Long-term gynaecological outcome of patients with persistent cloaca. *J Urol* 170:1493-1496, 2003.

Warne SA, Godley ML, Wilcox DT. Surgical reconstruction of cloacal malformations can alter bladder function: a comparative study with anorectal anomalies. *J Urol* 172:2377-2381, 2004.

Warot X, Fromental-Ramain C, Fraulob V, Chambon P, Dolle P. Gene dosage-dependent effects of the *Hoxa*-13 and *Hoxd-13* mutations on morphogenesis of the terminal parts of the digestive and urogenital tracts. *Development* 124:4781-4791, 1997.

Weber S, Mir S, Schlingmann KP, Nurnberg G, Becker C, Kara PE, Ozkayin N, Konrad M, Nurnberg P, Schaefer F. Gene locus ambiguity in posterior urethral valves/prune-belly syndrome. *Pediatr Nephrol* 20:1036-1042, 2005.

Welham SJ, Riley PR, Wade A, Hubank M, Woolf AS. Maternal diet programs embryonic kidney gene expression. *Physiol Genomics* 22:48-56, 2005.

Wilkie AO, Slaney SF, Oldridge M, Poole MD, Ashworth GJ, Hockley AD, Hayward RD, David DJ, Pulleyn LJ, Rutland P. Apert syndrome results from localized mutations of FGFR2 and is allelic with Crouzon syndrome. *Nat Genet* 9:165-172, 1995.

Williams I, Richardson J, Starkey A, Stansfield I. Genome-wide prediction of stop codin readthorugh during translation in the yeast *Saccharomyces cerevisiae*. *Nucleic Acids Res* 32:6605-6616, 2004.

Winyard PJD, Risdon RA, Sams VR, Dressler GR, Woolf AS. The PAX2 transcription factor is expressed in cystic and hyperproliferative dysplastic epithelia in human kidney malformations. *J Clin Invest* 98:451-459, 1996.

Winyard PJD, Nauta J, Lirenman DS, Hardman P, Sams VR, Risdon AR, Woolf AS. Deregulation of cell survival in cystic and dysplastic renal development. *Kidney Int* 49:135-146, 1996b.

Winyard PJD, Bao Q, Hughes RC, Woolf AS. Epithelial galectin-3 during human nephrogenesis and childhood cystic diseases. *J Am Soc Nephrol* 8:1647-1657, 1997.

Woolf AS, Kolatsi-Joannou M, Hardman P, Andermarcher E, Moorby C, Fine LG, Jat PS, Noble MD, Gherardi E. Roles of hepatocyte growth factor/scatter factor and met in early development of the metanephros. *J Cell Biol* 128:171-184, 1995.

Woolf AS, Welham SJM, Hermann MM, Winyard PJD. Maldevelopment of the human kidney and lower urinary tract: an overview. *In The Kidney: from Normal Development to Congenital Disease.* Eds Vize PD, Woolf AS, Bard JBL. Elsevier Science/Academic Press 377-393, 2003.

Woolf AS, Price KL, Scambler PJ, Winyard PJ. Evolving concepts in human renal dysplasia. *J Am Soc Nephrol* 15:998-1007, 2004.

Woolf AS, Wilcox DT. Understanding primary vesicoureteric reflux and associated nephropathies. *Curr Paediatr* 14:563-567, 2004.

Woolf AS, Jenkins D. Development of the kidney. In *Heptinstall's Pathology of the Kidney.* 6th edition. Eds Jennette JC, Olson JL, Schwartz MM, Silva FG. Lippincott-Raven, Philadelphia-New York, USA, 2006. *In press.*

Wu XR, Manabe M, Yu J, Sun TT. Large scale purification and immunlocalization of bovine uroplakins I, II and III. Molecular markers fo urothelial differentiation. *J Biol Chem* 265:19170-19179, 1990.

Wu XR, Sun TT. Molecular cloning of a 47 kDa tissue-specific and differentiation-dependent urothelial cell surface glycoprotein. *J Cell Sci* 106: 31-43, 1993.

Wu XR, Lin JH, Walz T, Haner M, Yu J, Aebi U, Sun TT. Mammalian uroplakins. A group of highly conserved urothelial differentiation-related membrane proteins. *J Biol Chem* 269: 13716-13724, 1994.

Wu XR, Medina JJ, Sun TT. Selective interactions of UPIa and UPIb, teo members of the transmembrane 4 superfamily, with distinct single transmembrane-domained proteins in differentiated urothelial cells. *J Biol Chem* 270:29752-29759, 1995.

Wu RL, Osman I, Wu XR, Lu ML, Zhang ZF, Liang FX, Hamza R, Scher H, Cordon-Cardo C, Sun TT. Uroplakin II gene is expressed in transitional cell carcinoma but not in bilharzial bladder squamous cell carcinoma: alternative pathways of bladder epithelial differentiation and tumor formation. *Cancer Res* 58:1291-1297, 1998.

Xu PX, Adams J, Peters H, Brown MC, Heaney S, Maas R. Eya1-deficient mice lack ears and kidneys and show abnormal apoptosis of organ primordia. *Nat Genet* 23:113-117, 1999.

Xu PX, Zheng W, Huang L, Maire P, Laclef C, Silvius D. Six1 is required for the early organogenesis of the mammalian kidney. *Development* 130:3085-3094, 2003.

Yang SP, Woolf AS, Yuan HT, Scott RJ, Risdon RA, O'Hare MJ, Winyard PJD. Potential biological role of transforming growth factor β1 in human congenital kidney malformations. *Am J Pathol* 157:1633-1647, 2000.

Yang J, Bardes ESG, Moore JD, Brennan J, Powers MA, Kornbluth S. Control of cyclin B1 localization through regulated binding of the nuclear export factor CRM1. *Genes Dev* 12:2131-2141, 1998.

Yang J, Kornbluth S. All aboard the cyclin train: subcellular trafficking of cyclins and their CDK partners. *Trends Cell Biol* 9:207-210, 1999.

Yang SP, Woolf AS, Quinn F, Winyard PJD. Deregulation of renal transforming growth factor-β1 after experimental short-term ureteric obstruction in fetal sheep. *Am J Pathol* 159:109-117, 2001.

Yu J, Carroll TJ, McMahon AP. Sonic hedgehog regulates proliferation and differentiation of mesenchymal cells in the mouse metanephric kidney. *Development* 129:5301-5312, 2002.

Yu J, Manabe M, Wu XR, Xu C, Surya B, Sun TT. Uroplakin I: a 27 kDa protein associated with the asymmetric unit membrane of mammalian urothelium. *J Cell Biol* 111:1207-1216, 1990.

Yu J, Lin JH, Wu XR, Sun TT. Uroplakins Ia and Ib, two major differentiation products of bladder epithelium, belong to a family of four transmembrane domain (4TM) proteins. *J Cell Biol* 125: 171-182, 1994.

Zent R, Bush KT, Pohl ML, Quaranta V, Koshikara N, Wang Z, Kreidberg JA, Sakurai H, Stuart RO, Nigam SK. Involvement of laminin binding integrins and laminin-5 in branching morphogenesis of the ureteric bud during kidney development. *Dev Biol* 238:289-302, 2001.

Zhao Z, Fu XY, Hewett-Emmett D, Boerwinkle E. Investigating single nucleotide polymorphism (SNP) density in the human genome and its implications for molecular evolution. *Gene* 312:207-213, 2003.

Zhou G, Mo WJ, Sebbel P, Min G, Neubert TA, Glockshuber R, Wu XR, Sun TT, Kong XP. Uroplakin Ia is the urothelial receptor for uropathogenic Escerichia coli: evidence from in vitro FimH binding. *J Cell Sci* 114:4095-4103, 2001.